

The Microbial Ecology of the Paediatric Oral Microbiome in Healthy and Sleep Disorder Breathers

by

Jessica Alice Pillay Carlson–Jones

Bachelor of Biotechnology (Hons)

Thesis

Submitted to Flinders University

for the degree of

Doctor of Philosophy

College of Science and Engineering

August 2019

Table of Contents

Summary.....	viii
Declaration.....	x
Acknowledgements.....	xi

CHAPTER 1

General introduction	1
The human microbiome.....	2
The oral microbiome	2
Microbial dispersal across anatomic sites.....	5
Paediatric sleep disorder breathing	5
Sleep and the microbiome.....	6
Microbial links to paediatric sleep disorders	7
Thesis aims and objectives	9
References.....	12

CHAPTER 2

Enumerating Virus-Like Particles and Bacterial Populations in the Sinuses of Chronic Rhinosinusitis Patients Using Flow Cytometry.....	24
Abstract.....	25
Introduction	26
Materials and Methods	27
Ethics statement	27

Sample collection.....	27
Sample preparation.....	28
Flow cytometric analysis	29
Data analysis	30
Results	31
Flow cytometric analysis	31
Bacterial sample preparation method optimisation	32
VLP sample preparation method optimisation	33
Bacterial rank abundance	33
VLP rank abundance	36
Lack of correlation with patient symptoms.....	39
Discussion.....	39
Acknowledgments	44
References.....	44
Supporting Information	51

CHAPTER 3

Flow cytometric enumeration of bacterial and virus-like particle populations in the human oral cavity pre and post sleep.....	54
Abstract.....	55
Poster presentation	56

CHAPTER 4

The microbial abundance dynamics of the human oral cavity before and after sleep

.....	57
Abstract.....	58
Introduction	59
Materials and methods	61
Ethics statement	61
Sample collection.....	61
Sample preparation.....	62
Flow cytometric analysis	63
Data analysis	65
Results	65
Flow cytometric analysis	65
Oral cavity bacterial abundance heterogeneity before sleep	68
Oral cavity bacterial abundance heterogeneity after sleep	70
Oral cavity VLP abundance heterogeneity before sleep	71
Oral cavity VLP abundance homogeneity after sleep	73
Bacterial and VLP increases during sleep	73
Bacterial and VLP network analysis	77
Discussion.....	81
Acknowledgements	86
References.....	86
Supporting information	95

CHAPTER 5

The microbial abundance dynamics in the oral cavity of paediatric sleep disorder breathers before and after sleep	103
Abstract.....	104
Introduction	105
Materials and Methods.....	106
Ethics statement	106
Sample collection.....	106
Swab sample preparation	107
Flow cytometry.....	108
Data analysis	108
Results.....	109
SDB bacterial abundance heterogeneity before sleep.....	109
SDB bacterial abundance heterogeneity after sleep	113
SDB VLP abundance heterogeneity before sleep	114
SDB VLP abundance homogeneity after sleep	117
Significant increase in bacterial and VLP counts during sleep.....	117
Significant differences in microbial concentrations between health states	121
Discussion.....	122
Acknowledgements	127
References.....	128
Supplementary information	135

CHAPTER 6

The spatial distribution of the bacterial communities within the healthy paediatric oral cavity before and after sleep	145
Abstract.....	146
Introduction	147
Materials and Methods	148
Ethics statement	148
Sample collection.....	148
Swab sample preparation	150
Bacteria 16S PCR amplification	150
Bioinformatics	151
Sequence analysis.....	151
Results	152
Overall sequence statistics	152
Relative abundance of oral bacteria differs among microhabitat	152
Bacterial populations shift in relative abundance during sleep	161
Differences in oral community composition based on collection time and microhabitat	164
Bacterial communities vary among participants	168
Discussion.....	170
Acknowledgements	175
References.....	175

CHAPTER 7

The spatial distribution of the oral microbiome in paediatric sleep disorder breathers

.....	184
Abstract.....	185
Introduction	186
Materials and Methods	187
Ethics statement	187
Sample collection.....	187
Swab preparation.....	188
Bacterial 16S PCR amplification	189
Bioinformatic analysis	189
Sequence analysis.....	190
Results	191
Overall sequence statistics	191
Oral microhabitats vary in bacterial composition in SDB	191
Bacterial community composition among microhabitats when split by time	197
Bacterial communities differ in composition among participants and between genders in SDB	198
Bacterial communities in paediatric SDB significantly differ to healthy participants ..	201
Discussion.....	204
Acknowledgements	209
References.....	209

CHAPTER 8

General discussion	219
Thesis overview	220
Synthesis of research.....	221
Flow cytometric enumeration of bacteria and VLP in maxillary sinus flush samples .	221
The healthy paediatric oral cavity is a numerically dynamic heterogeneous environment	222
Viral community abundances differ between healthy and SDB	223
Microbial communities shift anaerobically during sleep in healthy paediatric participants	224
Bacterial communities in SDB significantly differ to healthy individuals	225
Significance.....	227
Future directions	228
Conclusions	229
References.....	230
Appendices	239
Publications.....	239
Poster presentations	240
Response to reviewers (chapter 4).....	256

SUMMARY

The human body is colonised by an array of microorganisms that are involved in maintaining overall health and wellbeing. Disruption to these beneficial microbial communities is linked to the progression of numerous disease states. Regarded as the gateway to the body, the oral cavity has become a site for numerous taxonomic studies investigating microbial links between health and disease. Within the oral cavity are different microhabitats that support the colonisation of different bacterial communities. However, little is known about the absolute microbial abundance dynamics within and between these microhabitats, and whether they are different in disease states. Used as a tool for monitoring microbial dynamics in environmental studies, flow cytometry enables the rapid enumeration of bacteria and viruses within a community. In chapters 2, 3 and 4 of this thesis we demonstrate that flow cytometry can be used on medical samples to count bacteria and viruses within niches of the human body. We establish that the upper respiratory tract, specifically the sinuses and oral cavity, are colonised by 'high' numbers of microbes and that these counts are not homogeneous in their distribution spatially and among individuals. In addition, chapters 3 and 4 also establish that the microbial communities in the healthy paediatric oral cavity significantly increase in absolute abundance during sleep by counts of up to 100 million. In sleep disorder breathers (SDB), this microbial dynamic is predicted to be different as variations in sleeping patterns are suspected to change oral environmental conditions. Chapter 5 presents the first study to identify, using flow cytometry, a significant difference in the absolute microbial abundances, specifically in viruses, between microhabitats in the healthy and sleep disorder breathers' oral cavities. Chapter 6 characterises the relative taxonomic distribution of the microhabitats of the healthy paediatric oral cavity and shows for the first time that these bacterial communities significantly shift during sleep, specifically in anaerobic genera of bacteria. Finally, chapter 7 shows that paediatric sleep disorder breathers have significantly different oral taxonomic

profiles than healthy paediatric participants, specifically at the tip of the tongue after sleep. Overall, this thesis highlights the potential value in high frequency time series of healthy and SDB oral microbiomes. Here we show that the paediatric oral microbial communities significantly shift in abundance over time, suggesting of a highly dynamic community. Therefore, there is the need for careful interpretation when identifying shifts in oral microbial composition between health states. This thesis suggests the need for future microbial related research in paediatric SDB with a particular focus on the oral microbiome to determine if there is a causal relation between the microbial communities present and the health condition.

DECLARATION

I certify that this thesis: does not incorporate without acknowledgment any material previously submitted for a degree or diploma in any university; and to the best of my knowledge and belief, does not contain any material previously published or written by another person except where due reference is made in the text.

Signed..... Jessica Carlson-Jones.....

Date..... 16th of September 2018.....

ACKNOWLEDGEMENTS

Firstly, I would like to express my sincere gratitude to my primary supervisor, Professor Jim Mitchell, for his guidance and support throughout the course of this PhD. Thank you as well for providing me with the opportunity to travel around the world to attend workshops and to present at conferences.

To my supervisors at the Women's and Children's Hospital, Professor Declan Kennedy and Dr. James Martin, thank you for allowing me the opportunity to join your research team. Your insight, expertise and words of encouragement were greatly appreciated.

Thanks must also go to Associate Professor Peter Speck (Flinders University), Dr. Renee Smith (Flinders Medical Centre) and Professor Geraint Rogers (SAHMRI) for their advice throughout the course of this PhD. I would also like to acknowledge the financial contribution made by the Australian Government through the Research Training Program (RTP) Scholarship.

Thank you also to Professor Peter-John Wormald (Queen Elizabeth Hospital) for allowing me access into theatre to witness the incredible sinus procedures he conducted to collect the sinus flush samples.

I am also hugely appreciative to Dr. Anna Kontos of the Robinson Research Institute. Without your curiosity into the paediatric microbiome this project would never have existed. Thank you for your support throughout, but most importantly, thank you for the time and effort you put in to collecting the oral swab samples.

To Jody Fisher, thank you so much for your help with the statistical and network analysis components of this thesis. Your knowledge and expertise have been invaluable. Thank you as well for the friendship and support you gave me throughout and for having my back when things got tough.

To Dr. James Paterson and Dr. Kelly Newton, thank you for your training and expert advice in flow cytometry. I also really appreciated your words of encouragement throughout.

To my fellow lab mates Dr. Lisa Dann, Dr. Eloise Prime and Jacqueline Rochow, thank you for all the adventures we have shared together. Your support and friendship throughout have been invaluable.

To Annie Taylor, Michelle Clanahan and Sylvia Sapula, thank you for your words of advice, encouragement and support throughout my candidature.

I would also like to say a special thank you to my amazing Nanna who despite ill health during my candidature, still managed to provide unconditional support to me. Thank you also for providing the motivation I needed to finish.

A special mention also goes my late Poppa, Dr. Pillay, who sadly passed away just over a year out from my completion. Thank you for teaching me the value of an education. I know how proud you were when I started my PhD, I only wish you were around to see me finish.

Finally, to my incredible parents. Words cannot begin to describe how grateful I am for all the support you have given me, not only during this PhD, but throughout my life. Thank you for believing in me.

CHAPTER 1:

GENERAL INTRODUCTION

The human microbiome

The human body is host to an array of microorganisms including viruses, bacteria, archaea, protozoa and fungi. Collectively referred to as the microbiota, these microbes colonize our bodies shortly after birth [1], and over time develop into a diverse community of microorganisms [2]. Starting in 2008, the Human Microbiome Project (HMP) set out to understand how these microbial communities impacted human health and disease [3, 4]. Since then, aided by the rapid progression of high-throughput sequencing technologies [5], extensive amounts of research have been conducted showing how these microbial communities are involved in maintaining our overall health and well-being [4, 6]. This includes but is not limited to the development and regulation of our immune system, nutrient absorption, energy metabolism, mucosal barrier function, detoxification and the prevention of colonisation by pathogenic microorganisms [7-9]. Therefore, perturbations to these microbial communities can have a considerable impact on human health [6]. Another major outcome from these microbiome studies was the knowledge that different regions on the human body were colonised by different microbial communities, and that these communities were highly varied among individuals [10]. One region seen to be particularly complex and diverse was the oral cavity [4, 11].

The oral microbiome

The oral cavity contains various microhabitats that differ in microbial community structure [12, 13]. This includes the soft shedding mucosal surfaces of the tongue, palate, buccal mucosa and gingivae, along with the non-shedding surfaces of the teeth. The microhabitat variations are thought to be a result of numerous factors including salivary flow, oral anatomy, oral hygiene, moisture levels, abrasion (i.e. form

the tongue), surface structure (i.e. papillae), host immune response and oxygen, nutrient, temperature and pH gradients [4, 11-20]. As a result, the oral cavity is an extremely dynamic environment [13], where the microbiota have evolved to adapt to such changes to form a balanced equilibrium of resident microbiota [7, 21]. However, disturbances to this balance can result in numerous oral and systemic diseases.

Oral dysbiosis is where the diversity and taxonomy within an environment is disrupted [6]. Many oral pathogens have been identified within the oral microbiome, but they are found at a controlled level [7, 22]. When there is a disturbance to the natural balance of oral microbiota, an opportunity arises for these pathogenic bacteria to grow and dominate [23]. This has been observed in many oral related infections including dental caries [24] and periodontitis [25]. These oral infections have also been linked to other systemic diseases including preterm birth [26, 27], pneumonia [28], cardiovascular disease [29-32], diabetes [33] and stroke [34]. This shows that understanding the oral microbiome is an important area of research as the flow on effect from dysbiosis in this environment may have further implications in other systems in the body.

Saliva is one host derived mechanism that helps control the levels of bacteria in the oral cavity [35]. Recently shown to shape the spatial gradient of bacterial diversity in the oral cavity [17], saliva is also an important antimicrobial defence system [35]. Important enzymes and proteins in the saliva directly and indirectly regulate the oral microbiome [35]. An example of this is the production of the chemical hypothiocyanite, a reaction catalysed by the enzyme lactoperoxidase found in saliva [7]. Hypothiocyanite has an antimicrobial effect by inhibiting bacterial glycolysis [36].

Unlike bacteria, studies into the human oral virome are less extensive [37-40]. Most viruses in the oral cavity have been identified as bacteriophages [37], viruses that infect bacteria. Unlike eukaryotic viruses, bacteriophages have the capability to eliminate specific bacteria or act as reservoirs for genetic exchange via their lytic and lysogenic lifecycles [37, 41]. Therefore, studies have suggested that these viruses have the potential to shape the oral bacterial communities. One study found that the majority of bacteriophages in the oral cavity displayed homologs for integrase, an enzyme which enables genetic material to be integrated into their bacterial hosts DNA [37]. This implies that lysogeny is favoured, suggesting that bacteriophages in the oral cavity could act as a reservoir for genetic exchange among bacteria, including genes for antibiotic resistance [37, 42]. What role these bacteriophages play in oral health and disease remains largely unknown. However, some studies are beginning to show that the bacteriophage communities in periodontal disease vary to what is observed in healthy controls [39, 40, 43].

It is well established that the oral cavity undergoes changes at each postnatal developmental stage [44]. This is partly due to the eruption and replacement of teeth within the earlier years of life [13, 44]. Other physiological changes, such as hormonal fluctuations during puberty and pregnancy, also influence oral bacteria [45]. Therefore, care needs to be taken when comparing between health states as differences in oral microbiomes could reflect physiological variations due to age.

Microbial dispersal across anatomic sites

Although spatially situated apart, different anatomic sites in the human body are connected and are thought to act as possible sources of microbial inoculation for other body sites [46]. For example, the sinuses and oral cavity drain into the pharynx which is connected to the trachea and lungs, as well as the oesophagus, stomach and gut. [46]. Studies have shown certain sinus bacterial strains have been isolated in the lower respiratory tract of newly transplanted lungs [47]. However, latter work has also suggested that the oral cavity acts as a significant microbial source to the lungs, stomach and oesophagus as microbial communities among these anatomic regions possessed a greater level of similarity to each [48, 49]. This suggests that dysbiosis in one area of the human body could potentially have an undesirable effect on another region. This has already been observed with links between periodontitis and cardiovascular disease [29-31]. Therefore, it is important to monitor the microbial dynamics of various anatomical locations within the body of different health states, as the source microbial dysbiosis may originate from another anatomical location.

Paediatric sleep disorder breathing

Sleep disorder breathing (SDB) defines a broad spectrum of breathing disturbances during sleep. Ranging from mild snoring to obstructive sleep apnoea syndrome (OSA), SDB affects approximately 10% of the paediatric population [50]. One of the characteristics of this condition is the complete or partial blockage of the airways during sleep which leads to arousals events and disruptions of the normal sleeping pattern [51]. This obstruction is often caused by hypertrophy of the tonsillar and adenoid tissue [52]. There is also a peak prevalence in paediatric SDB between the ages of 2 and 8 as this is the age range where the tonsils and adenoids are at their

largest in relation to the airways [53, 54]. Children who are overweight or obese are also at a greater risk of developing SDB [55, 56]. However, the conventional form of treatment, an adenotonsillectomy [57, 58], is not as effective in this group as the narrowing of the airways is due to fat deposits in the pharyngeal wall [59, 60].

Due to the airway obstruction during sleep, children with SDB often display symptoms of snoring, restlessness, nocturnal sweating, noisy breathing, sleep terrors, mouth breathing and apnoea during the night [61, 62]. These disturbances can cause fatigue, inattention, hyperactivity and aggressiveness during the day [61, 62]. If left untreated, paediatric sleep apnoea can have harmful outcomes on the children's growth, cardiovascular, neurocognitive and behavioural wellbeing [57, 63].

Sleep and the microbiome

Interest into the microbiomes of SDB began when mice and human gut microbiota studies showed evidence of conforming to a circadian rhythm, a cycle of 24-hours in which various physiological processes in our body fluctuate up and down [64, 65]. Furthermore, sequencing of faecal samples from mice and humans exposed to diurnal fluctuations showed that circadian misalignment perturbs gut microbiota [64]. In 2016, research showed for the first time that short partial sleep deprivation and chronic sleep fragmentation in mice and healthy young men resulted in a shift of their gut microbiota [66, 67]. The study by Poroyket et al. reported an increase in the relative abundance of *Lachnospiraceae* and *Ruminococcaceae*, and a decrease in *Lactobacillaceae* families in the gut of sleep fragmented mice models [67]. Interestingly, these effects were reversed after 2 weeks of unfragmented normal sleep [67]. This study also reported that germ free mice, when transplanted with the faecal microbiota of sleep fragmented mice, displayed similar metabolic shifts to the sleep

fragmented cohort [67]. These studies suggested that restoring the gut microbiota in sleep fragmented cases, such as sleep apnoea, could be a future form of treatment.

A study by Moreno-Indias et al. was the first to specifically investigate how intermittent hypoxia, a trademark of obstructive sleep apnoea, impacted the microbial diversity of the gut [68]. Here, the faecal microbiomes of mice exposed to patterns of intermittent hypoxia for 6 weeks were compared to normoxic controls [68]. Results showed that, hypoxic mice had an increase in the relative abundance of Firmicutes, and a decrease in Bacteroidetes and Proteobacteria phyla [68]. This suggested that microbial equilibrium in the gut of OSA is perturbed, opening a new field of research in sleep apnoea. Since then, numerous studies have continued investigating the link between OSA and its symptoms (i.e. hypertension) with the gut microbiome [69-71]. However, no studies have investigated these gut microbial shifts in the paediatric population. As the human microbiome is known to change with age [44], it important to examine possible gut perturbances in all age groups, from the very young to the elderly.

Microbial links to paediatric sleep disorders

Recently a study has suggested that respiratory viruses may be involved in the inflammation of tonsillar tissue leading to the development of sleep apnoea [57]. It has been hypothesized that respiratory viral infections, in particular respiratory syncytial virus (RSV), can cause an increase of lymphoid tissue resulting in inflammation of the airways in young susceptible children [57, 72]. Infants who were infected with the RSV had a significantly higher obstructive sleep apnoea index (a scale which ranks the severity of the sleep apnoea) than children who were not infected with the virus. This suggests a role of early life respiratory viral infection in the

pathogenesis of sleep apnoea. However, more research is needed to show a strong connection between the microbiome and the pathogenesis of sleep apnoea.

Thesis aims and objectives

Overall, this thesis aims to understand the spatial distribution of the paediatric oral microbiota within various microhabitats of the oral cavity, and to see if these communities change in paediatric SDB. To do this, we looked at the microbial communities in the oral cavity of children with and without SDB before and after sleep to determine if there are any differences in the absolute or taxonomic community structure. With no studies investigating the dynamic of the paediatric SDB oral microbiome, this thesis will be an important piece in understanding whether further investigations into the oral microbiome will hold the key to the possibility of uncovering a pathogenic cause to sleep related conditions.

Specifically, the aims were:

- To develop a flow cytometry protocol that can be used on medical samples to successfully enumerate bacterial and viral populations. In addition, establish that viruses are prominent in the maxillary sinuses of Chronic Rhinosinusitis patients.
- To assess the spatial distribution and dynamics of the absolute bacterial and viral populations within the healthy paediatric oral cavity before and after sleep.
- To investigate the spatial distribution and dynamics of the absolute bacterial and viral populations within the SDB paediatric oral cavity before and after sleep, and to determine if they are as abundant and dynamic as healthy participants.
- To determine the taxonomic community distributions of bacteria within microhabitats of the healthy paediatric oral cavity and assess if these communities change during sleep.

- To determine the taxonomic community distributions of bacteria within microhabitats of the SDB paediatric oral cavity and assess if these communities change during sleep. In addition, determine if these bacterial communities are the same as healthy participants.

This thesis has been written in manuscript form to suit the submission criteria for scientific journals. Therefore, there is some redundancy in the introduction and methods sections of the chapters. The results from chapters 2, 3 and 4 have been published in or submitted to peer reviewed journals. Chapter 2 investigated the bacterial and viral concentrations within the maxillary sinuses of chronic rhinosinusitis patients using flow cytometry and was published in the journal PLOS ONE [73]. Chapter 3 presents the abundance dynamics of the healthy paediatric oral microbiome before and after sleep. The abstract of chapter 3 (the poster version of chapter 4) has been published in the peer reviewed Journal of Sleep Research [15]. Chapter 4 assesses the heterogeneity in the absolute bacterial and viral loads within the microhabitats of the healthy paediatric oral cavity and assesses by how much they fluctuate during sleep. Chapter 4 had been submitted for publication in the journal PLOS ONE (30th January 2018). Chapter 5 investigates the spatial distribution and heterogeneity of the absolute bacterial and viral populations within microhabitats of the SDB oral cavity and assesses if these microbial loads are displayed to the same extent as healthy participants. Chapter 6 investigates the bacterial taxonomic distribution within the microhabitats of the healthy paediatric oral cavity and how these communities change during sleep. Chapter 7 compares the taxonomic distribution of bacterial communities in the SDB oral cavity to the healthy oral cavity to determine if the oral microbiome in SDB is different. A summary of the results and the future implications they have on the field of SDB has been discussed in chapter 8. Future directions to come out of this thesis are also included in this chapter. This thesis provides the first insight into the absolute abundance dynamics of the healthy and SDB oral cavity during sleep. It provides a new option for monitoring microbial dynamics in microbial related health conditions.

References

1. Dominguez-Bello MG, Costello EK, Contreras M, Magris M, Hidalgo G, Fierer N, et al. Delivery mode shapes the acquisition and structure of the initial microbiota across multiple body habitats in newborns. *Proc Natl Acad Sci U S A*. 2010;107(26):11971-5. Epub 2010/06/23. doi: 10.1073/pnas.1002601107. PubMed PMID: 20566857; PubMed Central PMCID: PMC2900693.
2. Koenig JE, Spor A, Scalfone N, Fricker AD, Stombaugh J, Knight R, et al. Succession of microbial consortia in the developing infant gut microbiome. *Proc Natl Acad Sci U S A*. 2011;108 Suppl 1:4578-85. Epub 2010/07/30. doi: 10.1073/pnas.1000081107. PubMed PMID: 20668239; PubMed Central PMCID: PMC3063592.
3. Turnbaugh PJ, Ley RE, Hamady M, Fraser-Liggett CM, Knight R, Gordon JI. The human microbiome project. *Nature*. 2007;449(7164):804-10. doi: 10.1038/nature06244. PubMed PMID: 17943116; PubMed Central PMCID: PMC3709439.
4. Human Microbiome Project C. Structure, function and diversity of the healthy human microbiome. *Nature*. 2012;486(7402):207-14. doi: 10.1038/nature11234. PubMed PMID: 22699609; PubMed Central PMCID: PMC3564958.
5. Reuter JA, Spacek DV, Snyder MP. High-throughput sequencing technologies. *Mol Cell*. 2015;58(4):586-97. Epub 2015/05/23. doi: 10.1016/j.molcel.2015.05.004. PubMed PMID: 26000844; PubMed Central PMCID: PMC4494749.
6. Cho I, Blaser MJ. The human microbiome: at the interface of health and disease. *Nat Rev Genet*. 2012;13(4):260-70. Epub 2012/03/14. doi: 10.1038/nrg3182. PubMed PMID: 22411464; PubMed Central PMCID: PMC3418802.

7. Kilian M, Chapple ILC, Hannig M, Marsh PD, Meuric V, Pedersen AML, et al. The oral microbiome – an update for oral healthcare professionals. *Bdj*. 2016;221:657. doi: 10.1038/sj.bdj.2016.865.
8. Relman DA. The Human Microbiome and the Future Practice of Medicine. *JAMA*. 2015;314(11):1127-8. Epub 2015/09/16. doi: 10.1001/jama.2015.10700. PubMed PMID: 26372576.
9. Donohoe DR, Garge N, Zhang X, Sun W, O'Connell TM, Bunger MK, et al. The microbiome and butyrate regulate energy metabolism and autophagy in the mammalian colon. *Cell Metab*. 2011;13(5):517-26. Epub 2011/05/03. doi: 10.1016/j.cmet.2011.02.018. PubMed PMID: 21531334; PubMed Central PMCID: PMC3099420.
10. Costello EK, Lauber CL, Hamady M, Fierer N, Gordon JI, Knight R. Bacterial community variation in human body habitats across space and time. *Science*. 2009;326(5960):1694-7. Epub 2009/11/07. doi: 10.1126/science.1177486. PubMed PMID: 19892944; PubMed Central PMCID: PMC3602444.
11. Dewhirst FE, Chen T, Izard J, Paster BJ, Tanner AC, Yu WH, et al. The human oral microbiome. *Journal of bacteriology*. 2010;192(19):5002-17. doi: 10.1128/JB.00542-10. PubMed PMID: 20656903; PubMed Central PMCID: PMC2944498.
12. Aas JA, Paster BJ, Stokes LN, Olsen I, Dewhirst FE. Defining the normal bacterial flora of the oral cavity. *J Clin Microbiol*. 2005;43(11):5721-32. doi: 10.1128/JCM.43.11.5721-5732.2005. PubMed PMID: 16272510; PubMed Central PMCID: PMC1287824.

13. Xu X, He J, Xue J, Wang Y, Li K, Zhang K, et al. Oral cavity contains distinct niches with dynamic microbial communities. *Environ Microbiol.* 2015;17(3):699-710. Epub 2014/05/08. doi: 10.1111/1462-2920.12502. PubMed PMID: 24800728.
14. Simon-Soro A, Tomas I, Cabrera-Rubio R, Catalan MD, Nyvad B, Mira A. Microbial geography of the oral cavity. *Journal of dental research.* 2013;92(7):616-21. Epub 2013/05/16. doi: 10.1177/0022034513488119. PubMed PMID: 23674263.
15. Carlson-Jones J, Kontos A, Paterson J, Smith R, Dann L, Speck P, et al. Flow Cytometric Enumeration of Bacterial and Virus-Like Particle Populations in the Human Oral Cavity Pre and Post Sleep. *J Sleep Res.* 2016;25:86-. PubMed PMID: WOS:000393032700215.
16. Mager DL, Ximenez-Fyvie LA, Haffajee AD, Socransky SS. Distribution of selected bacterial species on intraoral surfaces. *J Clin Periodontol.* 2003;30(7):644-54. Epub 2003/07/02. PubMed PMID: 12834503.
17. Proctor DM, Fukuyama JA, Loomer PM, Armitage GC, Lee SA, Davis NM, et al. A spatial gradient of bacterial diversity in the human oral cavity shaped by salivary flow. *Nat Commun.* 2018;9(1):681. Epub 2018/02/16. doi: 10.1038/s41467-018-02900-1. PubMed PMID: 29445174; PubMed Central PMCID: PMC5813034.
18. Choi JE, Waddell JN, Lyons KM, Kieser JA. Intraoral pH and temperature during sleep with and without mouth breathing. *J Oral Rehabil.* 2016;43(5):356-63. Epub 2015/12/17. doi: 10.1111/joor.12372. PubMed PMID: 26666708.
19. Aframian DJ, Davidowitz T, Benoliel R. The distribution of oral mucosal pH values in healthy saliva secretors. *Oral diseases.* 2006;12(4):420-3. Epub 2006/06/24. doi: 10.1111/j.1601-0825.2005.01217.x. PubMed PMID: 16792729.

20. Dawes C. A mathematical model of salivary clearance of sugar from the oral cavity. *Caries research*. 1983;17(4):321-34. Epub 1983/01/01. doi: 10.1159/000260684. PubMed PMID: 6575870.
21. Avila M, Ojcius DM, Yilmaz O. The oral microbiota: living with a permanent guest. *DNA and cell biology*. 2009;28(8):405-11. doi: 10.1089/dna.2009.0874. PubMed PMID: 19485767; PubMed Central PMCID: PMC2768665.
22. Van Winkelhoff AJ, Boutaga K. Transmission of periodontal bacteria and models of infection. *J Clin Periodontol*. 2005;32 Suppl 6:16-27. Epub 2005/09/01. doi: 10.1111/j.1600-051X.2005.00805.x. PubMed PMID: 16128826.
23. Marsh PD, Head DA, Devine DA. Ecological approaches to oral biofilms: control without killing. *Caries research*. 2015;49 Suppl 1:46-54. Epub 2015/04/15. doi: 10.1159/000377732. PubMed PMID: 25871418.
24. Aas JA, Griffen AL, Dardis SR, Lee AM, Olsen I, Dewhirst FE, et al. Bacteria of dental caries in primary and permanent teeth in children and young adults. *J Clin Microbiol*. 2008;46(4):1407-17. doi: 10.1128/Jcm.01410-07. PubMed PMID: WOS:000254866400038.
25. Liu B, Faller LL, Klitgord N, Mazumdar V, Ghodsi M, Sommer DD, et al. Deep sequencing of the oral microbiome reveals signatures of periodontal disease. *Plos One*. 2012;7(6):e37919. doi: 10.1371/journal.pone.0037919. PubMed PMID: 22675498; PubMed Central PMCID: PMC3366996.
26. Offenbacher S, Jared HL, O'Reilly PG, Wells SR, Salvi GE, Lawrence HP, et al. Potential pathogenic mechanisms of periodontitis associated pregnancy complications. *Annals of periodontology / the American Academy of Periodontology*. 1998;3(1):233-50. doi: 10.1902/annals.1998.3.1.233. PubMed PMID: 9722707.

27. Shira Davenport E. Preterm low birthweight and the role of oral bacteria. *Journal of oral microbiology*. 2010;2. doi: 10.3402/jom.v2i0.5779. PubMed PMID: 21523222; PubMed Central PMCID: PMC3084577.
28. Awano S, Ansai T, Takata Y, Soh I, Akifusa S, Hamasaki T, et al. Oral health and mortality risk from pneumonia in the elderly. *Journal of dental research*. 2008;87(4):334-9. PubMed PMID: 18362314.
29. Loos BG, Craandijk J, Hoek FJ, Wertheim-van Dillen PM, van der Velden U. Elevation of systemic markers related to cardiovascular diseases in the peripheral blood of periodontitis patients. *Journal of periodontology*. 2000;71(10):1528-34. Epub 2000/11/04. doi: 10.1902/jop.2000.71.10.1528. PubMed PMID: 11063384.
30. Suzuki J, Aoyama N, Ogawa M, Hirata Y, Izumi Y, Nagai R, et al. Periodontitis and cardiovascular diseases. *Expert Opin Ther Targets*. 2010;14(10):1023-7. Epub 2010/08/04. doi: 10.1517/14728222.2010.511616. PubMed PMID: 20678026.
31. Beukers NG, van der Heijden GJ, van Wijk AJ, Loos BG. Periodontitis is an independent risk indicator for atherosclerotic cardiovascular diseases among 60 174 participants in a large dental school in the Netherlands. *J Epidemiol Community Health*. 2017;71(1):37-42. Epub 2016/08/10. doi: 10.1136/jech-2015-206745. PubMed PMID: 27502782; PubMed Central PMCID: PMCPMC5256268.
32. Ramirez JH, Parra B, Gutierrez S, Arce RM, Jaramillo A, Ariza Y, et al. Biomarkers of cardiovascular disease are increased in untreated chronic periodontitis: a case control study. *Australian dental journal*. 2014;59(1):29-36. doi: 10.1111/adj.12139. PubMed PMID: 24495202.
33. Genco RJ, Grossi SG, Ho A, Nishimura F, Murayama Y. A proposed model linking inflammation to obesity, diabetes, and periodontal infections. *Journal of*

periodontology. 2005;76(11 Suppl):2075-84. doi: 10.1902/jop.2005.76.11-S.2075.
PubMed PMID: 16277579.

34. Joshipura KJ, Hung HC, Rimm EB, Willett WC, Ascherio A. Periodontal disease, tooth loss, and incidence of ischemic stroke. *Stroke; a journal of cerebral circulation*. 2003;34(1):47-52. PubMed PMID: 12511749.

35. van 't Hof W, Veerman EC, Nieuw Amerongen AV, Ligtenberg AJ. Antimicrobial defense systems in saliva. *Monogr Oral Sci*. 2014;24:40-51. Epub 2014/05/28. doi: 10.1159/000358783. PubMed PMID: 24862593.

36. Takahashi N. Oral Microbiome Metabolism: From "Who Are They?" to "What Are They Doing?". *Journal of dental research*. 2015;94(12):1628-37. Epub 2015/09/18. doi: 10.1177/0022034515606045. PubMed PMID: 26377570.

37. Pride DT, Salzman J, Haynes M, Rohwer F, Davis-Long C, White RA, et al. Evidence of a robust resident bacteriophage population revealed through analysis of the human salivary virome. *ISME J*. 2012;6(5):915-26. doi: 10.1038/ismej.2011.169. PubMed PMID: WOS:000302950700002.

38. Bachrach G, Leizerovici-Zigmond M, Zlotkin A, Naor R, Steinberg D. Bacteriophage isolation from human saliva. *Letters in applied microbiology*. 2003;36(1):50-3. Epub 2002/12/18. PubMed PMID: 12485342.

39. Ly M, Abeles SR, Boehm TK, Robles-Sikisaka R, Naidu M, Santiago-Rodriguez T, et al. Altered oral viral ecology in association with periodontal disease. *mBio*. 2014;5(3):e01133-14. Epub 2014/05/23. doi: 10.1128/mBio.01133-14. PubMed PMID: 24846382; PubMed Central PMCID: PMC4030452.

40. Wang J, Gao Y, Zhao F. Phage-bacteria interaction network in human oral microbiome. *Environ Microbiol*. 2016;18(7):2143-58. Epub 2015/06/04. doi: 10.1111/1462-2920.12923. PubMed PMID: 26036920.

41. Rohwer F, Thurber RV. Viruses manipulate the marine environment. *Nature*. 2009;459(7244):207-12. doi: 10.1038/nature08060. PubMed PMID: WOS:000266036100031.
42. Canchaya C, Fournous G, Chibani-Chennoufi S, Dillmann ML, Brussow H. Phage as agents of lateral gene transfer. *Curr Opin Microbiol*. 2003;6(4):417-24. doi: 10.1016/S1369-5274(03)00086-9. PubMed PMID: WOS:000185173000018.
43. Santiago-Rodriguez TM, Naidu M, Abeles SR, Boehm TK, Ly M, Pride DT. Transcriptome analysis of bacteriophage communities in periodontal health and disease. *BMC genomics*. 2015;16:549. Epub 2015/07/29. doi: 10.1186/s12864-015-1781-0. PubMed PMID: 26215258; PubMed Central PMCID: PMC4515923.
44. Crielaard W, Zaura E, Schuller AA, Huse SM, Montijn RC, Keijser BJJ. Exploring the oral microbiota of children at various developmental stages of their dentition in the relation to their oral health. *Bmc Med Genomics*. 2011;4. doi: Artn 22 10.1186/1755-8794-4-22. PubMed PMID: WOS:000288378200001.
45. Zaura E, ten Cate JM. Towards understanding oral health. *Caries research*. 2015;49 Suppl 1:55-61. Epub 2015/04/15. doi: 10.1159/000377733. PubMed PMID: 25871419.
46. Proctor DM, Relman DA. The Landscape Ecology and Microbiota of the Human Nose, Mouth, and Throat. *Cell host & microbe*. 2017;21(4):421-32. doi: 10.1016/j.chom.2017.03.011. PubMed PMID: 28407480; PubMed Central PMCID: PMC5538306.
47. Ciofu O, Johansen HK, Aanaes K, Wassermann T, Alhede M, von Buchwald C, et al. *P. aeruginosa* in the paranasal sinuses and transplanted lungs have similar adaptive mutations as isolates from chronically infected CF lungs. *Journal of cystic*

fibrosis : official journal of the European Cystic Fibrosis Society. 2013;12(6):729-36.
doi: 10.1016/j.jcf.2013.02.004. PubMed PMID: 23478131.

48. Bassis CM, Erb-Downward JR, Dickson RP, Freeman CM, Schmidt TM, Young VB, et al. Analysis of the upper respiratory tract microbiotas as the source of the lung and gastric microbiotas in healthy individuals. *mBio*. 2015;6(2):e00037. doi: 10.1128/mBio.00037-15. PubMed PMID: 25736890; PubMed Central PMCID: PMC4358017.

49. Bik EM, Eckburg PB, Gill SR, Nelson KE, Purdom EA, Francois F, et al. Molecular analysis of the bacterial microbiota in the human stomach. *Proc Natl Acad Sci U S A*. 2006;103(3):732-7. doi: 10.1073/pnas.0506655103. PubMed PMID: 16407106; PubMed Central PMCID: PMC1334644.

50. Lumeng JC, Chervin RD. Epidemiology of pediatric obstructive sleep apnea. *Proceedings of the American Thoracic Society*. 2008;5(2):242-52. Epub 2008/02/06. doi: 10.1513/pats.200708-135MG. PubMed PMID: 18250218; PubMed Central PMCID: PMCPMC2645255.

51. Loughlin GM, Brouillette RT, Brooke LJ, Carroll JL, Chipps BE, England SJ, et al. Standards and indications for cardiopulmonary sleep studies in children (vol 153, pg 866, 1995). *Am J Resp Crit Care*. 1996;153(6):U54-U. PubMed PMID: WOS:A1996UR22300046.

52. Bhattacharjee R, Kheirandish-Goza L, Spruyt K, Mitchell RB, Promchiarak J, Simakajornboon N, et al. Adenotonsillectomy Outcomes in Treatment of Obstructive Sleep Apnea in Children A Multicenter Retrospective Study. *Am J Resp Crit Care*. 2010;182(5):676-83. doi: DOI 10.1164/rccm.200912-1930OC. PubMed PMID: WOS:000281492000013.

53. Jeans WD, Fernando DC, Maw AR, Leighton BC. A longitudinal study of the growth of the nasopharynx and its contents in normal children. *Br J Radiol.* 1981;54(638):117-21. Epub 1981/02/01. doi: 10.1259/0007-1285-54-638-117. PubMed PMID: 7459548.
54. Marcus CL. Sleep-disordered breathing in children. *Am J Respir Crit Care Med.* 2001;164(1):16-30. Epub 2001/07/04. doi: 10.1164/ajrccm.164.1.2008171. PubMed PMID: 11435234.
55. Rosen CL, Larkin EK, Kirchner HL, Emancipator JL, Bivins SF, Surovec SA, et al. Prevalence and risk factors for sleep-disordered breathing in 8- to 11-year-old children: association with race and prematurity. *The Journal of Pediatrics.* 2003;142(4):383-9. doi: 10.1067/mpd.2003.28.
56. Bixler EO, Vgontzas AN, Lin HM, Liao D, Calhoun S, Vela-Bueno A, et al. Sleep disordered breathing in children in a general population sample: prevalence and risk factors. *Sleep.* 2009;32(6):731-6. Epub 2009/06/24. PubMed PMID: 19544748; PubMed Central PMCID: PMCPMC2690559.
57. Yeshuroon-Koffler K, Shemer-Avni Y, Keren-Naus A, Goldbart AD. Detection of common respiratory viruses in tonsillar tissue of children with obstructive sleep apnea. *Pediatr Pulm.* 2014;n/a-n/a. doi: 10.1002/ppul.23005.
58. Marcus CL, Brooks LJ, Ward SD, Draper KA, Gozal D, Halbower AC, et al. Diagnosis and Management of Childhood Obstructive Sleep Apnea Syndrome. *Pediatrics.* 2012;130(3):E714-E55. doi: DOI 10.1542/peds.2012-1672. PubMed PMID: WOS:000309409300035.
59. O'Brien LM, Sitha S, Baur LA, Waters KA. Obesity increases the risk for persisting obstructive sleep apnea after treatment in children. *Int J Pediatr Otorhi.* 2006;70(9):1555-60. doi: 10.1016/j.ijporl.2006.04.003.

60. Horner RL, Mohiaddin RH, Lowell DG, Shea SA, Burman ED, Longmore DB, et al. Sites and sizes of fat deposits around the pharynx in obese patients with obstructive sleep apnoea and weight matched controls. *Eur Respir J.* 1989;2(7):613-22. Epub 1989/07/01. PubMed PMID: 2776867.
61. Chervin RD, Archbold KH, Dillon JE, Panahi P, Pituch KJ, Dahl RE, et al. Inattention, hyperactivity, and symptoms of sleep-disordered breathing. *Pediatrics.* 2002;109(3):449-56. Epub 2002/03/05. PubMed PMID: 11875140.
62. Sinha D, Guilleminault C. Sleep disordered breathing in children. *The Indian journal of medical research.* 2010;131:311-20. Epub 2010/03/24. PubMed PMID: 20308756.
63. Gozal D, O'Brien LM. Snoring and obstructive sleep apnoea in children: Why should we treat? *Paediatric Respiratory Reviews.* 2004;5, Supplement 1(0):S371-S6. doi: [http://dx.doi.org/10.1016/S1526-0542\(04\)90066-8](http://dx.doi.org/10.1016/S1526-0542(04)90066-8).
64. Thaiss CA, Zeevi D, Levy M, Zilberman-Schapira G, Suez J, Tengeler AC, et al. Transkingdom control of microbiota diurnal oscillations promotes metabolic homeostasis. *Cell.* 2014;159(3):514-29. Epub 2014/11/25. doi: 10.1016/j.cell.2014.09.048. PubMed PMID: 25417104.
65. Liang X, Bushman FD, FitzGerald GA. Rhythmicity of the intestinal microbiota is regulated by gender and the host circadian clock. *Proc Natl Acad Sci U S A.* 2015;112(33):10479-84. Epub 2015/08/05. doi: 10.1073/pnas.1501305112. PubMed PMID: 26240359; PubMed Central PMCID: PMC4547234.
66. Benedict C, Vogel H, Jonas W, Woting A, Blaut M, Schurmann A, et al. Gut microbiota and glucometabolic alterations in response to recurrent partial sleep deprivation in normal-weight young individuals. *Mol Metab.* 2016;5(12):1175-86. Epub

2016/12/03. doi: 10.1016/j.molmet.2016.10.003. PubMed PMID: 27900260; PubMed Central PMCID: PMC5123208.

67. Poroyko VA, Carreras A, Khalyfa A, Khalyfa AA, Leone V, Peris E, et al. Chronic Sleep Disruption Alters Gut Microbiota, Induces Systemic and Adipose Tissue Inflammation and Insulin Resistance in Mice. *Scientific reports*. 2016;6:35405. Epub 2016/10/16. doi: 10.1038/srep35405. PubMed PMID: 27739530; PubMed Central PMCID: PMC5064361.

68. Moreno-Indias I, Torres M, Montserrat JM, Sanchez-Alcoholado L, Cardona F, Tinahones FJ, et al. Intermittent hypoxia alters gut microbiota diversity in a mouse model of sleep apnoea. *Eur Respir J*. 2015;45(4):1055-65. Epub 2014/12/30. doi: 10.1183/09031936.00184314. PubMed PMID: 25537565.

69. Durgan DJ, Ganesh BP, Cope JL, Ajami NJ, Phillips SC, Petrosino JF, et al. Role of the Gut Microbiome in Obstructive Sleep Apnea-Induced Hypertension. *Hypertension*. 2016;67(2):469-74. Epub 2015/12/30. doi: 10.1161/HYPERTENSIONAHA.115.06672. PubMed PMID: 26711739; PubMed Central PMCID: PMC54713369.

70. Santisteban MM, Qi Y, Zubcevic J, Kim S, Yang T, Shenoy V, et al. Hypertension-Linked Pathophysiological Alterations in the Gut. *Circ Res*. 2017;120(2):312-23. Epub 2016/11/02. doi: 10.1161/CIRCRESAHA.116.309006. PubMed PMID: 27799253; PubMed Central PMCID: PMC5250568.

71. Li J, Zhao F, Wang Y, Chen J, Tao J, Tian G, et al. Gut microbiota dysbiosis contributes to the development of hypertension. *Microbiome*. 2017;5(1):14. Epub 2017/02/02. doi: 10.1186/s40168-016-0222-x. PubMed PMID: 28143587; PubMed Central PMCID: PMC5286796.

72. Goldbart AD, Mager E, Veling MC, Goldman JL, Kheirandish-Gozal L, Serpero LD, et al. Neurotrophins and tonsillar hypertrophy in children with obstructive sleep apnea. *Pediatr Res.* 2007;62(4):489-94. doi: Doi 10.1203/Pdr.0b013e31814257ed. PubMed PMID: WOS:000249862900022.
73. Carlson-Jones JA, Paterson JS, Newton K, Smith RJ, Dann LM, Speck P, et al. Enumerating Virus-Like Particles and Bacterial Populations in the Sinuses of Chronic Rhinosinusitis Patients Using Flow Cytometry. *Plos One.* 2016;11(5):e0155003. doi: 10.1371/journal.pone.0155003. PubMed PMID: 27171169; PubMed Central PMCID: PMC4865123.

CHAPTER 2:

ENUMERATING VIRUS-LIKE PARTICLES AND BACTERIAL POPULATIONS IN THE SINUSES OF CHRONIC RHINOSINUSITIS PATIENTS USING FLOW CYTOMETRY

This chapter has been accepted and published in the journal PLOS ONE.

Citation: Carlson-Jones JAP, Paterson JS, Newton K, Smith RJ, Dann LM, Speck P, et al. (2016) Enumerating Virus-Like Particles and Bacterial Populations in the Sinuses of Chronic Rhinosinusitis Patients Using Flow Cytometry. PLoS ONE 11(5): e0155003. <https://doi.org/10.1371/journal.pone.0155003>

Contribution to publication: Conceived and designed the experiments, performed the experiments, analysed the data, contributed reagents/materials/analysis tools and wrote the publication.

Research Design: 80%

Data collection and analysis: 100%

Writing and editing: 80%

Abstract

There is increasing evidence to suggest that the sinus microbiome plays a role in the pathogenesis of chronic rhinosinusitis (CRS). However, the concentration of these microorganisms within the sinuses is still unknown. We show that flow cytometry can be used to enumerate bacteria and virus-like particles (VLPs) in sinus flush samples of CRS patients. This was achieved through trialling 5 sample preparation techniques for flow cytometry. We found high concentrations of bacteria and VLPs in these samples. Untreated samples produced the highest average bacterial and VLP counts with $3.3 \pm 0.74 \times 10^7$ bacteria ml^{-1} and $2.4 \pm 1.23 \times 10^9$ VLP ml^{-1} of sinus flush ($n = 9$). These counts were significantly higher than most of the treated samples ($p < 0.05$). Results showed 10^3 and 10^4 times inter-patient variation for bacteria and VLP concentrations. This wide variation suggests that diagnosis and treatment need to be personalised and that utilising flow cytometry is useful and efficient for this. This study is the first to enumerate bacterial and VLP populations in the maxillary sinus of CRS patients. The relevance of enumeration is that with increasing antimicrobial resistance, antibiotics are becoming less effective at treating bacterial infections of the sinuses, so alternative therapies are needed. Phage therapy has been proposed as one such alternative, but for dosing, the abundance of bacteria is required. Knowledge of whether phages are normally present in the sinuses will assist in gauging the safety of applying phage therapy to sinuses. Our finding, that large numbers of VLP are frequently present in sinuses, indicates that phage therapy may represent a minimally disruptive intervention towards the nasal microbiome. We propose that flow cytometry can be used as a tool to assess microbial biomass dynamics in sinuses and other anatomical locations where infection can cause disease.

Introduction

Chronic rhinosinusitis (CRS) is a common disease amongst the human population, and there is increasing evidence to show that microorganisms are involved in the inflammation of the sinus mucosal layer leading to exacerbation of the disease [1-3]. It is well established that the healthy sinus is not sterile, but is colonised by a diverse community of microorganisms [1, 2, 4, 5]. These microorganisms exist in the sinuses within exopolysaccharide biofilms, the presence of which leads to difficulties in treating the disease [6-12]. As antibiotics are a common treatment option for CRS patients, there is concern surrounding the growing antimicrobial resistance [13, 14]. Bacteria within these biofilms are able to secrete a polysaccharide matrix that acts as a protective barrier against host defences and antimicrobial agents [15]. This protective barrier makes it difficult when it comes to treating CRS with antibiotics. An alternative treatment is phage therapy which utilises specific bacteriophages (phage) that infect and kill pathogenic bacteria [16]. Trials of bacteriophage cocktails consisting of multiple types of phage, on sheep models of sinusitis have proven to be effective in eliminating *Staphylococcus aureus* in biofilms and its free floating form [17]. Through the use of these phage cocktails, the development of phage resistant bacteria is reduced [18]. Knowledge of population abundance of bacteria and phage in the sinuses is important for the development of appropriate phage concentrations for use in this therapy [19].

Flow cytometry has been used as a method for enumerating heterotrophic bacteria and virus-like particles (VLPs) in environmental samples for decades [20-22]. This non-culture based technology is a quick, inexpensive way to rapidly enumerate a large number of cells and particles to provide data without the enrichment bias

culturing introduces [20]. This technique yields highly reproducible counts and enumeration of VLPs at a concentration that would be too low for transmission electron microscopy (TEM) [20]. Here, we investigate methods to enumerate bacteria and VLPs within sinus flush fluid samples and present the first data, produced using flow cytometry, describing bacterial and VLP abundance within the maxillary sinuses of CRS patients. We, therefore, aim to measure the variation in abundance of bacteria and VLPs in the sinuses of CRS patients to determine if they are present at the same level among patients.

Materials and Methods

Ethics statement

Maxillary sinus flush fluid samples were obtained from nine patients diagnosed with CRS in accordance to criteria defined by the Chronic Rhinosinusitis Task Force [23]. This study was approved by The Queen Elizabeth Hospital Human Research Ethics Committee, reference number: HREC/13/TQEHLMH/49. All nine patients involved in the study gave written consent prior to their sinus surgery. All sinus flush fluid samples were collected by the senior author (P.J.W) during the patient's endoscopic sinus surgery. Due to the highly invasive nature of the operating procedure, healthy controls were not ethically justifiable, nor are they relevant to the question of how much abundance variation is there among infected patients.

Sample collection

Immediately after opening the maxillary sinus, approximately 5 ml of sterile saline was used to flush the sinus and re-collected in sterile specimen containers. Volume of flush fluid collected ranged from approximately 2 to 4 ml. Once samples

were collected, they were transported on ice ready for immediate fixation with glutaraldehyde (0.5% final concentration) on ice in the dark, then snap freezing in liquid nitrogen and storage at -80°C until analysis [21].

Sample preparation

Five sample preparation techniques for flow cytometry were investigated. Fixed sinus flush fluid samples were thawed before each treatment was applied.

Sputasol. Sputasol was made using 0.02 µm filtered MilliQ water according to the manufacturer's instructions (Oxoid). Equal volumes of Sputasol and fixed sinus sample were mixed together then incubated at 37°C for 15 minutes.

Methanol. Methanol, 0.2 µm filtered, was added to fixed sinus samples to a final concentration of 20% [24]. Samples were incubated at 37°C for 15 minutes then sonicated for 30 seconds in a SoniClean™ sonicating bath (Model 160TD, 60 W, 50/60Hz).

Potassium citrate. Potassium citrate tribasic solution (1M, Sigma) was added to the fixed sample to a 1% final concentration [24]. The sample was then vortexed for 30 seconds [24].

Sodium pyrophosphate. Sodium pyrophosphate solution was added to 100 µl of fixed sample to a final concentration of 10 mM [24]. Samples were vortexed for 1 minute and incubated at room temperature for 15 minutes [24]. Samples were then sonicated for 30 seconds in a SoniClean™ sonicating bath (Model 160TD, 60 W, 50/60Hz).

Untreated. Fixed samples were diluted in 0.2µm filtered TE buffer (10 mM Tris, 1 mM EDTA, pH 7.4) without pre-treatment [21].

Flow cytometric analysis

Bacterial and VLP populations present in sinus flush fluid were identified and enumerated using a BD ACCURI C6 flow cytometer (Becton Dickinson). Samples using each extraction technique were run in triplicate for each patient. Samples were diluted (1:100) in 0.2 µm filtered TE buffer, stained with the DNA-binding dye SYBR-I Green (1:20,000 final dilution; Molecular Probes) then incubated at 80°C in the dark for 10 minutes [21]. For each preparation method control samples were generated prior to each flow cytometry session. These samples were prepared in the same manner as patient samples in 0.9% sterile saline, the same concentration used to flush patient sinuses. These samples were used to eliminate background artefacts introduced during sample preparation.

Samples were analysed using an Accuri C6 flow cytometer (Accuri C6) and BD ACCURI CFlow software. All samples were run for 2 minutes at machine fluidics setting of fast, with the threshold set to FL-1 (green fluorescence). As a control, 1 µm diameter fluorescent beads (Molecular Probes) were used. Beads were added to each sample to a final concentration of 10^5 beads ml^{-1} [25]. The beads allow for flow cytometric parameters to be normalised according to bead fluorescence and concentration, and to give an indication of viral and bacterial cell size [25]. Phosphate-buffered saline (PBS) was used as sheath fluid for flow cytometry analysis. For each sample, green fluorescence, side angle light scatter and forward angle light scatter were recorded.

Data analysis

Flow cytometry data was analysed using FlowJo software (Tree Star, Inc.). VLP and bacterial populations were categorised based on variations in side scatter, a representation of cell size, and SYBR Green fluorescence, an indication of nucleic acid content [20, 21, 26]. For some patients, only one bacterial population was observed, whereas others showed multiple. Therefore, one overall bacterial population was created to remain consistent across all patient samples.

Rank abundance plots were generated for bacterial and VLP concentrations using all method triplicates and their averages to distinguish between any patient groupings formed on abundance. Comparisons between bacterial and VLP abundances for each treatment method were made using the statistical analysis program SPSS version 22 (IBM Corp. Released 2013. IBM SPSS Statistics for Windows, Version 22.0. Armonk, NY: IBM Corp.) using the Wilcoxon signed-rank test. Statistical significance between treatments was considered when $p < 0.05$.

Results

Flow cytometric analysis

Cytograms showed discrete bacterial and VLP populations present within the sinus fluid of CRS patients (Fig 1). Some patients exhibited one distinct bacterial population, whereas others patients exhibited up to four (Fig 1). Variations in bacterial and VLP abundance were observed between patients regardless of the treatment method used on the samples. Mean bacterial and VLP abundances for each treatment method are shown in Table 1.

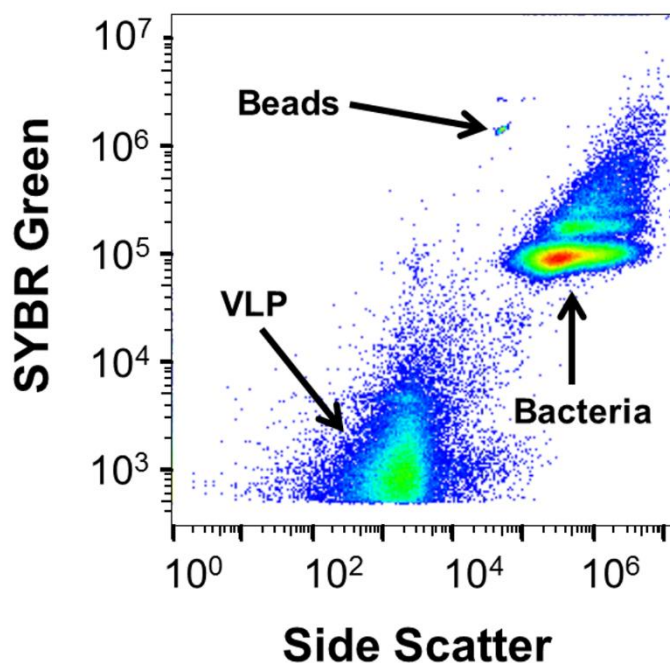


Fig 1. Bacterial and VLP identification using side-scatter and green fluorescence. Representative cytogram shows the VLP and bacterial populations in a patient's untreated sinus wash.

Table 1. Mean concentration of bacteria and VLP per ml of sinus flush fluid for each treatment method tested. Error represents standard error of the mean.

Treatment	Bacteria ml⁻¹ (\pmSEM)	VLP ml⁻¹ (\pmSEM)
Untreated	3.3 x 10 ⁷ (7.4 x 10 ⁶)	2.4 x 10 ⁹ (1.2 x 10 ⁹)
Sodium pyrophosphate	2.9 x 10 ⁷ (6.7 x 10 ⁶)	2.0 x 10 ⁹ (9.9 x 10 ⁸)
Sputasol	2.2 x 10 ⁷ (6.6 x 10 ⁶)	1.8 x 10 ⁹ (9.4 x 10 ⁸)
Methanol	2.0 x 10 ⁷ (4.3 x 10 ⁶)	2.2 x 10 ⁹ (9.9 x 10 ⁸)
Potassium citrate	1.9 x 10 ⁷ (4.6 x 10 ⁶)	2.1 x 10 ⁹ (1.1 x 10 ⁹)

Bacterial sample preparation method optimisation

For patient samples, the mean bacterial abundance for untreated samples was the highest of all treatments, with $3.3 \pm 0.74 \times 10^7$ cells ml⁻¹ (n = 27; Table 1). The lowest mean abundance was for potassium citrate treated samples with $1.9 \pm 0.46 \times 10^7$ cells ml⁻¹ (n = 27; Table 1). In testing the differences between treatments, the untreated and sodium pyrophosphate samples yielded significantly higher bacterial abundance than potassium citrate (p < 0.001 and p < 0.001), methanol (p = 0.002 and p < 0.001) and Sputasol (p = 0.003 and p < 0.001). There was no significant difference in bacterial abundance between sodium pyrophosphate treated and untreated samples (p = 0.39).

VLP sample preparation method optimisation

VLP mean abundance for the untreated method was the highest for all patient samples with $2.4 \pm 1.2 \times 10^9$ cells ml⁻¹ (n = 27; Table 1). Sputasol treated patient samples yielded the lowest VLP abundances with $1.8 \pm 0.91 \times 10^9$ cells ml⁻¹ (n = 27; Table 1). Untreated samples yielded significantly higher VLP abundances than potassium citrate (p = 0.031), methanol (p = 0.010), and Sputasol (p = 0.019) treated samples. There was no significant difference between VLP abundance for untreated samples and sodium pyrophosphate treated samples (p = 0.08). Sodium pyrophosphate also did not yield significantly higher VLP abundances than potassium citrate (p = 0.44) and methanol (p = 0.53) treated samples. There was, however, a significant difference between VLP abundances for sodium pyrophosphate and Sputasol (p = 0.008).

Bacterial rank abundance

Rank abundance was used to identify possible groupings among the patient's bacterial abundance. Breaks in the plot suggest 3 groupings of patients with bacterial abundances classified as high, greater than 10^7 cells ml⁻¹, medium, between 10^5 to 10^6 cells ml⁻¹, and low, less than 10^5 cells ml⁻¹ (Fig 2). The high bacterial group consisted of triplicates from 5 patients. The medium bacterial group contained triplicates from 3 patients and the low bacterial abundance group consisted of 1 patient. There was approximately one order of magnitude difference between each of the 3 groups (Fig 2). The overall average bacterial rank abundance using all treatment triplicates fit a logarithmic trend; however this was achieved by a series of step down power laws for each bacterial group (Fig 3).

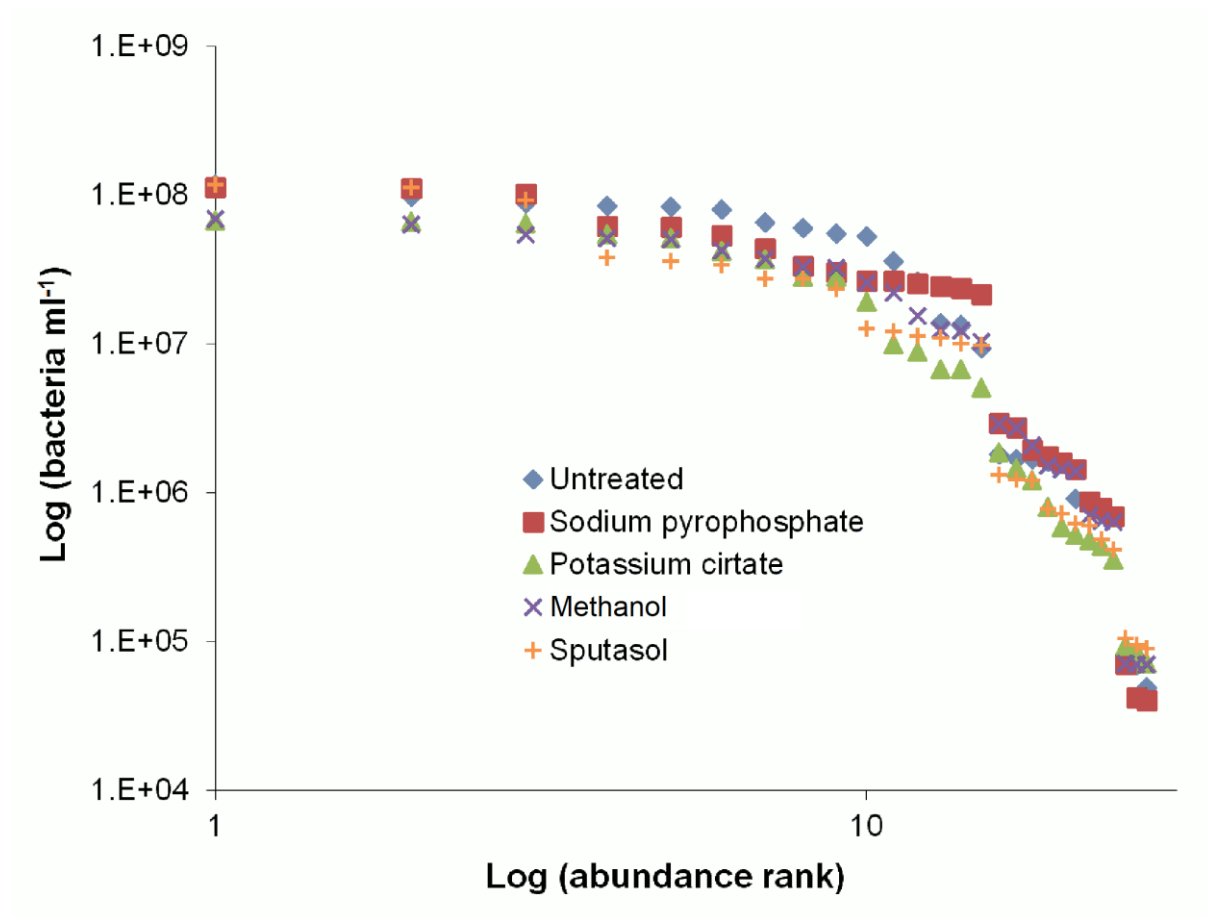


Fig 2. Rank abundance for each patient's bacterial abundance for each sample treatment method, with triplicates shown. Three clear groups of patients with high, medium and low bacterial abundances are apparent. Differences in treatments used on the samples can be seen not to influence steps of bacterial abundance for patients.

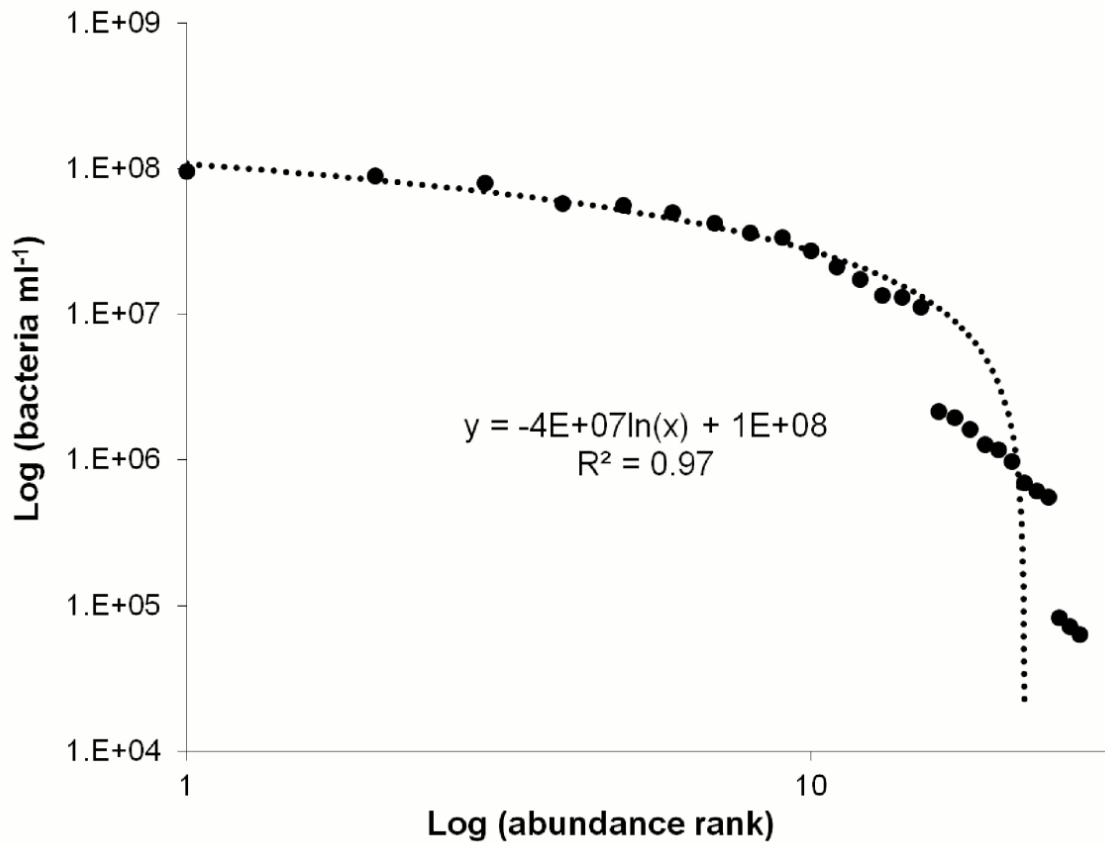


Fig 3. Average bacterial rank abundance using all treatment triplicates. Data points follow a logarithmic trend achieved by steps of power laws for each observed group. High medium and low bacterial concentration groups fit the power law equations $y = 2E+08x^{-0.84}$ ($R^2 = 0.84$), $y = 5E+10x^{-3.57}$ ($R^2 = 0.98$) and $y = 6E+09x^{-3.49}$ ($R^2 = 1$) respectively.

VLP rank abundance

A rank abundance plot for VLP abundance was generated using the method triplicates of untreated, sodium pyrophosphate, potassium citrate, Sputasol and methanol samples (Fig 4). VLP abundances show an even distribution across 5 orders of magnitude. Three patients had values above 10^8 VLP ml⁻¹. These are classified as high VLP, with the proviso that they are separated from each other by an order of magnitude (Fig 4). Three patients make up the medium concentration group between 10^7 and 10^8 VLP ml⁻¹. However, in this group the loss of VLPs in the methanol and sodium pyrophosphate treatments makes the group appear fused with the lowest group. The lowest group was classified as concentrations below 10^7 VLP ml⁻¹. In this group the methanol treatment showed considerable loss of VLPs and in one patient a complete absence of VLPs (Fig 4). The overall average VLP rank abundance using all treatment triplicates fit a steep power law (Fig 5).

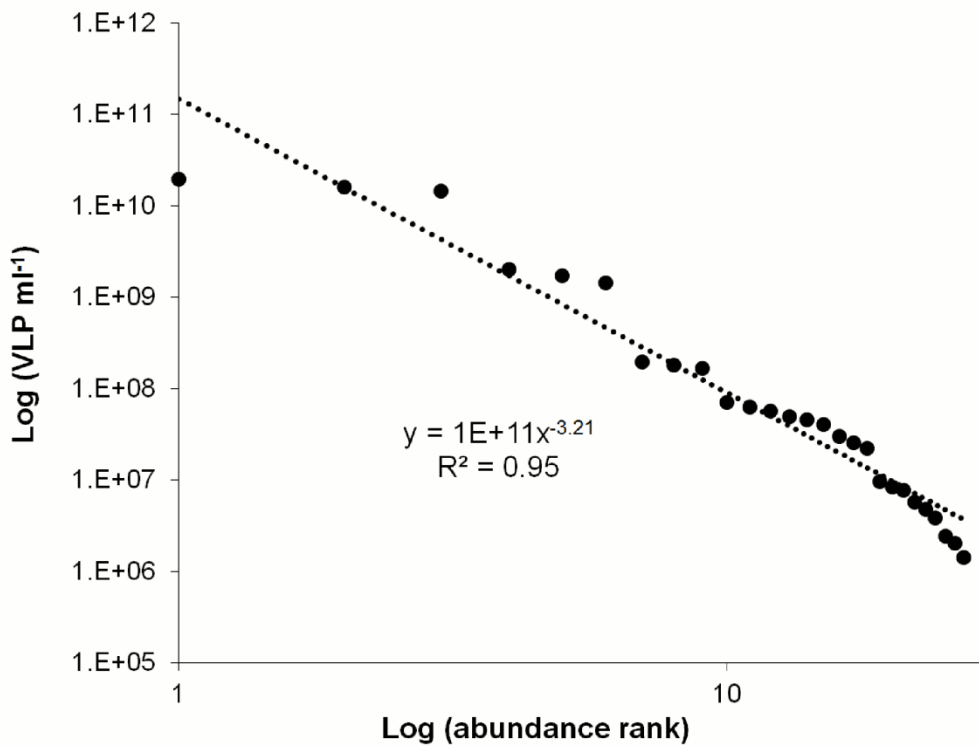


Fig 4. Rank abundance for each patient’s VLP abundance for each sample preparation method, with triplicates shown. Highest abundances are rare while lower abundances are common. Differences in treatments used on the patient samples can be seen not to influence the high range of VLP origination levels.

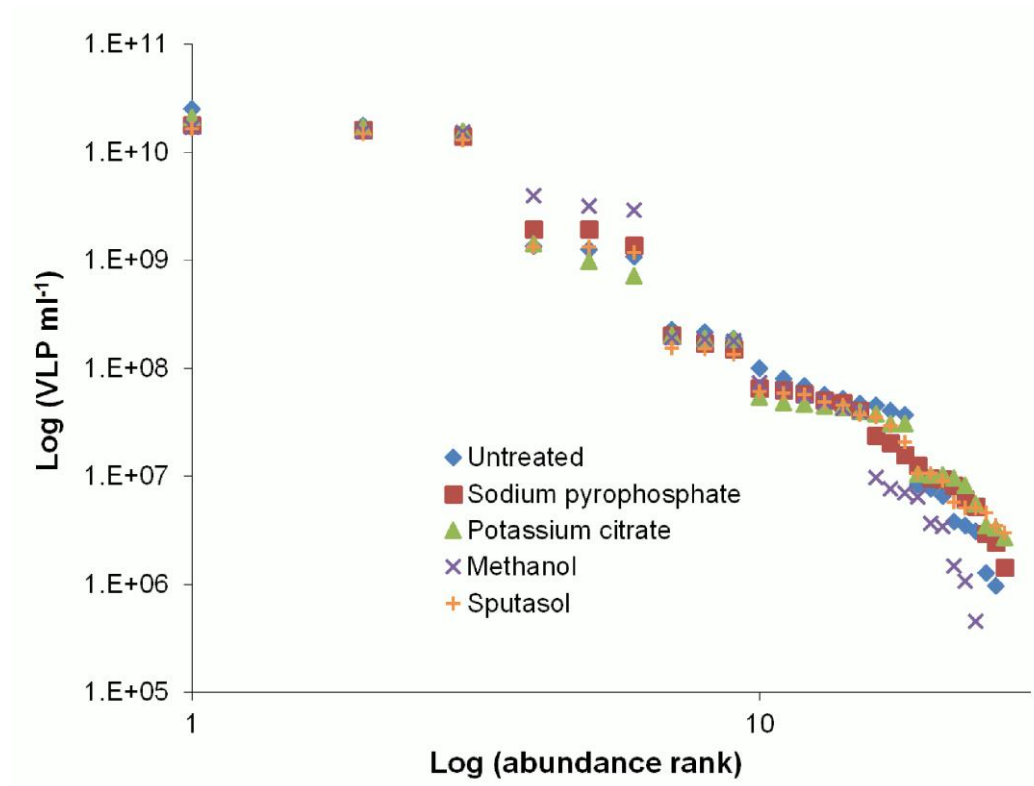


Fig 5. Average VLP rank abundance using all treatment triplicates. Data points follow a power law.

Lack of correlation with patient symptoms

Prior to sinus surgery, each patient completed a questionnaire regarding basic clinical information and provided a severity score from 0, being no problem, to 5, being a problem as bad as it can be, for CRS symptoms for the past two weeks. Based on the rank abundance plots (Figs 2 and 3), possible trends in the patient groups were investigated. There were no trends observed within the rank abundance patient groups for bacteria or VLPs.

Discussion

This is the first study to use flow cytometry to enumerate bacteria and VLPs within the maxillary sinus of CRS patients. We present a number of snapshot enumerations, using flow cytometry, of the microbial composition of sinuses of CRS patients. We tested a number of sample preparation techniques for bacterial and VLP enumeration that are used for environmental samples, in particular, techniques used for disruption of coral mucus, for microscopy [24, 27]. Our results showed that the sinus, at least in patients requiring sinus surgery, is an active microbiological environment. We speculate that most VLPs detected are likely to be bacteriophages as they are the most commonly found in association with their hosts, bacteria, which we find to be present in abundance in sinuses. The proposal that phages can be used to treat bacterial infections of the sinus [17] can now be viewed in the light of this data showing that phages appear to be present in sinuses in large numbers (Table 1).

Although the primary focus of this study was to enumerate the bacteria and VLPs in the sinus fluid, there was concern surrounding the presence of small fragments of mucus or biofilms within the samples prepared for flow cytometry. The

mucus may have caused the bacteria and VLPs to clump together resulting in an overestimation on particle size, shape and DNA content. This is a similar concern in regards to analyzing bacteria and VLPs in coral mucus using microscopy [24, 27]. As bacterial and VLP flow cytometry on human samples is a new approach, various flow cytometry methods were investigated.

Common chemicals used in environmental sample preparation include potassium citrate, sodium pyrophosphate and methanol. Sodium pyrophosphate and potassium citrate are commonly used in environmental microbiology for desorbing viral particles from soil and marine sediment [28, 29]. Potassium citrate increases the electrostatic repulsion between viruses and bacteria, and the mucus to which they are attached to by raising pH [24]. Sodium pyrophosphate weakens the hydrophilic links in mucus allowing for viruses and bacteria to be separated [30]. Dithiothreitol (DTT) has been used on sinus samples to improve the yield of fungal cultures and in studies involving quantification of inflammatory cells in nasal secretions [31-33]. Sputasol contains DTT and has been used to liquefy mucus in nasal lavage [34]. It does this by breaking disulfide bonds within mucin, causing liquefaction, releasing trapped viruses and bacteria [35, 36]. Methanol has the ability to break up exopolymeric substances in mucus which entrap bacteria and viruses [37].

Our results show that the untreated and sodium pyrophosphate treatment methods yielded significantly higher bacterial abundances than all other methods tested ($p < 0.05$). For VLP enumeration, no treatment (as in the untreated samples) was the optimal method. Although there was no significant difference between untreated and sodium pyrophosphate treated samples ($p < 0.05$), sodium pyrophosphate did not yield significantly higher VLP abundances than methanol and

potassium citrate ($p < 0.05$). This result contrasts to previous microscopy studies which found potassium citrate better for viral enumeration in coral mucus [24]. Unlike sample preparation for coral mucus for microscopy, flow cytometry includes an incubation period after addition of SYBR Green. During this step viral capsids may partially and temporarily denature, facilitating a greater uptake of SYBR Green [20]. This may result in brighter VLP fluorescence resulting in higher counts for all samples. It is also possible that the extra processing steps involved with each treatment resulted in the loss of bacteria and VLPs. All samples were diluted for flow cytometry in TE buffer which contained 1 mM of EDTA. EDTA has been used to extract bacteria and viruses from photosynthetic microbial mats as it destroys cation links within exopolymeric substances, releasing bound bacteria and viruses [38]. It also permeabilises outer membranes, facilitating greater uptake of SYBR Green [39]. Additional treatment to each sample could have an adverse effect, causing damage to viral capsid proteins or to bacterial cell walls. Our data suggests that the least possible number of processing steps and addition of chemicals is the optimal method for analyzing sinus flush samples.

Previous studies have shown that the human sinus is colonized with an array of microbes [1, 2, 6-12, 40]. Flow cytometry enables categorization and enumeration of these microbes based on size and DNA content [21, 26]. Some patient's cytograms revealed numerous bacterial sub-populations (Fig. 1). These populations displayed increased green fluorescence, an indication of DNA content, and size. These different sub-populations may be reflecting different bacterial replication stages or are indicative of different bacterial species with different sized genomes. In the Sputasol treated patient samples, an unusual population was observed between the bacterial and VLP regions. This population appears to be an artifact of the Sputasol as it was also

observed in the control samples (S1 Fig). Thus, there may be a component within Sputasol which autofluorescences or binds to SYBR Green.

Large variations were observed between patients bacterial and VLP concentrations, which is not uncommon with human microbial flora studies [41-45]. These findings suggest that the maxillary sinus is either extremely dynamic or highly individualised. These differences in the patient microbial concentrations could indicate the need for personalised dosages when treating CRS with antibiotics or with phage. The rank abundance plot for patient bacterial abundance revealed 3 groupings of high, medium and low abundance (Fig 2). As the treatments used on the samples were not seen to account for the differences in bacterial and VLP levels (Figs 2 and 4), an average of all treatment values was used to clearly demonstrate the obvious trends in bacterial concentration groups (Fig 3) and high episodic nature of the VLPs (Fig 5).

For the bacterial rank abundance, the three orders of magnitude range among the 9 patients may reflect temporal variation or that the bacterial abundances are defined by processes or a variable that was not measured. The skew of the distribution towards the lower concentrations in the VLP rank abundance is consistent with the highly episodic nature of viral infections, particularly in bacteriophage where large burst sizes can quickly reduce the concentrations of particular bacterial species, leaving high bacteriophage concentrations at least temporarily [46]. From this, one might posit that time series sampling would show an eventual decline in VLP concentration. While bacteriophage dynamics is one likely explanation for the observed distribution, at this point we cannot discount that some patients have chronically high VLP concentrations. To investigate this and its clinical significance would require flow cytometric and nucleic acid sequence analysis of time series

samples from the identified patients. Due to the invasive nature of sampling used in this study, healthy controls and a time series using the same sampling method may not be a feasible option. Therefore, there is the need to develop a proxy for an alternative less invasive sampling strategy, such as nasal swabbing. While this is beyond the scope of this paper, it is a potentially valuable future direction.

Knowledge of the abundance of microorganisms in CRS will further our understanding of the disease as the presence of certain bacterial species does not always imply infection. The aim of this research was to produce a snapshot enumeration of the sinus microbes of 9 patients known to suffer from CRS, and to determine if they had similar abundances of bacteria and VLPs. Within the group of 9 patients sampled, there was 3 orders of magnitude difference in abundance for bacterial populations and almost 4 orders of magnitude difference for VLPs. This suggests that not all CRS patients are infected at the same level of bacteria and VLPs. Knowledge of the differences in bacterial abundances may facilitate the development of personalised treatment options.

This work indicates the potential for future studies in other microbial disease related health conditions. We propose that flow cytometry has potential as a tool to monitor microbial dynamics in patients and in future may assist in determining appropriate dosages required when treating microbial related health conditions.

Acknowledgments

We would like to thank all the staff at the Flow Cytometry Unit in the Flinders Medical Centre for their technical support throughout the duration of this study. We would also like to extend our gratitude to the tissue registrars in Professor Wormald's research group for conducting the patient surveys and their assistance in sample collection.

References

1. Feazel LM, Robertson CE, Ramakrishnan VR, Frank DN. Microbiome complexity and *Staphylococcus aureus* in chronic rhinosinusitis. *The Laryngoscope*. 2012;122(2):467-72. doi: 10.1002/lary.22398. PubMed PMID: 22253013; PubMed Central PMCID: PMC3398802.
2. Boase S, Foreman A, Cleland E, Tan L, Melton-Kreft R, Pant H, et al. The microbiome of chronic rhinosinusitis: culture, molecular diagnostics and biofilm detection. *BMC infectious diseases*. 2013;13:210. doi: 10.1186/1471-2334-13-210. PubMed PMID: 23656607; PubMed Central PMCID: PMC3654890.
3. Ooi EH, Wormald PJ, Tan LW. Innate immunity in the paranasal sinuses: a review of nasal host defenses. *American journal of rhinology*. 2008;22(1):13-9. doi: 10.2500/ajr.2008.22.3127. PubMed PMID: 18284853.
4. Jiang RS, Liang KL, Jang JW, Hsu CY. Bacteriology of endoscopically normal maxillary sinuses. *The Journal of laryngology and otology*. 1999;113(9):825-8. PubMed PMID: 10664686.
5. Wilson MT, Hamilos DL. The nasal and sinus microbiome in health and disease. *Current allergy and asthma reports*. 2014;14(12):485. doi: 10.1007/s11882-014-0485-x. PubMed PMID: 25342392.

6. Cryer J, Schipor I, Perloff JR, Palmer JN. Evidence of bacterial biofilms in human chronic sinusitis. *ORL; journal for oto-rhino-laryngology and its related specialties*. 2004;66(3):155-8. doi: 10.1159/000079994. PubMed PMID: 15316237.
7. Ferguson BJ, Stolz DB. Demonstration of biofilm in human bacterial chronic rhinosinusitis. *American journal of rhinology*. 2005;19(5):452-7. PubMed PMID: 16270598.
8. Ramadan HH, Sanclement JA, Thomas JG. Chronic rhinosinusitis and biofilms. *Otolaryngology--head and neck surgery : official journal of American Academy of Otolaryngology-Head and Neck Surgery*. 2005;132(3):414-7. doi: 10.1016/j.otohns.2004.11.011. PubMed PMID: 15746854.
9. Sanclement JA, Webster P, Thomas J, Ramadan HH. Bacterial biofilms in surgical specimens of patients with chronic rhinosinusitis. *The Laryngoscope*. 2005;115(4):578-82. doi: 10.1097/01.mlg.0000161346.30752.18. PubMed PMID: 15805862.
10. Sanderson AR, Leid JG, Hunsaker D. Bacterial biofilms on the sinus mucosa of human subjects with chronic rhinosinusitis. *The Laryngoscope*. 2006;116(7):1121-6. doi: 10.1097/01.mlg.0000221954.05467.54. PubMed PMID: 16826045.
11. Psaltis AJ, Ha KR, Beule AG, Tan LW, Wormald PJ. Confocal scanning laser microscopy evidence of biofilms in patients with chronic rhinosinusitis. *The Laryngoscope*. 2007;117(7):1302-6. doi: 10.1097/MLG.0b013e31806009b0. PubMed PMID: 17603329.
12. Foreman A, Psaltis AJ, Tan LW, Wormald PJ. Characterization of bacterial and fungal biofilms in chronic rhinosinusitis. *Am J Rhinol Allergy*. 2009;23(6):556-61. doi: 10.2500/ajra.2009.23.3413. PubMed PMID: 19958600.

13. Kingdom TT, Swain RE, Jr. The microbiology and antimicrobial resistance patterns in chronic rhinosinusitis. *American journal of otolaryngology*. 2004;25(5):323-8. PubMed PMID: 15334396.
14. Bhattacharyya N, Kepnes LJ. Assessment of trends in antimicrobial resistance in chronic rhinosinusitis. *Ann Oto Rhinol Laryn*. 2008;117(6):448-52. PubMed PMID: WOS:000257026300008.
15. Flemming HC, Wingender J. The biofilm matrix. *Nature reviews Microbiology*. 2010;8(9):623-33. doi: 10.1038/nrmicro2415. PubMed PMID: 20676145.
16. Abedon ST, Kuhl SJ, Blasdel BG, Kutter EM. Phage treatment of human infections. *Bacteriophage*. 2011;1(2):66-85. Epub 2012/02/16. doi: 10.4161/bact.1.2.15845

2159-7073-1-2-2 [pii]. PubMed PMID: 22334863; PubMed Central PMCID: PMC3278644.
17. Drilling A, Morales S, Jardeleza C, Vreugde S, Speck P, Wormald PJ. Bacteriophage reduces biofilm of *Staphylococcus aureus* ex vivo isolates from chronic rhinosinusitis patients. *American journal of rhinology & allergy*. 2014;28(1):3-11. doi: 10.2500/ajra.2014.28.4001. PubMed PMID: 24717868.
18. Fu W, Forster T, Mayer O, Curtin JJ, Lehman SM, Donlan RM. Bacteriophage cocktail for the prevention of biofilm formation by *Pseudomonas aeruginosa* on catheters in an in vitro model system. *Antimicrob Agents Chemother*. 2010;54(1):397-404. Epub 2009/10/14. doi: 10.1128/AAC.00669-09

AAC.00669-09 [pii]. PubMed PMID: 19822702; PubMed Central PMCID: PMC2798481.

19. Payne RJ, Phil D, Jansen VA. Phage therapy: the peculiar kinetics of self-replicating pharmaceuticals. *Clin Pharmacol Ther.* 2000;68(3):225-30. Epub 2000/10/03. doi: S0009923600889559 [pii]
10.1067/mcp.2000.109520. PubMed PMID: 11014403.
20. Marie D, Brussaard CPD, Thyrhaug R, Bratbak G, Vaulot D. Enumeration of marine viruses in culture and natural samples by flow cytometry. *Appl Environ Microbiol.* 1999;65(1):45-52. PubMed PMID: 9872758; PubMed Central PMCID: PMC90981.
21. Brussaard CP. Optimization of procedures for counting viruses by flow cytometry. *Appl Environ Microbiol.* 2004;70(3):1506-13. PubMed PMID: 15006772; PubMed Central PMCID: PMC368280.
22. Robertson BR, Button DK. Characterizing aquatic bacteria according to population, cell size, and apparent DNA content by flow cytometry. *Cytometry.* 1989;10(1):70-6. doi: 10.1002/cyto.990100112. PubMed PMID: 2465113.
23. Benninger MS, Ferguson BJ, Hadley JA, Hamilos DL, Jacobs M, Kennedy DW, et al. Adult chronic rhinosinusitis: definitions, diagnosis, epidemiology, and pathophysiology. *Otolaryngology--head and neck surgery : official journal of American Academy of Otolaryngology-Head and Neck Surgery.* 2003;129(3 Suppl):S1-32. Epub 2003/09/06. doi: S0194599803013974 [pii]. PubMed PMID: 12958561.
24. Leruste A, Bouvier T, Bettarel Y. Enumerating viruses in coral mucus. *Appl Environ Microbiol.* 2012;78(17):6377-9. Epub 2012/06/26. doi: 10.1128/AEM.01141-12
AEM.01141-12 [pii]. PubMed PMID: 22729548; PubMed Central PMCID: PMC3416620.

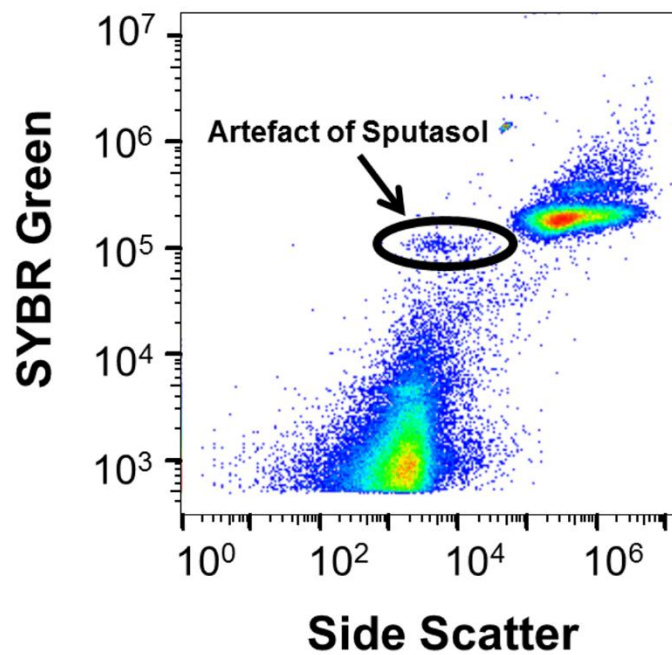
25. Gasol JM, Del Giorgio PA. Using flow cytometry for counting natural planktonic bacteria and understanding the structure of planktonic bacterial communities. *Sci Mar.* 2000;64(2):197-224. PubMed PMID: ISI:000088019800007.
26. Marie D, Partensky F, Jacquet S, Vaulot D. Enumeration and cell cycle analysis of natural populations of marine picoplankton by flow cytometry using the nucleic acid stain SYBR Green I. *Appl Environ Microb.* 1997;63(1):186-93. PubMed PMID: WOS:A1997WA16800029.
27. Garren M, Azam F. New method for counting bacteria associated with coral mucus. *Appl Environ Microbiol.* 2010;76(18):6128-33. doi: 10.1128/AEM.01100-10. PubMed PMID: 20656857; PubMed Central PMCID: PMC2937480.
28. Danovaro R, Dell'Anno A, Trucco A, Serresi M, Vanucci S. Determination of virus abundance in marine sediments. *Appl Environ Microbiol.* 2001;67(3):1384-7. Epub 2001/03/07. doi: 10.1128/AEM.67.3.1384-1387.2001. PubMed PMID: 11229937; PubMed Central PMCID: PMC92740.
29. Williamson KE, Wommack KE, Radosevich M. Sampling natural viral communities from soil for culture-independent analyses. *Appl Environ Microbiol.* 2003;69(11):6628-33. Epub 2003/11/07. PubMed PMID: 14602622; PubMed Central PMCID: PMC262263.
30. Danovaro R, Middelboe M. Separation of free virus particles from sediments in aquatic systems. *Manual of Aquatic Viral Ecology ASLO.* 2010:74-81.
31. Lee HS, Majima Y, Sakakura Y, Shinogi J, Kawaguchi S, Kim BW. Quantitative cytology of nasal secretions under various conditions. *The Laryngoscope.* 1993;103(5):533-7. Epub 1993/05/01. doi: 10.1288/00005537-199305000-00010. PubMed PMID: 8483371.

32. Shinogi J, Majima Y, Takeuchi K, Harada T, Sakakura Y. Quantitative cytology of nasal secretions with perennial allergic rhinitis in children: comparison of noninfected and infected conditions. *The Laryngoscope*. 1998;108(5):703-5. Epub 1998/05/20. doi: 10.1097/00005537-199805000-00014. PubMed PMID: 9591549.
33. Chisholm KM, Getsinger D, Vaughan W, Hwang PH, Banaei N. Pretreatment of sinus aspirates with dithiothreitol improves yield of fungal cultures in patients with chronic sinusitis. *International forum of allergy & rhinology*. 2013. Epub 2013/10/15. doi: 10.1002/alr.21230. PubMed PMID: 24124079.
34. Hajjiannou J, Maraki S, Vlachaki E, Panagiotaki I, Lagoudianakis G, Skoulakis C, et al. Mycology of the Nasal Cavity of Chronic Rhinosinusitis Patients with Nasal Polyps in the Island of Crete. *Research in Otolaryngology*. 2012;1(2):6-10.
35. Cleland WW. Dithiothreitol, a New Protective Reagent for Sh Groups. *Biochemistry*. 1964;3:480-2. Epub 1964/04/01. PubMed PMID: 14192894.
36. Grebski E, Peterson C, Medici TC. Effect of physical and chemical methods of homogenization on inflammatory mediators in sputum of asthma patients. *Chest*. 2001;119(5):1521-5. Epub 2001/05/12. PubMed PMID: 11348963.
37. Lunau M, Lemke A, Walther K, Martens-Habbena W, Simon M. An improved method for counting bacteria from sediments and turbid environments by epifluorescence microscopy. *Environ Microbiol*. 2005;7(7):961-8. Epub 2005/06/11. doi: EMI767 [pii]
10.1111/j.1462-2920.2005.00767.x. PubMed PMID: 15946292.
38. Carreira C, Staal M, Middelboe M, Brussaard CP. Counting viruses and bacteria in photosynthetic microbial mats. *Appl Environ Microbiol*. 2015;81(6):2149-55. doi: 10.1128/AEM.02863-14. PubMed PMID: 25595761; PubMed Central PMCID: PMC4345377.

39. Vaara M. Agents That Increase the Permeability of the Outer-Membrane. *Microbiol Rev.* 1992;56(3):395-411. PubMed PMID: WOS:A1992JN45300002.
40. Human Microbiome Project C. Structure, function and diversity of the healthy human microbiome. *Nature.* 2012;486(7402):207-14. doi: 10.1038/nature11234. PubMed PMID: 22699609; PubMed Central PMCID: PMC3564958.
41. Costello EK, Lauber CL, Hamady M, Fierer N, Gordon JI, Knight R. Bacterial community variation in human body habitats across space and time. *Science.* 2009;326(5960):1694-7. doi: 10.1126/science.1177486. PubMed PMID: 19892944; PubMed Central PMCID: PMC3602444.
42. Turnbaugh PJ, Hamady M, Yatsunencko T, Cantarel BL, Duncan A, Ley RE, et al. A core gut microbiome in obese and lean twins. *Nature.* 2009;457(7228):480-4. doi: 10.1038/nature07540. PubMed PMID: 19043404; PubMed Central PMCID: PMC2677729.
43. Biswas K, Hoggard M, Jain R, Taylor MW, Douglas RG. The nasal microbiota in health and disease: variation within and between subjects. *Front Microbiol.* 2015;9:134. doi: 10.3389/fmicb.2015.00134. PubMed PMID: 25784909; PubMed Central PMCID: PMC4345913.
44. Nasidze I, Li J, Quinque D, Tang K, Stoneking M. Global diversity in the human salivary microbiome. *Genome research.* 2009;19(4):636-43. doi: 10.1101/gr.084616.108. PubMed PMID: 19251737; PubMed Central PMCID: PMC2665782.
45. Grice EA, Kong HH, Conlan S, Deming CB, Davis J, Young AC, et al. Topographical and temporal diversity of the human skin microbiome. *Science.* 2009;324(5931):1190-2. doi: 10.1126/science.1171700. PubMed PMID: 19478181; PubMed Central PMCID: PMC2805064.

46. Mitchell JG, Seuront L. Towards a seascape topology II: Zipf analysis of one-dimensional patterns. *J Marine Syst.* 2008;69(3-4):328-38. doi: 10.1016/j.jmarsys.2006.03.026. PubMed PMID: WOS:000252044800015.

Supporting Information



S1 Fig. Representative cytogram showing the Sputasol artefact population observed between the VLP and bacterial populations.

S1 Table. Patients total bacterial abundances for each optimisation method. Replicates (Rep) for each method are shown.

	Untreated			Sodium pyrophosphate			Potassium citrate			Methanol			Sputasol		
	Rep 1	Rep 2	Rep 3	Rep 1	Rep 2	Rep 3	Rep 1	Rep 2	Rep 3	Rep 1	Rep 2	Rep 3	Rep 1	Rep 2	Rep 3
Patient 1	1.82E+06	1.60E+06	1.62E+06	6.94E+05	8.73E+05	7.93E+05	3.54E+05	4.75E+05	4.39E+05	2.10E+06	2.92E+06	2.76E+06	1.32E+06	1.22E+06	1.24E+06
Patient 2	8.63E+05	7.33E+05	6.99E+05	1.45E+06	1.94E+06	1.75E+06	5.20E+05	5.83E+05	7.98E+05	1.44E+06	1.41E+06	1.52E+06	6.18E+05	4.89E+05	4.17E+05
Patient 3	8.52E+07	1.17E+08	9.83E+07	1.02E+08	1.11E+08	1.12E+08	4.21E+07	5.18E+07	5.42E+07	4.29E+07	3.77E+07	5.15E+07	3.80E+07	3.61E+07	3.38E+07
Patient 4	6.91E+04	4.92E+04	7.96E+04	6.98E+04	4.00E+04	4.23E+04	9.37E+04	8.53E+04	7.17E+04	6.99E+04	6.99E+04	7.10E+04	1.05E+05	9.43E+04	9.00E+04
Patient 5	1.69E+06	1.67E+06	9.17E+05	1.59E+06	2.73E+06	2.96E+06	1.22E+06	1.86E+06	1.45E+06	6.32E+05	7.08E+05	6.42E+05	7.22E+05	6.03E+05	7.75E+05
Patient 6	8.84E+07	6.54E+07	5.56E+07	2.36E+07	2.68E+07	4.40E+07	2.84E+07	2.82E+07	3.72E+07	1.55E+07	3.30E+07	5.47E+07	1.13E+07	1.21E+07	1.01E+07
Patient 7	1.38E+07	9.32E+06	1.33E+07	3.03E+07	3.35E+07	2.17E+07	1.91E+07	6.71E+06	8.86E+06	5.06E+07	6.38E+07	6.96E+07	1.10E+07	1.26E+07	9.79E+06
Patient 8	6.04E+07	8.00E+07	8.42E+07	6.09E+07	5.39E+07	6.24E+07	6.75E+07	6.65E+07	6.52E+07	3.25E+07	2.23E+07	2.61E+07	1.19E+08	1.13E+08	9.20E+07
Patient 9	3.59E+07	2.65E+07	5.31E+07	2.56E+07	2.44E+07	2.68E+07	9.96E+06	5.07E+06	6.70E+06	1.04E+07	1.24E+07	1.25E+07	2.76E+07	2.76E+07	2.35E+07

S2 Table. Patients total VLP abundances for each optimisation method. Replicates (Rep) for each method are shown.

	Untreated			Sodium pyrophosphate			Potassium citrate			Methanol			Sputasol		
	<u>Rep 1</u>	<u>Rep 2</u>	<u>Rep 3</u>	<u>Rep 1</u>	<u>Rep 2</u>	<u>Rep 3</u>	<u>Rep 1</u>	<u>Rep 2</u>	<u>Rep 3</u>	<u>Rep 1</u>	<u>Rep 2</u>	<u>Rep 3</u>	<u>Rep 1</u>	<u>Rep 2</u>	<u>Rep 3</u>
Patient 1	1.00E+08	8.12E+07	6.86E+07	2.06E+07	2.39E+07	1.58E+07	4.51E+07	3.08E+07	4.68E+07	4.29E+07	6.35E+07	5.63E+07	2.92E+07	4.56E+07	3.74E+07
Patient 2	6.66E+06	7.76E+06	8.42E+06	8.23E+06	6.15E+06	9.61E+06	1.03E+07	1.04E+07	1.04E+07	3.70E+06	3.46E+06	6.48E+06	5.08E+06	2.99E+06	5.15E+06
Patient 3	3.75E+07	4.77E+07	4.09E+07	5.78E+07	6.60E+07	6.35E+07	3.09E+07	4.32E+07	3.99E+07	1.07E+06	4.60E+05	9.75E+06	6.13E+07	5.76E+07	5.95E+07
Patient 4	3.49E+06	3.85E+06	3.14E+06	2.46E+06	1.45E+06	2.94E+06	3.51E+06	3.36E+06	2.71E+06	0	0	0	5.80E+06	4.63E+06	3.52E+06
Patient 5	0	9.79E+05	1.27E+06	5.27E+06	9.45E+06	1.28E+07	5.60E+06	9.70E+06	8.24E+06	7.04E+06	1.48E+06	7.72E+06	9.16E+06	1.07E+07	1.06E+07
Patient 6	2.55E+10	1.78E+10	1.55E+10	1.43E+10	1.80E+10	1.63E+10	1.72E+10	1.57E+10	2.12E+10	1.57E+10	1.71E+10	1.55E+10	1.50E+10	1.30E+10	1.66E+10
Patient 7	1.26E+09	1.09E+09	1.36E+09	1.38E+09	1.95E+09	1.94E+09	7.27E+08	9.87E+08	1.42E+09	3.20E+09	4.03E+09	2.96E+09	1.18E+09	1.33E+09	1.34E+09
Patient 8	1.88E+08	2.28E+08	2.16E+08	1.52E+08	1.72E+08	2.02E+08	1.87E+08	2.05E+08	1.89E+08	1.87E+08	1.79E+08	1.93E+08	1.36E+08	1.51E+08	1.55E+08
Patient 9	5.22E+07	4.61E+07	5.67E+07	5.04E+07	4.86E+07	4.06E+07	4.86E+07	3.77E+07	5.41E+07	7.40E+07	4.92E+07	3.98E+07	3.55E+07	4.94E+07	2.09E+07

Chapter 3:

FLOW CYTOMETRIC ENUMERATION OF BACTERIAL AND VIRUS-LIKE PARTICLE POPULATIONS IN THE HUMAN ORAL CAVITY PRE AND POST SLEEP

This poster was presented at the Sleep Down Under conference and the abstract published in the Journal of Sleep Research.

Citation: Carlson-Jones, J., Kontos, A., Paterson, J., Smith, R., Dann, L., Speck, P., Lushington, K., Martin, J., Kennedy, D. and Mitchell, J., 2016, October. FLOW CYTOMETRIC ENUMERATION OF BACTERIAL AND VIRUS-LIKE PARTICLE POPULATIONS IN THE HUMAN ORAL CAVITY PRE AND POST SLEEP. In *JOURNAL OF SLEEP RESEARCH* (Vol. 25, pp. 86-86). 111 RIVER ST, HOBOKEN 07030-5774, NJ USA: WILEY-BLACKWELL.

Contribution to publication: Conceived and designed the experiments, performed the experiments, analysed the data, contributed reagents/materials/analysis tools and wrote the poster/abstract.

Research Design: 80%

Data collection and analysis: 100%

Writing and editing: 90%

Abstract

Within the oral cavity are various ecological niches which provide unique surfaces for the colonisation of distinct microbial communities. Such surfaces include the tongue, throat, palate, gingivae and teeth. Although there is increasing genomic sequence data to show how these niches differ, the overall concentrations of bacteria and viruses at these locations still remains unclear. Here, we examined the spatial distribution of the paediatric oral microbiota of 10 healthy volunteers using flow cytometry as a tool to enumerate populations of bacteria and virus-like particles (VLPs). The highest concentrations of bacteria were found at the back of the tongue with an average of $2.90 \pm 0.76 \times 10^7$ bacteria mL^{-1} before sleep and $1.35 \pm 0.20 \times 10^8$ bacteria mL^{-1} after sleep. The temporomandibular joint had the highest percentage increase in VLPs with $5.68 \pm 1.86 \times 10^6$ VLPs mL^{-1} before sleep and $5.96 \pm 2.30 \times 10^7$ VLP mL^{-1} after sleep. These increases in bacterial and VLP concentrations were found to be significantly different from one another ($p < 0.05$), as were all other sampled locations. These detectable differences in bacterial and VLP concentrations in the oral cavity further demonstrates that the oral cavity is a heterogeneous environment with unique niches that change over time. Through understanding the changes in microbial abundances within these niches, we can further our understanding of the healthy paediatric oral microbiome, and determine in the future, how shifts in these abundances relate to various health conditions.

Flow cytometric enumeration of bacterial and virus-like particle populations in the human oral cavity pre and post sleep

Jessica Carlson-Jones¹, Anna Kontos², James S Paterson¹, Renee J Smith¹, Lisa M Dann¹, Peter Speck¹, James Martin³, Declan Kennedy³, James G Mitchell¹
¹Flinders University, Australia, ²The University of Adelaide, Australia, ³Department of Respiratory and Sleep Medicine, Australia

Introduction¹⁻¹⁰

- Various microhabitats within the oral cavity
 - Tongue, palate, teeth, gingiva
- Different oral surfaces = different microbial communities
- Changes in oral environment over time
 - Oxygen levels, pH, dryness, nutrients (food)
- Flow cytometry as a tool for enumeration
 - Rapid enumeration of cells
 - Allows for counts of virus-like particles (VLPs) at low concentrations
 - Reduces enrichment biases

Objectives

To examine the spatial distribution of bacteria and VLPs within the healthy paediatric oral cavity

To determine changes in bacterial and VLP concentrations in the oral cavity after sleep

Methodology⁷⁻¹⁰

Sample collection:

- Oral swabs collected at Women's and Children's Hospital, Adelaide
 - Roof of mouth
 - Back of throat
 - Back of tongue
 - Tip of tongue
 - Top of molars
 - Gingiva
- Swabs taken before and after sleep

Enumeration:

- FACSCanto II flow cytometer

Results

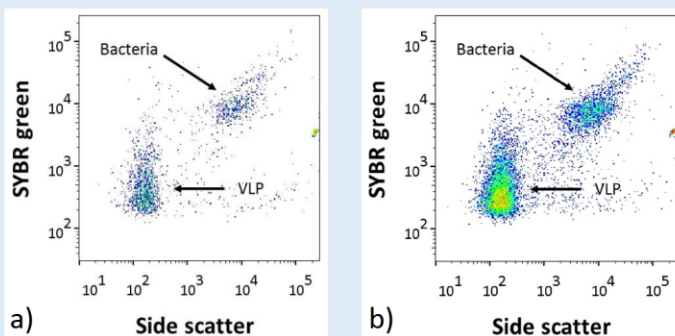


Figure 1: Cytofluorograms from swab samples taken at the back of the throat a) before and b) after sleep from one healthy volunteer. An increase in both bacteria and VLP abundance can be seen after sleep.

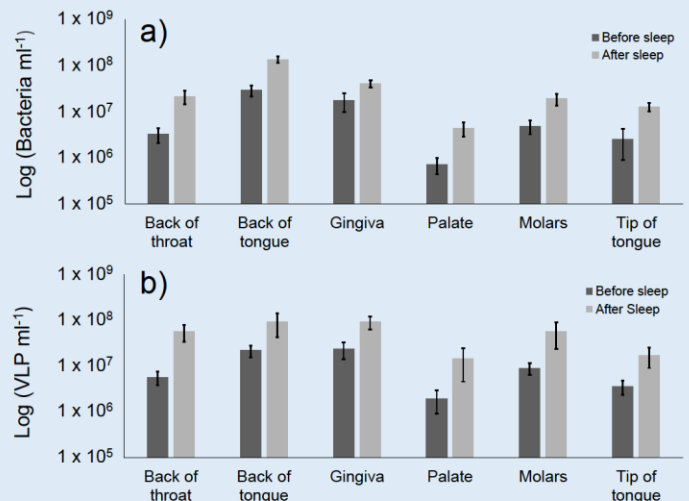


Figure 2: Average abundances of a) bacteria ml⁻¹ and b) VLP ml⁻¹ at various locations within the oral cavity. Error bars represent the standard error of the mean.

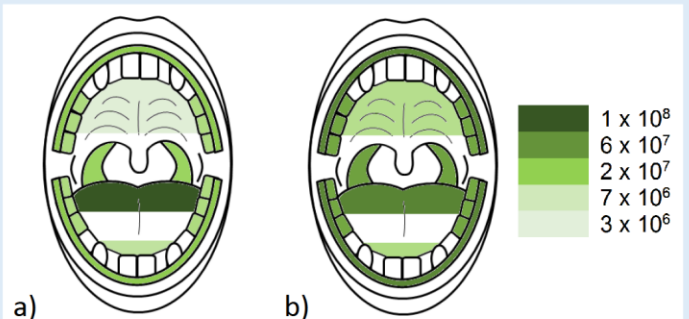


Figure 3: Heat maps showing the average increase in a) bacteria ml⁻¹ and b) VLP ml⁻¹ after sleep at sampled locations.

- Significant increase in both bacteria and VLP for all locations after sleep ($p < 0.05$)

Conclusions

Flow cytometry can be used as a tool to enumerate bacteria and VLPs from oral swab samples

The back of the tongue and gingiva have the highest abundances of bacteria and VLPs

The palate and tip of tongue have the lowest abundances of bacteria and VLPs

There is an average increase in the abundance of bacteria and VLP by 1000% during sleep

Bacterial abundances in the oral cavity can increase by a count of up to 100 million during sleep

References

- Dewhirst et al. (2010) Journal of bacteriology. 192(19):5002-17
- Human Microbiome Project (2012) Nature. 486(7402):207-14.
- Xu et al. (2014) Environmental Microbiology. n/a-n/a.
- Aas et al. (2005) J Clin Microbiol. 43(11):5721-32.
- Humphrey et al (2001) The Journal of prosthetic dentistry. 85(2):162-9.
- Schneyer et al. (1956) Journal of dental research. 35(1):109-14.
- Marie D et al. (1999) Appl Environ Microbiol. 65(1):45-52.
- Brussaard et al. (2004) Applied and environmental microbiology. 70(3):1506-13.
- Robertson et al (1989) Cytometry. 10(1):70-6.
- Carlson-Jones et al. (2016) PloS one. 11(5):e0155003

Email: jessica.carlsonjones@flinders.edu.au

Ethics: REC2495/3/16(HREC/12/WCHN/52;SSA/12/WCH/53)

Chapter 4

THE MICROBIAL ABUNDANCE DYNAMICS OF THE HUMAN ORAL CAVITY BEFORE AND AFTER SLEEP

Contribution to publication: Conceived and designed the experiments, performed the experiments, analysed the data, contributed reagents/materials/analysis tools and wrote the publication.

Research Design: 80%

Data collection and analysis: 100%

Writing and editing: 80%

Abstract

Microhabitats in the oral cavity provide a variety of surfaces for colonisation of microbial communities. These include the teeth, gingivae, tongue, palate and temporomandibular joint. Recent focus has been on oral microbial taxonomy, characterising oral microhabitats. However, the bacterial and viral abundances are unknown. In this study, bacterial and virus-like particle (VLP) abundances in 10 healthy children were enumerated using flow cytometry before and after sleep. Bacterial counts in the oral cavity ranged from $7.2 \pm 2.8 \times 10^5$ bacteria at the palate before sleep to $1.3 \pm 0.2 \times 10^8$ bacteria at the back of the tongue after sleep, a range difference of 187 times. VLPs changed by a difference of 48 times with counts ranging from $1.9 \pm 1.0 \times 10^6$ VLP at the palate before sleep to $9.2 \pm 5.0 \times 10^7$ VLP at the back of the tongue after sleep. A significant increase in bacterial and VLP abundances was observed for all locations after sleep ($p < 0.05$). Here, we show that the oral cavity is a dynamic numerically heterogeneous microbial environment where bacteria and VLPs can increase by a count of 100 million and 70 million cells and particles respectively during sleep. Quantification of the paediatric oral microbiome complements taxonomic diversity information to show how biomass varies and shifts in space and time.

Introduction

The human body has many ecological habitats, each with their own unique environment. Within each of these habitats are complex ecosystems of coexisting microbial communities [1]. These microbial communities are collectively referred to as the human microbiome. One area that has been extensively investigated is the oral cavity [1-3]. The oral cavity contains multiple microhabitats [1, 4, 5]. These include the tongue, palate, cheek, lip, gingivae and teeth with each area differing in their surface structure, thereby providing unique microbial habitats for the colonisation of distinct microbial communities [3, 5]. Recent taxonomic studies have begun to focus on defining the oral microbiome by these various microhabitats [5, 6]. This enables a well characterised analysis of possible disease sites in the oral cavity and allows for a more focused analysis of the oral microbiome in health and disease [7, 8]. However, the absolute bacterial and viral abundance dynamics of these microhabitats are still relatively unknown.

One tool used for monitoring microbial dynamics and population abundances is flow cytometry. Used for decades in monitoring microbial dynamics in environmental samples [9-11] and more recently in medical samples [12], flow cytometry provides an inexpensive way to rapidly enumerate cells and particles within a sample. As the majority of bacteria are non-culturable, flow cytometry provides a rapid, culture-free enumeration alternative that eliminates enrichment biases culturing introduces [9]. This highly reproducible technique also produces counts of virus-like particles (VLPs) at concentrations that would be too low for epifluorescence and transmission electron microscopy [9]. Flow cytometric absolute abundances adds a new dimension to microbial community analysis compared to relative abundances. It allows for

comparison across studies to determine not just the presence or absence of a potential pathogen, but assessment of whether critical concentrations are required for pathogenesis and what those concentrations are [13]. We seek to ultimately answer where the balance lies between bacterial community composition and bacterial community absolute abundance in causing and reacting to pathologies. The first step is to be able to measure absolute abundance, which frequently applied sequencing techniques are unable to do [13, 14].

During sleep, the microbial dynamics of the oral cavity changes due to shifts in environmental conditions, such as saliva flow, pH and oxygen distribution [6, 15-17]. In this study we investigate the changes in absolute microbial abundance in the healthy oral cavity of children during sleep. Samples were collected from 6 microhabitats in the oral cavity before and after sleep in 10 healthy children. Using flow cytometry as a method of enumeration, the absolute bacterial and VLP abundance distributions of the oral cavity were accessed. Therefore, the objective of this study was to measure the microhabitat microbial dynamics in the paediatric oral cavity and what impact sleep has on those dynamics.

Materials and methods

Ethics statement

Participants in this study were a subgroup of healthy, control children from a larger study investigating the effects of sleep disordered breathing on development, which was approved by the Human Research Ethics Committees of the Women's and Children's Hospital and the University of Adelaide, South Australia. The study has been conducted in accordance with the 1964 Declaration of Helsinki and its later amendments. Parents of participants provided written consent and children written assent for involvement in the study. Parents also completed a child's health and behaviour questionnaire prior to sample collection.

Sample collection

Samples were collected from 10 children (male $n = 7$, female $n = 3$) undergoing an overnight polysomnography sleep test at the Women's and Children's Hospital, Adelaide, Australia. Participants involved in the study were asked to refrain from oral hygiene practices, such as brushing teeth or antimicrobial rinses, for the duration of the study. Ages ranged from 6.08 to 16.58 years (mean 10.3 ± 1.2 years). The average BMI for all participants was 20.1 ± 1.8 .

Sterile rayon swabs (Copan, Brescia, Italy; product code: 155C) were used to collect samples from participants. These swabs were individually packaged in their own sterile polypropylene tube. Each swab was approximately 5 mm in diameter and had a 13.3 cm plastic shaft to allow for precise sampling. Swab samples were always collected from the left temporomandibular joint, the middle of the back of the tongue, the occlusal site of the last two distal molars on the bottom jaw on the right side, the

gingival margin of the last proximal molar on the right lower jaw, the middle of the palate and the middle of the tip of the tongue. These samples will be referred to in this article as temporomandibular joint, back of tongue, molars, gingivae, palate and tip of tongue respectively. These samples were taken just before lights out between 8.30-9.00 pm, referred to as before sleep, and immediately on waking the following day between 6.00-6.30 am, referred to as after sleep. Each swab was rotated clockwise 6 times at each location for sample collection. All participants' samples were collected by the same researcher at the same locations before and after sleep using the same sampling technique described. Once the swab samples were collected they were immediately placed back into the polypropylene tube and stored at -80°C until flow cytometric analysis.

Sample preparation

Swab samples were thawed at room temperature immediately prior to sample preparation. Once thawed, swab tips were cut off into 1 ml of sterile (0.2 µm filtered and UV treated) TE buffer (10 mM Tris, 1 mM EDTA, pH 7.4, Sigma). Samples were then vortexed for 3 minutes to elute the bacteria and viruses from the swab tip.

Eluted swab samples were diluted (1:100) in 0.2 µm filtered TE buffer for optimal visualisation of bacterial and VLP populations. Diluted samples were then stained with SYBR-I Green (1:20,000 final dilution; Molecular Probes) and incubated for 10 minutes in the dark at 80°C [10]. Control samples of sterile rayon swabs eluted in sterile TE buffer were prepared in the same manner as the participant swab samples. These samples were used to eliminate any background artefacts introduced during sample preparation or from the rayon swabs themselves. Triplicates of each swab sample were prepared for analysis (S1-S4 Tables).

Fluorescent beads (1 μm , Molecular Probes) were added to each sample at a concentration of 10^5 beads ml^{-1} [18]. Using the bead fluorescence and concentration as a control, flow cytometric parameters were normalised [18].

Flow cytometric analysis

Bacterial and VLP populations from the oral swab samples were identified and enumerated using a FACSCanto II flow cytometer (Becton Dickinson) fitted with a blue (488 nm, 20 mW) laser. Green fluorescence, side angle light scatter and forward angle light scatter were recorded for all samples. Phosphate-buffered saline was used as sheath fluid for the duration of the study.

Bacterial and VLP populations were analysed and enumerated using FlowJo software (Tree Star, Inc). SYBR Green fluorescence and side scatter were used to differentiate between bacterial and VLP populations [9, 10, 19]. For consistency among participants, one bacterial population and one VLP population were compared and analysed (Fig 1).

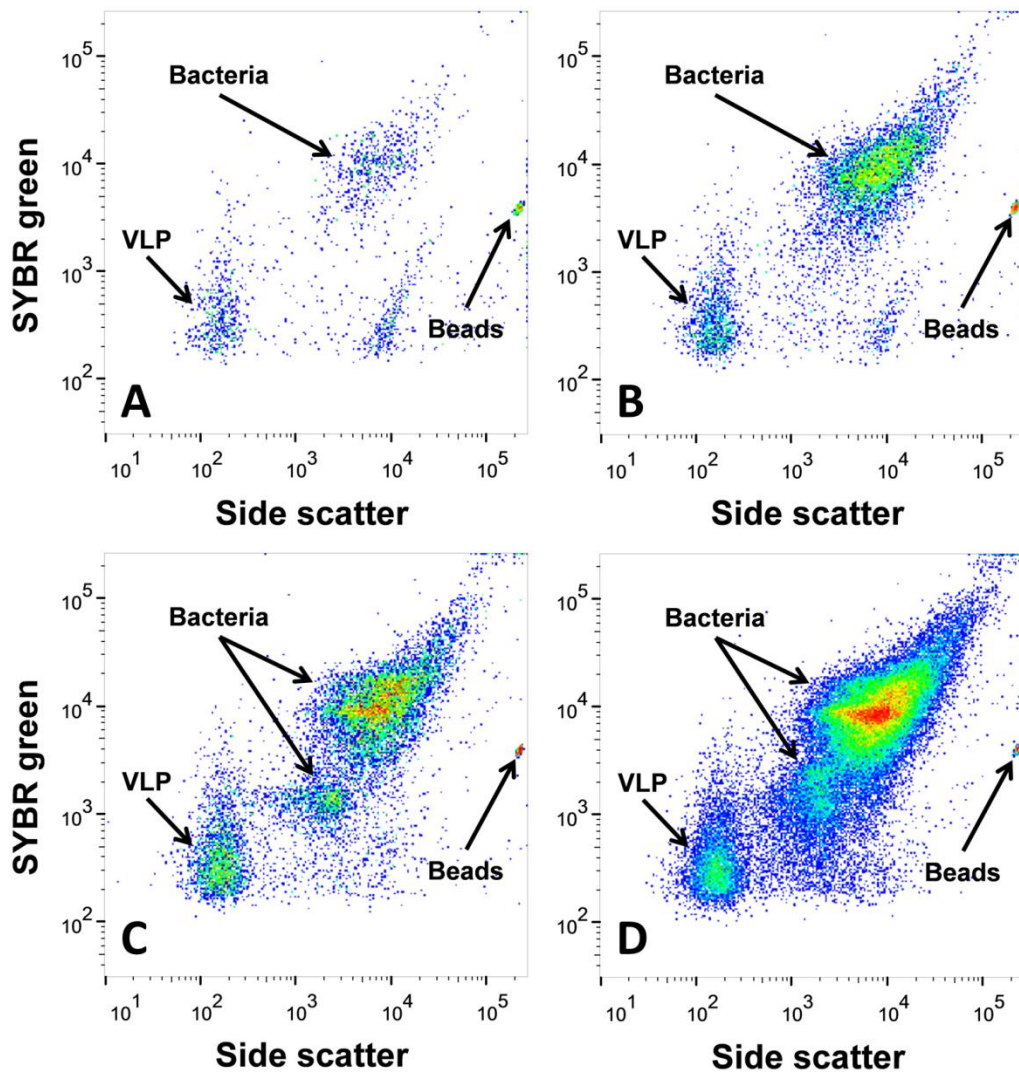


Fig 1. Flow cytometric identification of bacterial and VLP populations. Representative cytograms from one participant showing the bacterial and VLP populations at (A) the tip of the tongue before sleep (B) the tip of the tongue after sleep (C) the back of the tongue before sleep and (D) the back of the tongue after sleep. Bacterial and VLP abundances increased after sleep. Differences in bacterial and VLP abundances can also be seen between both sample locations.

Data analysis

Mann-Whitney U and Wilcoxon sign rank tests were run on the average participant bacterial and VLP concentrations using the program MATLAB (MathWorks, Natick, Massachusetts, United States). The p values calculated were corrected using the multiple comparisons hypothesis for false discovery [20]. Statistical significance was considered when $p < 0.05$. Cytoscape (version 3.5.1, <http://www.cytoscape.org/>) was used to create and visualise $p < 0.05$ filtered Pearson correlation coefficient networks for bacteria and VLPs both before and after sleep [21].

Results

Flow cytometric analysis

Bacterial and VLP populations were present in all sampled locations before and after sleep (an example is shown in Fig 1). For most participants, there was an increase in bacterial and VLP populations after sleep through visualisation of the cytograms (Fig 1). This observation was confirmed through calculations of the average counts of both bacteria and VLP populations before and after sleep (Tables 1 and 2; S5-S8 Tables).

Table 1. Average bacterial abundances within the paediatric oral cavity. Error represents the standard error of the mean (SEM). Wilcoxon sign rank tests p values were corrected for false discovery rates. Percentage increases were calculated by taking an average of each participant's percentage increase/decrease in bacteria for each location.

Sample location	Bacteria before sleep (± SEM)	Bacteria after sleep (± SEM)	Average increase in bacteria (± SEM)	Percentage increase (± SEM)	p value
Temporomandibular joint	3.3 x 10 ⁶ (1.2 x 10 ⁶)	2.1 x 10 ⁷ (7.0 x 10 ⁶)	1.8 x 10 ⁷ (6.3 x 10 ⁶)	2098% (1464%)	0.0025
Back of tongue	2.9 x 10 ⁷ (7.6 x 10 ⁶)	1.3 x 10 ⁸ (2.0 x 10 ⁷)	1.1 x 10 ⁸ (2.2 x 10 ⁷)	764% (290%)	0.0032
Gingivae	1.7 x 10 ⁷ (7.7 x 10 ⁶)	4.1 x 10 ⁷ (7.6 x 10 ⁶)	2.3 x 10 ⁷ (8.6 x 10 ⁶)	784% (445%)	0.0056
Palate	7.2 x 10 ⁵ (2.8 x 10 ⁵)	4.3 x 10 ⁶ (1.5 x 10 ⁶)	3.6 x 10 ⁶ (1.4 x 10 ⁶)	1436% (803%)	0.0013
Molars	4.8 x 10 ⁶ (1.6 x 10 ⁶)	1.9 x 10 ⁷ (5.4 x 10 ⁶)	1.4 x 10 ⁷ (5.6 x 10 ⁶)	714% (340%)	0.0012
Tip of tongue	2.6 x 10 ⁶ (1.7 x 10 ⁶)	1.3 x 10 ⁷ (2.8 x 10 ⁶)	1.0 x 10 ⁷ (3.1 x 10 ⁶)	2391% (1226%)	0.0016

Table 2. Average VLP abundances within the paediatric oral cavity. Error represents the standard error of the mean (SEM). Wilcoxon sign rank tests p values were corrected for false discovery rates. Percentage increases were calculated by taking an average of each participant's percentage increase/decrease in VLPs for each location.

Sample location	VLP before sleep (± SEM)	VLP after sleep (± SEM)	Average increase in VLP (± SEM)	Percentage increase (± SEM)	p value
Temporomandibular joint	5.7 x 10 ⁶ (1.9 x 10 ⁶)	5.7 x 10 ⁷ (2.3 x 10 ⁷)	5.1 x 10 ⁷ (2.2 x 10 ⁷)	3638% (3125%)	0.00025
Back of tongue	2.2 x 10 ⁷ (6.3 x 10 ⁶)	9.2 x 10 ⁷ (5.0 x 10 ⁷)	7.0 x 10 ⁷ (4.7 x 10 ⁷)	416% (240%)	0.00018
Gingivae	2.4 x 10 ⁷ (9.5 x 10 ⁶)	9.2 x 10 ⁷ (2.9 x 10 ⁷)	6.8 x 10 ⁷ (2.8 x 10 ⁷)	1614% (963%)	0.00021
Palate	1.9 x 10 ⁶ (1.0 x 10 ⁶)	1.4 x 10 ⁷ (9.9 x 10 ⁶)	1.2 x 10 ⁷ (9.7 x 10 ⁶)	700% (323%)	0.000025
Molars	9.0 x 10 ⁶ (2.6 x 10 ⁶)	5.7 x 10 ⁷ (3.3 x 10 ⁷)	4.8 x 10 ⁷ (3.1 x 10 ⁷)	662% (180%)	0.00016
Tip of tongue	3.6 x 10 ⁶ (1.2 x 10 ⁶)	1.7 x 10 ⁷ (8.2 x 10 ⁶)	1.4 x 10 ⁷ (8.4 x 10 ⁶)	2083% (1911%)	0.00020

Oral cavity bacterial abundance heterogeneity before sleep

The Mann-Whitney U test was used to compare average bacterial abundances between samples before sleep to identify regions of heterogeneity in the oral cavity (Fig 2). No significant difference in bacterial abundances were detected between the back of the tongue ($2.9 \pm 0.8 \times 10^7$ bacteria) and gingivae ($1.7 \pm 0.8 \times 10^7$ bacteria) before sleep ($p > 0.05$) (Table 1; Fig 2). These two areas had the highest average bacterial counts, with participant averages ranging from 5.3×10^5 (gingivae) to 8.7×10^7 (back of tongue) bacteria (S5 Table). Both the back of the tongue and gingivae were found to have bacterial abundances significantly higher than the temporomandibular joint ($p = 0.0018$ and $p = 0.016$), palate ($p = 0.0015$ and $p = 0.0012$), molars ($p = 0.0021$ and $p = 0.031$) and tip of the tongue ($p = 0.0012$ and 0.0062) respectively (Table1; Fig 2). The palate was the area in the mouth with the lowest bacterial abundances before sleep with participant's averages ranging from 8.4×10^4 to 2.2×10^6 bacterial with an overall group average of $7.2 \pm 2.8 \times 10^5$ bacteria (Table 1; S5 Table). Although not significantly different to the tip of the tongue ($p > 0.05$), the palate was found to be significantly lower in bacterial abundance than the molars ($p = 0.0059$) and the temporomandibular joint ($p = 0.0068$) (Table 1; Fig 2). All other locations when compared to one another were not significantly different ($p > 0.05$) (Fig 2). Overall, there was approximately a 2.8×10^7 abundance difference between the locations with the highest and lowest bacterial counts before sleep.

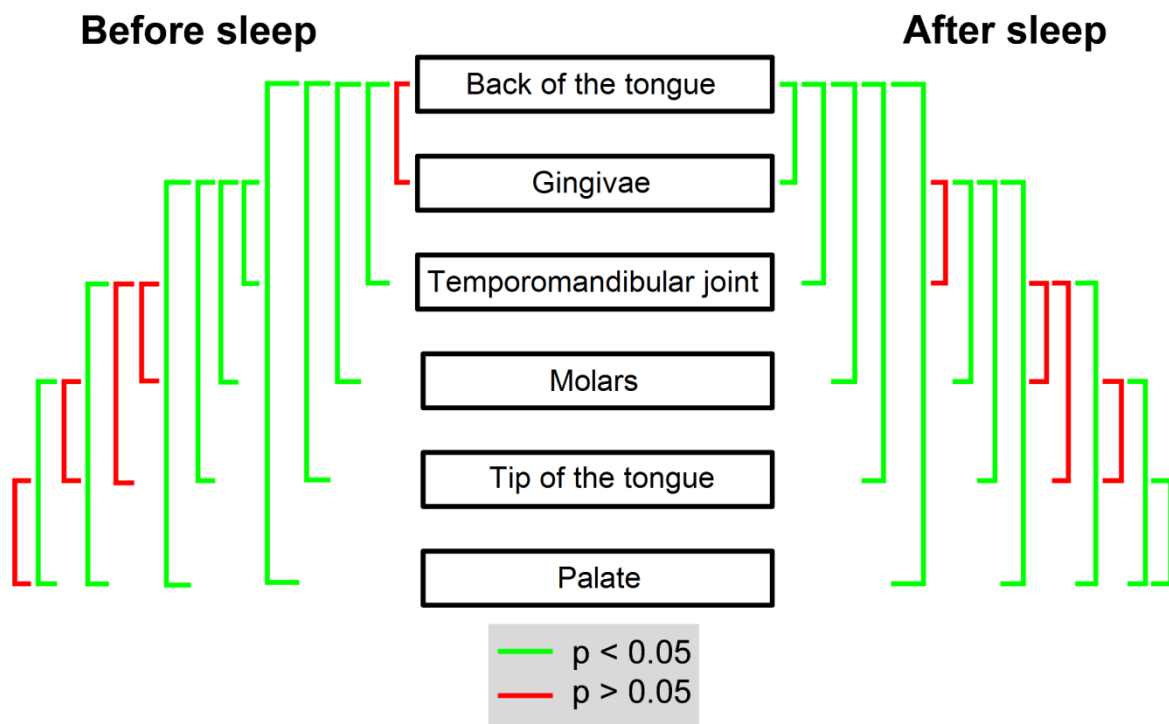


Fig 2. Mann-Whitney U tests for bacterial heterogeneity in the oral cavity before and after sleep. Significant differences between locations are shown in green ($p < 0.05$). Non-significant differences are shown in red ($p > 0.05$). Mann-Whitney U test comparisons have been corrected for false discovery rates.

Oral cavity bacterial abundance heterogeneity after sleep

The back of the tongue was the location with the highest bacterial abundances after sleep with participant's averages ranging from 4.0×10^7 to 2.1×10^8 bacteria with an overall group average of $1.3 \pm 0.2 \times 10^8$ bacteria (Table 1; S6 Table). The back of the tongue also had significantly higher abundances after sleep when compared to all other locations (temporomandibular joint $2.1 \pm 0.7 \times 10^7$, $p = 0.00088$; gingivae $4.1 \pm 0.8 \times 10^7$, $p = 0.0028$; palate $4.3 \pm 1.5 \times 10^6$, $p = 0.0018$; molars $1.9 \pm 0.5 \times 10^7$, $p = 0.00061$ and tip of tongue $1.3 \pm 0.3 \times 10^7$, $p = 0.00091$) (Table 1; Fig 2). The gingivae had significantly higher bacterial abundances after sleep than the molars ($p = 0.016$), the tip of the tongue ($p = 0.0051$) and the palate ($p = 0.00061$) (Table 1; Fig 2). The palate was the location with significantly lower counts of bacteria after sleep with participant averages ranging from 3.6×10^5 to 1.4×10^7 and an overall group average of $4.3 \pm 1.5 \times 10^6$ bacteria (Table 1; S6 Table). The palate was again significantly lower in abundance than the temporomandibular joint ($p = 0.019$), molars ($p = 0.0072$) and the tip of the tongue ($p = 0.014$) (Table 1; Fig 2). All other paired comparisons between locations were not significantly different ($p > 0.05$) (Fig 2). Overall, there was approximately a 1.3×10^8 range in bacteria after sleep.

Oral cavity VLP abundance heterogeneity before sleep

Less heterogeneity was observed between VLP abundances in the oral cavity before sleep than bacteria before sleep. The back of the tongue ($2.2 \pm 0.6 \times 10^7$ VLP) was found to be significantly higher in VLPs than the temporomandibular joint ($5.7 \pm 1.9 \times 10^6$ VLP; $p = 0.037$), tip of the tongue ($3.6 \pm 1.2 \times 10^6$ VLP; $p = 0.016$) and the palate ($1.9 \pm 1.0 \times 10^6$ VLP; $p = 0.0087$; Table 2; Fig 3). The gingivae ($2.4 \pm 1.0 \times 10^7$ VLP) were also significantly higher in VLP abundance than the tip of the tongue ($p = 0.019$) and the palate ($p = 0.013$; Table 2; Fig 3). All other paired comparisons between oral sites did not show a significant difference ($p > 0.05$; Fig 3). Overall there was a range of 2.2×10^7 VLPs before sleep.

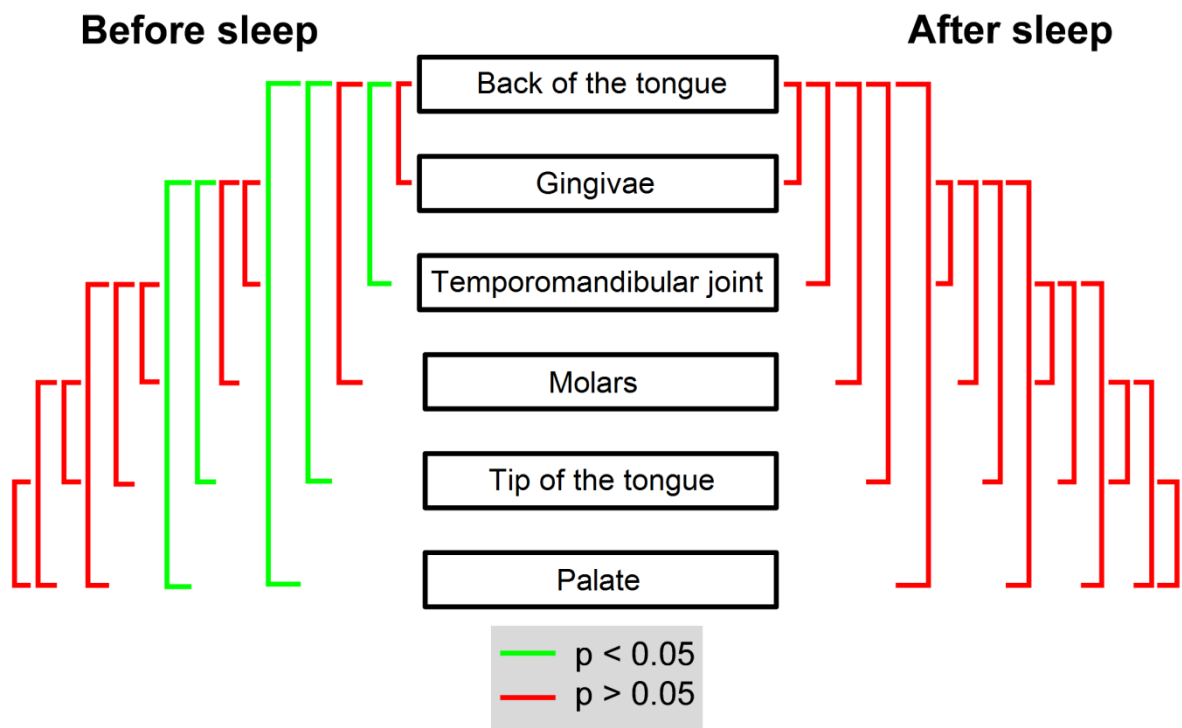


Fig 3. Mann-Whitney U tests for VLP heterogeneity in the oral cavity before and after sleep. Significant differences between locations are shown in green ($p < 0.05$). Non-significant differences are shown in red ($p > 0.05$). Mann-Whitney U test comparisons have been corrected for false discovery rates.

Oral cavity VLP abundance homogeneity after sleep

Homogeneity was observed among the average abundances of VLPs at each sampled location in the oral cavity after sleep ($p > 0.05$) (Table 2; Fig 3). The average VLP abundances after sleep ranged from $1.4 \pm 1.0 \times 10^7$ at the palate to $9.2 \pm 5.0 \times 10^7$ at the back of the tongue (Table 2). Therefore, the average VLP abundance for all locations after sleep was $5.5 \pm 1.2 \times 10^7$.

Bacterial and VLP increases during sleep

Corrected Wilcoxon sign rank test p values revealed that all sampled locations in the oral cavity significantly increased in bacterial and VLP abundances after sleep ($p < 0.05$; Tables 1 and 2; Fig 4). The back of the tongue was the location with the largest increase in bacteria with an overall average count increase of $1.1 \pm 0.2 \times 10^8$ bacteria ($p = 0.0032$; Table 1; Fig 4). This was followed by the gingivae ($p = 0.0056$), temporomandibular joint ($p = 0.0025$), molars ($p = 0.0012$) and tip of tongue ($p = 0.0016$) with average count increases of $2.3 \pm 0.9 \times 10^7$, $1.8 \pm 0.6 \times 10^7$, $1.4 \pm 0.6 \times 10^7$ and $1.0 \pm 0.3 \times 10^7$ bacteria respectively (Table 1; Fig 4). The palate was the location with the lowest average increase in bacteria with $3.6 \pm 1.4 \times 10^6$ bacteria ($p = 0.0013$; Table 1; Fig 4).

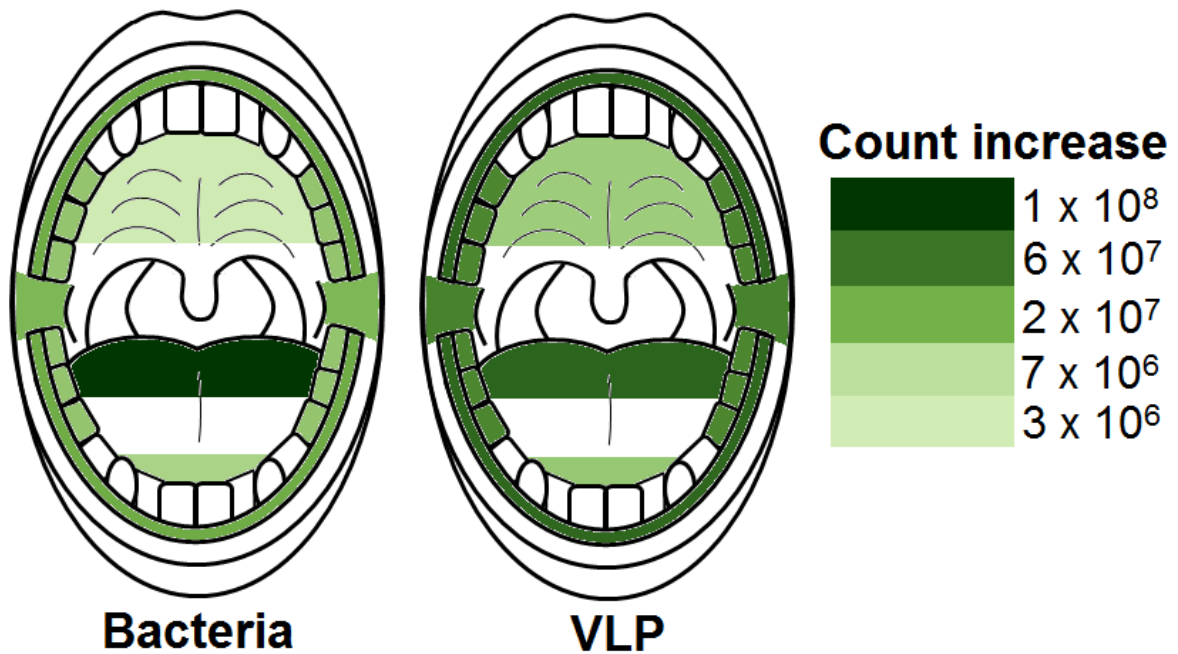


Fig 4. Heat maps showing the average increase in bacteria and VLP after sleep at sampled locations. All sampled oral locations significantly increased in bacteria and VLP during sleep ($p < 0.05$). The back of the tongue was the location that increased the most in both bacteria and VLPs during sleep with counts of $1.1 \pm 0.2 \times 10^8$ and $7.0 \pm 4.7 \times 10^7$ respectively. The palate increased the least in both bacteria and VLP with counts of $3.6 \pm 1.4 \times 10^6$ and $1.2 \pm 1.0 \times 10^7$ respectively.

For VLP, the back of the tongue was also the location with the largest increase with an average count of $7.0 \pm 4.7 \times 10^7$ VLP ($p = 0.00018$; Table 2; Fig 4). This was again followed by the gingivae ($p = 0.00021$), temporomandibular joint ($p = 0.00025$), molars ($p = 0.00016$) and tip of tongue ($p = 0.00020$) with increases of $6.8 \pm 2.8 \times 10^7$, $5.1 \pm 2.2 \times 10^7$, $4.8 \pm 3.1 \times 10^7$ and $1.4 \pm 0.8 \times 10^7$ VLP respectively (Table 2; Fig 4). The palate was also the location with the lowest average increase in VLP with $1.2 \pm 1.0 \times 10^7$ VLP ($p < 0.0001$; Table 2; Fig 4).

The largest percentage increases in bacteria were reported at the tip of the tongue and the temporomandibular joint with 2400% and 2100% increases respectively (Fig 5; Table 1). The gingivae, back of tongue and molars had the lowest percentage increases with 780%, 760% and 710% respectively (Fig 5; Table 1). A similar trend could be observed with the percentage increases for VLPs with the temporomandibular joint and tip of tongue having the highest increases with 3600% and 2100% (Fig 5; Table 2). The back of the tongue had the lowest VLP percentage increase with 420% (Fig 5; Table 2).

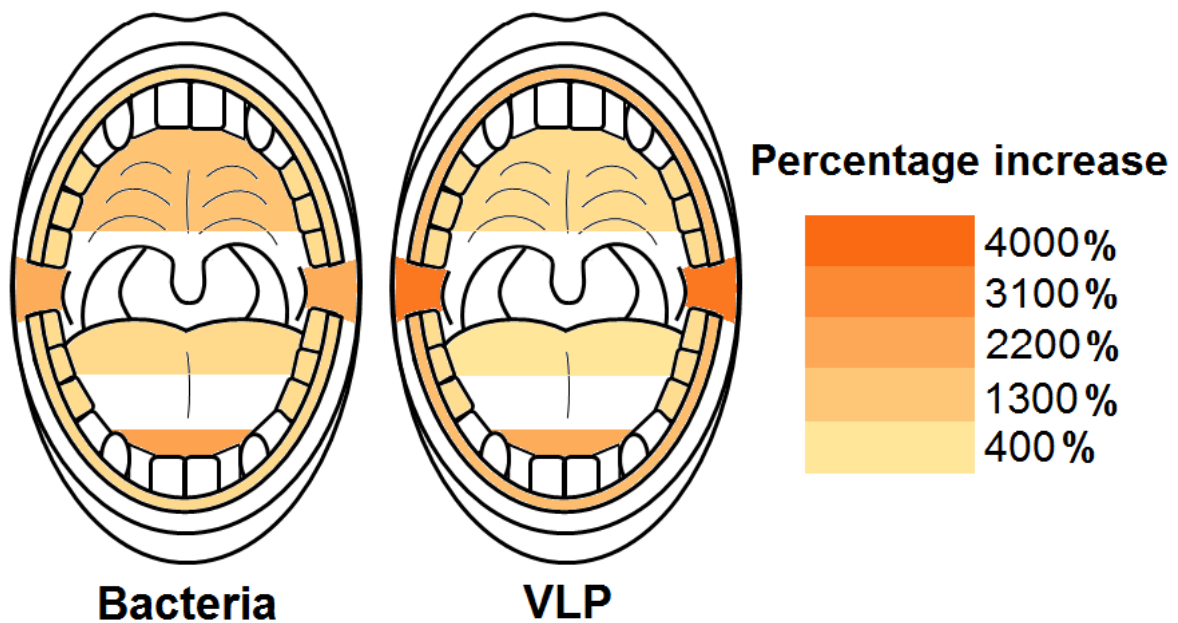


Fig 5. Heat maps showing the average percentage increase in bacteria and VLP after sleep at sampled locations. The molars, back of the tongue and gingivae were the locations with the lowest bacterial percentage increase during sleep (714%, 764% and 784% respectively). Likewise, the back of the tongue also had the lowest VLP percentage increase (416%). The tip of the tongue was the area with the highest bacterial percentage increase (2391%) and the temporomandibular joint the highest VLP percentage increase (3638%).

Bacterial and VLP network analysis

Pearson correlation coefficient bacterial abundance interaction network analysis before sleep revealed 9 connections between the 6 sampled locations, the strongest being between the gingivae and the temporomandibular joint (0.91) (Fig 6A). The palate was the only node connected to all other sample sites before sleep (Fig 6A). After sleep, the bacterial network breaks down with the gingivae no longer part of the abundance network (Fig 6B). The 5 connections seen in the network are no longer as strongly correlated compared to before sleep (Fig 6B). However, the correlation between the temporomandibular joint and the palate remains as strong as before. A new correlation is also formed between the molars and the temporomandibular joint (0.53) (Fig 6B). The palate is again the location with the greatest number of connections, this time with only 3. The strongest correlation in bacterial abundance after sleep was between the palate and the temporomandibular joint (0.73) (Fig 6B).

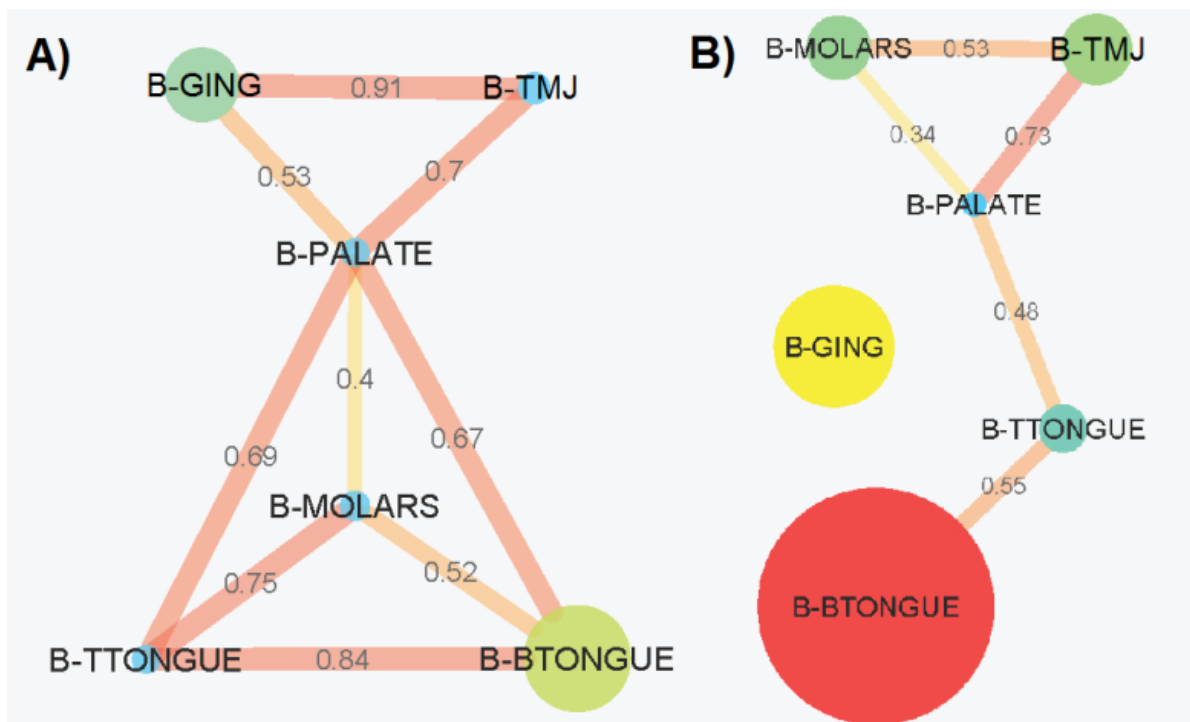


Fig 6. Pearson correlation coefficient bacterial abundance networks ($p < 0.05$ filtered). Networks show the Pearson correlations between bacterial abundances for all samples locations (A) before sleep and (B) after sleep. The wider and warmer the colour of the edge, the stronger the Pearson correlation coefficient. The colour and size of the nodes corresponds to the abundance of bacteria. B-GING = bacteria at the gingivae, B-TMJ = bacteria at the temporomandibular joint, B-PALATE = bacteria at the palate, B-MOLARS = bacteria at the molars, B-TTONGUE = bacteria at the tip of the tongue and B-BTONGUE = bacteria at the back of the tongue.

Eleven connections were observed in the Pearson correlation coefficient VLP abundance network before sleep, 5 of which were from all locations connecting with the back of the tongue (Fig 7A). The strongest correlation was between the molars and the tip of the tongue (0.84). Like with bacteria, the VLP network after sleep also broke down with fewer connections observed (Fig 7B). However, most of the correlations after sleep that are present remained strong. The correlations the back of the tongue has with the molars, palate and temporomandibular joint increased in strength after sleep (Fig 7B). The palate formed new strong correlations between the molars and the temporomandibular joint (Fig 7B). Of the 8 connections after sleep, the correlation between VLP abundances at the palate and the back of the tongue was the strongest (0.99). The gingivae and the temporomandibular joint were the areas with the weakest connection in the network (0.47; Fig 7B). All locations after sleep were correlated to the temporomandibular joint.

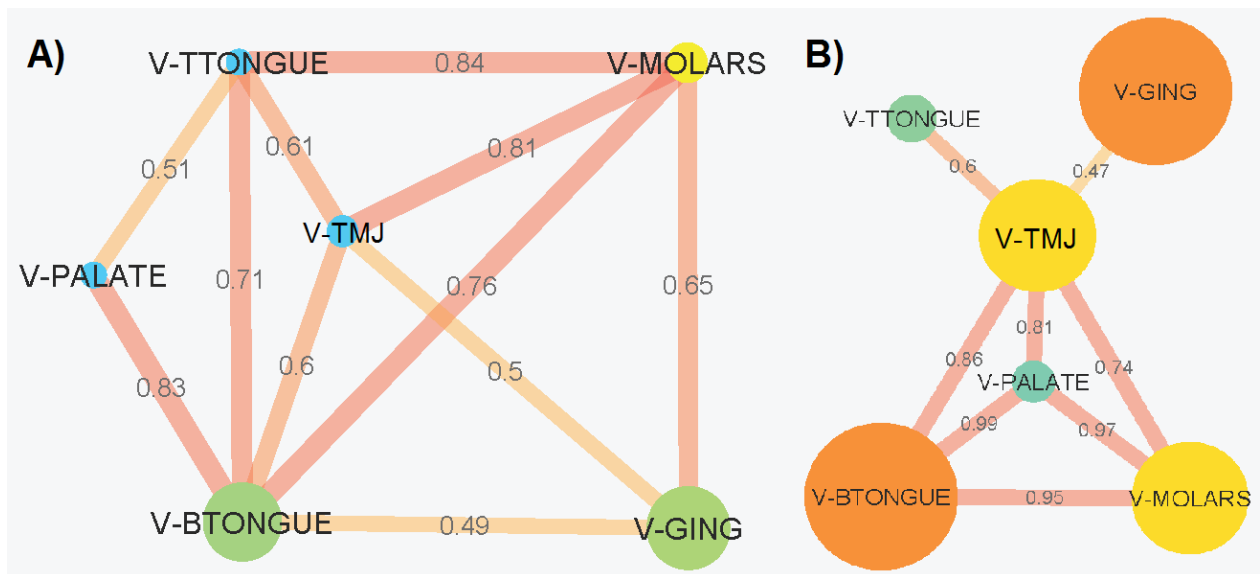


Fig 7. Pearson correlation coefficient VLP abundance networks ($p < 0.05$ filtered). Networks show the Pearson correlations between VLP abundances for all samples locations (A) before sleep and (B) after sleep. The wider and warmer the colour of the edge, the stronger the Pearson correlation coefficient. The colour and size of the nodes corresponds to the abundance of VLPs. V-GING = VLP at the gingivae, V-TMJ = VLP at the temporomandibular joint, V-PALATE = VLP at the palate, V-MOLARS = VLP at the molars, V-TTONGUE = VLP at the tip of the tongue and V-BTONGUE = VLP at the back of the tongue.

Discussion

Here we present the paediatric bacterial and VLP numerical diversity within the oral cavity. Our data shows that the various microhabitats within the oral cavity of healthy children differ in absolute microbial abundances; and increase by counts of up to 10^8 overnight during sleep (Fig 1; Tables 1 and 2). This result suggests that the oral cavity is a dynamic and numerically heterogeneous environment. Here we see that there are large ranges in healthy individual's oral cavities (S5-S8 Tables). These large ranges could indicate that high microbial abundances may not be indicative of oral related illnesses. This suggests, like taxonomy, microbial abundances are distinct to individuals even at the paediatric age group, where there has been less time for community and abundance divergence.

Regarded as a niche within the human body, the oral cavity contains numerous microhabitats [1, 4, 5]. Most of these microhabitats are lined with mucosal epithelia (i.e. tongue, palate, gingivae and temporomandibular joint) that shed into the saliva bringing with it the microbial rich biofilm [5, 22, 23]. One area sampled in this study expected to be a high shedding environment is the palate. We speculate that the increased friction caused by the rough surface of the tongue on the palate results in a higher rate of mucosal shedding compared to other locations in the oral cavity. Therefore, there is less time between mucosal shedding events for a complex and abundant microbial community on this surface. This makes it a good model for the early development of mouth microbial communities. This is consistent with our finding of lower bacterial and VLP counts at this location compared to other microhabitats (Table 1; Fig 2).

Low abundances of bacteria were also observed at the tip of the tongue (Table 1). These low abundances support previous culture-based studies where lower bacterial colony forming units (CFU) were produced from samples collected from the dorsal anterior of the tongue [24]. As with the palate, the lower abundance values here are expected to be a result of mucosal shedding due to friction at the tip of the tongue through speech and swallowing. It is also the area in the oral cavity most exposed to the external environment. As a result, it is likely a constantly changing environment, for example, changes in moisture content due to breathing through the mouth.

Interestingly, the tongue was also the location in the oral cavity with the highest microbial abundances. Higher bacterial abundances were reported at the back of the tongue before and after sleep (Table 1; Fig 2). This result also supports previous bacterial culture based topographic tongue studies where the highest CFU counts were in the area posterior to the circumvallate papillae [24]. It is likely that the papillae structures at the back of the tongue contribute to these high abundances by providing an environment with a large surface area that encourages microbial growth. The crevasses and fissures formed by these structures trap small food particles and provide refuge for microbes from saliva flow and clearance [24].

Post-nasal drip from the sinuses down the back of the throat to the back of the tongue may also be a contributing factor to the high microbial abundances at the back of the tongue. It is well established that the sinuses are colonised by bacteria and viruses and that these microbes can be found at 'high' concentrations [12, 25, 26]. Previous studies have shown certain strains of sinus bacteria are also found in the lower respiratory tract of newly transplanted lungs [27], suggesting the upper respiratory tract, including the sinuses, act as a microbial inoculant source. Therefore,

it is likely that post-nasal drip facilitates the addition and inoculation of bacteria and viruses from the sinuses to the oral cavity [28]. It is also likely that the mucus from the sinuses provides nutrients in the form of metabolites and proteins for the existing bacterial communities found at the back of the tongue [29].

High abundances of bacteria and VLPs were also found along the gingivae before and after sleep. Collected where the teeth and gums meet, it is possible that these samples consisted of plaque from the teeth as well as gum mucosa. Understanding the microbiology in this area is of significant interest to dental professionals as it is the site of for such oral diseases as dental caries and periodontal disease [30-32]. Plaque build-up on the teeth during the day and at night occurs through the attachment of specific genera of bacteria to the surface of the tooth to form a complex organised multi-genera consortium of microorganisms known as a biofilm [33-35]. This biofilm growth can extend below the gum into the periodontal pocket where it is protected from salivary clearance and daily oral hygiene practices. The periodontal pocket would also provide refuge for trapped food particles, which can be used as nutrients to support microbial growth. However, although some plaque fragments may have been removed, an analysis of the total plaque community in this study is unlikely as plaque is not as easily removed by a swab. Therefore, the microbial abundances presented in this study are ones loosely associated with surfaces that can easily be removed by a swab.

Although bacterial heterogeneity was observed among locations before and after sleep, it was only observed in VLP abundances before sleep (Fig 3). Why VLPs were homogeneous after sleep is beyond the scope of this study. However, it warrants

further investigations into what, if any, factor is controlling viral dispersal in the oral cavity during sleep.

During sleep, all sampled locations in the oral cavity significantly increased in bacteria and VLPs ($p < 0.05$; Figs 4 and 5). These increases may well be explained by differences in saliva secretion rates during the day and at night. Recently it has been shown that salivary flow creates gradients that influence the spatial organisation of the oral microbial communities [46]. It is known that saliva production and flow rate is elevated during the day compared to night during sleep [15, 16, 47, 48]. When food is consumed, predominantly during the day, an increase in saliva production is triggered to start the digestion process [8, 49]. Likewise, increased jaw movement as a result of speech also stimulates an increase in saliva production to lubricate the oral cavity [47]. When deglutition occurs to clear excess saliva or food, epithelial cells lining areas such as the palate, tongue, temporomandibular joint and gum line shed into the saliva taking with it the microbial rich mucosal layer [5, 22, 23]. Similarly, for the non-shedding epithelial surfaces such as the teeth, it is likely small plaque biofilm fragments break off and shed into the saliva. Therefore, during sleep when there is reduced saliva production and deglutition it would be expected that less microbial shedding would occur allowing more time for bacterial and VLP microbial community development.

Saliva also contains mucin molecules that play a role in controlling the microbial communities in the oral cavity due to their antibacterial properties [15, 50-52]. These mucins promote aggregation and removal of oral bacteria [15, 50-52]. Therefore, it could be postulated that when there is a reduction in saliva secretion during sleep, antimicrobial mucins will be at a lower concentration and will therefore result in an

increase in the oral bacteria. Here we show that during sleep oral bacteria significantly increase by up to 10^8 bacteria. Therefore, it is reasonable to suggest that saliva is involved in regulating oral microbial abundance.

Along with its antimicrobial properties, saliva is also involved in the dilution of sugars and buffering acids derived from both microbes and dietary intake [15, 53]. With reduced 'flushing' of saliva through the oral cavity during sleep, it could be postulated that each microbial habitat in the oral cavity becomes more distinct and individualised based on its environment (i.e. pH or nutrient concentrations). This is supported by the breakdown of the bacterial network during sleep (Fig 6). This shows that there are fewer interactions between locations with each area acting more independently. However, although there is also a breakdown in the number of connections between locations for VLP during sleep, the strength of most of the correlations increases (Fig 7). This suggests that unlike bacteria, the VLP in the oral cavity are less likely to be impacted by the individualised conditions of each oral environment. This is again supported by the homogenisation of VLP abundances after sleep (Fig 3).

For this study, the participants involved did not engage in oral hygiene practices before sleep. The reasoning for this was to control for any biases introduced through individuality in the cleaning process. Therefore, it is expected that the abundance profiles generated in this study are on the higher end of the spectrum as plaque and nutrients in the form of trapped food particles that would have typically been removed remained. This too could provide another possible explanation for the significant increases in microbial concentrations.

In conclusion, our results demonstrate that flow cytometry can successfully be used as a tool to enumerate bacteria and VLPs from oral swab samples. Here we show that the oral cavity is a numerically dynamic heterogeneous environment. This further highlights and supports the importance of defining the oral cavity by its various microhabitats rather than as a whole. In addition, the microbial abundances within the oral cavity change over time and counts increase by up to 100 million bacteria and 70 million VLPs during sleep. This demonstrates that the oral cavity is an active bacterial and viral environment during sleep and that changes in oral environmental conditions can have a large impact on the absolute microbial abundances. As the oral microbiome taxonomically changes with each developmental stage of life [5, 54], future studies into the absolute microbial counts at different age groups will assist in identifying if these microbial abundance dynamics are specific to age. Knowledge of the differences in the microbial abundance dynamics of the oral cavity may aid in the diagnosis and the development of personalised treatment options for oral related diseases.

Acknowledgements

We would like to thank the staff at the Flinders Medical Centre Flow Cytometry Unit for their technical support throughout the study.

References

1. Dewhirst FE, Chen T, Izard J, Paster BJ, Tanner AC, Yu WH, et al. The human oral microbiome. *Journal of bacteriology*. 2010;192(19):5002-17. doi: 10.1128/JB.00542-10. PubMed PMID: 20656903; PubMed Central PMCID: PMC2944498.

2. Bik EM, Long CD, Armitage GC, Loomer P, Emerson J, Mongodin EF, et al. Bacterial diversity in the oral cavity of 10 healthy individuals. *Isme J.* 2010;4(8):962-74. doi: 10.1038/ismej.2010.30. PubMed PMID: 20336157; PubMed Central PMCID: PMC2941673.
3. Aas JA, Paster BJ, Stokes LN, Olsen I, Dewhirst FE. Defining the normal bacterial flora of the oral cavity. *J Clin Microbiol.* 2005;43(11):5721-32. doi: 10.1128/JCM.43.11.5721-5732.2005. PubMed PMID: 16272510; PubMed Central PMCID: PMC1287824.
4. Human Microbiome Project C. Structure, function and diversity of the healthy human microbiome. *Nature.* 2012;486(7402):207-14. doi: 10.1038/nature11234. PubMed PMID: 22699609; PubMed Central PMCID: PMC3564958.
5. Xu X, He J, Xue J, Wang Y, Li K, Zhang K, et al. Oral cavity contains distinct niches with dynamic microbial communities. *Environ Microbiol.* 2015;17(3):699-710. Epub 2014/05/08. doi: 10.1111/1462-2920.12502. PubMed PMID: 24800728.
6. Simon-Soro A, Tomas I, Cabrera-Rubio R, Catalan MD, Nyvad B, Mira A. Microbial geography of the oral cavity. *Journal of dental research.* 2013;92(7):616-21. doi: 10.1177/0022034513488119. PubMed PMID: 23674263.
7. Nyvad B, Crielaard W, Mira A, Takahashi N, Beighton D. Dental caries from a molecular microbiological perspective. *Caries research.* 2013;47(2):89-102. doi: 10.1159/000345367. PubMed PMID: 23207320.
8. Wade WG. The oral microbiome in health and disease. *Pharmacological research.* 2013;69(1):137-43. doi: 10.1016/j.phrs.2012.11.006. PubMed PMID: 23201354.
9. Marie D, Brussaard CPD, Thyraug R, Bratbak G, Vaulot D. Enumeration of marine viruses in culture and natural samples by flow cytometry. *Appl Environ*

Microbiol. 1999;65(1):45-52. PubMed PMID: 9872758; PubMed Central PMCID: PMC90981.

10. Brussaard CP. Optimization of procedures for counting viruses by flow cytometry. *Applied and environmental microbiology*. 2004;70(3):1506-13. PubMed PMID: 15006772; PubMed Central PMCID: PMC368280.

11. Robertson BR, Button DK. Characterizing aquatic bacteria according to population, cell size, and apparent DNA content by flow cytometry. *Cytometry*. 1989;10(1):70-6. doi: 10.1002/cyto.990100112. PubMed PMID: 2465113.

12. Carlson-Jones JA, Paterson JS, Newton K, Smith RJ, Dann LM, Speck P, et al. Enumerating Virus-Like Particles and Bacterial Populations in the Sinuses of Chronic Rhinosinusitis Patients Using Flow Cytometry. *PloS one*. 2016;11(5):e0155003. doi: 10.1371/journal.pone.0155003. PubMed PMID: 27171169.

13. Props R, Kerckhof FM, Rubbens P, De Vrieze J, Hernandez Sanabria E, Waegeman W, et al. Absolute quantification of microbial taxon abundances. *Isme J*. 2017;11(2):584-7. doi: 10.1038/ismej.2016.117. PubMed PMID: 27612291; PubMed Central PMCID: PMC5270559.

14. Widder S, Allen RJ, Pfeiffer T, Curtis TP, Wiuf C, Sloan WT, et al. Challenges in microbial ecology: building predictive understanding of community function and dynamics. *Isme J*. 2016;10(11):2557-68. doi: 10.1038/ismej.2016.45. PubMed PMID: 27022995; PubMed Central PMCID: PMC5113837 declare no conflict of interest.

15. Humphrey SP, Williamson RT. A review of saliva: normal composition, flow, and function. *The Journal of prosthetic dentistry*. 2001;85(2):162-9. doi: 10.1067/mpr.2001.113778. PubMed PMID: 11208206.

16. Schneyer LH, Pigman W, Hanahan L, Gilmore RW. Rate of flow of human parotid, sublingual, and submaxillary secretions during sleep. *Journal of dental research*. 1956;35(1):109-14. PubMed PMID: 13286394.
17. Choi JE, Waddell JN, Lyons KM, Kieser JA. Intraoral pH and temperature during sleep with and without mouth breathing. *J Oral Rehabil*. 2016;43(5):356-63. doi: 10.1111/joor.12372. PubMed PMID: WOS:000374339900005.
18. Gasol JM, Del Giorgio PA. Using flow cytometry for counting natural planktonic bacteria and understanding the structure of planktonic bacterial communities. *Sci Mar*. 2000;64(2):197-224. PubMed PMID: ISI:000088019800007.
19. Marie D, Partensky F, Jacquet S, Vaultot D. Enumeration and Cell Cycle Analysis of Natural Populations of Marine Picoplankton by Flow Cytometry Using the Nucleic Acid Stain SYBR Green I. *Appl Environ Microbiol*. 1997;63(1):186-93. PubMed PMID: 16535483; PubMed Central PMCID: PMC1389098.
20. Storey JD. A direct approach to false discovery rates. *J Roy Stat Soc B*. 2002;64:479-98. doi: Unsp 1369-7412/02/64479
Doi 10.1111/1467-9868.00346. PubMed PMID: WOS:000177425500009.
21. Shannon P, Markiel A, Ozier O, Baliga NS, Wang JT, Ramage D, et al. Cytoscape: a software environment for integrated models of biomolecular interaction networks. *Genome research*. 2003;13(11):2498-504. doi: 10.1101/gr.1239303. PubMed PMID: 14597658; PubMed Central PMCID: PMC403769.
22. Li Y, Ku CY, Xu J, Saxena D, Caufield PW. Survey of oral microbial diversity using PCR-based denaturing gradient gel electrophoresis. *Journal of dental research*. 2005;84(6):559-64. PubMed PMID: 15914595.
23. Fabian TK, Fejerdy P, Csermely P. Salivary Genomics, Transcriptomics and Proteomics: The Emerging Concept of the Oral Ecosystem and their Use in the Early

Diagnosis of Cancer and other Diseases. *Curr Genomics*. 2008;9(1):11-21. doi: 10.2174/138920208783884900. PubMed PMID: 19424479; PubMed Central PMCID: PMC2674305.

24. Allaker RP, Waite RD, Hickling J, North M, McNab R, Bosma MP, et al. Topographic distribution of bacteria associated with oral malodour on the tongue. *Archives of oral biology*. 2008;53 Suppl 1:S8-S12. doi: 10.1016/S0003-9969(08)70003-7. PubMed PMID: 18460402.

25. Jiang RS, Liang KL, Jang JW, Hsu CY. Bacteriology of endoscopically normal maxillary sinuses. *The Journal of laryngology and otology*. 1999;113(9):825-8. PubMed PMID: 10664686.

26. Wilson MT, Hamilos DL. The nasal and sinus microbiome in health and disease. *Current allergy and asthma reports*. 2014;14(12):485. doi: 10.1007/s11882-014-0485-x. PubMed PMID: 25342392.

27. Ciofu O, Johansen HK, Aanaes K, Wassermann T, Alhede M, von Buchwald C, et al. *P. aeruginosa* in the paranasal sinuses and transplanted lungs have similar adaptive mutations as isolates from chronically infected CF lungs. *Journal of cystic fibrosis : official journal of the European Cystic Fibrosis Society*. 2013;12(6):729-36. doi: 10.1016/j.jcf.2013.02.004. PubMed PMID: 23478131.

28. Whiteson KL, Bailey B, Bergkessel M, Conrad D, Delhaes L, Felts B, et al. The Upper Respiratory Tract as a Microbial Source for Pulmonary Infections in Cystic Fibrosis: Parallels from Island Biogeography. *Am J Resp Crit Care*. 2014;189(11):1309-15. doi: 10.1164/rccm.201312-2129PP. PubMed PMID: WOS:000336823200007.

29. Armstrong SK. Bacterial Metabolism in the Host Environment: Pathogen Growth and Nutrient Assimilation in the Mammalian Upper Respiratory Tract.

Microbiology spectrum. 2015;3(3). doi: 10.1128/microbiolspec.MBP-0007-2014. PubMed PMID: 26185081.

30. Simon-Soro A, Mira A. Solving the etiology of dental caries. Trends in microbiology. 2015;23(2):76-82. doi: 10.1016/j.tim.2014.10.010. PubMed PMID: 25435135.

31. Aas JA, Griffen AL, Dardis SR, Lee AM, Olsen I, Dewhirst FE, et al. Bacteria of dental caries in primary and permanent teeth in children and young adults. J Clin Microbiol. 2008;46(4):1407-17. doi: 10.1128/Jcm.01410-07. PubMed PMID: WOS:000254866400038.

32. Hajishengallis G, Lamont RJ. Beyond the red complex and into more complexity: the polymicrobial synergy and dysbiosis (PSD) model of periodontal disease etiology. Molecular oral microbiology. 2012;27(6):409-19. doi: 10.1111/j.2041-1014.2012.00663.x. PubMed PMID: 23134607; PubMed Central PMCID: PMC3653317.

33. Mark Welch JL, Rossetti BJ, Rieken CW, Dewhirst FE, Borisy GG. Biogeography of a human oral microbiome at the micron scale. Proc Natl Acad Sci U S A. 2016;113(6):E791-800. doi: 10.1073/pnas.1522149113. PubMed PMID: 26811460; PubMed Central PMCID: PMC4760785.

34. Zijng V, van Leeuwen MB, Degener JE, Abbas F, Thurnheer T, Gmur R, et al. Oral biofilm architecture on natural teeth. Plos One. 2010;5(2):e9321. Epub 2010/03/03. doi: 10.1371/journal.pone.0009321. PubMed PMID: 20195365; PubMed Central PMCID: PMCPMC2827546.

35. Dige I, Gronkjaer L, Nyvad B. Molecular studies of the structural ecology of natural occlusal caries. Caries research. 2014;48(5):451-60. Epub 2014/05/24. doi: 10.1159/000357920. PubMed PMID: 24852305.

36. Pride DT, Salzman J, Haynes M, Rohwer F, Davis-Long C, White RA, et al. Evidence of a robust resident bacteriophage population revealed through analysis of the human salivary virome. *ISME J.* 2012;6(5):915-26. doi: 10.1038/ismej.2011.169. PubMed PMID: WOS:000302950700002.
37. Abeles SR, Pride DT. Molecular bases and role of viruses in the human microbiome. *Journal of molecular biology.* 2014;426(23):3892-906. doi: 10.1016/j.jmb.2014.07.002. PubMed PMID: 25020228.
38. Ly M, Abeles SR, Boehm TK, Robles-Sikisaka R, Naidu M, Santiago-Rodriguez T, et al. Altered oral viral ecology in association with periodontal disease. *mBio.* 2014;5(3):e01133-14. doi: 10.1128/mBio.01133-14. PubMed PMID: 24846382; PubMed Central PMCID: PMC4030452.
39. Knowles B, Silveira CB, Bailey BA, Barott K, Cantu VA, Cobian-Guemes AG, et al. Lytic to temperate switching of viral communities. *Nature.* 2016;531(7595):466-70. doi: 10.1038/nature17193. PubMed PMID: 26982729.
40. Silveira CB, Rohwer FL. Piggyback-the-Winner in host-associated microbial communities. *NPJ biofilms and microbiomes.* 2016;2:16010. doi: 10.1038/npjbiofilms.2016.10. PubMed PMID: 28721247; PubMed Central PMCID: PMC5515262.
41. Willi K, Sandmeier H, Kulik EM, Meyer J. Transduction of antibiotic resistance markers among *Actinobacillus actinomycetemcomitans* strains by temperate bacteriophages Aa phi 23. *Cellular and molecular life sciences : CMLS.* 1997;53(11-12):904-10. PubMed PMID: 9447241.
42. Stevens RH, Porras OD, Delisle AL. Bacteriophages induced from lysogenic root canal isolates of *Enterococcus faecalis*. *Oral microbiology and immunology.*

2009;24(4):278-84. doi: 10.1111/j.1399-302X.2009.00506.x. PubMed PMID: 19572888.

43. Bachrach G, Leizerovici-Zigmond M, Zlotkin A, Naor R, Steinberg D. Bacteriophage isolation from human saliva. *Letters in applied microbiology*. 2003;36(1):50-3. PubMed PMID: 12485342.

44. Sandmeier H, van Winkelhoff AJ, Bar K, Ankli E, Maeder M, Meyer J. Temperate bacteriophages are common among *Actinobacillus actinomycetemcomitans* isolates from periodontal pockets. *Journal of periodontal research*. 1995;30(6):418-25. PubMed PMID: 8544106.

45. Abeles SR, Robles-Sikisaka R, Ly M, Lum AG, Salzman J, Boehm TK, et al. Human oral viruses are personal, persistent and gender-consistent. *Isme J*. 2014;8(9):1753-67. doi: 10.1038/ismej.2014.31. PubMed PMID: 24646696; PubMed Central PMCID: PMC4139723.

46. Proctor DM, Fukuyama JA, Loomer PM, Armitage GC, Lee SA, Davis NM, et al. A spatial gradient of bacterial diversity in the human oral cavity shaped by salivary flow. *Nature communications*. 2018;9(1):681. doi: 10.1038/s41467-018-02900-1. PubMed PMID: 29445174; PubMed Central PMCID: PMC5813034.

47. Thie NM, Kato T, Bader G, Montplaisir JY, Lavigne GJ. The significance of saliva during sleep and the relevance of oromotor movements. *Sleep medicine reviews*. 2002;6(3):213-27. PubMed PMID: 12531122.

48. Dawes C. Circadian rhythms in human salivary flow rate and composition. *The Journal of physiology*. 1972;220(3):529-45. PubMed PMID: 5016036; PubMed Central PMCID: PMC1331668.

49. Dawes C. A mathematical model of salivary clearance of sugar from the oral cavity. *Caries research*. 1983;17(4):321-34. Epub 1983/01/01. doi: 10.1159/000260684. PubMed PMID: 6575870.
50. Murray PA, Prakobphol A, Lee T, Hoover CI, Fisher SJ. Adherence of oral streptococci to salivary glycoproteins. *Infection and immunity*. 1992;60(1):31-8. PubMed PMID: 1729194; PubMed Central PMCID: PMC257499.
51. Plummer C, Douglas CWI. Relationship between the ability of oral streptococci to interact with platelet glycoprotein Ib alpha and with the salivary low-molecular-weight mucin, MG2. *FEMS immunology and medical microbiology*. 2006;48(3):390-9. doi: 10.1111/j.1574-695X.2006.00161.x. PubMed PMID: WOS:000242487500012.
52. Frenkel ES, Ribbeck K. Salivary mucins in host defense and disease prevention. *Journal of oral microbiology*. 2015;7:29759. doi: 10.3402/jom.v7.29759. PubMed PMID: 26701274; PubMed Central PMCID: PMC4689954.
53. Dawes C, MacPherson LM. The distribution of saliva and sucrose around the mouth during the use of chewing gum and the implications for the site-specificity of caries and calculus deposition. *Journal of dental research*. 1993;72(5):852-7. doi: 10.1177/00220345930720050401. PubMed PMID: 8501281.
54. Crielaard W, Zaura E, Schuller AA, Huse SM, Montijn RC, Keijser BJ. Exploring the oral microbiota of children at various developmental stages of their dentition in the relation to their oral health. *Bmc Med Genomics*. 2011;4:22. Epub 2011/03/05. doi: 10.1186/1755-8794-4-22. PubMed PMID: 21371338; PubMed Central PMCID: PMCPMC3058002.

Supporting information

S1 Table. Bacterial abundances in the oral cavity before sleep for each participant. Eluted swab samples were prepared and run three times on the flow cytometer as method replicates (R). Participant's average bacterial abundances before sleep were calculated using these three values (S5 Table).

		Participant									
		1	2	3	4	5	6	7	8	9	10
Temporomandibular joint	R1	1.6E+07	4.4E+06	4.2E+06	3.7E+06	3.7E+06	2.3E+05	4.7E+05	5.4E+05	1.2E+06	2.3E+06
	R2	1.0E+07	4.2E+06	4.5E+06	3.4E+06	3.8E+06	2.5E+05	4.5E+05	6.8E+05	1.4E+06	2.3E+06
	R3	1.2E+07	3.9E+06	4.1E+06	3.9E+06	1.2E+06	2.2E+05	5.8E+05	7.0E+05	7.2E+05	2.1E+06
Back of tongue	R1	2.6E+07	8.9E+07	3.3E+07	4.6E+07	9.6E+06	2.4E+07	3.9E+07	1.6E+07	9.4E+06	8.1E+06
	R2	2.3E+07	9.8E+07	2.9E+07	4.6E+07	5.8E+06	2.6E+07	3.6E+07	1.9E+07	9.2E+06	6.9E+06
	R3	2.2E+07	7.3E+07	2.5E+07	4.6E+07	8.8E+06	2.8E+07	3.9E+07	1.3E+07	8.0E+06	7.6E+06
Gingivae	R1	6.8E+07	1.4E+07	2.2E+07	3.8E+06	1.1E+07	6.2E+05	1.4E+07	1.1E+07	1.4E+07	4.7E+06
	R2	8.9E+07	1.8E+07	1.8E+07	2.8E+06	7.4E+06	4.5E+05	1.6E+07	1.3E+07	1.2E+07	3.2E+06
	R3	9.9E+07	1.7E+07	1.4E+07	3.3E+06	9.7E+06	5.0E+05	1.3E+07	9.1E+06	1.1E+07	4.5E+06
Palate	R1	2.1E+06	2.1E+06	2.3E+05	1.7E+06	1.9E+05	1.5E+05	7.3E+04	9.2E+04	4.4E+05	2.4E+05
	R2	1.9E+06	2.3E+06	1.9E+05	1.6E+06	1.6E+05	1.6E+05	9.8E+04	7.5E+04	4.7E+05	2.5E+05
	R3	2.1E+06	2.3E+06	1.2E+05	1.5E+06	8.2E+04	1.7E+05	8.9E+04	8.5E+04	3.7E+05	1.9E+05
Molars	R1	9.8E+05	1.7E+07	8.2E+06	3.7E+06	4.9E+06	5.3E+05	5.4E+05	3.8E+05	1.0E+07	3.9E+06
	R2	1.9E+06	1.5E+07	7.7E+06	3.3E+06	4.5E+06	5.3E+05	6.4E+05	3.4E+05	9.8E+06	3.4E+06
	R3	1.7E+06	1.6E+07	6.9E+06	2.9E+06	4.0E+06	4.6E+05	4.6E+05	2.0E+05	1.2E+07	3.1E+06
Tip of tongue	R1	2.3E+06	1.7E+07	4.6E+05	1.6E+06	2.3E+05	1.8E+05	5.4E+05	3.2E+05	1.2E+06	2.2E+06
	R2	2.0E+06	1.9E+07	5.6E+05	1.6E+06	3.4E+05	1.9E+05	4.3E+05	2.2E+05	9.6E+05	1.3E+06
	R3	3.0E+06	1.6E+07	5.0E+05	1.4E+06	1.1E+05	2.2E+05	3.8E+05	2.4E+05	9.7E+05	1.5E+06

S2 Table. Bacterial abundances in the oral cavity after sleep for each participant. Eluted swab samples were prepared and run three times on the flow cytometer as method replicates (R). Participant's average bacterial abundances after sleep were calculated using these three values (S6 Table).

		Participant									
		1	2	3	4	5	6	7	8	9	10
Temporomandibular joint	R1	8.1E+07	3.9E+06	2.5E+06	4.1E+07	7.1E+06	3.3E+07	6.8E+06	2.9E+06	1.2E+07	2.0E+07
	R2	5.0E+07	3.3E+06	3.4E+06	5.1E+07	8.6E+06	3.9E+07	1.3E+07	2.9E+06	8.6E+06	3.3E+07
	R3	7.4E+07	2.8E+06	2.9E+06	4.4E+07	8.4E+06	3.6E+07	9.4E+06	1.7E+06	1.2E+07	2.7E+07
Back of tongue	R1	1.4E+08	8.0E+07	1.9E+08	1.5E+08	8.9E+07	1.2E+08	4.0E+07	7.5E+07	2.3E+08	2.3E+08
	R2	1.2E+08	1.6E+08	1.6E+08	2.4E+08	7.5E+07	7.6E+07	4.6E+07	5.7E+07	2.1E+08	2.3E+08
	R3	1.6E+08	1.9E+08	1.7E+08	2.4E+08	4.8E+07	1.0E+08	3.4E+07	5.7E+07	1.7E+08	1.7E+08
Gingivae	R1	6.3E+07	5.5E+07	8.3E+06	1.8E+07	2.7E+07	2.3E+07	2.2E+07	7.9E+07	3.2E+07	7.5E+07
	R2	6.5E+07	6.5E+07	2.4E+07	1.7E+07	3.4E+07	2.6E+07	1.8E+07	7.4E+07	4.5E+07	7.0E+07
	R3	7.5E+07	3.1E+07	1.9E+07	1.7E+07	1.8E+07	2.3E+07	2.0E+07	5.1E+07	3.6E+07	9.3E+07
Palate	R1	9.6E+06	1.2E+06	2.2E+06	3.0E+06	2.4E+06	1.2E+07	4.9E+05	4.1E+05	4.3E+06	2.2E+06
	R2	1.5E+07	2.2E+06	1.5E+06	4.8E+06	2.3E+06	1.5E+07	7.1E+05	3.3E+05	5.5E+06	1.8E+06
	R3	9.9E+06	2.5E+06	1.6E+06	3.0E+06	3.3E+06	1.4E+07	6.2E+05	3.4E+05	4.6E+06	1.5E+06
Molars	R1	5.5E+07	1.1E+07	1.3E+07	1.3E+07	4.7E+07	2.6E+06	4.2E+06	3.3E+06	2.4E+07	1.6E+07
	R2	4.9E+07	1.7E+07	1.7E+07	1.4E+07	4.2E+07	2.9E+06	3.4E+06	2.5E+06	2.4E+07	2.1E+07
	R3	6.8E+07	1.6E+07	1.4E+07	2.0E+07	2.3E+07	2.6E+06	2.8E+06	2.0E+06	2.7E+07	1.5E+07
Tip of tongue	R1	9.2E+06	1.4E+07	5.4E+06	2.0E+07	1.0E+07	2.5E+07	1.1E+06	3.9E+06	2.7E+07	2.3E+07
	R2	7.0E+06	1.4E+07	5.2E+06	1.6E+07	1.1E+07	2.6E+07	1.5E+06	4.5E+06	2.6E+07	1.6E+07
	R3	6.5E+06	1.5E+07	4.6E+06	1.7E+07	6.6E+06	2.7E+07	9.3E+05	3.5E+06	2.4E+07	1.7E+07

S3 Table. VLP abundances in the oral cavity before sleep for each participant. Eluted swab samples were prepared and run three times on the flow cytometer as method replicates (R). Participant's average VLP abundances before sleep were calculated using these three values (S7 Table).

		Participant									
		1	2	3	4	5	6	7	8	9	10
Temporomandibular joint	R1	1.4E+07	8.2E+06	2.1E+06	6.0E+06	3.2E+06	2.5E+05	1.9E+06	1.2E+06	1.3E+06	1.5E+07
	R2	1.4E+07	1.0E+07	2.7E+06	6.7E+06	4.1E+06	4.7E+05	1.5E+06	1.6E+06	1.2E+06	2.7E+07
	R3	1.4E+07	8.9E+06	2.0E+06	5.3E+06	3.1E+06	4.1E+05	2.1E+06	1.3E+06	1.1E+06	9.2E+06
Back of tongue	R1	5.2E+07	3.3E+07	8.7E+06	7.6E+07	9.9E+06	3.9E+06	2.2E+06	1.0E+07	2.1E+07	2.5E+07
	R2	4.4E+07	3.6E+07	7.5E+06	5.8E+07	8.8E+06	3.8E+06	1.1E+06	1.2E+07	2.0E+07	2.7E+07
	R3	4.9E+07	2.6E+07	1.2E+07	4.9E+07	1.0E+07	4.2E+06	1.5E+06	6.3E+06	1.2E+07	2.9E+07
Gingivae	R1	8.9E+07	4.3E+07	1.6E+07	1.3E+07	1.1E+07	1.5E+06	1.7E+07	2.5E+07	4.9E+06	3.3E+06
	R2	9.6E+07	4.9E+07	1.4E+07	1.4E+07	1.4E+07	1.3E+06	1.2E+07	2.4E+07	5.8E+06	2.8E+06
	R3	1.2E+08	5.6E+07	2.2E+07	1.2E+07	8.4E+06	1.3E+06	1.7E+07	1.2E+07	4.8E+06	4.6E+06
Palate	R1	3.2E+06	1.6E+06	2.3E+05	9.1E+06	2.3E+05	1.4E+06	8.7E+04	4.9E+05	1.4E+06	8.4E+05
	R2	2.4E+06	1.6E+06	8.0E+04	1.3E+07	6.1E+05	1.5E+06	9.0E+04	2.4E+05	8.9E+05	6.8E+05
	R3	3.0E+06	2.1E+06	1.8E+05	1.1E+07	2.2E+05	1.2E+06	1.1E+05	1.9E+05	5.6E+05	4.6E+05
Molars	R1	1.9E+07	1.9E+07	1.2E+06	1.3E+07	3.4E+06	1.1E+06	9.2E+04	7.3E+06	7.8E+06	1.3E+07
	R2	1.7E+07	2.3E+07	1.6E+06	9.1E+06	3.1E+06	1.2E+06	1.3E+05	7.9E+06	8.1E+06	2.1E+07
	R3	2.4E+07	2.4E+07	1.1E+06	1.5E+07	2.0E+06	8.1E+05	8.6E+04	3.9E+06	7.7E+06	1.4E+07
Tip of tongue	R1	3.6E+06	1.0E+07	4.1E+05	9.1E+06	2.7E+05	5.5E+05	3.4E+05	2.2E+06	8.5E+05	6.4E+06
	R2	4.0E+06	1.2E+07	6.3E+05	7.6E+06	8.1E+05	3.9E+05	1.5E+05	2.0E+06	8.5E+05	8.7E+06
	R3	4.1E+06	1.2E+07	8.3E+05	7.9E+06	5.2E+05	4.0E+05	2.0E+05	4.7E+06	6.9E+05	4.6E+06

S4 Table. VLP abundances in the oral cavity after sleep for each participant. Eluted swab samples were prepared and run three times on the flow cytometer as method replicates (R). Participant's average VLP abundances after sleep were calculated using these three values (S8 Table).

		Participant									
		1	2	3	4	5	6	7	8	9	10
Temporomandibular joint	R1	1.9E+08	2.4E+06	9.5E+05	7.4E+07	1.7E+06	1.1E+08	4.0E+06	8.2E+06	7.9E+06	1.3E+08
	R2	2.5E+08	7.6E+06	1.0E+06	1.4E+08	3.4E+06	1.1E+08	2.4E+06	7.9E+06	1.3E+07	1.0E+08
	R3	1.8E+08	6.4E+06	8.4E+05	1.0E+08	4.0E+06	1.4E+08	2.9E+06	3.1E+06	1.1E+07	9.6E+07
Back of tongue	R1	3.9E+08	3.1E+07	1.7E+07	8.3E+07	8.9E+06	8.2E+07	1.0E+07	1.2E+07	1.2E+07	5.6E+07
	R2	4.6E+08	6.2E+07	1.4E+07	1.5E+08	6.6E+06	1.0E+08	8.4E+06	1.2E+07	1.2E+07	6.1E+07
	R3	7.3E+08	6.2E+07	2.1E+07	1.5E+08	6.6E+06	1.1E+08	8.0E+06	7.9E+06	1.1E+07	6.9E+07
Gingivae	R1	1.7E+08	2.1E+08	4.0E+06	4.3E+07	7.0E+06	8.8E+07	3.9E+06	1.2E+08	3.0E+07	3.2E+08
	R2	1.1E+08	2.7E+08	5.3E+06	9.2E+07	1.6E+07	1.1E+08	5.6E+06	1.1E+08	3.5E+07	2.3E+08
	R3	1.6E+08	6.0E+07	6.8E+06	2.6E+07	4.8E+06	8.0E+07	7.6E+06	8.0E+07	3.0E+07	3.1E+08
Palate	R1	8.7E+07	2.9E+06	4.2E+05	1.1E+07	3.3E+06	1.3E+07	2.6E+05	9.8E+05	1.7E+06	6.7E+06
	R2	1.6E+08	2.8E+06	5.5E+05	1.6E+07	3.6E+06	1.4E+07	4.9E+05	1.4E+06	2.3E+06	5.2E+06
	R3	6.3E+07	1.5E+06	6.1E+05	1.1E+07	4.2E+06	1.3E+07	4.9E+05	9.0E+05	2.1E+06	5.3E+06
Molars	R1	2.6E+08	1.7E+07	1.2E+07	1.8E+07	3.3E+07	1.0E+07	1.1E+06	4.1E+06	6.9E+07	7.0E+07
	R2	2.4E+08	1.6E+07	1.0E+07	2.6E+07	2.4E+07	1.0E+07	1.3E+06	4.8E+06	4.4E+07	5.8E+07
	R3	5.4E+08	2.1E+07	1.6E+07	2.6E+07	3.0E+07	9.7E+06	2.1E+06	4.3E+06	6.9E+07	5.8E+07
Tip of tongue	R1	3.6E+07	4.9E+06	7.2E+05	3.6E+07	1.2E+06	8.2E+07	4.9E+05	7.1E+06	3.4E+06	2.3E+07
	R2	1.8E+07	5.3E+06	5.6E+05	2.6E+07	1.7E+06	9.3E+07	3.7E+05	1.0E+07	3.0E+06	2.0E+07
	R3	1.7E+07	4.0E+06	9.9E+05	1.4E+07	1.3E+06	8.4E+07	1.8E+05	7.6E+06	2.9E+06	1.6E+07

S5 Table. Participant's average bacterial counts for each sample site in the oral cavity before sleep.

Participant	Temporomandibular joint	Back of tongue	Gingivae	Palate	Molars	Tip of tongue
1	1.28E+07	2.38E+07	8.52E+07	2.05E+06	1.51E+06	2.45E+06
2	4.19E+06	8.66E+07	1.62E+07	2.22E+06	1.59E+07	1.74E+07
3	4.28E+06	2.91E+07	1.79E+07	1.80E+05	7.61E+06	5.05E+05
4	3.67E+06	4.60E+07	3.32E+06	1.63E+06	3.29E+06	1.57E+06
5	2.91E+06	8.05E+06	9.52E+06	1.44E+05	4.45E+06	2.29E+05
6	2.36E+05	2.61E+07	5.25E+05	1.61E+05	5.06E+05	1.99E+05
7	4.99E+05	3.82E+07	1.46E+07	8.65E+04	5.46E+05	4.50E+05
8	6.39E+05	1.62E+07	1.12E+07	8.41E+04	3.08E+05	2.64E+05
9	1.08E+06	8.85E+06	1.23E+07	4.29E+05	1.07E+07	1.03E+06
10	2.25E+06	7.53E+06	4.16E+06	2.27E+05	3.48E+06	1.64E+06

S6 Table. Participant's average bacterial counts for each sample site in the oral cavity after sleep.

Participant	Temporomandibular joint	Back of tongue	Gingivae	Palate	Molars	Tip of tongue
1	6.83E+07	1.40E+08	6.78E+07	1.17E+07	5.73E+07	7.59E+06
2	3.36E+06	1.42E+08	5.00E+07	1.99E+06	1.44E+07	1.42E+07
3	2.94E+06	1.75E+08	1.69E+07	1.73E+06	1.48E+07	5.07E+06
4	4.50E+07	2.07E+08	1.75E+07	3.60E+06	1.58E+07	1.74E+07
5	8.05E+06	7.06E+07	2.60E+07	2.66E+06	3.72E+07	9.30E+06
6	3.61E+07	9.99E+07	2.41E+07	1.39E+07	2.69E+06	2.59E+07
7	9.73E+06	3.99E+07	1.99E+07	6.06E+05	3.47E+06	1.18E+06
8	2.49E+06	6.31E+07	6.81E+07	3.60E+05	2.62E+06	3.94E+06
9	1.09E+07	2.03E+08	3.78E+07	4.82E+06	2.51E+07	2.53E+07
10	2.68E+07	2.10E+08	7.97E+07	1.83E+06	1.74E+07	1.86E+07

S7 Table. Participant's average VLP counts for each sample site in the oral cavity before sleep.

Participant	Temporomandibular joint	Back of tongue	Gingivae	Palate	Molars	Tip of tongue
1	1.41E+07	4.83E+07	1.00E+08	2.89E+06	2.04E+07	3.90E+06
2	9.14E+06	3.15E+07	4.93E+07	1.77E+06	2.23E+07	1.13E+07
3	2.23E+06	9.23E+06	1.73E+07	1.63E+05	1.33E+06	6.24E+05
4	5.97E+06	6.12E+07	1.27E+07	1.08E+07	1.24E+07	8.18E+06
5	3.49E+06	9.70E+06	1.11E+07	3.55E+05	2.82E+06	5.29E+05
6	3.76E+05	3.96E+06	1.37E+06	1.37E+06	1.02E+06	4.45E+05
7	1.82E+06	1.62E+06	1.52E+07	9.42E+04	1.04E+05	2.28E+05
8	1.40E+06	9.63E+06	2.01E+07	3.04E+05	6.39E+06	2.97E+06
9	1.19E+06	1.80E+07	5.19E+06	9.54E+05	7.86E+06	7.98E+05
10	1.71E+07	2.69E+07	3.56E+06	6.57E+05	1.59E+07	6.55E+06

S8 Table. Participant's average VLP counts for each sample site in the oral cavity after sleep.

Participant	Temporomandibular joint	Back of tongue	Gingivae	Palate	Molars	Tip of tongue
1	2.07E+08	5.28E+08	1.49E+08	1.02E+08	3.44E+08	2.36E+07
2	5.44E+06	5.16E+07	1.82E+08	2.42E+06	1.80E+07	4.73E+06
3	9.47E+05	1.74E+07	5.38E+06	5.30E+05	1.28E+07	7.53E+05
4	1.05E+08	1.26E+08	5.39E+07	1.29E+07	2.34E+07	2.52E+07
5	3.01E+06	7.38E+06	9.25E+06	3.71E+06	2.92E+07	1.40E+06
6	1.20E+08	9.83E+07	9.39E+07	1.33E+07	1.00E+07	8.62E+07
7	3.11E+06	8.84E+06	5.71E+06	4.12E+05	1.52E+06	3.48E+05
8	6.38E+06	1.05E+07	1.04E+08	1.08E+06	4.39E+06	8.20E+06
9	1.07E+07	1.16E+07	3.19E+07	2.03E+06	6.07E+07	3.09E+06
10	1.08E+08	6.20E+07	2.87E+08	5.70E+06	6.16E+07	1.96E+07

Chapter 5

THE MICROBIAL ABUNDANCE DYNAMICS IN THE ORAL
CAVITY OF PAEDIATRIC SLEEP DISORDER BREATHERS
BEFORE AND AFTER SLEEP

Abstract

In this study we measured the absolute microbial abundance variation in the oral cavity of paediatric sleep disorder breathers (SDB). Using flow cytometry, bacterial and virus-like particle (VLP) populations at 6 locations in the oral cavity of SDB were enumerated and analysed for regions of heterogeneity. Oral swab samples were collected from 20 paediatric SDB participants at the temporomandibular joint, back of the tongue, tip of the tongue, palate, gingivae and molars prior to and preceding their polysomnography sleep analysis. We report that, like the healthy paediatric oral microbiome, the paediatric SDB oral cavity is numerically heterogeneous in microbial communities, and that these communities significantly increase in abundance during sleep by counts of up to 70 million. We also report significant VLP count differences of up to 23 million between the healthy and SDB paediatric oral microbiome. Here we show that oral biomass varies between healthy and SDB oral cavities. Therefore, we highlight the importance of controlling for time and location in comparative human microbiome studies as this biomass changes based on space and time.

Introduction

During sleep, the pharyngeal muscles in the upper airway are in a complex balance [1]. If this balance is disrupted, airway collapsibility may result, increasing upper airway resistance and reducing air flow [1]. Defined as a continuum respiratory disorder ranging from mild snoring to severe obstructive sleep apnoea syndrome (OSA), sleep disorder breathing (SDB) affects 10% of the paediatric population [2]. One major factor to the disorder is the impairment of normal ventilation and sleep pattern due to upper airway obstruction in the form of adenotonsillar hypertrophy [3]. If left untreated, paediatric SDB can lead to numerous behavioural, neurocognitive, cardiovascular and growth issues [4].

The oral cavity is part of the upper airway and has been a site of interest for numerous microbiome studies as it is thought to be the gateway to the respiratory and digestive systems [5]. It has been well established that the oral cavity is colonised by an array of microbes [5-7] and that these microbes are niche specific based on the various microhabitats present [8]. These microhabitats differ not only in surface structure but also in environmental conditions including oxygen, pH and temperature [7, 9, 10]. These microhabitats in the healthy paediatric oral cavity are numerically heterogeneous and increase in abundance during sleep [11, 12].

With increasing evidence suggesting sleep perturbations alter the gut microbiota [13-15]; it is reasonable to suggest that perturbations in sleeping patterns could also have a similar effect on the oral microbiome. Using flow cytometry we investigated the oral microbial abundance profiles of SDB before and after sleep. Flow cytometry can enumerate bacteria and virus-like particles (VLPs) based on particle size and DNA content. For this study, VLPs refer to small particles with a low DNA

concentration, the characteristics of viruses. We, therefore, aim to investigate the abundance variation in bacteria and VLPs in paediatric SDB to determine if they are different to previously reported healthy paediatric populations.

Materials and Methods

Ethics statement

This study was approved by The Human Research Ethics Committees of the Women's and Children's Hospital and University of Adelaide, South Australia. Participants involved were a subgroup of SDB children from a larger study investigating the effects of SDB on development. The study was conducted in accordance with the 1964 Declaration of Helsinki and its later amendments. Parents of participants provided written consent and children written assent for involvement in the study. Child's health and behaviour questionnaire were completed by the parents of the participants prior to sample collection.

Sample collection

Samples were collected from 20 paediatric SDB (female $n = 8$, male $n = 12$) undergoing a polysomnography sleep test. Participant ages ranged from 4.75 to 18.92 years with a group average of 12.26 ± 1.00 years. BMI's were between 12.50 and 38.30 with an overall group average of 22.83 ± 1.55 . Participants were asked to refrain from oral hygiene practices for the duration of the study.

Oral microhabitats were sampled using individually packaged sterile rayon swabs (Copan, Brescia, Italy; product code: 155C) as previously described [12]. Each swab, stored in its own individual polypropylene tube, had a diameter of approximately 5 mm and a plastic shaft length of 13.3 cm. Swabs were collected from each participant

at the left temporomandibular joint, the middle of the back of the tongue, the occlusal site of the last two distal molars on the bottom jaw on the right side, the gingival margin of the last proximal molar on the right lower jaw, the middle of the palate and the middle of the tip of the tongue. These samples will be referred to in this article as the temporomandibular joint, back of tongue, molars, gingivae, palate and tip of tongue respectively. Swabs were collected from participants between 8.30-9.00 pm just prior to lights out (before sleep) and between 6.00-6.30 am the following morning upon awakening (after sleep). Samples were collected from participants by the same researcher before and after sleep at the same location by rotating the swab clockwise 6 times. Once collected, swabs were placed back into their polypropylene tubes and stored at -80°C until analysis.

Swab sample preparation

Swab samples were prepared according to methods previously described [12]. Briefly, thawed swab tips were cut off and vortexed for 3 minutes in 1 ml of sterile (0.2 µm filtered and UV treated) TE buffer (10 mM Tris, 1 mM EDTA, pH 7.4, Sigma). Swab elute was diluted 1:100 in 0.2 µm filtered and UV treated TE buffer, then stained with SYBR-I Green (1:20,00 final dilution; Molecular Probes) [16]. Samples were then incubated in the dark at 80°C for 10 minutes [16]. Sterile rayon swabs were used as a control and were prepared in the same manner as the participant samples. These samples were used to eliminate any background artefacts introduced from the swab or the sample preparation. Each swab sample was prepared in triplicate for analysis (S1-S4 Tables). Flow cytometric parameters were normalised based on the fluorescence and concentration of 1 µm fluorescent beads (Molecular Probes) [17]. These beads were added to each sample at a concentration of 10^5 beads ml⁻¹ [17].

Flow cytometry

A FACSCanto II flow cytometer (Becton Dickinson) fitted with red (633 nm, 17 mW), Violet (405 nm, 30 mW) and blue (488 nm, 20 mW) lasers was used to identify and enumerate bacterial and VLP populations from the swab samples. For each sample, green fluorescence, forward angle light scatter and side angle light scatter were recorded. Phosphate-buffered saline was used as sheath fluid in the flow cytometer.

FlowJo software (Tree Star, Inc) was used to enumerate and analyse bacterial and VLP populations. Bacterial and VLP populations in the samples were differentiated using SYBR Green fluorescence and side scatter [16, 18, 19]

Data analysis

Statistical analysis of the abundance data was analysed using the program MATLAB (MathWorks, Natick, Massachusetts, United States). Paired comparisons of bacterial and VLP abundances among locations before and after sleep were analysed using the Mann-Whitney U test. The Wilcoxon sign rank test was used to compare bacterial and VLP abundances before and after sleep in SDB. The Mann-Whitney U test was also used to compare SDB bacterial and VLP abundances to microbial counts previously published on the healthy paediatric oral cavity [12]. P values were corrected for false positives using the multiple comparisons hypothesis for false discovery [20]. Statistical significance was considered when $p < 0.05$.

Results

SDB bacterial abundance heterogeneity before sleep

The average bacterial abundances for each microhabitat in the SDB oral cavity before sleep are presented in Table 1. The palate was the area in the oral cavity with the lowest abundances of bacteria before sleep with participant averages ranging from 3.80×10^4 to 6.79×10^6 bacteria (Table 1; S5 Table). The group average of $9.55 \pm 3.88 \times 10^5$ bacteria for this location was significantly lower in abundance than tip of the tongue ($1.96 \pm 0.54 \times 10^6$ bacteria; $p = 0.006$), molars ($3.19 \pm 0.86 \times 10^6$ bacteria; $p = 0.001$), temporomandibular joint ($4.50 \pm 0.95 \times 10^6$ bacteria; $p < 0.0001$), back of the tongue ($1.90 \pm 0.36 \times 10^7$ bacteria; $p < 0.0001$) and gingivae ($2.56 \pm 0.70 \times 10^7$ bacteria; $p < 0.0001$). No significant difference was observed between the average bacterial abundances at the gingivae ($2.56 \pm 0.70 \times 10^7$ bacteria) and the back of the tongue ($1.90 \pm 0.36 \times 10^7$ bacteria) before sleep (Fig 1; Table 1; $p > 0.05$). Participants bacterial counts at these two locations ranged from 2.83×10^5 (back of the tongue) to 1.05×10^8 (gingivae) with a combined average of $2.23 \pm 0.39 \times 10^7$ bacteria for both locations (Table 1; S5 Table). The gingivae ($2.56 \pm 0.70 \times 10^7$ bacteria) were significantly higher in bacterial abundance before sleep than the temporomandibular joint ($4.50 \pm 0.95 \times 10^6$ bacteria; $p = 0.0039$), palate ($9.55 \pm 3.88 \times 10^5$ bacteria; $p < 0.0001$), molars ($3.19 \pm 0.86 \times 10^6$ bacteria; $p = 0.00031$) and tip of tongue ($1.96 \pm 0.54 \times 10^6$ bacteria; $p < 0.0001$; Fig 1; Table 1). A significantly higher bacterial abundance at the back of tongue was also reported compared to the temporomandibular joint ($4.50 \pm 0.95 \times 10^6$ bacteria; $p = 0.0012$), palate ($9.55 \pm 3.88 \times 10^5$ bacteria; $p < 0.0001$), molars ($3.19 \pm 0.86 \times 10^6$ bacteria; $p = 0.00026$) and tip of tongue ($1.96 \pm 0.54 \times 10^6$ bacteria; $p < 0.0001$; Fig 1; Table 1). Finally, the

temporomandibular joint ($4.50 \pm 0.95 \times 10^6$ bacteria) was reported to be significantly higher in bacterial abundance than the tip of the tongue ($1.96 \pm 0.54 \times 10^6$ bacteria; $p = 0.013$; Fig 1; Table 1). All other locations, when paired with each other, did not show a significant difference in bacterial abundances (Fig 1; $p > 0.05$). Overall there was a 2.47×10^7 range difference between the highest and lowest bacterial counts before sleep in the oral cavity, a difference of approximately 27 times (Table 1).

Table 1. Average bacterial abundances within the paediatric SDB oral cavity.

Error represents the standard error of the mean. Wilcoxon sign rank tests p values were corrected for false discovery rates. Percentage increases were calculated by taking an average of each patient's percentage increase/decrease in bacteria for each location.

Sample location	Bacteria before sleep (\pm SEM)	Bacteria after sleep (\pm SEM)	Average increase in bacteria (\pm SEM)	Percentage increase (\pm SEM)	p value
Temporomandibular joint	4.50 x 10 ⁶ (9.46 x 10 ⁵)	2.65 x 10 ⁷ (6.88 x 10 ⁶)	2.21 x 10 ⁷ (7.08 x 10 ⁶)	2097 (1112%)	< 0.0001
Back of tongue	1.90 x 10 ⁷ (3.64 x 10 ⁶)	8.94 x 10 ⁷ (1.49 x 10 ⁷)	7.04 x 10 ⁷ (1.33 x 10 ⁷)	1005 (425%)	< 0.0001
Gingivae	2.56 x 10 ⁷ (6.96 x 10 ⁶)	5.80 x 10 ⁷ (1.65 x 10 ⁷)	3.24 x 10 ⁷ (1.26 x 10 ⁷)	485 (175%)	< 0.0001
Palate	9.55 x 10 ⁵ (3.88 x 10 ⁵)	3.88 x 10 ⁶ (9.15 x 10 ⁵)	2.93 x 10 ⁶ (9.81 x 10 ⁵)	2080 (560%)	< 0.0001
Molars	3.19 x 10 ⁶ (8.61 x 10 ⁵)	1.59 x 10 ⁷ (4.98 x 10 ⁶)	1.27 x 10 ⁷ (4.75 x 10 ⁶)	1312 (395%)	< 0.0001
Tip of tongue	1.96 x 10 ⁶ (5.38 x 10 ⁵)	1.50 x 10 ⁷ (4.79 x 10 ⁶)	1.30 x 10 ⁷ (4.41 x 10 ⁶)	1297 (321%)	< 0.0001

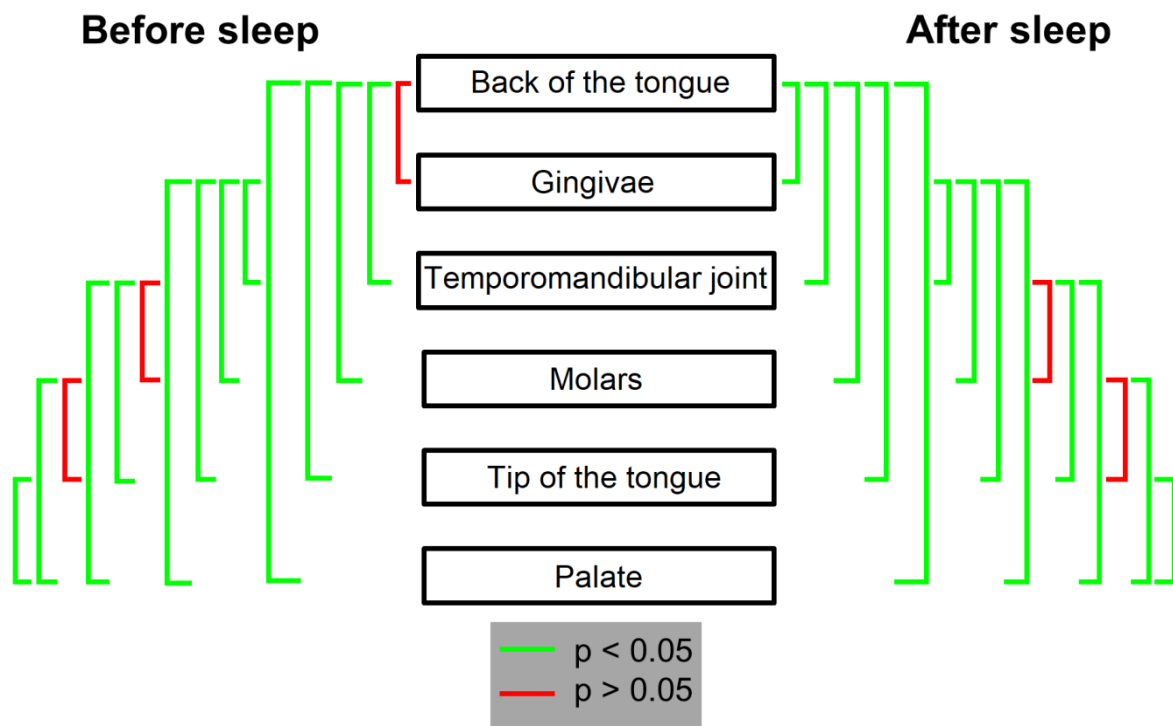


Figure 1. Mann-Whitney U tests for bacterial heterogeneity in the oral cavity before and after sleep in SDB. Significant differences between locations are shown in green ($p < 0.05$). Non-significant differences are shown in red ($p > 0.05$). Mann-Whitney U test comparisons have been corrected for false discovery rates.

SDB bacterial abundance heterogeneity after sleep

Bacterial counts of $3.88 \pm 0.92 \times 10^6$ at the palate were significantly lower than the temporomandibular joint ($2.65 \pm 0.69 \times 10^7$ bacteria; $p = 0.00023$), back of tongue ($8.94 \pm 1.49 \times 10^7$ bacteria; $p < 0.0001$), gingivae ($5.80 \pm 1.65 \times 10^7$ bacteria; $p < 0.0001$), molars ($1.59 \pm 0.50 \times 10^7$ bacteria; $p = 0.00096$) and tip of tongue ($1.50 \pm 0.48 \times 10^7$ bacteria; $p = 0.0068$) in SDB after sleep (Fig 1; Table 1). The back of the tongue ($8.94 \pm 1.49 \times 10^7$ bacteria) was the location with the highest abundance of bacteria after sleep and was significantly higher than the temporomandibular joint ($2.65 \pm 0.69 \times 10^7$ bacteria; $p = 0.00092$), gingivae ($5.80 \pm 1.65 \times 10^7$ bacteria; $p = 0.046$), palate ($3.88 \pm 0.92 \times 10^6$ bacteria; $p < 0.0001$), molars ($1.59 \pm 0.50 \times 10^7$ bacteria; $p < 0.0001$) and tip of tongue ($1.50 \pm 0.48 \times 10^7$ bacteria; $p < 0.0001$; Fig 1; Table 1). The gingivae ($5.80 \pm 1.65 \times 10^7$ bacteria) were the location with the second highest abundance of bacteria in the oral cavity after sleep and were also significantly higher in bacterial counts than the temporomandibular joint ($2.65 \pm 0.69 \times 10^7$ bacteria; $p = 0.047$), palate ($3.88 \pm 0.92 \times 10^6$ bacteria; $p < 0.0001$), molars ($1.59 \pm 0.50 \times 10^7$ bacteria; $p = 0.0039$) and tip of tongue ($1.50 \pm 0.48 \times 10^7$ bacteria; $p = 0.0015$; Fig 1; Table 1). Finally, the temporomandibular joint ($2.65 \pm 0.69 \times 10^7$ bacteria) was also reported to be significantly higher in bacterial counts than the tip of the tongue ($1.50 \pm 0.48 \times 10^7$ bacteria; $p = 0.049$) after sleep (Fig 1; Table 1). No significant difference was observed between bacterial counts at the molars and the temporomandibular joint or tip of the tongue after sleep (Fig 1; $p > 0.05$). Overall there was a bacterial range difference of 23 times between the palate and the back of the tongue after sleep (Table 1).

SDB VLP abundance heterogeneity before sleep

VLP counts of $1.38 \pm 0.64 \times 10^6$ at the palate were significantly lower than the temporomandibular joint ($6.36 \pm 2.17 \times 10^6$ VLP; $p = 0.0036$), back of tongue ($1.05 \pm 0.23 \times 10^7$ VLP; $p = 0.00013$), gingivae ($3.05 \pm 1.00 \times 10^7$ VLP; $p = 0.00012$), molars ($4.69 \pm 1.43 \times 10^6$ VLP; $p = 0.0027$) and tip of tongue ($3.87 \pm 1.48 \times 10^6$ VLP; $p = 0.014$) before sleep (Fig 2; Table 2). No significant difference was observed between VLP abundances at the back of the tongue ($1.05 \pm 0.23 \times 10^7$ VLP) and gingivae ($3.05 \pm 1.00 \times 10^7$ VLP) before sleep ($p > 0.05$; Fig 2). However, VLPs at both locations were significantly higher than the molars ($p = 0.035$ and 0.021 respectively) and tip of the tongue ($p = 0.014$ and 0.012 respectively) before sleep (Fig 2; Table 2). All other paired comparisons among locations did not show a significant difference in VLP abundance before sleep ($p > 0.05$; Fig 2). A 22 times VLP difference was observed between the location with the highest (gingivae) and lowest (palate) VLP abundances in the oral cavity before sleep (Table 2).

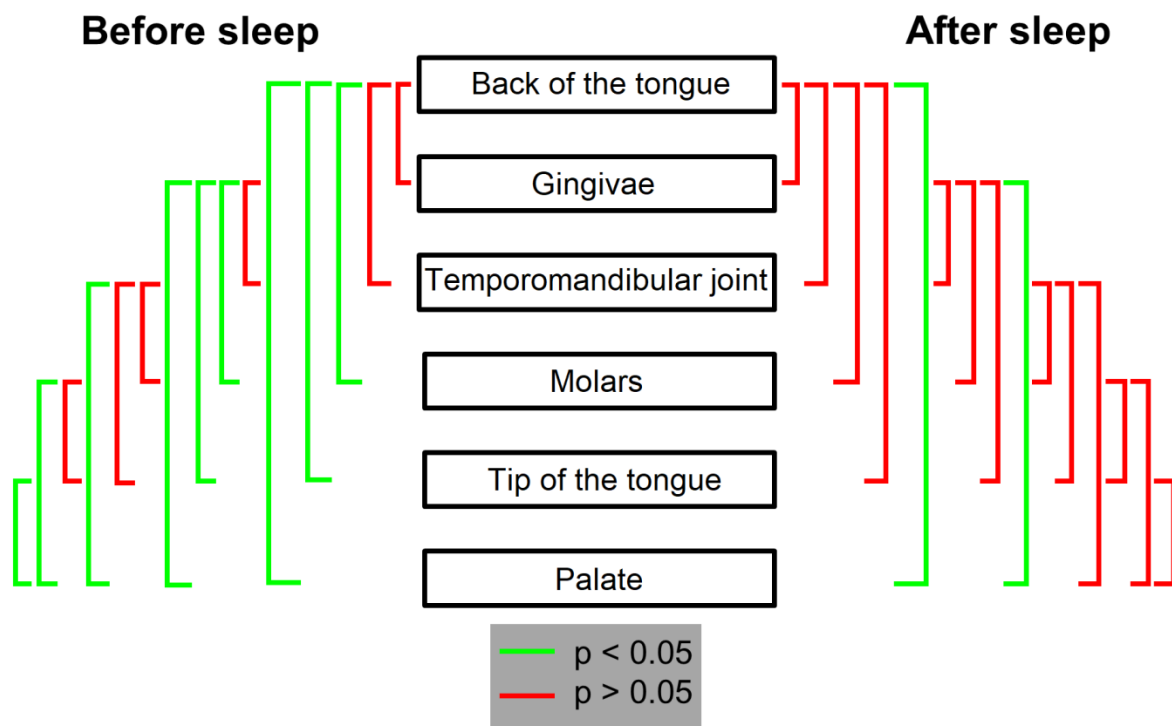


Figure 2. Mann-Whitney U tests for VLP heterogeneity in the oral cavity before and after sleep in SDB. Significant differences between locations are shown in green ($p < 0.05$). Non-significant differences are shown in red ($p > 0.05$). Mann-Whitney U test comparisons have been corrected for false discovery rates.

Table 2. Average VLP abundances within the SDB paediatric oral cavity. Error represents the standard error of the mean. Wilcoxon sign rank tests p values were corrected for false discovery rates. Percentage increases were calculated by taking an average of each patient's percentage increase/decrease in VLPs for each location.

Sample location	VLP before sleep (± SEM)	VLP after sleep (± SEM)	Average increase in VLP (± SEM)	Percentage increase (± SEM)	p value
Temporomandibular joint	6.36 x 10 ⁶ (2.17 x 10 ⁶)	3.43 x 10 ⁷ (1.22 x 10 ⁷)	2.08 x 10 ⁷ (1.07 x 10 ⁷)	3698 (2195%)	0.0001
Back of tongue	1.05 x 10 ⁷ (2.29 x 10 ⁶)	7.20 x 10 ⁷ (2.60 x 10 ⁷)	6.16 x 10 ⁷ (2.51 x 10 ⁷)	1038 (377%)	< 0.0001
Gingivae	3.05 x 10 ⁷ (1.00 x 10 ⁷)	7.72 x 10 ⁷ (3.13 x 10 ⁷)	4.67 x 10 ⁷ (2.48 x 10 ⁷)	1035 (587%)	0.0003
Palate	1.38 x 10 ⁶ (6.35 x 10 ⁵)	1.35 x 10 ⁷ (6.72 x 10 ⁶)	1.21 x 10 ⁷ (6.27 x 10 ⁶)	5443 (2195%)	< 0.0001
Molars	4.69 x 10 ⁶ (1.43 x 10 ⁶)	3.55 x 10 ⁷ (1.62 x 10 ⁷)	3.08 x 10 ⁷ (1.50 x 10 ⁷)	2160 (1183%)	< 0.0001
Tip of tongue	3.87 x 10 ⁶ (1.48 x 10 ⁶)	7.38 x 10 ⁷ (5.55 x 10 ⁷)	6.99 x 10 ⁷ (5.42 x 10 ⁷)	969 (366%)	< 0.0001

SDB VLP abundance homogeneity after sleep

Participant VLP averages ranged from $1.21 \pm 0.63 \times 10^7$ at the palate to $7.72 \pm 3.13 \times 10^7$ at the gingivae after sleep (S8 Table), a difference of approximately 6 times. Both the gingivae ($7.72 \pm 3.13 \times 10^7$ VLP) and the back of tongue ($7.20 \pm 2.60 \times 10^7$ VLP) were reported to have significantly higher VLP counts than the palate ($7.72 \pm 3.13 \times 10^7$ VLP) after sleep ($p = 0.018$ and $p = 0.015$ respectively; Fig 2; Table 2). All other locations when compared with each other did not show significant differences in VLP abundance after sleep ($p > 0.05$; Fig 2).

Significant increase in bacterial and VLP counts during sleep

All sampled locations in SDB increased in average bacterial abundance during sleep (Fig 3). These increases were all significant ($p < 0.05$; Table 1). The area with the greatest average increase in bacteria after sleep was the back of the tongue with a 5 times count increase of $7.04 \pm 1.33 \times 10^7$ bacteria ($p < 0.0001$; Table 1). The palate was the location with the smallest increase in bacteria with a 4 times increase of $2.93 \pm 0.98 \times 10^6$ bacteria during sleep ($p < 0.0001$; Table 1). The temporomandibular joint, gingivae, molars and tip of tongue increased by 6, 2, 5 and 8 times respectively ($p < 0.0001$; Table 1). Percentage increases ranged from approximately 490% at the gingivae to 2100% at the temporomandibular joint and palate (Table 1).

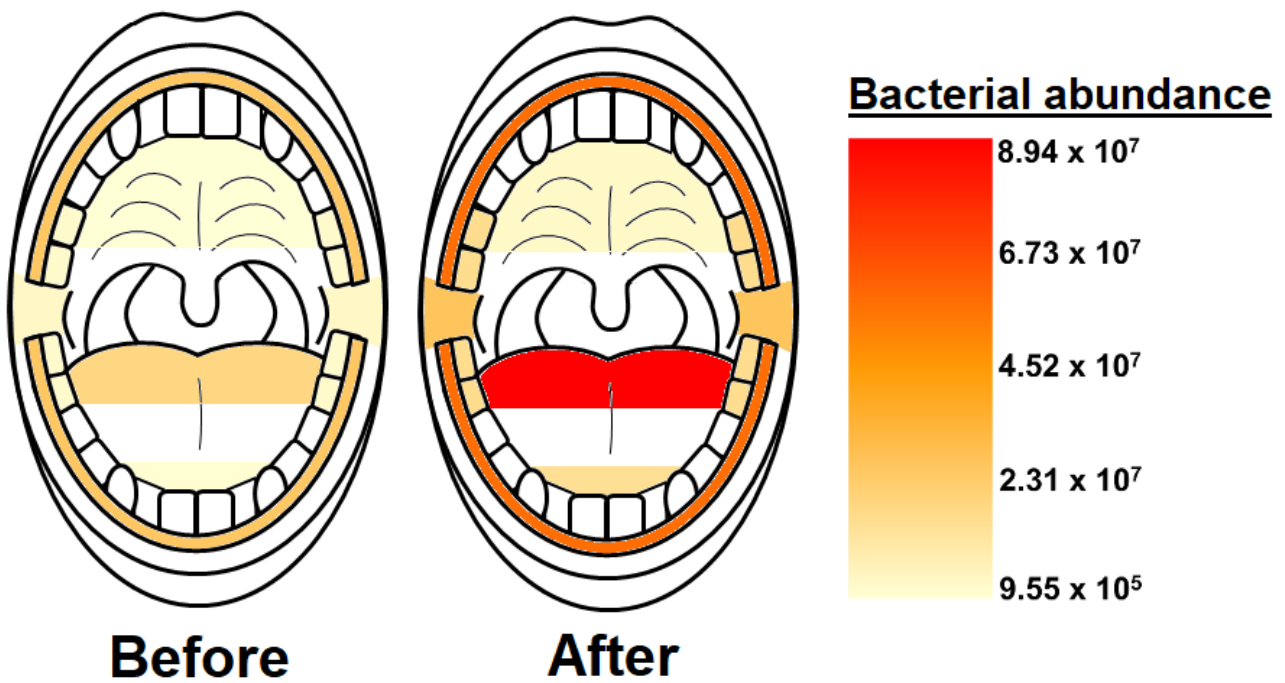


Figure 3. Bacterial loads in the paediatric SDB oral cavity before and after sleep.

A significant increase in bacterial abundances was observed for all microhabitats after sleep ($p < 0.05$). The back of tongue and gingivae were the locations with the highest bacterial counts both before and after sleep. The lowest bacterial counts were recorded at the palate.

Similarly, with VLPs, all sample locations in SDB showed a significant increase in VLP abundance after sleep ($p < 0.05$; Fig 4; Table 2). The tip and the back of the tongue were the areas with the greatest increases in VLPs after sleep with $6.99 \pm 5.42 \times 10^7$ and $6.16 \pm 2.51 \times 10^7$ VLP count increases respectively ($p < 0.0001$; Table 2). However, the tip of the tongue was the location with the lowest percentage increase in VLP with 970% (Table 2). The location with the lowest increase in VLPs was the palate with a count increase of $1.21 \pm 6.3 \times 10^7$ VLP ($p < 0.0001$; Table 2). However, the palate was the location with the highest percentage increase in VLP with 5400% (Table 2). The temporomandibular joint, gingivae and molars increased in VLPs during sleep by approximately 5 ($p = 0.00011$), 3 ($p = 0.00026$) and 8 ($p < 0.0001$) times respectively (Table 2).

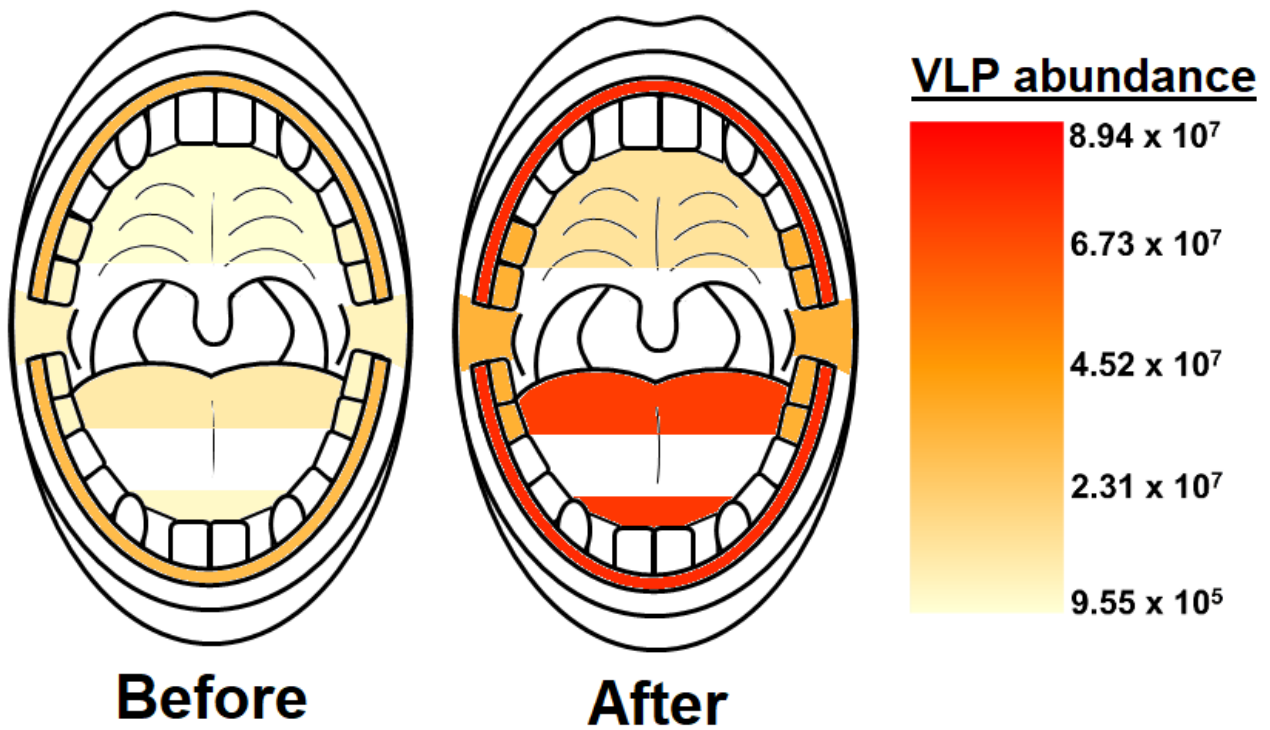


Figure 4. VLP loads in the paediatric SDB oral cavity before and after sleep. A significant increase in VLP abundances was observed for all microhabitats after sleep ($p < 0.05$). The gingivae and palate were the locations with the highest and lowest VLP counts before and after sleep respectively.

Significant differences in microbial concentrations between health states

Mann-Whitney U comparisons were made between healthy and SDB bacterial and VLP abundances before and after sleep using previously published data [11, 12]. The average bacterial abundance at the back of the tongue in SDB ($1.90 \pm 0.36 \times 10^7$ bacteria) was significantly lower ($p = 0.047$) than healthy individuals ($2.90 \pm 0.76 \times 10^7$ bacteria) before sleep, with SDB having approximately 1.01×10^7 less bacteria than healthy participants at that location (S9 Table) [11, 12]. All other paired location comparisons before sleep between healthy and SDB did not show any significant differences in bacterial concentration ($p > 0.05$; S9 Table). After sleep, bacterial abundances at the back of the tongue in SDB ($8.94 \pm 1.49 \times 10^7$ bacteria) were also significantly lower than healthy participants ($1.35 \pm 1.49 \times 10^7$ bacteria) by approximately 4.56×10^7 bacteria ($p = 0.019$; S9 Table). No other paired location comparisons between healthy and SDB bacterial counts after sleep showed a significant difference ($p > 0.05$; S9 Table).

Significant differences in VLP concentrations were identified for all locations before sleep between healthy and SDB participants ($p < 0.05$; S10 Table). Before sleep, SDB were 6.78×10^5 VLP higher at the temporomandibular joint ($p = 0.013$), 6.89×10^6 VLP higher at the gingivae ($p = 0.0089$) and 3.23×10^5 VLP higher at the tip of the tongue ($p = 0.018$) than healthy participants (S10 Table) [12]. However, SDBs were significantly lower in VLP abundances than healthy individuals at the back of the tongue ($p = 0.0041$), palate ($p = 0.0052$) and molars ($p = 0.0052$) with 1.15×10^7 , 5.57×10^5 and 4.36×10^6 less VLP respectively (S10 Table). After sleep, SDB had significantly lower VLP abundances than healthy individuals at the temporomandibular joint ($p = 0.045$), back of the tongue ($p = 0.045$), gingivae ($p = 0.025$) and molars ($p = 0.022$) with count differences of 2.26×10^7 , 2.02×10^7 , 1.49×10^7 and 2.11×10^7 VLP

respectively between health states (S10 Table) [12]. No significant difference was observed between VLP concentrations in healthy and SDBs at the palate and the tip of the tongue ($p > 0.05$; S10 Table).

Mann-Whitney U comparisons were also used to identify any significant differences in the average increases in bacteria and VLPs between healthy and SDB for each location. Average increases in bacterial concentrations at all locations in SDBs were not significantly different to the average bacterial increases at the corresponding location in healthy individuals ($p > 0.05$). The same could be said for the average VLP increases for each location between healthy and SDBs ($p > 0.05$).

Discussion

In this study, we present the absolute microbial abundances of oral microhabitats in SDB before and after sleep. Our results suggest that like the healthy paediatric oral microbiome [11, 12], the paediatric SDB oral cavity is numerically heterogeneous in bacteria and VLP among microhabitats. Our data also supports our previous finding of a significant increase in bacterial and VLP populations at each microhabitat during sleep ($p < 0.05$; Figs 3 and 4; Tables 1 and 2) [11, 12]. Furthermore, we show the absolute VLP abundances in SDB significantly differ to healthy controls ($p < 0.05$). However, based on this study alone we cannot corroborate if these differences are a cause or result of SDB.

Previous taxonomic and absolute abundance profiles of the microbial communities in the healthy oral cavity have identified regions of heterogeneity among microhabitats [8, 11, 12]. These microbial patterns of spatial variation are thought to be influenced by factors such as oral anatomy, oral hygiene, moisture levels,

temperature gradients, pH gradients, salivary flow, abrasion (i.e. from the tongue), surface structure (i.e. soft shedding mucosa and non-shedding tooth surfaces) and host immune response [5, 7-11, 21-24]. Absolute abundance counts of the healthy paediatric oral cavity showed that bacterial heterogeneity was observed among locations before and after sleep, but only in VLP before sleep [11, 12]. Our data on SDB is consistent with this finding, but also shows heterogeneity in VLP after sleep (Figs 1 and 2). However, more regions of heterogeneity were observed in SDB than healthy participants. Most significant and non-significant bacterial microhabitat abundance comparisons in SDB were seen to closely resemble what was identified in healthy controls (Figs 1 and 2) [11, 12]. In addition, bacterial abundances before sleep at the tip of the tongue in SDB were approximately 3 million counts lower than the temporomandibular joint and 1 million counts higher than the palate ($p < 0.05$; Fig 1; Table 1). After sleep the temporomandibular joint was 12 million counts higher than the tip of the tongue, but 31 million counts lower than the gingivae ($p < 0.05$; Fig 1; Table 1). These regions of bacterial heterogeneity in SDB were not reported in healthy participants [11, 12].

In addition to the regions of VLP heterogeneity reported in healthy participants [12], SDB VLP counts at the palate were approximately 2, 3 and 5 million counts lower than the tip of tongue, molars and temporomandibular joint respectively, making it the location with significantly lower VLP in the SDB oral cavity before sleep ($p < 0.05$; Fig 2; Table 2). Other regions of VLP heterogeneity identified in SDB that were not identified in healthy controls were the 6 and 26 million lower counts of VLP at the molars compared to the back of tongue and gingivae respectively ($p < 0.05$; Fig 2; Table 2). However, the 16 million count difference reported between the back of the tongue and temporomandibular joint before sleep in healthy participants was not seen

to be significant in SDB ($p < 0.05$; Fig 2) [12]. All microhabitat VLP counts in the healthy paediatric oral cavity have been reported to be homogeneous after sleep [12]. Most sampled locations in SDB were also homogeneous in abundance to each other after sleep. However, unlike in healthy participants, VLP abundances at the back of the tongue and gingivae were 59 and 64 million counts higher than the palate after sleep respectively ($p < 0.05$; Fig 2; Table 2). As more regions of heterogeneity were observed in SDB this could suggest that the microhabitats in SDB are more distinct compared to healthy controls. This could be a result of greater differences in the anatomical and environmental factors mentioned above between microhabitats in SDB compared to healthy [5, 7-11, 21-24]. However, as these factors were not examined in this study, further research is required to understand if and how these conditions vary within the oral microhabitats of SDB.

We speculate that the majority of VLPs presented in this study are bacteriophages due to their close association with their bacterial hosts and high abundance in the environment [25-27]. Bacteriophages are an established component of the oral microbiome and are thought to be involved in shaping the bacterial communities residing there through their lytic and lysogenic lifecycles [25, 28, 29]. However, it is speculated that most of the oral bacteriophages are lysogenic, which enhances the transfer of genetic material within the environment [30-32]. It is through the transfer of genetic material that bacteria acquire new gene functions [31], such as antibiotic resistance [33]. Therefore, it is important to monitor bacteriophage abundances in various health states as they have the potential to alter the microbial community's resistance to antibiotic treatments.

Individuals experiencing sleep related breathing disorders, such as OSA, are frequent mouth breathers throughout the day and during sleep [36, 37]. As a result, dry mouth has been reported with some studies proposing it as a significant symptom of OSA [37]. Upper airway resistance due to enlarged tonsils and adenoids are thought to be major contributors to why SDB breathe through their mouth [38]. As a result, the tip of the tongue in SDBs is expected to be the location most exposed to and influenced by the external environment. This means the microbial community residing there are constantly adapting to the changes in environmental conditions, making the tip of the tongue a competitive environment for the bacterial hosts. This competitive environment potentially makes it a location prone to invading pathogens. Therefore, viral lysis at this location could act as a line of defence against invading pathogens introduced from the external environment [39].

Snoring is another characteristic of SDB, where the soft palate, epiglottis, pharyngeal walls and tongue oscillate [40]. We speculate that snoring introduces friction at the back of the tongue that is not normally displayed to the same extent in healthy individuals. We speculate that the increased friction at the back of the tongue in SDB results in the shedding or dislodgment of mucosal fragments, bringing with it the bacterial communities residing there. As a result, the bacterial communities are less likely to develop to as high of abundance as healthy non-snorers. This may be reflected in the 46 million lower bacterial count at the back of the tongue after sleep in SDB than healthy controls ($p = 0.020$) [11, 12]. Bacterial counts were also 10 million counts lower in SDB at the back of the tongue before sleep compared to healthy controls ($p = 0.047$). Again, this may be a result of a dryer oral cavity due to mouth breathing throughout the day [36].

It has been reported that recurrent vibrations of the upper airways [41, 42] and exposure to respiratory viruses [43] results in localised inflammation and mucosal swelling [44-46]. Specifically, early life exposure to respiratory syncytial virus has been shown to increase upper airway lymphoid tissue and result in a higher obstructive apnoea-hypopnea index [43], highlighting a potential role for viruses in the pathophysiology of sleep apnoea. Here we show that VLP abundances in SDB were significantly different to healthy controls before and after sleep ($p < 0.05$). Half of the locations had significantly higher VLP counts than the healthy controls with differences of up to 7 million. The other half had significantly lower VLP, by counts of up to 12 million. After sleep, healthy controls were 23, 20, 15 and 21 million counts higher in VLP abundance at the temporomandibular joint, back of tongue, gingivae and molars respectively compared to SDB ($p < 0.05$). These differences in VLPs could again be due to variations in environmental conditions between health states, such as the already mentioned factors of salivary flow, oral dryness, anatomical differences or immune responses [5, 7-11, 21-24]. However, they could also indicate a difference in bacterial community structure between health states. Although no significant difference was observed in the bacterial abundances between healthy and SDB for most microhabitats, differences in the bacterial taxonomy could still be present. The differences in VLP abundance between healthy and SDB may reflect different viral communities present with different host ranges. Therefore, bacterial 16S analysis is required to identify these possible taxonomic differences as flow cytometry without specific bacterial probes cannot identify taxonomy.

In conclusion, we observed that oral microhabitats in paediatric SDB significantly differ in microbial abundance to healthy paediatric participants. The main differences were observed between VLPs, suggesting a possible difference in the

bacterial taxonomy as opposed to abundance. With increasing studies showing the importance of the oral microbiome in many metabolic pathways, it is imperative to understand what effect perturbations to these communities have on our health. This is none so more important than in the paediatric age group where growth and development is still taking place. Further studies in characterising the bacterial taxonomy of microhabitats in paediatric SDB before and after sleep will provide further insight into what, if any, differences are present in the oral microbiome, and the potential impact these changes have on overall health. However, care should be taken when interoperating results, as we have shown biomass in the oral cavity varies through space and time.

Acknowledgements

This study was supported by Flinders University, Adelaide University and grants from the Australian Research Council, Channel 7 Research Foundation and the Australian Office of Learning and Teaching. We would like to thank the staff at the Flinders Medical Centre Flow Cytometry Unit for their technical support throughout the study.

References

1. Katz ES, D'Ambrosio CM. Pathophysiology of pediatric obstructive sleep apnea. *Proceedings of the American Thoracic Society*. 2008;5(2):253-62. doi: 10.1513/pats.200707-111MG. PubMed PMID: 18250219; PubMed Central PMCID: PMC2645256.
2. Lumeng JC, Chervin RD. Epidemiology of pediatric obstructive sleep apnea. *Proceedings of the American Thoracic Society*. 2008;5(2):242-52. doi: 10.1513/pats.200708-135MG. PubMed PMID: 18250218; PubMed Central PMCID: PMC2645255.
3. Marcus CL. Sleep-disordered breathing in children. *Am J Respir Crit Care Med*. 2001;164(1):16-30. doi: 10.1164/ajrccm.164.1.2008171. PubMed PMID: 11435234.
4. Gozal D, O'Brien LM. Snoring and obstructive sleep apnoea in children: why should we treat? *Paediatr Respir Rev*. 2004;5 Suppl A:S371-6. Epub 2004/02/26. PubMed PMID: 14980299.
5. Dewhirst FE, Chen T, Izard J, Paster BJ, Tanner AC, Yu WH, et al. The human oral microbiome. *Journal of bacteriology*. 2010;192(19):5002-17. doi: 10.1128/JB.00542-10. PubMed PMID: 20656903; PubMed Central PMCID: PMC2944498.
6. Bik EM, Long CD, Armitage GC, Loomer P, Emerson J, Mongodin EF, et al. Bacterial diversity in the oral cavity of 10 healthy individuals. *The ISME journal*. 2010;4(8):962-74. doi: 10.1038/ismej.2010.30. PubMed PMID: 20336157; PubMed Central PMCID: PMC2941673.
7. Aas JA, Paster BJ, Stokes LN, Olsen I, Dewhirst FE. Defining the normal bacterial flora of the oral cavity. *Journal of clinical microbiology*. 2005;43(11):5721-32.

doi: 10.1128/JCM.43.11.5721-5732.2005. PubMed PMID: 16272510; PubMed Central PMCID: PMC1287824.

8. Xu X, He J, Xue J, Wang Y, Li K, Zhang K, et al. Oral cavity contains distinct niches with dynamic microbial communities. *Environ Microbiol.* 2015;17(3):699-710. doi: 10.1111/1462-2920.12502. PubMed PMID: 24800728.

9. Aframian DJ, Davidowitz T, Benoliel R. The distribution of oral mucosal pH values in healthy saliva secretors. *Oral diseases.* 2006;12(4):420-3. Epub 2006/06/24. doi: 10.1111/j.1601-0825.2005.01217.x. PubMed PMID: 16792729.

10. Choi JE, Waddell JN, Lyons KM, Kieser JA. Intraoral pH and temperature during sleep with and without mouth breathing. *J Oral Rehabil.* 2016;43(5):356-63. Epub 2015/12/17. doi: 10.1111/joor.12372. PubMed PMID: 26666708.

11. Carlson-Jones J, Kontos A, Paterson J, Smith R, Dann L, Speck P, et al. Flow Cytometric Enumeration of Bacterial and Virus-Like Particle Populations in the Human Oral Cavity Pre and Post Sleep. *J Sleep Res.* 2016;25:86-. PubMed PMID: WOS:000393032700215.

12. Carlson-Jones JA, Kontos A, Kennedy D, Martin J, McKerral J, Paterson JS, et al. The microbial abundance dynamics of the human oral cavity before and after sleep. *Plos One (Submitted).* 2018.

13. Benedict C, Vogel H, Jonas W, Woting A, Blaut M, Schurmann A, et al. Gut microbiota and glucometabolic alterations in response to recurrent partial sleep deprivation in normal-weight young individuals. *Mol Metab.* 2016;5(12):1175-86. Epub 2016/12/03. doi: 10.1016/j.molmet.2016.10.003. PubMed PMID: 27900260; PubMed Central PMCID: PMCPMC5123208.

14. Anderson JR, Carroll I, Azcarate-Peril MA, Rochette AD, Heinberg LJ, Peat C, et al. A preliminary examination of gut microbiota, sleep, and cognitive flexibility in

healthy older adults. *Sleep medicine*. 2017;38:104-7. doi: 10.1016/j.sleep.2017.07.018. PubMed PMID: 29031742.

15. Voigt RM, Forsyth CB, Green SJ, Mutlu E, Engen P, Vitaterna MH, et al. Circadian disorganization alters intestinal microbiota. *Plos One*. 2014;9(5):e97500. doi: 10.1371/journal.pone.0097500. PubMed PMID: 24848969; PubMed Central PMCID: PMC4029760.

16. Brussaard CP. Optimization of procedures for counting viruses by flow cytometry. *Appl Environ Microbiol*. 2004;70(3):1506-13. PubMed PMID: 15006772; PubMed Central PMCID: PMC368280.

17. Gasol JM, Del Giorgio PA. Using flow cytometry for counting natural planktonic bacteria and understanding the structure of planktonic bacterial communities. *Sci Mar*. 2000;64(2):197-224. PubMed PMID: ISI:000088019800007.

18. Marie D, Brussaard CPD, Thyraug R, Bratbak G, Vaulot D. Enumeration of marine viruses in culture and natural samples by flow cytometry. *Appl Environ Microbiol*. 1999;65(1):45-52. Epub 1999/01/05 21:58. PubMed PMID: 9872758; PubMed Central PMCID: PMCPMC90981.

19. Marie D, Partensky F, Jacquet S, Vaulot D. Enumeration and Cell Cycle Analysis of Natural Populations of Marine Picoplankton by Flow Cytometry Using the Nucleic Acid Stain SYBR Green I. *Appl Environ Microbiol*. 1997;63(1):186-93. PubMed PMID: 16535483; PubMed Central PMCID: PMC1389098.

20. Storey JD. A direct approach to false discovery rates. *J Roy Stat Soc B*. 2002;64:479-98. doi: Unsp 1369-7412/02/64479

Doi 10.1111/1467-9868.00346. PubMed PMID: WOS:000177425500009.

21. Human Microbiome Project C. Structure, function and diversity of the healthy human microbiome. *Nature*. 2012;486(7402):207-14. doi: 10.1038/nature11234. PubMed PMID: 22699609; PubMed Central PMCID: PMC3564958.
22. Simon-Soro A, Tomas I, Cabrera-Rubio R, Catalan MD, Nyvad B, Mira A. Microbial geography of the oral cavity. *Journal of dental research*. 2013;92(7):616-21. Epub 2013/05/16. doi: 10.1177/0022034513488119. PubMed PMID: 23674263.
23. Mager DL, Ximenez-Fyvie LA, Haffajee AD, Socransky SS. Distribution of selected bacterial species on intraoral surfaces. *J Clin Periodontol*. 2003;30(7):644-54. Epub 2003/07/02. PubMed PMID: 12834503.
24. Proctor DM, Fukuyama JA, Loomer PM, Armitage GC, Lee SA, Davis NM, et al. A spatial gradient of bacterial diversity in the human oral cavity shaped by salivary flow. *Nat Commun*. 2018;9(1):681. Epub 2018/02/16. doi: 10.1038/s41467-018-02900-1. PubMed PMID: 29445174; PubMed Central PMCID: PMC5813034.
25. Pride DT, Salzman J, Haynes M, Rohwer F, Davis-Long C, White RA, 3rd, et al. Evidence of a robust resident bacteriophage population revealed through analysis of the human salivary virome. *ISME J*. 2012;6(5):915-26. Epub 2011/12/14. doi: 10.1038/ismej.2011.169. PubMed PMID: 22158393; PubMed Central PMCID: PMC3329113.
26. Abeles SR, Pride DT. Molecular bases and role of viruses in the human microbiome. *Journal of molecular biology*. 2014;426(23):3892-906. doi: 10.1016/j.jmb.2014.07.002. PubMed PMID: 25020228.
27. Carlson-Jones JA, Paterson JS, Newton K, Smith RJ, Dann LM, Speck P, et al. Enumerating Virus-Like Particles and Bacterial Populations in the Sinuses of Chronic Rhinosinusitis Patients Using Flow Cytometry. *Plos One*. 2016;11(5):e0155003. doi:

10.1371/journal.pone.0155003. PubMed PMID: 27171169; PubMed Central PMCID: PMC4865123.

28. Hitch G, Pratten J, Taylor PW. Isolation of bacteriophages from the oral cavity. *Letters in applied microbiology*. 2004;39(2):215-9. doi: 10.1111/j.1472-765X.2004.01565.x. PubMed PMID: 15242464.

29. Ly M, Abeles SR, Boehm TK, Robles-Sikisaka R, Naidu M, Santiago-Rodriguez T, et al. Altered oral viral ecology in association with periodontal disease. *mBio*. 2014;5(3):e01133-14. doi: 10.1128/mBio.01133-14. PubMed PMID: 24846382; PubMed Central PMCID: PMC4030452.

30. Roberts AP, Mullany P. Genetic basis of horizontal gene transfer among oral bacteria. *Periodontol 2000*. 2006;42:36-46. doi: 10.1111/j.1600-0757.2006.00149.x. PubMed PMID: 16930305.

31. Stevens RH, Porras OD, Delisle AL. Bacteriophages induced from lysogenic root canal isolates of *Enterococcus faecalis*. *Oral microbiology and immunology*. 2009;24(4):278-84. doi: 10.1111/j.1399-302X.2009.00506.x. PubMed PMID: 19572888.

32. Edlund A, Santiago-Rodriguez TM, Boehm TK, Pride DT. Bacteriophage and their potential roles in the human oral cavity. *Journal of oral microbiology*. 2015;7:27423. doi: 10.3402/jom.v7.27423. PubMed PMID: 25861745; PubMed Central PMCID: PMC4393417.

33. Abeles SR, Robles-Sikisaka R, Ly M, Lum AG, Salzman J, Boehm TK, et al. Human oral viruses are personal, persistent and gender-consistent. *Isme J*. 2014;8(9):1753-67. Epub 2014/03/22. doi: 10.1038/ismej.2014.31. PubMed PMID: 24646696; PubMed Central PMCID: PMCPMC4139723.

34. Knowles B, Silveira CB, Bailey BA, Barott K, Cantu VA, Cobian-Guemes AG, et al. Lytic to temperate switching of viral communities. *Nature*. 2016;531(7595):466-70. doi: 10.1038/nature17193. PubMed PMID: 26982729.
35. Silveira CB, Rohwer FL. Piggyback-the-Winner in host-associated microbial communities. *NPJ biofilms and microbiomes*. 2016;2:16010. Epub 2017/07/20. doi: 10.1038/npjbiofilms.2016.10. PubMed PMID: 28721247; PubMed Central PMCID: PMC5515262.
36. Izu SC, Itamoto CH, Pradella-Hallinan M, Pizarro GU, Tufik S, Pignatari S, et al. Obstructive sleep apnea syndrome (OSAS) in mouth breathing children. *Brazilian journal of otorhinolaryngology*. 2010;76(5):552-6. PubMed PMID: 20963335.
37. Oksenberg A, Fromm P, Melamed S. Dry mouth upon awakening in obstructive sleep apnea. *J Sleep Res*. 2006;15(3):317-20. doi: DOI 10.1111/j.1365-2869.2006.00527.x. PubMed PMID: WOS:000239691900010.
38. Marcus CL. Sleep-disordered breathing in children. *Current opinion in pediatrics*. 2000;12(3):208-12. PubMed PMID: 10836154.
39. Barr JJ, Youle M, Rohwer F. Innate and acquired bacteriophage-mediated immunity. *Bacteriophage*. 2013;3(3):e25857. doi: 10.4161/bact.25857. PubMed PMID: 24228227; PubMed Central PMCID: PMC3821666.
40. Liistro G, Stanescu DC, Veriter C, Rodenstein DO, Aubert-Tulkens G. Pattern of snoring in obstructive sleep apnea patients and in heavy snorers. *Sleep*. 1991;14(6):517-25. PubMed PMID: 1798885.
41. Puig F, Rico F, Almendros I, Montserrat JM, Navajas D, Farre R. Vibration enhances interleukin-8 release in a cell model of snoring-induced airway inflammation. *Sleep*. 2005;28(10):1312-6. PubMed PMID: 16295217.

42. Almendros I, Carreras A, Ramirez J, Montserrat JM, Navajas D, Farre R. Upper airway collapse and reopening induce inflammation in a sleep apnoea model. *Eur Respir J*. 2008;32(2):399-404. doi: 10.1183/09031936.00161607. PubMed PMID: 18448490.
43. Snow A, Dayyat E, Montgomery-Downs HE, Kheirandish-Gozal L, Gozal D. Pediatric obstructive sleep apnea: a potential late consequence of respiratory syncytial virus bronchiolitis. *Pediatr Pulmonol*. 2009;44(12):1186-91. doi: 10.1002/ppul.21109. PubMed PMID: 19911395.
44. Serpero LD, Kheirandish-Gozal L, Dayyat E, Goldman JL, Kim J, Gozal D. A mixed cell culture model for assessment of proliferation in tonsillar tissues from children with obstructive sleep apnea or recurrent tonsillitis. *The Laryngoscope*. 2009;119(5):1005-10. doi: 10.1002/lary.20147. PubMed PMID: 19266584; PubMed Central PMCID: PMC2892471.
45. Kim J, Bhattacharjee R, Dayyat E, Snow AB, Kheirandish-Gozal L, Goldman JL, et al. Increased cellular proliferation and inflammatory cytokines in tonsils derived from children with obstructive sleep apnea. *Pediatr Res*. 2009;66(4):423-8. doi: 10.1203/PDR.0b013e3181b453e3. PubMed PMID: 19581829; PubMed Central PMCID: PMC2892472.
46. Goldbart AD, Mager E, Veling MC, Goldman JL, Kheirandish-Gozal L, Serpero LD, et al. Neurotrophins and tonsillar hypertrophy in children with obstructive sleep apnea. *Pediatr Res*. 2007;62(4):489-94. doi: 10.1203/PDR.0b013e31814257ed. PubMed PMID: 17667845; PubMed Central PMCID: PMC3693447.

Supplementary information

S1 Table. SDB bacterial abundances in the oral cavity before sleep for each participant. Eluted swab samples were prepared and run three times on the flow cytometer as a method replicate (R).

Participant	Temporomandibular joint			Back of tongue			Gingivae			Palate			Molars			Tip of tongue		
	R1	R2	R3	R1	R2	R3	R1	R2	R3	R1	R2	R3	R1	R2	R3	R1	R2	R3
1	9.3E+06	8.9E+06	1.0E+07	2.7E+07	2.5E+07	2.8E+07	9.0E+07	6.4E+07	5.9E+07	3.4E+06	3.8E+06	2.7E+06	6.9E+06	5.1E+06	5.1E+06	3.6E+06	3.7E+06	3.0E+06
2	8.2E+06	1.0E+07	8.7E+06	4.0E+07	2.8E+07	3.4E+07	5.9E+07	6.3E+07	6.8E+07	7.0E+06	6.7E+06	6.7E+06	6.2E+06	6.7E+06	7.9E+06	1.1E+07	9.8E+06	9.5E+06
3	2.0E+07	1.5E+07	1.7E+07	5.4E+07	5.9E+07	5.6E+07	1.2E+08	9.1E+07	1.1E+08	1.0E+06	9.9E+05	9.9E+05	8.4E+06	6.3E+06	5.9E+06	3.9E+06	4.1E+06	4.2E+06
4	3.6E+06	4.5E+06	5.4E+06	1.3E+07	1.1E+07	1.1E+07	7.2E+07	7.4E+07	1.0E+08	4.9E+05	3.0E+05	7.1E+05	7.4E+05	5.4E+05	1.2E+06	2.0E+06	1.3E+06	1.7E+06
5	8.2E+06	1.0E+07	7.0E+06	3.3E+07	3.0E+07	2.4E+07	5.1E+07	4.7E+07	3.2E+07	4.4E+05	2.1E+05	3.7E+05	1.1E+07	1.1E+07	7.5E+06	1.8E+06	2.0E+06	2.4E+06
6	3.2E+06	4.4E+06	2.8E+06	1.4E+07	1.6E+07	1.8E+07	1.5E+06	2.4E+06	2.3E+06	1.2E+05	2.9E+05	2.1E+05	3.1E+06	2.5E+06	3.5E+06	6.1E+06	6.1E+06	5.2E+06
7	6.9E+06	7.8E+06	7.9E+06	5.2E+07	5.3E+07	6.3E+07	1.7E+07	1.4E+07	2.0E+07	1.0E+06	9.1E+05	1.1E+06	8.1E+05	1.6E+06	1.1E+06	4.8E+05	6.4E+05	7.2E+05
8	6.7E+06	6.2E+06	6.7E+06	8.2E+06	8.3E+06	8.4E+06	1.6E+07	1.5E+07	1.1E+07	2.9E+05	2.8E+05	2.7E+05	5.4E+05	4.3E+05	6.5E+05	3.8E+05	6.6E+05	7.8E+05
9	2.2E+06	2.3E+06	2.2E+06	2.6E+07	3.2E+07	2.8E+07	2.6E+06	2.8E+06	3.7E+06	3.1E+05	3.1E+05	3.6E+05	3.0E+05	2.3E+05	2.2E+05	1.5E+06	1.6E+06	1.6E+06
10	1.9E+06	1.9E+06	1.8E+06	7.5E+06	8.0E+06	7.4E+06	5.2E+06	4.8E+06	4.1E+06	1.5E+05	1.2E+05	4.4E+04	1.6E+06	1.2E+06	1.4E+06	8.1E+05	8.5E+05	5.9E+05
11	2.0E+06	4.1E+06	2.6E+06	7.1E+06	8.4E+06	6.8E+06	3.3E+06	4.2E+06	3.2E+06	1.6E+04	3.6E+04	6.2E+04	4.0E+05	5.2E+05	6.3E+05	1.9E+06	2.4E+06	3.0E+06
12	1.9E+06	1.3E+06	1.7E+06	4.5E+06	4.7E+06	3.5E+06	2.5E+07	2.2E+07	1.9E+07	8.3E+04	6.8E+04	7.2E+04	7.5E+06	9.8E+06	7.7E+06	4.8E+05	4.3E+05	3.7E+05
13	1.0E+06	1.4E+06	1.1E+06	1.1E+07	9.4E+06	1.1E+07	3.7E+06	4.4E+06	4.6E+06	9.8E+04	1.1E+05	9.5E+04	1.1E+06	1.4E+06	1.6E+06	4.7E+04	7.8E+04	4.0E+04
14	5.3E+05	7.0E+05	6.1E+05	2.2E+07	1.9E+07	1.6E+07	2.0E+06	2.7E+06	1.8E+06	1.2E+05	1.2E+05	1.5E+05	1.4E+06	1.3E+06	1.2E+06	2.8E+05	3.6E+05	1.3E+05
15	3.6E+05	3.0E+05	5.0E+05	1.6E+06	1.1E+06	9.1E+05	1.2E+06	4.8E+05	7.9E+05	8.9E+04	1.4E+05	6.5E+04	4.2E+05	2.0E+05	3.0E+05	9.7E+05	1.3E+06	7.4E+05
16	4.7E+05	3.9E+05	4.4E+05	1.7E+05	3.1E+05	2.3E+05	3.8E+06	7.1E+06	8.2E+06	2.8E+04	4.5E+04	6.1E+04	4.3E+05	3.6E+05	4.1E+05	1.2E+05	8.6E+04	1.5E+05
17	3.3E+06	4.5E+06	3.2E+06	2.4E+07	1.9E+07	1.9E+07	1.0E+07	1.0E+07	8.6E+06	4.3E+06	3.9E+06	3.8E+06	1.2E+07	1.7E+07	1.1E+07	2.6E+06	1.4E+06	2.1E+06
18	6.2E+05	8.5E+05	7.8E+05	7.8E+05	6.6E+05	6.1E+05	3.9E+06	4.5E+06	3.7E+06	1.9E+05	2.0E+05	1.5E+05	1.3E+05	1.2E+05	1.1E+05	1.2E+06	1.3E+06	9.0E+05
19	5.5E+06	3.5E+06	8.6E+06	1.4E+07	1.5E+07	1.6E+07	2.2E+07	2.2E+07	2.0E+07	3.1E+05	2.8E+05	2.2E+05	1.0E+06	9.4E+05	1.0E+06	6.6E+05	6.6E+05	4.6E+05
20	2.9E+06	1.6E+06	2.2E+06	2.9E+07	2.4E+07	2.4E+07	2.8E+07	3.5E+07	3.0E+07	4.4E+05	3.3E+05	3.5E+05	6.2E+05	8.3E+05	9.8E+05	5.7E+05	4.8E+05	6.4E+05

S2 Table. SDB bacterial abundances in the oral cavity after sleep for each participant. Eluted swab samples were prepared and run three times on the flow cytometer as a method replicate (R).

Participant	Temporomandibular joint			Back of tongue			Gingivae			Palate			Molars			Tip of tongue		
	R1	R2	R3	R1	R2	R3	R1	R2	R3	R1	R2	R3	R1	R2	R3	R1	R2	R3
1	4.5E+07	2.4E+07	3.7E+07	6.5E+07	1.0E+08	8.8E+07	6.4E+07	5.6E+07	4.0E+07	6.3E+05	4.2E+05	3.5E+05	1.1E+07	2.2E+07	1.5E+07	9.3E+06	1.4E+07	1.1E+07
2	5.9E+07	5.8E+07	6.9E+07	1.7E+08	1.4E+08	1.4E+08	1.1E+08	1.1E+08	1.3E+08	9.1E+06	7.7E+06	7.5E+06	8.4E+07	1.1E+08	9.5E+07	4.2E+07	6.3E+07	1.7E+08
3	3.3E+06	7.9E+06	5.9E+06	1.9E+08	2.4E+08	2.8E+08	2.8E+08	4.0E+08	3.1E+08	6.1E+06	8.0E+06	6.8E+06	5.3E+06	9.4E+06	6.6E+06	2.2E+07	3.3E+07	2.2E+07
4	2.2E+06	2.4E+06	1.7E+06	2.3E+07	8.3E+06	2.4E+07	5.4E+07	3.1E+07	5.0E+07	5.6E+05	4.0E+05	3.5E+05	2.0E+06	1.6E+06	1.3E+06	1.0E+06	1.2E+06	1.3E+06
5	1.7E+07	2.0E+07	1.4E+07	1.4E+08	1.6E+08	1.6E+08	1.2E+08	1.2E+08	1.5E+08	1.4E+07	1.7E+07	1.4E+07	5.5E+07	6.6E+07	5.0E+07	2.3E+07	3.6E+07	3.0E+07
6	1.9E+07	1.4E+07	1.9E+07	1.3E+08	1.7E+08	1.2E+08	2.4E+07	2.3E+07	1.5E+07	7.3E+05	9.8E+05	9.7E+05	3.6E+06	2.8E+06	3.4E+06	3.4E+06	4.8E+06	2.9E+06
7	2.6E+06	2.1E+06	3.1E+06	1.1E+08	8.7E+07	9.9E+07	2.3E+07	2.1E+07	3.1E+07	6.3E+05	6.8E+05	7.1E+05	5.9E+06	6.9E+06	4.6E+06	3.3E+06	3.5E+06	3.4E+06
8	4.2E+07	5.1E+07	4.3E+07	6.3E+07	6.2E+07	5.5E+07	4.5E+07	3.7E+07	5.8E+07	4.1E+05	4.2E+05	3.8E+05	1.7E+06	2.6E+06	2.6E+06	2.5E+06	2.8E+06	2.8E+06
9	3.7E+06	4.2E+06	4.4E+06	3.1E+07	3.5E+07	3.0E+07	1.5E+06	2.7E+06	1.5E+06	3.1E+06	3.4E+06	2.6E+06	2.2E+07	1.7E+07	1.4E+07	1.4E+06	2.1E+06	2.0E+06
10	6.3E+07	3.6E+07	5.8E+07	6.4E+07	7.9E+07	7.3E+07	3.0E+06	2.1E+06	3.4E+06	4.5E+06	3.4E+06	5.0E+06	2.9E+06	3.8E+06	4.2E+06	9.5E+05	8.7E+05	9.6E+05
11	1.4E+07	8.9E+06	8.3E+06	5.2E+07	5.2E+07	6.4E+07	8.4E+06	1.0E+07	8.9E+06	1.0E+06	1.8E+06	1.0E+06	1.1E+07	6.7E+06	1.3E+07	2.8E+06	3.3E+06	3.2E+06
12	1.3E+07	1.3E+07	8.4E+06	2.6E+07	2.8E+07	2.5E+07	5.6E+06	5.4E+06	4.2E+06	1.1E+06	1.2E+06	9.7E+05	8.9E+06	6.8E+06	8.1E+06	8.9E+06	9.8E+06	8.4E+06
13	3.1E+07	2.6E+07	3.5E+07	1.2E+08	1.4E+08	1.2E+08	4.6E+07	4.9E+07	4.5E+07	3.1E+06	2.7E+06	2.3E+06	6.9E+06	5.6E+06	5.9E+06	2.3E+06	3.1E+06	2.5E+06
14	1.4E+08	1.3E+08	1.2E+08	1.9E+08	1.6E+08	8.7E+07	4.2E+07	7.2E+07	4.6E+07	5.8E+06	1.1E+07	9.9E+06	2.8E+07	3.0E+07	1.9E+07	8.3E+06	6.1E+06	5.7E+06
15	4.1E+07	3.2E+07	4.3E+07	1.2E+08	1.0E+08	1.2E+08	1.4E+07	2.1E+07	3.3E+07	1.0E+07	7.5E+06	7.1E+06	8.0E+06	1.3E+07	6.1E+06	1.5E+07	2.4E+07	1.9E+07
16	6.2E+06	7.7E+06	8.3E+06	4.8E+06	4.3E+06	2.7E+06	7.7E+06	1.4E+07	7.0E+06	1.5E+06	1.2E+06	1.8E+06	9.2E+06	1.6E+07	1.8E+07	4.4E+06	6.1E+06	3.8E+06
17	3.4E+07	6.6E+07	2.9E+07	9.2E+07	3.7E+08	1.4E+08	7.5E+07	1.1E+08	1.4E+08	7.3E+05	7.3E+05	6.4E+05	2.2E+06	3.0E+06	8.1E+06	1.4E+07	3.9E+07	2.5E+07
18	2.3E+06	2.3E+06	2.2E+06	1.6E+07	7.8E+06	1.1E+07	3.8E+07	3.5E+07	3.5E+07	9.7E+06	9.3E+06	7.6E+06	3.2E+06	3.3E+06	5.6E+06	3.6E+07	3.6E+07	3.8E+07
19	4.2E+06	4.1E+06	4.1E+06	2.2E+07	1.8E+07	2.1E+07	6.7E+07	6.4E+07	4.7E+07	2.9E+06	4.4E+06	3.3E+06	1.6E+07	1.3E+07	1.4E+07	1.9E+06	2.0E+06	2.0E+06
20	9.4E+06	1.0E+07	7.6E+06	3.9E+07	4.0E+07	3.6E+07	3.3E+07	5.2E+07	2.8E+07	7.1E+05	6.1E+05	5.9E+05	1.4E+07	1.3E+07	9.1E+06	1.5E+07	1.6E+07	1.5E+07

S3 Table. SDB VLP abundances in the oral cavity before sleep for each participant. Eluted swab samples were prepared and run three times on the flow cytometer as a method replicate (R).

Participant	Temporomandibular joint			Back of tongue			Gingivae			Palate			Molars			Tip of tongue		
	R1	R2	R3	R1	R2	R3	R1	R2	R3	R1	R2	R3	R1	R2	R3	R1	R2	R3
1	7.1E+06	6.0E+06	9.3E+06	1.2E+07	1.1E+07	1.3E+07	1.1E+08	9.9E+07	9.0E+07	1.4E+06	1.6E+06	1.4E+06	1.3E+07	1.4E+07	1.3E+07	2.9E+06	2.7E+06	3.5E+06
2	3.7E+07	4.7E+07	3.9E+07	4.4E+07	2.7E+07	3.9E+07	1.3E+08	1.5E+08	7.9E+07	1.2E+07	1.1E+07	1.3E+07	2.5E+07	2.4E+07	2.3E+07	3.1E+07	2.5E+07	2.8E+07
3	1.0E+07	9.3E+06	1.0E+07	1.3E+07	1.4E+07	1.7E+07	1.5E+08	1.1E+08	1.4E+08	4.8E+05	5.0E+05	5.1E+05	4.8E+06	4.1E+06	4.5E+06	1.1E+06	9.3E+05	9.5E+05
4	4.8E+06	3.1E+06	5.6E+06	2.5E+06	2.6E+06	3.9E+06	1.3E+07	1.2E+07	1.6E+07	8.6E+05	7.6E+05	6.2E+05	9.0E+05	1.2E+06	1.1E+06	1.0E+06	6.3E+05	1.1E+06
5	2.0E+07	1.7E+07	1.7E+07	2.1E+07	2.1E+07	1.6E+07	1.5E+07	1.0E+07	1.3E+07	4.9E+05	4.5E+05	4.8E+05	1.5E+07	1.9E+07	1.4E+07	1.1E+07	1.4E+07	1.7E+07
6	4.6E+05	6.7E+05	5.2E+05	2.1E+06	2.4E+06	3.1E+06	1.1E+06	1.6E+06	1.4E+06	7.0E+04	4.4E+04	3.4E+04	1.7E+06	1.5E+06	1.7E+06	3.4E+06	4.5E+06	3.8E+06
7	1.6E+06	7.6E+05	1.3E+06	1.8E+07	1.5E+07	2.4E+07	5.3E+06	4.7E+06	5.5E+06	4.2E+05	3.1E+05	5.1E+05	1.4E+06	8.6E+05	5.9E+05	1.1E+06	4.4E+05	1.5E+06
8	3.8E+06	5.8E+06	3.2E+06	3.2E+06	3.0E+06	2.3E+06	6.0E+06	4.6E+06	6.1E+06	1.1E+05	7.9E+04	1.2E+05	6.6E+05	1.0E+06	1.2E+06	5.4E+05	8.3E+05	7.3E+05
9	9.8E+06	8.5E+06	3.8E+06	4.6E+06	4.9E+06	5.0E+06	2.7E+06	4.2E+06	2.2E+06	3.0E+06	2.2E+06	3.3E+06	3.0E+05	2.5E+05	2.5E+05	8.1E+06	7.9E+06	1.0E+07
10	1.2E+06	9.6E+05	1.4E+06	2.5E+06	3.3E+06	2.8E+06	1.6E+06	8.7E+05	9.4E+05	9.9E+04	4.9E+04	6.7E+04	4.7E+05	4.1E+05	1.1E+06	3.4E+05	2.4E+05	3.1E+05
11	1.4E+07	1.9E+07	1.9E+07	2.2E+06	2.3E+06	4.2E+06	6.1E+06	4.5E+06	7.1E+06	7.0E+03	2.9E+04	1.6E+05	1.0E+06	1.3E+06	7.7E+05	4.0E+06	2.7E+06	4.9E+06
12	5.4E+06	4.3E+06	6.4E+06	4.0E+06	3.2E+06	3.4E+06	5.9E+07	3.5E+07	4.8E+07	1.7E+05	2.0E+05	1.2E+05	4.5E+06	5.0E+06	4.8E+06	1.1E+06	1.5E+06	1.1E+06
13	7.4E+05	1.3E+06	1.6E+06	1.5E+07	1.4E+07	2.3E+07	1.8E+06	2.7E+06	2.5E+06	3.0E+05	8.8E+04	5.6E+04	2.4E+06	4.1E+06	6.2E+06	1.1E+06	6.1E+05	4.1E+05
14	3.3E+05	3.1E+05	6.7E+04	2.9E+06	2.2E+06	2.2E+06	2.3E+06	1.9E+06	2.1E+06	1.8E+04	9.9E+03	1.0E+04	3.8E+06	8.0E+06	2.5E+06	4.8E+04	5.2E+04	3.8E+04
15	5.1E+05	2.3E+05	1.9E+05	2.2E+06	8.1E+05	1.7E+06	1.1E+06	1.3E+06	3.6E+06	4.1E+04	5.8E+04	5.5E+04	2.6E+05	2.5E+05	1.8E+05	3.2E+06	1.6E+06	1.4E+06
16	1.7E+05	1.6E+05	9.4E+04	3.1E+05	3.9E+05	2.3E+05	3.1E+05	5.0E+05	5.3E+05	3.4E+04	6.5E+04	3.7E+04	1.7E+05	3.3E+05	1.8E+05	2.2E+05	1.8E+05	2.5E+05
17	2.2E+06	2.8E+06	2.2E+06	2.6E+07	1.6E+07	2.3E+07	5.3E+06	7.9E+06	5.5E+06	5.6E+06	6.1E+06	5.6E+06	5.6E+06	1.0E+07	1.4E+07	1.8E+06	2.0E+06	1.8E+06
18	6.7E+05	1.3E+06	1.5E+06	6.0E+05	4.8E+05	7.2E+05	6.1E+05	6.7E+05	1.1E+06	2.2E+05	2.8E+05	1.7E+05	1.9E+05	3.0E+05	4.2E+05	2.1E+06	8.9E+05	4.4E+05
19	1.5E+06	1.7E+06	2.8E+06	1.9E+07	2.7E+07	2.9E+07	5.2E+07	3.7E+07	6.5E+07	1.5E+06	1.8E+06	1.1E+06	4.2E+06	2.4E+06	2.9E+06	1.1E+06	8.7E+05	1.4E+06
20	1.9E+06	8.1E+05	1.9E+06	1.6E+07	1.7E+07	1.5E+07	1.1E+08	1.1E+08	8.4E+07	1.6E+06	6.6E+05	8.2E+05	1.5E+06	1.6E+06	1.5E+06	3.3E+06	3.2E+06	4.3E+06

S4 Table. SDB VLP abundances in the oral cavity after sleep for each participant. Eluted swab samples were prepared and run three times on the flow cytometer as a method replicate (R).

Participant	Temporomandibular joint			Back of tongue			Gingivae			Palate			Molars			Tip of tongue		
	R1	R2	R3	R1	R2	R3	R1	R2	R3	R1	R2	R3	R1	R2	R3	R1	R2	R3
1	2.8E+07	3.0E+07	3.5E+07	7.3E+06	8.3E+06	9.7E+06	5.8E+07	4.7E+07	6.8E+07	7.8E+04	8.6E+05	1.2E+05	9.5E+06	1.1E+07	9.2E+06	2.5E+06	3.2E+06	2.5E+06
2	2.0E+08	2.5E+08	2.4E+08	2.0E+08	1.3E+08	1.4E+08	4.6E+08	4.2E+08	3.3E+08	1.7E+08	1.1E+08	8.6E+07	2.9E+08	2.9E+08	2.3E+08	5.2E+08	7.1E+08	2.1E+09
3	3.1E+06	1.1E+07	7.6E+06	9.8E+07	1.3E+08	2.4E+08	6.2E+08	5.3E+08	4.3E+08	6.5E+06	9.9E+06	8.5E+06	7.4E+06	8.0E+06	6.9E+06	7.1E+06	7.0E+06	6.0E+06
4	4.2E+05	4.3E+05	8.1E+05	5.6E+06	4.8E+06	1.1E+07	1.1E+07	6.3E+06	1.2E+07	6.1E+05	6.0E+05	4.6E+05	8.5E+05	8.1E+05	2.4E+05	1.2E+06	8.8E+05	6.7E+05
5	4.8E+07	6.6E+07	1.2E+08	4.6E+08	4.3E+08	4.6E+08	5.7E+07	5.3E+07	5.9E+07	6.0E+07	6.7E+07	7.8E+07	1.7E+08	1.9E+08	2.8E+08	2.5E+08	1.8E+08	2.2E+08
6	2.5E+06	2.1E+06	2.7E+06	1.2E+08	2.8E+08	8.5E+07	2.3E+07	2.4E+07	1.8E+07	2.8E+06	1.9E+06	3.6E+06	3.6E+06	4.1E+06	4.4E+06	7.3E+06	9.2E+06	6.2E+06
7	2.4E+05	1.5E+05	1.8E+05	7.6E+06	5.5E+06	8.4E+06	3.9E+06	3.9E+06	5.2E+06	4.1E+05	6.5E+05	1.4E+06	3.6E+06	1.5E+06	2.7E+06	6.1E+05	5.7E+05	1.4E+06
8	4.3E+06	5.9E+06	3.9E+06	1.8E+06	1.6E+06	1.7E+06	2.2E+07	1.3E+07	3.0E+07	9.5E+04	7.1E+04	9.1E+04	3.0E+05	6.7E+05	3.9E+05	2.1E+05	2.0E+05	3.5E+05
9	4.7E+06	2.7E+06	3.4E+06	1.6E+07	1.3E+07	1.2E+07	2.0E+06	6.4E+06	3.8E+06	7.0E+06	5.5E+06	9.5E+06	7.1E+07	6.4E+07	5.1E+07	4.0E+06	4.2E+06	5.0E+06
10	2.7E+07	2.7E+07	2.6E+07	1.6E+07	1.2E+07	1.4E+07	1.2E+06	8.9E+05	7.0E+05	4.9E+06	6.2E+06	5.3E+06	4.3E+06	5.9E+06	5.3E+06	7.0E+05	1.1E+06	8.5E+05
11	4.6E+06	4.0E+06	6.4E+06	7.2E+06	4.6E+06	5.2E+06	4.7E+06	6.6E+06	7.1E+06	2.8E+06	2.4E+06	2.7E+06	6.1E+06	1.2E+07	1.0E+07	2.8E+06	1.7E+06	3.6E+06
12	5.3E+06	4.3E+06	4.2E+06	4.1E+06	5.1E+06	4.7E+06	2.8E+06	2.8E+06	2.6E+06	2.9E+05	4.3E+05	4.5E+05	4.3E+06	4.5E+06	3.4E+06	6.6E+05	6.9E+05	1.3E+06
13	4.7E+07	5.4E+07	7.9E+07	3.7E+07	4.7E+07	5.4E+07	1.2E+07	1.5E+07	1.7E+07	4.5E+06	4.4E+06	4.0E+06	1.4E+07	1.3E+07	1.2E+07	3.7E+06	3.8E+06	3.5E+06
14	9.4E+07	8.3E+07	1.1E+08	3.9E+07	3.7E+07	3.0E+07	5.1E+07	5.4E+07	5.4E+07	4.1E+06	4.6E+06	5.4E+06	3.0E+07	3.0E+07	2.4E+07	3.4E+06	2.9E+06	2.7E+06
15	8.9E+07	5.9E+07	4.9E+07	5.9E+07	4.9E+07	7.7E+07	1.6E+07	1.5E+07	3.3E+07	1.3E+07	1.2E+07	1.5E+07	1.2E+07	2.2E+07	2.0E+07	4.4E+07	5.4E+07	5.7E+07
16	1.7E+06	2.4E+06	2.4E+06	2.1E+06	1.7E+06	1.7E+06	2.0E+06	2.9E+06	1.6E+06	4.5E+05	4.8E+05	5.9E+05	2.8E+06	4.2E+06	5.2E+06	1.2E+06	4.3E+06	2.6E+06
17	4.6E+07	8.2E+07	2.1E+07	1.3E+08	5.9E+08	1.1E+08	1.1E+08	8.8E+07	2.5E+08	2.3E+06	1.1E+06	1.4E+06	5.3E+06	6.8E+06	1.1E+07	3.2E+07	4.4E+07	2.7E+07
18	2.8E+06	3.0E+06	3.3E+06	2.7E+07	1.3E+07	2.4E+07	9.0E+07	1.1E+08	8.1E+07	1.3E+07	1.9E+07	2.1E+07	1.3E+07	1.2E+07	1.3E+07	1.2E+07	1.1E+07	1.3E+07
19	8.7E+05	6.9E+05	1.0E+06	6.8E+06	4.1E+06	5.9E+06	6.4E+06	6.3E+06	3.9E+06	4.8E+06	5.6E+06	5.1E+06	1.0E+07	1.1E+07	9.0E+06	3.3E+06	2.2E+06	2.2E+06
20	1.8E+07	1.7E+07	1.3E+07	1.1E+07	1.1E+07	1.0E+07	7.0E+07	1.1E+08	9.1E+07	1.8E+06	1.9E+06	1.2E+06	3.6E+07	2.3E+07	2.2E+07	1.1E+07	1.3E+07	1.1E+07

S5 Table. Mean bacterial abundances for each sample site in the oral cavity before sleep for each SDB participant.

Participant	Temporomandibular joint	Back of tongue	Gingivae	Palate	Molars	Tip of tongue
1	9.42E+06	2.66E+07	7.10E+07	3.28E+06	5.70E+06	3.41E+06
2	9.04E+06	3.41E+07	6.35E+07	6.79E+06	6.93E+06	1.01E+07
3	1.72E+07	5.67E+07	1.05E+08	9.93E+05	6.86E+06	4.06E+06
4	4.49E+06	1.16E+07	8.29E+07	4.98E+05	8.23E+05	1.66E+06
5	8.44E+06	2.89E+07	4.35E+07	3.41E+05	9.54E+06	2.04E+06
6	3.46E+06	1.60E+07	2.06E+06	2.07E+05	3.03E+06	5.80E+06
7	7.51E+06	5.58E+07	1.69E+07	1.00E+06	1.17E+06	6.15E+05
8	6.53E+06	8.28E+06	1.41E+07	2.79E+05	5.40E+05	6.09E+05
9	2.24E+06	2.88E+07	3.04E+06	3.26E+05	2.50E+05	1.59E+06
10	1.89E+06	7.64E+06	4.71E+06	1.02E+05	1.42E+06	7.52E+05
11	2.87E+06	7.42E+06	3.59E+06	3.80E+04	5.16E+05	2.46E+06
12	1.65E+06	4.23E+06	2.20E+07	7.42E+04	8.34E+06	4.27E+05
13	1.20E+06	1.08E+07	4.24E+06	1.01E+05	1.38E+06	5.51E+04
14	6.15E+05	1.88E+07	2.16E+06	1.27E+05	1.32E+06	2.55E+05
15	3.85E+05	1.20E+06	8.19E+05	9.78E+04	3.05E+05	1.01E+06
16	4.32E+05	2.38E+05	6.39E+06	4.47E+04	4.00E+05	1.17E+05
17	3.68E+06	2.08E+07	9.80E+06	3.98E+06	1.33E+07	2.03E+06
18	7.50E+05	6.82E+05	4.03E+06	1.82E+05	1.20E+05	1.14E+06
19	5.91E+06	1.50E+07	2.14E+07	2.71E+05	1.01E+06	5.93E+05
20	2.23E+06	2.57E+07	3.08E+07	3.71E+05	8.11E+05	5.64E+05

S6 Table. Mean bacterial abundances for each sample site in the oral cavity after sleep for each SDB participant.

Participant	Temporomandibular joint	Back of tongue	Gingivae	Palate	Molars	Tip of tongue
1	3.54E+07	8.44E+07	5.33E+07	4.70E+05	1.62E+07	1.14E+07
2	6.22E+07	1.50E+08	1.16E+08	8.10E+06	9.47E+07	9.30E+07
3	5.69E+06	2.36E+08	3.30E+08	6.96E+06	7.11E+06	2.57E+07
4	2.11E+06	1.83E+07	4.49E+07	4.34E+05	1.65E+06	1.16E+06
5	1.70E+07	1.52E+08	1.29E+08	1.51E+07	5.70E+07	2.97E+07
6	1.74E+07	1.40E+08	2.07E+07	8.92E+05	3.26E+06	3.69E+06
7	2.58E+06	9.89E+07	2.53E+07	6.73E+05	5.79E+06	3.43E+06
8	4.53E+07	5.99E+07	4.71E+07	4.02E+05	2.31E+06	2.72E+06
9	4.12E+06	3.21E+07	1.90E+06	3.04E+06	1.78E+07	1.85E+06
10	5.25E+07	7.21E+07	2.83E+06	4.31E+06	3.61E+06	9.27E+05
11	1.03E+07	5.61E+07	9.27E+06	1.29E+06	9.97E+06	3.12E+06
12	1.15E+07	2.61E+07	5.09E+06	1.07E+06	7.90E+06	9.04E+06
13	3.05E+07	1.29E+08	4.67E+07	2.72E+06	6.12E+06	2.62E+06
14	1.30E+08	1.45E+08	5.31E+07	8.77E+06	2.56E+07	6.70E+06
15	3.87E+07	1.13E+08	2.26E+07	8.23E+06	8.94E+06	1.96E+07
16	7.44E+06	3.93E+06	9.45E+06	1.48E+06	1.45E+07	4.76E+06
17	4.30E+07	2.00E+08	1.10E+08	7.03E+05	4.45E+06	2.61E+07
18	3.54E+07	8.44E+07	5.33E+07	4.70E+05	1.62E+07	1.14E+07
19	6.22E+07	1.50E+08	1.16E+08	8.10E+06	9.47E+07	9.30E+07
20	5.69E+06	2.36E+08	3.30E+08	6.96E+06	7.11E+06	2.57E+07

S7 Table. Mean VLP abundances for each sample site in the oral cavity before sleep for each SDB participant.

Participant	Temporomandibular joint	Back of tongue	Gingivae	Palate	Molars	Tip of tongue
1	7.44E+06	1.21E+07	9.82E+07	1.48E+06	1.34E+07	3.03E+06
2	4.09E+07	3.66E+07	1.18E+08	1.19E+07	2.40E+07	2.80E+07
3	9.96E+06	1.46E+07	1.33E+08	4.98E+05	4.48E+06	9.89E+05
4	4.47E+06	3.01E+06	1.39E+07	7.45E+05	1.07E+06	9.33E+05
5	1.80E+07	1.97E+07	1.27E+07	4.73E+05	1.62E+07	1.42E+07
6	5.50E+05	2.54E+06	1.38E+06	4.94E+04	1.64E+06	3.88E+06
7	1.23E+06	1.91E+07	5.19E+06	4.14E+05	9.58E+05	1.00E+06
8	4.25E+06	2.84E+06	5.58E+06	1.02E+05	9.59E+05	7.02E+05
9	7.35E+06	4.84E+06	3.06E+06	2.84E+06	2.67E+05	8.66E+06
10	1.16E+06	2.87E+06	1.12E+06	7.18E+04	6.70E+05	2.98E+05
11	1.75E+07	2.91E+06	5.90E+06	6.42E+04	1.04E+06	3.86E+06
12	5.35E+06	3.53E+06	4.73E+07	1.61E+05	4.78E+06	1.26E+06
13	1.22E+06	1.73E+07	2.32E+06	1.48E+05	4.20E+06	6.94E+05
14	2.37E+05	2.42E+06	2.12E+06	1.26E+04	4.74E+06	4.61E+04
15	7.44E+06	1.21E+07	9.82E+07	1.48E+06	1.34E+07	3.03E+06
16	4.09E+07	3.66E+07	1.18E+08	1.19E+07	2.40E+07	2.80E+07
17	9.96E+06	1.46E+07	1.33E+08	4.98E+05	4.48E+06	9.89E+05
18	4.47E+06	3.01E+06	1.39E+07	7.45E+05	1.07E+06	9.33E+05
19	1.80E+07	1.97E+07	1.27E+07	4.73E+05	1.62E+07	1.42E+07
20	5.50E+05	2.54E+06	1.38E+06	4.94E+04	1.64E+06	3.88E+06

S8 Table. Mean VLP abundances for each sample site in the oral cavity after sleep for each SDB participant.

Participant	Temporomandibular joint	Back of tongue	Gingivae	Palate	Molars	Tip of tongue
1	3.08E+07	8.44E+06	5.77E+07	3.54E+05	9.94E+06	2.71E+06
2	2.28E+08	1.55E+08	4.04E+08	1.24E+08	2.68E+08	1.11E+09
3	7.31E+06	1.54E+08	5.28E+08	8.27E+06	7.46E+06	6.71E+06
4	5.53E+05	7.04E+06	9.71E+06	5.61E+05	6.35E+05	9.12E+05
5	7.90E+07	4.49E+08	5.62E+07	6.82E+07	2.15E+08	2.18E+08
6	2.42E+06	1.63E+08	2.17E+07	2.77E+06	4.00E+06	7.58E+06
7	1.92E+05	7.17E+06	4.35E+06	8.25E+05	2.61E+06	8.72E+05
8	4.72E+06	1.71E+06	2.16E+07	8.60E+04	4.51E+05	2.52E+05
9	3.57E+06	1.37E+07	4.06E+06	7.30E+06	6.23E+07	4.39E+06
10	2.69E+07	1.39E+07	9.34E+05	5.45E+06	5.17E+06	8.67E+05
11	5.00E+06	5.66E+06	6.14E+06	2.63E+06	9.48E+06	2.67E+06
12	4.61E+06	4.61E+06	2.76E+06	3.91E+05	4.06E+06	8.82E+05
13	6.01E+07	4.62E+07	1.49E+07	4.31E+06	1.28E+07	3.66E+06
14	9.58E+07	3.54E+07	5.31E+07	4.69E+06	2.79E+07	3.00E+06
15	6.57E+07	6.16E+07	2.14E+07	1.32E+07	1.80E+07	5.15E+07
16	2.16E+06	1.82E+06	2.17E+06	5.07E+05	4.08E+06	2.71E+06
17	4.97E+07	2.76E+08	1.48E+08	1.64E+06	7.81E+06	3.43E+07
18	3.03E+06	2.12E+07	9.29E+07	1.76E+07	1.27E+07	1.18E+07
19	8.68E+05	5.57E+06	5.52E+06	5.16E+06	1.01E+07	2.57E+06
20	1.56E+07	1.07E+07	8.91E+07	1.65E+06	2.71E+07	1.18E+07

S9 Table. The average oral bacterial abundances in healthy [12] and SDB before and after sleep (Healthy n = 10, SDB n = 20). Significant differences were calculated using Mann-Whitney tests that were corrected for false discovery rates. Significantly higher bacterial counts were identified in healthy participants at the back of the tongue both before and after sleep compared to SDB.

	Sample location	Healthy (\pm SEM)	SDB (\pm SEM)	P value
Before sleep	Temporomandibular joint	3.26×10^6 ($\pm 1.17 \times 10^6$)	4.50×10^6 ($\pm 9.46 \times 10^5$)	> 0.05
	Back of tongue	2.90×10^7 ($\pm 7.60 \times 10^6$)	1.90×10^7 ($\pm 3.64 \times 10^6$)	0.047
	Gingivae	1.75×10^7 ($\pm 7.74 \times 10^6$)	2.56×10^7 ($\pm 6.96 \times 10^6$)	> 0.05
	Palate	7.21×10^5 ($\pm 2.77 \times 10^5$)	9.55×10^5 ($\pm 3.88 \times 10^5$)	> 0.05
	Molars	4.83×10^6 ($\pm 1.62 \times 10^6$)	3.19×10^6 ($\pm 8.61 \times 10^5$)	> 0.05
	Tip of tongue	2.57×10^6 ($\pm 1.66 \times 10^6$)	1.96×10^6 ($\pm 5.38 \times 10^5$)	> 0.05
After sleep	Temporomandibular joint	2.14×10^7 ($\pm 7.03 \times 10^6$)	2.65×10^7 ($\pm 6.88 \times 10^6$)	> 0.05
	Back of tongue	1.35×10^8 ($\pm 2.02 \times 10^7$)	8.94×10^7 ($\pm 1.49 \times 10^7$)	0.019
	Gingivae	4.08×10^7 ($\pm 7.56 \times 10^6$)	5.80×10^7 ($\pm 1.65 \times 10^7$)	> 0.05
	Palate	4.32×10^6 ($\pm 1.48 \times 10^6$)	3.88×10^6 ($\pm 9.15 \times 10^5$)	> 0.05
	Molars	1.91×10^7 ($\pm 5.44 \times 10^6$)	1.59×10^7 ($\pm 4.98 \times 10^6$)	> 0.05
	Tip of tongue	1.29×10^7 ($\pm 2.78 \times 10^6$)	1.50×10^7 ($\pm 4.79 \times 10^6$)	> 0.05

S10 Table. The average oral VLP abundances in healthy [12] and SDB before and after sleep (Healthy n = 10, SDB n = 20). Significant differences were calculated using Mann-Whitney tests that were corrected for false discovery rates. Error represents the standard error of the mean (\pm SEM).

	Sample location	Healthy (\pm SEM)	SDB (\pm SEM)	P value
Before sleep	Temporomandibular joint	5.68 x 10 ⁶ (\pm 1.86 x 10 ⁶)	6.36 x 10 ⁶ (\pm 2.17 x 10 ⁶)	0.013
	Back of tongue	2.20 x 10 ⁷ (\pm 6.30 x 10 ⁶)	1.05 x 10 ⁷ (\pm 2.29 x 10 ⁶)	0.0041
	Gingivae	2.36 x 10 ⁷ (\pm 9.54 x 10 ⁶)	3.05 x 10 ⁷ (\pm 1.00 x 10 ⁷)	0.0089
	Palate	1.94 x 10 ⁶ (\pm 1.03 x 10 ⁶)	1.38 x 10 ⁶ (\pm 6.35 x 10 ⁵)	0.0052
	Molars	9.05 x 10 ⁶ (\pm 2.61 x 10 ⁶)	4.69 x 10 ⁶ (\pm 1.43 x 10 ⁶)	0.0052
	Tip of tongue	3.55 x 10 ⁶ (\pm 1.23 x 10 ⁶)	3.87 x 10 ⁶ (\pm 1.48 x 10 ⁶)	0.018
After sleep	Temporomandibular joint	5.69 x 10 ⁷ (\pm 2.30 x 10 ⁷)	3.43 x 10 ⁷ (\pm 1.22 x 10 ⁷)	0.045
	Back of tongue	9.22 x 10 ⁷ (\pm 5.02 x 10 ⁷)	7.20 x 10 ⁷ (\pm 2.60 x 10 ⁷)	0.045
	Gingivae	9.21 x 10 ⁷ (\pm 2.91 x 10 ⁷)	7.72 x 10 ⁷ (\pm 3.13 x 10 ⁷)	0.025
	Palate	1.44 x 10 ⁷ (\pm 9.88 x 10 ⁶)	1.35 x 10 ⁷ (\pm 6.72 x 10 ⁶)	> 0.05
	Molars	5.66 x 10 ⁷ (\pm 3.26 x 10 ⁷)	3.55 x 10 ⁷ (\pm 1.62 x 10 ⁷)	0.022
	Tip of tongue	1.73 x 10 ⁷ (\pm 8.24 x 10 ⁶)	7.38 x 10 ⁷ (\pm 5.55 x 10 ⁷)	> 0.05

Chapter 6

THE SPATIAL DISTRIBUTION OF THE BACTERIAL
COMMUNITIES WITHIN THE HEALTHY PAEDIATRIC ORAL
CAVITY BEFORE AND AFTER SLEEP

Abstract

Regarded as the gateway to the body, the oral cavity is comprised of various microhabitats that provide unique surfaces for the colonisation of distinct microbial communities. It is recognised that these microhabitats are heterogeneous in their absolute bacterial distribution and increase significantly during sleep. However, there are no taxonomic studies that investigate if and how these bacterial communities change in the paediatric oral cavity during sleep. Here, we present the paediatric oral taxonomic microbial dynamics of 6 individuals before and after sleep using 16S ribosomal RNA gene sequencing. Differences among microhabitats were driven by differences in the relative abundance of 'core' taxa characteristic to the healthy oral microbiome. Furthermore, an increase in the relative abundance of anaerobic bacteria, specifically *Veillonella* and *Prevotella*, during sleep was observed. This suggests that in addition to controlling for sample location, care must also be taken when interpreting differences in taxonomic profiles in the oral cavity as differences may reflect inconsistencies in the collection time of the sample.

Introduction

The oral cavity is estimated to harbour over 600 species of bacteria [1, 2]. These bacteria play an important role in maintaining oral health [3]. However, dysbiosis of these communities have also been linked to oral and systemic diseases such as dental caries, periodontitis and cardiovascular disease [4-8]. With different oral surfaces having distinct microbial communities, the oral microbiome is now being defined by its various microhabitats rather than as a whole [9]. These communities are further influenced by changes in environmental factors including diet, smoking, hosts immunity and oral hygiene [8, 10, 11]. One factor that has not been investigated is the impact of sleep on these microbial communities. During sleep, the environmental conditions of the oral cavity change due to a reduction in saliva flow, oxygen exposure and pH [12-15]. The microbial communities of healthy oral cavities are dynamic, with bacterial and viral concentrations significantly increasing during sleep [16]. However, taxonomic shifts in these communities remain unclear.

Here, we present an evaluation of the bacterial taxonomic shifts in the oral cavity of 6 healthy children during sleep using 16S ribosomal RNA sequencing. The overall aims for this study were to (i) characterise the microhabitats of the paediatric oral cavity before and after sleep, (ii) to use this data to determine if there is a change in the oral microbiome during sleep and (iii) to identify if there are significant differences in the resulting bacterial communities between genders and participants. Overall, we hypothesised that during sleep, the bacterial communities in the paediatric oral cavity would significantly change. Ultimately, by understanding the 'normal' microbial shifts during sleep, further studies into what impact sleeping disturbances have on our oral microbiome can be investigated.

Materials and Methods

Ethics statement

The healthy participants involved in this study were a control subgroup from a larger study investigating effects of sleep disorder breathing on development. This study was approved by The Human Research Ethics Committees of the Women's and Children's Hospital and University of Adelaide, South Australia; and was conducted in accordance with the 1964 Declaration of Helsinki and its later amendments. Written consent was provided by the parents of the participants and written assent by the participants. A child's health and behaviour questionnaire was completed by the parents prior to sample collection.

Sample collection

Oral swab samples were collected from 6 healthy children undergoing an overnight polysomnography sleep test at the Women's and Children's Hospital. The Children's ages ranged from 7.75 to 16.58 years with the overall average of 10.40 ± 3.99 years. Of the 6 participants sampled 2 were female and 4 were male. The average BMI for the group samples was 18.63 ± 3.92 with a range between 14.2 to 19.7.

Individually polypropylene packaged sterile rayon swabs (Copan, Brescia, Italy; product code: 155C; length 13.3 cm, diameter 5 mm) were used to collect the oral samples using methods previously described [16, 17]. Briefly samples were collected from the middle of the palate, the gingival margin of the last proximal molar on the right lower jaw, the occlusal site of the last two distal molars on the bottom jaw on the right side, the left temporomandibular joint, the middle of the back of the tongue and the middle of the tip of the tongue for all participants (Fig. 1). For the duration of this

manuscript these locations will be referred to as the palate, gingivae, molars, temporomandibular joint, back of tongue and tip of tongue respectively (Fig. 1). Each participant had these locations sampled twice, once just before lights out between 8.30-9.00 pm, referred to as before sleep, and immediately on waking the following day between 6.00-6.30 am, referred to as after sleep. Therefore, each participant was sampled 12 times (6 before sleep and 6 after sleep). Swabs were collected from each location by rotating the swab tip clockwise 6 times. All samples in this study were collected by the same researcher at the same locations before and after sleep using the same methods described. Once collected, swab sampled were placed back into their polypropylene tube and frozen at -80°C until analysis.

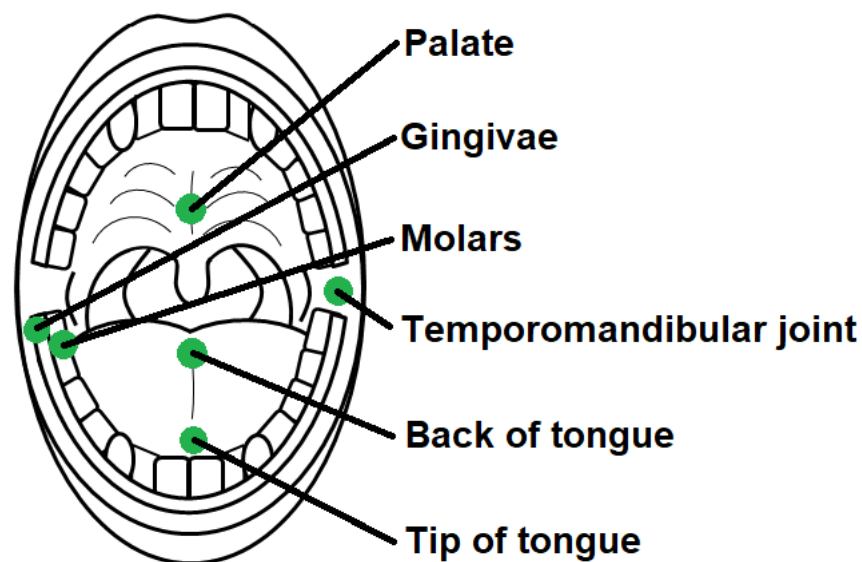


Figure 1. Microhabitat sample locations in the paediatric oral cavity. Separate swabs were rotated clockwise 6 times at each location to collect oral samples.

Swab sample preparation

Flow cytometry was performed on swab samples prior to 16S analysis [16]. Briefly, preparation of the swab samples for flow cytometry involved thawing the swabs at room temperature then cutting the tips off into 1 ml of sterile (0.2 µm filtered and UV treated) TE buffer (10 mM Tris, 1 mM EDTA, pH 7.4, Sigma). The swab tip and TE buffer were vortexed for 3 minutes to elute the bacteria and viruses from the swab tip. A small volume from each sample was taken at this stage for flow cytometric analysis [16]. The remainder of each sample was snap frozen in liquid nitrogen and stored at -80°C until 16S analysis.

Bacteria 16S PCR amplification

Eluted oral swab samples were thawed at room temperature and briefly vortexed to ensure uniform microbial distribution. Direct PCR amplification [18] was used to amplify the V3-V4 region of the 16S gene using the forward primer 341F and the reverse primer 805R. Illumina overhang adaptor sequences were added to both the 341F forward and 805R reverse primer sequences. PCR amplification of the samples was performed in 25 µl reactions using KAPA Taq HiFi Hotstart (Kapa Biosystems, Boston, MA, USA). For each 25µl PCR reaction, 10 µl of eluted swab sample was used. Negative control samples were prepared with sterile (0.2 µm filtered and UV treated) water and were run with each PCR reaction. PCR reactions were performed as followed: initial denaturing step at 95°C for 3 minutes followed by 30 cycles of 95°C for 30 seconds, 55°C for 30 seconds and 72°C for 30 seconds. A final extension step was performed at 72°C for 5 minutes. PCR products were run on agarose gel (2.5%) to verify amplification success and negative controls. DNA sequences were

then generated on an Illumina MiSeq run (Genomics Facility, Flinders Medical Centre, Adelaide, Australia).

Bioinformatics

A total of 7,660,611 pair-end reads successfully assembled and quality filtered at a Phred score of 30 using the bioinformatics program Paired-End reAd mergeR (PEAR) v0.9.4 [19]. Samples were then processed as previously described [20] using both Quantitative Insights Into Microbial Ecology (QIIME) v.1.8.0 [21] and UPARSE [22]. In brief, sequences were quality filtered to a minimum quality score of 30, a minimum 200 bp in length, no more than 6 ambiguous bases and no primer mismatches using QIIME. VSEARCH [23] was used to dereplicate sequences and singletons were removed using USEARCH [24]. Chimeras were removed, and remaining sequences clustered in to operational taxonomic units (OTUs) at 97% using the *cluster_otus* command in USEARCH. Greengenes database (13_08) was used to assign taxonomy using the default program UCLUST [24] in QIIME. Sequences were rarefied to 4920 to remove biases due to differing sequencing depths.

Sequence analysis

Bray-Curtis similarity matrices were calculated from square root transformed relative abundance data using the multivariate statistics program PRIMER (version 7, Primer-E, Plymouth) [25, 26]. The non-parametric distribution free Analysis of Similarity (ANOSIM) test was used to test the null hypothesis of no differences among a *a priori* group to determine patterns of bacterial community variation [25]. Permutational Multivariate Analysis of Variance (PERMANOVA+, version 1.0.3) was used to determine differences in overall bacterial composition between locations, time, gender and participants using 9999 unrestricted permutations of the raw data [26]. The

distance-based test for homogeneity (PERMDISP) was used to test the multivariate dispersions within a group [27]. When statistical significance was observed through PERMANOVA and ANOSIM analysis ($p < 0.05$), a similarity percentage analysis (SIMPER) was used to identify what genera of bacteria were driving the dissimilarity among groups (90% cut off) [27]. Bootstrap averaged metric Multidimensional Scaling (MDS) analysis was run on samples to establish the spread and separation of samples bases on the results from ANOSIM [25]. A bootstrap region of 95% was used and 500 bootstraps per group were run. The average of these 500 bootstraps were used to determine the average centroid and where 95% of the averages lied within the multivariate space.

Results

Overall sequence statistics

Sixty-five of 72 samples were successfully sequenced. The back of the tongue was the area with the least number of successful samples, with 4 of the 6 samples amplifying before sleep and only 1 of the 6 samples after sleep. The healthy participants used in this study were a subset group from a larger study with sleep-disorder breathers where 7,660,611 reads were successfully joined after paired-end assembly. After 97% OTU clustering 3,143,387 sequences were clustered into 536 OTUs. Each sample contained an average of 47,627 ($\pm 38,475$ SD) sequences, with a minimum of 1,491 and a maximum of 253,489 sequences.

Relative abundance of oral bacteria differs among microhabitat

ANOSIM and PERMANOVA tests revealed healthy oral bacterial populations separated into groups based on microhabitat (ANOSIM $R = 0.157$, $p = 0.002$;

PERMANOVA pseudo-F = 2.58, $p < 0.0001$). Pairwise comparisons in ANOSIM revealed of the 15 paired comparisons between microhabitats, 11 were seen to be significant (Table 1; $R < 0.5$, $p < 0.04$). The tip of the tongue was observed to be significantly different to all other oral microhabitats (Table 1; $R < 0.5$, $p < 0.04$). The temporomandibular joint, gingivae and molars were similar in bacterial composition (Table 1; $R < 0.034$, $p \geq 0.232$), as were the palate and back of tongue (Table 1; $R = 0.1$, $p = 0.181$). The low R values for the significantly different comparisons indicate that although these locations do not have the same bacterial community composition, there is strong overlap in bacterial communities present.

Table 1. ANOSIM pairwise tests between microhabitats in the paediatric oral cavity. A significant difference in the patterns of bacterial community composition between microhabitats is denoted by an asterisk (*). No significant difference was observed in bacterial community structure among the temporomandibular joint, gingivae and molars; or the back of the tongue and palate. The tip of the tongue was significantly different to all microhabitats.

Pairwise tests	R statistic	P value
Temporomandibular joint, Back of tongue	0.32	0.019*
Temporomandibular joint, Gingivae	0.01	0.351
Temporomandibular joint, Palate	0.14	0.036*
Temporomandibular joint, Molars	0.034	0.232
Temporomandibular joint, Tip of tongue	0.27	0.0002*
Back of tongue, Gingivae	0.36	0.010*
Back of tongue, Palate	0.10	0.181
Back of tongue, Molars	0.27	0.040*
Back of tongue, Tip of tongue	0.46	0.004*
Gingivae, Palate	0.23	0.005*
Gingivae, Molars	-0.035	0.698
Gingivae, Tip of tongue	0.30	0.0001*
Palate, Molars	0.12	0.038*
Palate, Tip of tongue	0.14	0.030*
Molars, Tip of tongue	0.22	0.001*

PERMDISP analysis based on microhabitat revealed an overall significant difference in the dispersion of data ($F= 4.00$, $p = 0.011$). Pairwise PERMDISP tests showed that there was a significant difference in the dispersion of data between the tip of the tongue and the temporomandibular joint ($t = 3.99$, $p = 0.001$), gingivae ($t = 4.45$, $p = 0.0005$), palate ($t = 2.97$, $p = 0.012$) and molars ($t = 3.98$, $p = 0.0012$) (Figure 1). The microhabitat with the greatest level of variability in data was the molars with a Bray-Curtis distance-to-centroid of 22.82 ± 1.45 . The tip of the tongue was the least dispersed with 16.29 ± 0.76 . Separation of each microhabitat was observed using metric MDS of the Bray-Curtis dissimilarity (Fig. 2). However, there was some overlap among locations (Fig. 2). The greatest spread of the 95% bootstrap region was at the back of the tongue (Fig. 2).

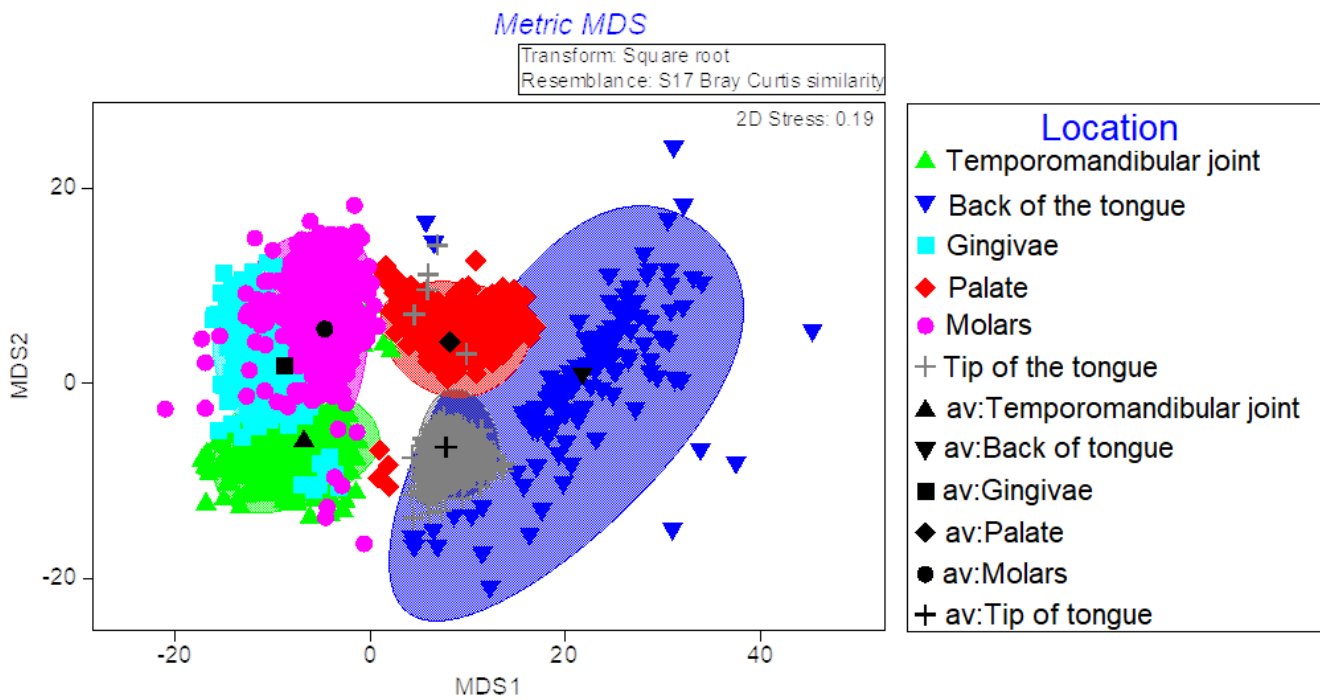


Figure 2. Metric Multidimensional Scaling (MDS) plot based on the Bray-Curtis dissimilarity for all samples at the temporomandibular joint (green triangle), back of the tongue (inverted dark blue triangles), gingivae (light blue squares), palate (red diamonds) and tip of the tongue (grey crosses) in the paediatric oral cavity. Centroid values are for each microhabitat are surrounded by a smooth bootstrap region where 95% of the 500 bootstrap averages lie.

SIMPER analysis on each microhabitat revealed an average Bray-Curtis similarity of 67.65 for the temporomandibular joint, 70.28 for the back of the tongue, 67.26 for the gingivae, 69.70 for the palate, 66.31 for the molars and 76.19 for the tip of the tongue. *Streptococcus* and *Haemophilus* were the top two relatively abundant genera contributing to a combined total of 35.99%, 34.37%, 25.94%, 30.75% and 29.22% of the total within group similarity at the temporomandibular joint, gingivae, palate, molars and tip of the tongue respectively. *Streptococcus* and *Veillonella* were the top relatively abundant taxa at the back of the tongue contributing to 27.30% of the within group similarity at that location. Pairwise SIMPER analysis on the significantly different microhabitats, as identified by ANOSOM, revealed that the dissimilarities among locations were driven predominantly by differences in the relative abundance of *Veillonella*, *Streptococcus*, *Prevotella*, *Haemophilus* and *Rothia* genera.

Table 2. The relative abundance of the top bacterial genera driving the dissimilarity among microhabitats. Values are the average percentage contribution for each genus to the total bacterial community identified at each microhabitat. Error represents the standard error of the mean.

	<i>Streptococcus</i>	<i>Haemophilus</i>	<i>Veillonella</i>	<i>Prevotella</i>	<i>Rothia</i>
Palate	32.36% (± 1.91%)	8.95% (± 1.61%)	10.32% (± 2.09%)	9.40% (± 2.41%)	2.44% (± 0.59%)
Gingivae	39.08% (± 3.24%)	12.41% (± 2.08%)	10.20% (± 2.87%)	5.41% (± 1.88%)	0.32% (± 0.19%)
Molars	40.08% (± 4.98%)	9.62% (± 1.68%)	5.01% (± 0.80%)	5.98% (± 2.40%)	1.26% (± 0.31%)
Temporomandibular joint	46.50% (± 4.96%)	8.90% (± 1.50%)	8.15% (± 2.75%)	8.53% (± 2.95%)	0.34% (± 0.090%)
Back of tongue	25.14% (± 6.03%)	5.85% (± 1.82%)	23.83% (± 5.23%)	9.57% (± 2.97%)	1.79% (± 0.32%)
Tip of tongue	33.00% (± 1.68%)	15.73% (± 2.51%)	11.83% (± 1.90%)	5.29% (± 1.36%)	4.67% (± 1.02%)

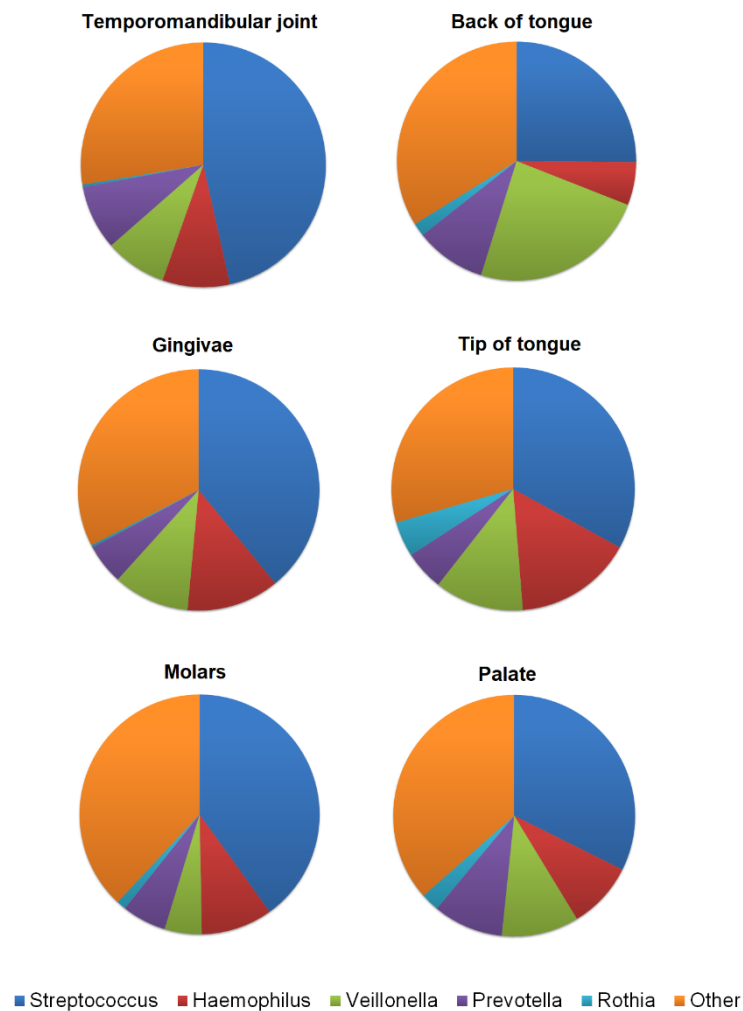


Figure 3. The top 5 bacterial genera driving the dissimilarity between microhabitats in the oral cavity, additional bacterial identified at each location are grouped into other. The back of the tongue and palate were characterised by a higher relative abundance of *Veillonella* and *Prevotella*. The Tip of the tongue was characterised by a higher abundance of *Veillonella*, *Rothia* and *Haemophilus*. The Temporomandibular joint, Gingivae and Molars were characterised by a higher relative abundance of *Streptococcus*. The percentage contribution for each of the 5 genera to the total bacterial communities identified at each microhabitat can be found in Table 2.

A higher relative abundance of *Veillonella*, *Rothia* and *Haemophilus* at the tip of the tongue were seen to be the main taxa driving the dissimilarity among other microhabitats. Specifically, pairwise SIMPER comparisons with the temporomandibular joint revealed a higher abundance of *Veillonella*, *Rothia* and *Haemophilus* at the tip of the tongue. These taxa contributed to 19.97% of the Bray-Curtis dissimilarity between locations (31.24). Comparisons between the gingivae and the tip of the tongue showed a Bray-Curtis dissimilarity measure of 31.74. Of that, 13.37% of the dissimilarity was driven by a higher relative abundance of *Rothia* and *Veillonella*. A higher relative abundance of *Haemophilus* and *Veillonella* at the tip of the tongue contributed to 11.54% of the 31.57 Bray-Curtis dissimilarity measure with the molars. Finally, the higher abundance of *Haemophilus* at the tip of the tongue compared to the back of the tongue and palate contributed to 7.30% and 6.26% of the 30.45 and 28.52 Bray-Curtis dissimilarity between these microhabitats respectively.

A higher abundance of *Veillonella* and *Prevotella* taxa, and a lower relative abundance of *Streptococcus* at the back of the tongue, were the main discriminating genera identified by pairwise SIMPER analysis between the temporomandibular joint (37.74), gingivae (38.37) and molars (37.85). These taxa contributed to 26.38, 23 and 23.36% of the dissimilarity at each microhabitat respectively. *Veillonella* was also higher in relative abundance at the palate compared to the temporomandibular joint, gingivae and molars. These differences contributed to 6.43, 6.15 and 5.20% of the dissimilarity observed respectively. Pairwise SIMPER comparisons between the back and tip of the tongue identified that a higher abundance of *Veillonella* at the back of the tongue, and a higher abundance of *Haemophilus* at the tip of the tongue, were the top taxa contributing to 14.47% of the 30.45 Bray-Curtis dissimilarity. The temporomandibular joint was higher in relative abundance of *Streptococcus* than the

palate (33.40) and tip of the tongue (31.24) and contributed to 5.43 and 5.99% of the dissimilarity at each location respectively. However, the palate was higher in relative abundance of *Prevotella* than the temporomandibular joint and contributed a further 10.55% of the dissimilarity between these microhabitats.

Bacterial populations shift in relative abundance during sleep

The overall analysis of all samples split by time of collection (i.e. before and after sleep) showed a significant difference in bacterial community composition (ANOSIM $R = 0.151$, $p < 0.0001$; PERMANOVA pseudo- $F = 5.093$, $p = 0.0002$). Data distributions before and after sleep were also homogeneous in their dispersion (PERMDISP $F = 2.51$, $p = 0.14$). A metric MDS showed clear separation of samples collected before and after sleep based on the Bray-Curtis dissimilarity measures (Fig. 4). Both groups had a similar spread in the distribution of data (Fig. 4).

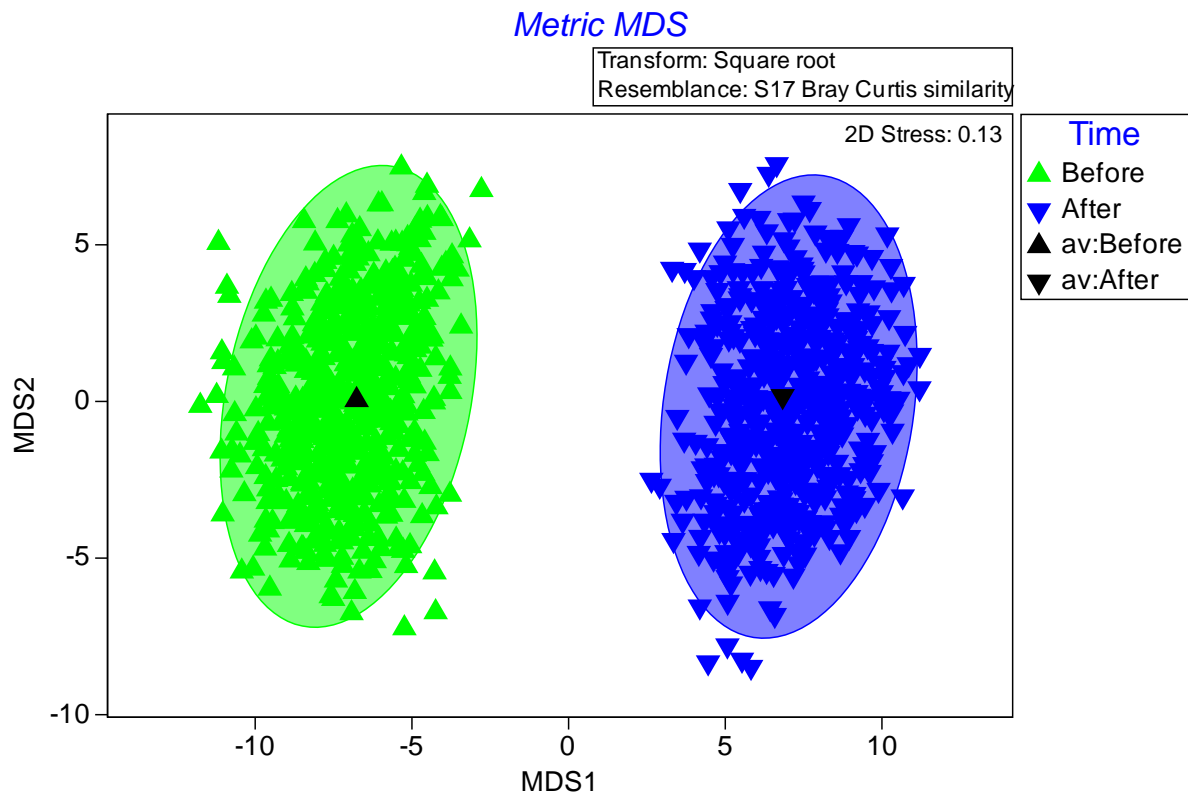


Figure 4. Metric Multidimensional Scaling (MDS) plot based on the Bray-Curtis dissimilarity for all samples before (green triangle) and after (inverted dark blue triangle) sleep in the paediatric oral cavity. Centroid values are for each microhabitat are surrounded by a smooth bootstrap region where 95% of the 500 bootstrap averages lie.

SIMPER analysis revealed that there was a Bray-Curtis similarity of 67.12 among all samples collected before sleep and 70.34 among all samples collected after sleep. *Streptococcus* and *Haemophilus* were the genera of bacteria dominating the before sleep samples and contributed to 31.90% of the Bray-Curtis similarity. After sleep, *Streptococcus* and *Veillonella* were the most relatively abundant taxa contributing to 29.21% of the Bray-Curtis similarity. SIMPER pairwise comparisons showed that there was an average Bray-Curtis dissimilarity of 33.40 between taxa before and after sleep. The increase in relative abundance of *Veillonella* from 9.23% before sleep to 11.34% after sleep and *Prevotella* 3.84% before sleep to 10.74% after sleep were the top two discriminating genera driving the dissimilarity between time points. Combined, both taxa contributed to 16.64% of the Bray-Curtis dissimilarity.

Based on this dissimilarity in bacterial composition with time, samples collected at each microhabitat before sleep were then compared among each other and samples collected after sleep compared to one another (i.e. bacterial populations at the molars before sleep compared to bacterial populations at the palate before sleep). Through grouping the samples based on time of sampling and microhabitat, comparisons into the specific bacterial shifts at each microhabitat during sleep could be made.

Differences in oral community composition based on collection time and microhabitat

Significantly different bacterial community compositions were revealed overall when data was grouped by sample time and microhabitat (ANOSIM $R = 0.238$, $p < 0.0001$; PERMANOVA pseudo- $F = 2.27$, $p < 0.0001$). However, by splitting the sample in this way, the sample size for each group is reduced. Therefore, there is a lower number of possible permutations that can be run for each pairwise test. These permutations ranged from 5 to 462. As there was only one sample for the back of the tongue after sleep, any pairwise comparisons with that data point were disregarded as there was not enough replicates to form a sensible significance test.

Before sleep, ANOSIM pairwise tests revealed a significant difference in bacterial community structure between the back of the tongue and the tip of the tongue ($R = 0.71$, $p = 0.005$), temporomandibular joint ($R = 0.65$, $p = 0.005$), gingivae ($R = 0.45$, $p = 0.014$), palate ($R = 0.43$, $p = 0.029$) and molars ($R = 0.50$, $p = 0.01$). The bacterial communities at the tip of the tongue were also seen to differ from the gingivae ($R = 0.27$, $p = 0.009$), molars ($R = 0.20$, $p = 0.03$) and temporomandibular joint ($R = 0.36$, $p = 0.006$). After sleep, bacterial community composition at the tip of the tongue was significantly different to the palate ($R = 0.33$, $p = 0.009$), molars ($R = 0.19$, $p = 0.026$), temporomandibular joint ($R = 0.24$, $p = 0.035$) and the gingivae ($R = 0.52$, $p = 0.002$). The palate was also different in bacterial composition compared to the gingivae ($R = 0.47$, $p = 0.015$) and the temporomandibular joint ($R = 0.27$, $p = 0.043$). When comparing bacterial community composition at each microhabitat before sleep to its corresponding microhabitat after sleep, only the palate ($R = 0.32$, $p = 0.028$) and tip of tongue ($R = 0.41$, $p = 0.013$) showed a significant difference.

Overall, distributions based on the time of microhabitat sampling were seen to be homogeneous in their dispersions (PERMDISP $F = 4.11$, $p = 0.054$). However, pairwise PERMDISP comparisons revealed heterogeneity in the dispersion of multivariate data between the tip of the tongue and the temporomandibular joint ($t = 3.86$ and 3.02 , $p = 0.0039$ and 0.010), gingivae ($t = 4.36$ and 2.65 , $p = 0.0021$ and 0.035) and molars ($t = 4.56$ and 3.24 , $p = 0.0036$ and 0.0066) before and after sleep respectively. The tip of the tongue had the least dispersal before (14.28 ± 0.91) and after (13.85 ± 0.88) sleep. The molars had the largest dispersal of data before (22.93 ± 1.67) and after (20.94 ± 2.01) sleep.

Before sleep, pairwise SIMPER analysis between the tip and the back of the tongue revealed that higher relative abundance of *Veillonella* and *Prevotella* at the back of the tongue and a higher relative abundance of *Haemophilus* and *Streptococcus* at the tip of the tongue, were the top relatively abundant taxa contributing to the dissimilarity. These differences in relative abundance were responsible for 29.23% of the 34.23 Bray-Curtis dissimilarity reported between locations. SIMPER also revealed that the higher relative abundance of *Veillonella* and *Prevotella* at the back of the tongue contributed to 17.93, 16.92, 15.50 and 18.03% of the Bray-Curtis dissimilarity between pairwise comparisons with the temporomandibular joint (42.86), gingivae (40.64), palate (36.08) and molars (42.00) respectively. Pairwise comparisons also showed that a high relative abundance of *Haemophilus* at the tip of the tongue contributed to 7.69 and 6.06% of the dissimilarity at the temporomandibular joint (31.32) and molars (31.81) respectively. A lower abundance of *Streptococcus* at the back of the tongue compared to the temporomandibular joint (42.86), gingivae (40.64), molars (42.00) and palate (36.08) also contributed to 8.89, 4.77, 6.29 and 5.29% of the dissimilarity between pairwise

comparisons at those locations respectively. A higher relative abundance of *Rothia* at the tip of the tongue was also responsible for contributing 7.50 and 7.76% of the dissimilarity between the temporomandibular joint (31.32) and gingivae (30.88) respectively. Other main differences observed between pairwise SIMPER comparisons of the genera that responsible for driving dissimilarity were: the high relative abundances of *Streptococcus* at the temporomandibular joint contributing 7.63% of the dissimilarity between the tip of the tongue (31.32), the high relative abundance of *Haemophilus* at the gingivae contributing to 4.81% of the dissimilarity between the back of the tongue (40.64), the high relative abundance of *Veillonella* at the tip of the tongue contributing 6.32% of the dissimilarity between the gingivae (30.88) and the high relative abundance of *Neisseria* at the tip of the tongue contributing to 5.80% of the dissimilarity between the molars (31.18).

After sleep, pairwise SIMPER analysis showed that a higher relative abundance of *Veillonella* at the tip of the tongue contributed to 9.03, 6.36 and 7.15% of the dissimilarity at the temporomandibular joint (27.86), gingivae (30.32) and molars (29.46) respectively. *Veillonella* was also higher in relative abundance at the palate compared to the gingivae (34.53) and temporomandibular joint (31.78) and was responsible for 5.44 and 7.00% of the dissimilarity at these locations respectively. *Prevotella* was also higher in relative abundance at the palate when pairwise comparisons were made to the tip of the tongue (26.78), gingivae (34.52) and temporomandibular joint (37.78). This difference in abundance contributed to 9.28, 11.59 and 11.65% of the dissimilarity at each location respectively. Other differences that were main dissimilarity drivers between locations after sleep were the higher relative abundance of *Rothia* at the tip of the tongue contributing to 6.15% of the dissimilarity between the gingivae (30.32), and the higher relative abundance of

CW040 at the gingivae contributing to 5.60% of the dissimilarity between the palate (34.52).

Before sleep, the average Bray-Curtis similarity measure for the palate was 70.74. The top two most abundant genera for this group were *Streptococcus* and *Haemophilus* contributing to 29.61% of the similarity within the group. After sleep the palate had a Bray-Curtis similarity measure of 70.34 with *Streptococcus* and *Veillonella* the top two genera with the highest relative abundance within the group. Both genera contributed to 23.27% of the total similarity within the group. When the palate was compared before and after sleep, the average dissimilarity measure between groups was 32.39. An increase in the relative abundance of *Prevotella* and *Veillonella* during sleep were the top genera driving the dissimilarity between these two groups. These genera were responsible for 16.93% of the dissimilarity.

With an average Bray-Curtis similarity of 77.92, the tip of the tongue before sleep was also populated with a higher relative abundance of *Streptococcus* and *Haemophilus*. Both genera contributed to a cumulative total of 31.73% to the similarity within this group. After sleep, the tip of the tongue had an average Bray-Curtis similarity of 78.64. *Streptococcus* and *Veillonella* were now the two genera with the highest relative abundance within the group contributing to a combined total of 28.52% of the dissimilarity. The average dissimilarity between the before and after sleep groups at the tip of the tongue was 25.55, with *Haemophilus* and *Veillonella* the main genera driving the dissimilarity between groups. *Haemophilus* was higher in relative abundance before sleep and *Veillonella* after sleep. These genera contributed to a total of 15.25% of the observed dissimilarity.

Bacterial communities vary among participants

Participants were seen to have significantly different bacterial community composition to each other (ANOSIM $R = 0.428$, $p < 0.0001$; PERMANOVA pseudo- $F = 5.71$, $p < 0.0001$). Overall, bacterial dispersion among participants was homogeneous (PERMDISP $F = 1.21$, $p = 0.41$), with the slight exception of a significant difference in dispersion between participants 2 and 4 (PERMDISP $t = 2.77$, $p = 0.017$). Each participant's average Bray-Curtis similarity measure was between 69.35 and 75.54 (SIMPER). *Streptococcus* was the most abundant within all participants and contributed the most to the similarity with anywhere between 15.56-23.32% (SIMPER). No significant difference was observed in bacterial composition between genders (ANOSIM $R = 0.088$, $p = 0.052$). A metric MDS of participant's samples showed that oral samples from the same participant grouped together with minimal overlap (Fig. 5). A slight overlap in samples between participants 2 and 6 was observed (Fig. 5). Participants 2 and 5 had the greatest spread of samples (Fig. 5).

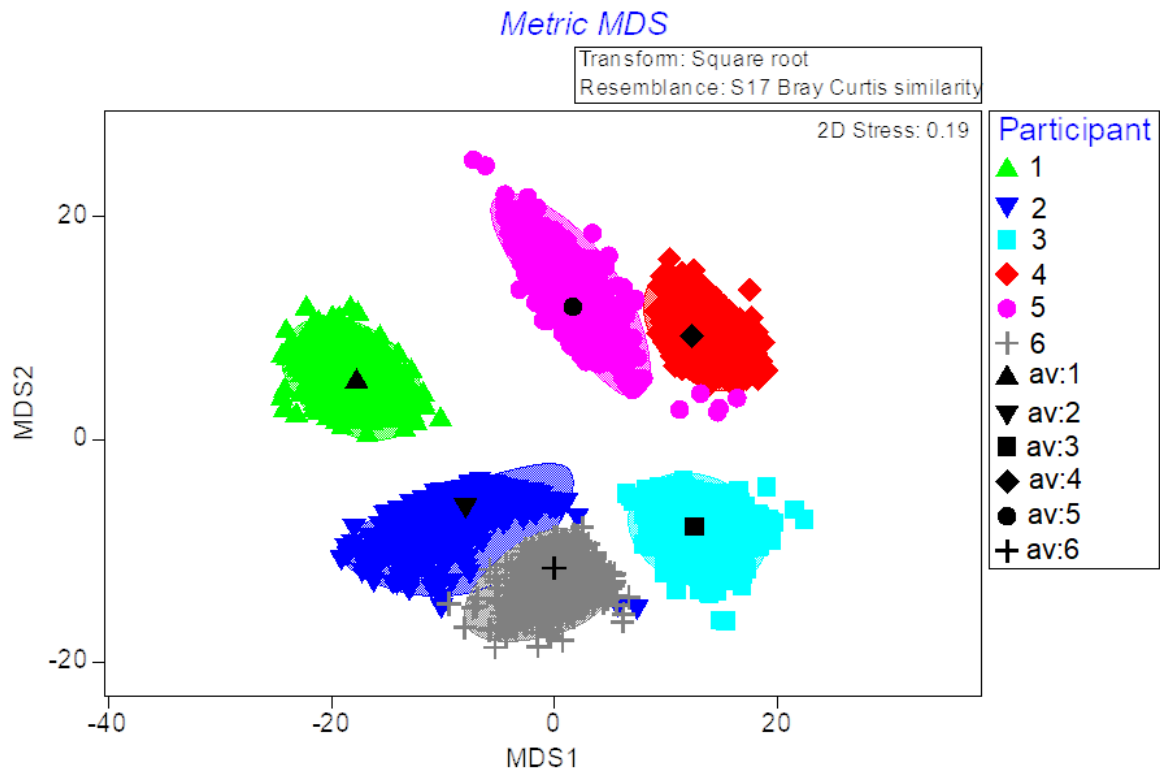


Figure 5. Metric Multidimensional Scaling (MDS) plot based on the Bray-Curtis dissimilarity for all oral samples collected from each of the 6 participants involved in this study. Centroid values are for each microhabitat are surrounded by a smooth bootstrap region where 95% of the 500 bootstrap averages lie.

Discussion

The purpose of this study was to understand the taxonomic shifts in the bacterial communities within microhabitats of the healthy paediatric oral cavity during sleep. This was achieved through 16S ribosomal RNA sequencing of 6 oral microhabitats (Fig. 1) before and after sleep in 6 healthy paediatric participants. We identified significant differences in the relative abundance of 'core' taxa among oral microhabitats, and a shift in these taxa during sleep, specifically in the anaerobic bacteria *Veillonella* and *Prevotella*. Here we present, to the best of our knowledge, the first study to address taxonomic bacterial microhabitat variation in the paediatric oral cavity during sleep. The influence of sleep on the oral microbiome adds complexity in understanding the healthy microbiome and suggests that the bacterial communities within the microhabitats could be influenced by a circadian cycle.

Previously it has been reported that the adult oral cavity contains distinct niches with significantly different microbial communities [28, 29]. Most of the dissimilarities identified were due to differences in the relative abundance of a 'core' set of taxa among oral locations [28-30]. This study supports this finding as bacterial dissimilarities in the paediatric oral microbiome were driven by differences in the relative abundance of the top abundant taxa. This has previously been suggested to be a result of the continuous dispersal of microorganisms through saliva [9, 31]. Microorganisms from the surfaces of the microhabitats within the oral cavity shed into the saliva. Saliva then facilitates the transport of these microbial communities to other surfaces within the oral cavity [32]. Based on the conditions of the new microhabitat, such as the pH, bacterial binding receptors and oxygen concentrations, depends on what bacteria from the saliva will colonise [9, 33].

Bacterial community analysis on overall microhabitats revealed each microhabitat assembled into one of three groups. These groups consisted of: the temporomandibular joint, gingivae and molars; back of tongue and palate; and the tip of the tongue. The microhabitats within each of these groups did not display an overall significant difference in the bacterial communities present (ANOSIM $p > 0.05$; Table 1). Spatially, the temporomandibular joint, gingivae and molars are near one other (Figure 1). Interestingly, this group consists of both soft shedding mucosal surfaces (temporomandibular joint and gingivae) and non-shedding tooth surfaces (molars), factors used to explain differences among these microhabitats in the past [28, 33]. We have previously reported that the absolute bacterial abundance at the molars and the temporomandibular joint are similar [16]. However, the bacterial counts at these two microhabitats were generally lower than the gingivae [16]. This demonstrates that significant differences in the absolute microbial abundances among microhabitats in the oral cavity do not reflect a difference in bacterial taxonomic structure. In this study, these three microhabitats were generally higher in relative abundance of *Streptococcus* compared to the palate, tip of the tongue and back of the tongue.

Streptococcus was identified as the most abundant genus in the paediatric oral cavity (Fig. 3). This supports previous oral microbiome studies in adults and children [1, 28, 30, 34, 35]. It is likely the samples collected at the molars and gingival margin contained small fragments of plaque. Recent studies have shown that the plaque biofilm consists of a highly spatially and taxonomically organised consortium of microorganisms [36]. *Streptococcus* initially attaches to the surface of the tooth and acts as a substrate for the attachment of other bacterial species [36, 37]. However, due to its facultative aerobic nature, *Streptococcus* also colonise towards the surface of the plaques 'corn-cob' structure and is involved in driving many biochemical

gradients in the biofilm [36]. Due to its high abundance at other microhabitats in the oral cavity, *Streptococcus* is also believed to be a wide-ranging coloniser of multiple surfaces [36]. The *Veillonella* genera of bacteria, also abundant in the paediatric oral cavity, depend on the organic acids produced by *Streptococcus* from the breakdown of carbohydrates in the oral cavity [38].

The back of the tongue and the palate were similar in bacterial composition and were higher in the relative abundance of the anaerobic bacteria *Prevotella* and *Veillonella*. Although different in their surface structure, these two microhabitats are often in contact with one another, possibly explaining the similarities observed. Dissimilarity among oral microhabitats and the tip of the tongue was also driven by a higher relative abundance of *Veillonella*, suggesting that a higher abundance of this genus of bacteria is characteristic of the tongue. This supports previous topographic tongue microbiome studies that show a skew towards these anaerobic bacteria [33, 39, 40]. The high relative abundance of this taxa at this anatomical location is likely due to the papillae on the surface of the tongue. These structures create small anaerobic pockets where nutrients are trapped, and bacteria are protected from salivary clearance [41]. *Prevotella* and *Veillonella* are commonly identified in the healthy oral microbiome [29, 30]. However, these hydrogen-sulfide producing bacteria found within the tongue biofilm are also responsible for oral malodour when increased in abundance [39, 42].

A higher relative abundance of *Haemophilus* and *Rothia* at the tip of the tongue were driving the dissimilarity among all other oral microhabitats, including the back of the tongue. These genera of bacteria are aerobic or facultative anaerobic, which suggests a decreasing oxygen gradient from the tip to the back of the tongue. As the

tip of the tongue is most exposed to the external environment, and is directly exposed to the air we breathe, it is logically consistent that this location is higher in aerobic species of bacteria compared to other locations.

During sleep, the dynamics of the oral cavity change. Healthy individuals breathe predominantly through their nose during sleep [43], creating an anaerobic environment within the mouth. Salivary flow and intraoral pH have also been reported to decrease during sleep [12, 15, 44]. Saliva plays an important role in the buffering of the intraoral pH by neutralising acids, some of which are produced by bacteria including *Streptococcus* [12, 45]. Therefore, during sleep when there is reduced salivary flow, the intraoral pH declines creating a slightly acidic environment [15]. During sleep, *Veillonella* and *Prevotella* increased in relative abundance and were the top taxa driving the dissimilarity between oral samples collected before and after sleep (Fig. 4). Both these bacteria are acid-tolerant and benefit from these acidic conditions [46, 47]. As previously mentioned *Veillonella* is dependent on the production of organic acids and utilises them as a carbon source [38]. However, *Prevotella* can act as an acid neutraliser through the fermentation of amino acids [46, 48]. This then facilitates the growth of periodontopathic bacteria that require a pH neutral environment [48].

Participants in this study had significantly different oral bacterial community structures to one another as evident by the grouping of oral samples according to participant (Fig. 5). Individualisation in human microbiomes occurs for the oral cavity, skin and gut [35, 49-52]. Differences in environments, diets and immune systems are thought to be involved in creating the dissimilarity among individuals [8, 10, 11]. The indication that individuals' oral samples group together regardless of the sample location suggest of the potential need for personalised oral care in disease states.

Previous studies have suggested the differences in the microbial profiles of saliva between health and disease is not dependent on the time of sampling [53-55]. This is supported by reports of no diurnal variation in the microbiota of stimulated saliva samples from healthy adult individuals over 20 hours [56]. Other studies have reported temporal stability in saliva from 5 days to 7 years [53, 57]. Here we show that over approximately 9 hours of sleep, microhabitats within the oral cavity significantly differ in bacterial community composition. Therefore, unlike saliva, careful regulation in the time of sampling for oral microhabitats needs to be considered when investigating oral microbial related diseases.

Limitations of this study include the heterogeneity in the spread of the data as identified by the PERMDISP results. The tip of the tongue was significantly less dispersed than most other microhabitats in the oral cavity (PERMDISP $p > 0.05$; Fig. 2). This could suggest that the significant pairwise ANOSIM comparisons between the tip of the tongue and these locations are likely a result of differences in dispersion rather than location. Larger sampling size could help explain whether these differences in relative abundance of taxa with the tip of the tongue are a result of difference in the dispersal of data. Another limitation of this study was that no oral hygiene was implemented before sleep. Therefore, the increase in the anaerobic genera *Veillonella* and *Prevotella* may reflect the increase in sugars and carbohydrates in the oral cavity. Further work should investigate what effect oral hygiene has on the microbial community in the paediatric oral cavity before and after sleep.

Here we show that microhabitat variation in the paediatric oral cavity is driven by differences in the relative abundance of 'core' taxa characteristic to the healthy oral microbiome. Our work suggests that the microhabitats in the oral cavity follow a

circadian cycle, and that the anaerobic bacteria, *Veillonella* and *Prevotella*, increase during sleep. Therefore, care must be taken when collecting microhabitat samples for taxonomic comparisons between health states, as differences in community structure could be due to discrepancies in sample collection time.

Acknowledgements

This study was supported by Flinders University, Adelaide University and grants from the Australian Research Council, Channel 7 Research Foundation and the Australian Office of Learning and Teaching.

References

1. Dewhirst FE, Chen T, Izard J, Paster BJ, Tanner AC, Yu WH, et al. The human oral microbiome. *Journal of bacteriology*. 2010;192(19):5002-17. doi: 10.1128/JB.00542-10. PubMed PMID: 20656903; PubMed Central PMCID: PMC2944498.
2. Paster BJ, Boches SK, Galvin JL, Ericson RE, Lau CN, Levanos VA, et al. Bacterial diversity in human subgingival plaque. *Journal of bacteriology*. 2001;183(12):3770-83. Epub 2001/05/24. doi: 10.1128/JB.183.12.3770-3783.2001. PubMed PMID: 11371542; PubMed Central PMCID: PMCPMC95255.
3. Wade WG. The oral microbiome in health and disease. *Pharmacological research*. 2013;69(1):137-43. Epub 2012/12/04. doi: 10.1016/j.phrs.2012.11.006. PubMed PMID: 23201354.
4. Belstrom D, Constancias F, Liu Y, Yang L, Drautz-Moses DI, Schuster SC, et al. Metagenomic and metatranscriptomic analysis of saliva reveals disease-associated microbiota in patients with periodontitis and dental caries. *NPJ biofilms and*

microbiomes. 2017;3:23. Epub 2017/10/06. doi: 10.1038/s41522-017-0031-4. PubMed PMID: 28979798; PubMed Central PMCID: PMC5624903.

5. Belda-Ferre P, Alcaraz LD, Cabrera-Rubio R, Romero H, Simon-Soro A, Pignatelli M, et al. The oral metagenome in health and disease. *Isme J.* 2012;6(1):46-56. Epub 2011/07/01. doi: 10.1038/ismej.2011.85. PubMed PMID: 21716308; PubMed Central PMCID: PMC3246241.

6. Aas JA, Griffen AL, Dardis SR, Lee AM, Olsen I, Dewhirst FE, et al. Bacteria of dental caries in primary and permanent teeth in children and young adults. *J Clin Microbiol.* 2008;46(4):1407-17. Epub 2008/01/25. doi: 10.1128/JCM.01410-07. PubMed PMID: 18216213; PubMed Central PMCID: PMC2292933.

7. Beck JD, Offenbacher S. Systemic effects of periodontitis: epidemiology of periodontal disease and cardiovascular disease. *Journal of periodontology.* 2005;76(11 Suppl):2089-100. Epub 2005/11/10. doi: 10.1902/jop.2005.76.11-S.2089. PubMed PMID: 16277581.

8. Kilian M, Chapple IL, Hannig M, Marsh PD, Meuric V, Pedersen AM, et al. The oral microbiome - an update for oral healthcare professionals. *British dental journal.* 2016;221(10):657-66. Epub 2016/11/20. doi: 10.1038/sj.bdj.2016.865. PubMed PMID: 27857087.

9. Xu X, He J, Xue J, Wang Y, Li K, Zhang K, et al. Oral cavity contains distinct niches with dynamic microbial communities. *Environ Microbiol.* 2015;17(3):699-710. Epub 2014/05/08. doi: 10.1111/1462-2920.12502. PubMed PMID: 24800728.

10. Adler CJ, Dobney K, Weyrich LS, Kaidonis J, Walker AW, Haak W, et al. Sequencing ancient calcified dental plaque shows changes in oral microbiota with dietary shifts of the Neolithic and Industrial revolutions. *Nat Genet.* 2013;45(4):450-5,

5e1. Epub 2013/02/19. doi: 10.1038/ng.2536. PubMed PMID: 23416520; PubMed Central PMCID: PMC3996550.

11. Wu J, Peters BA, Dominianni C, Zhang Y, Pei Z, Yang L, et al. Cigarette smoking and the oral microbiome in a large study of American adults. *Isme J.* 2016;10(10):2435-46. Epub 2016/03/26. doi: 10.1038/ismej.2016.37. PubMed PMID: 27015003; PubMed Central PMCID: PMC5030690.

12. Humphrey SP, Williamson RT. A review of saliva: normal composition, flow, and function. *The Journal of prosthetic dentistry.* 2001;85(2):162-9. doi: 10.1067/mpr.2001.113778. PubMed PMID: 11208206.

13. Schneyer LH, Pigman W, Hanahan L, Gilmore RW. Rate of flow of human parotid, sublingual, and submaxillary secretions during sleep. *Journal of dental research.* 1956;35(1):109-14. PubMed PMID: 13286394.

14. Simon-Soro A, Tomas I, Cabrera-Rubio R, Catalan MD, Nyvad B, Mira A. Microbial geography of the oral cavity. *Journal of dental research.* 2013;92(7):616-21. doi: 10.1177/0022034513488119. PubMed PMID: 23674263.

15. Choi JE, Waddell JN, Lyons KM, Kieser JA. Intraoral pH and temperature during sleep with and without mouth breathing. *J Oral Rehabil.* 2016;43(5):356-63. doi: 10.1111/joor.12372. PubMed PMID: WOS:000374339900005.

16. Carlson-Jones JA, Kontos A, Kennedy D, Martin J, McKerral J, Paterson JS, et al. The microbial abundance dynamics of the human oral cavity before and after sleep. *Plos One* (Submitted). 2018.

17. Carlson-Jones J, Kontos A, Paterson J, Smith R, Dann L, Speck P, et al. Flow Cytometric Enumeration of Bacterial and Virus-Like Particle Populations in the Human Oral Cavity Pre and Post Sleep. *J Sleep Res.* 2016;25:86-. PubMed PMID: WOS:000393032700215.

18. Dann LM, Smith RJ, Tobe SS, Paterson JS, Oliver RL, Mitchell JG. Microscale distributions of freshwater planktonic viruses and prokaryotes are patchy and taxonomically distinct. *Aquatic Microbial Ecology*. 2016;77(2):65-77.
19. Zhang J, Kobert K, Flouri T, Stamatakis A. PEAR: a fast and accurate Illumina Paired-End reAd mergeR. *Bioinformatics*. 2014;30(5):614-20. doi: 10.1093/bioinformatics/btt593. PubMed PMID: 24142950; PubMed Central PMCID: PMC3933873.
20. Pylro VS, Roesch LF, Morais DK, Clark IM, Hirsch PR, Totola MR. Data analysis for 16S microbial profiling from different benchtop sequencing platforms. *Journal of microbiological methods*. 2014;107:30-7. doi: 10.1016/j.mimet.2014.08.018. PubMed PMID: 25193439.
21. Kuczynski J, Stombaugh J, Walters WA, Gonzalez A, Caporaso JG, Knight R. Using QIIME to analyze 16S rRNA gene sequences from microbial communities. *Current protocols in bioinformatics*. 2011;Chapter 10:Unit 10 7. doi: 10.1002/0471250953.bi1007s36. PubMed PMID: 22161565; PubMed Central PMCID: PMC3249058.
22. Edgar RC. UPARSE: highly accurate OTU sequences from microbial amplicon reads. *Nature methods*. 2013;10(10):996-8. doi: 10.1038/nmeth.2604. PubMed PMID: 23955772.
23. Rognes T, Flouri T, Nichols B, Quince C, Mahe F. VSEARCH: a versatile open source tool for metagenomics. *PeerJ*. 2016;4:e2584. doi: 10.7717/peerj.2584. PubMed PMID: 27781170; PubMed Central PMCID: PMC5075697.
24. Edgar RC. Search and clustering orders of magnitude faster than BLAST. *Bioinformatics*. 2010;26(19):2460-1. doi: 10.1093/bioinformatics/btq461. PubMed PMID: 20709691.

25. Clarke K, Gorley, RN. PRIMER v7: User Manual/Tutorial. Plymouth: PRIMER-E; 2015.
26. Anderson M, Gorley R, Clarke K. PERMANOVA+ for PRIMER: Guide to Software and Statistical Methods. Plymouth UK: PRIMER-E; 2008.
27. Clarke KR. Non-parametric multivariate analyses of changes in community structure. *Austral ecology*. 1993;18(1):117-43.
28. Xu X, He J, Xue J, Wang Y, Li K, Zhang K, et al. Oral cavity contains distinct niches with dynamic microbial communities. *Environmental Microbiology*. 2014:n/a-n/a. doi: 10.1111/1462-2920.12502.
29. Aas JA, Paster BJ, Stokes LN, Olsen I, Dewhirst FE. Defining the normal bacterial flora of the oral cavity. *J Clin Microbiol*. 2005;43(11):5721-32. doi: 10.1128/JCM.43.11.5721-5732.2005. PubMed PMID: 16272510; PubMed Central PMCID: PMC1287824.
30. Zaura E, Keijser BJ, Huse SM, Crielaard W. Defining the healthy "core microbiome" of oral microbial communities. *BMC microbiology*. 2009;9:259. doi: 10.1186/1471-2180-9-259. PubMed PMID: 20003481; PubMed Central PMCID: PMC2805672.
31. Kaplan JB. Biofilm dispersal: mechanisms, clinical implications, and potential therapeutic uses. *Journal of dental research*. 2010;89(3):205-18. doi: 10.1177/0022034509359403. PubMed PMID: 20139339; PubMed Central PMCID: PMC3318030.
32. Rudney JD. Saliva and dental plaque. *Adv Dent Res*. 2000;14:29-39. doi: 10.1177/08959374000140010401. PubMed PMID: 11842921.

33. Mager DL, Ximenez-Fyvie LA, Haffajee AD, Socransky SS. Distribution of selected bacterial species on intraoral surfaces. *J Clin Periodontol*. 2003;30(7):644-54. Epub 2003/07/02. PubMed PMID: 12834503.
34. Mashima I, Theodorea CF, Thaweboon B, Thaweboon S, Scannapieco FA, Nakazawa F. Exploring the salivary microbiome of children stratified by the oral hygiene index. *Plos One*. 2017;12(9):e0185274. Epub 2017/09/22. doi: 10.1371/journal.pone.0185274. PubMed PMID: 28934367; PubMed Central PMCID: PMC5608389.
35. Bik EM, Long CD, Armitage GC, Loomer P, Emerson J, Mongodin EF, et al. Bacterial diversity in the oral cavity of 10 healthy individuals. *Isme J*. 2010;4(8):962-74. Epub 2010/03/26. doi: 10.1038/ismej.2010.30. PubMed PMID: 20336157; PubMed Central PMCID: PMC2941673.
36. Mark Welch JL, Rossetti BJ, Rieken CW, Dewhirst FE, Borisy GG. Biogeography of a human oral microbiome at the micron scale. *Proc Natl Acad Sci U S A*. 2016;113(6):E791-800. doi: 10.1073/pnas.1522149113. PubMed PMID: 26811460; PubMed Central PMCID: PMC4760785.
37. Whitmore SE, Lamont RJ. The pathogenic persona of community-associated oral streptococci. *Molecular microbiology*. 2011;81(2):305-14. Epub 2011/06/04. doi: 10.1111/j.1365-2958.2011.07707.x. PubMed PMID: 21635580; PubMed Central PMCID: PMC3248243.
38. Mashima I, Nakazawa F. The influence of oral *Veillonella* species on biofilms formed by *Streptococcus* species. *Anaerobe*. 2014;28:54-61. Epub 2014/05/28. doi: 10.1016/j.anaerobe.2014.05.003. PubMed PMID: 24862495.
39. Seerangaiyan K, van Winkelhoff AJ, Harmsen HJM, Rossen JWA, Winkel EG. The tongue microbiome in healthy subjects and patients with intra-oral halitosis. *J*

Breath Res. 2017;11(3):036010. Epub 2017/09/07. doi: 10.1088/1752-7163/aa7c24.
PubMed PMID: 28875948.

40. Palmer RJ, Jr. Composition and development of oral bacterial communities. *Periodontol* 2000. 2014;64(1):20-39. Epub 2013/12/11. doi: 10.1111/j.1600-0757.2012.00453.x. PubMed PMID: 24320954; PubMed Central PMCID: PMC3876289.

41. Allaker RP, Waite RD, Hickling J, North M, McNab R, Bosma MP, et al. Topographic distribution of bacteria associated with oral malodour on the tongue. *Archives of oral biology*. 2008;53 Suppl 1:S8-S12. doi: 10.1016/S0003-9969(08)70003-7. PubMed PMID: 18460402.

42. Washio J, Sato T, Koseki T, Takahashi N. Hydrogen sulfide-producing bacteria in tongue biofilm and their relationship with oral malodour. *Journal of medical microbiology*. 2005;54(Pt 9):889-95. Epub 2005/08/11. doi: 10.1099/jmm.0.46118-0. PubMed PMID: 16091443.

43. Pevernagie DA, De Meyer MM, Claeys S. Sleep, breathing and the nose. *Sleep medicine reviews*. 2005;9(6):437-51. Epub 2005/10/26. doi: 10.1016/j.smr.2005.02.002. PubMed PMID: 16242364.

44. Dawes C. Circadian rhythms in human salivary flow rate and composition. *The Journal of physiology*. 1972;220(3):529-45. PubMed PMID: 5016036; PubMed Central PMCID: PMC1331668.

45. Dawes C, Pedersen AM, Villa A, Ekstrom J, Proctor GB, Vissink A, et al. The functions of human saliva: A review sponsored by the World Workshop on Oral Medicine VI. *Archives of oral biology*. 2015;60(6):863-74. Epub 2015/04/05. doi: 10.1016/j.archoralbio.2015.03.004. PubMed PMID: 25841068.

46. Takahashi N. Oral Microbiome Metabolism: From "Who Are They?" to "What Are They Doing?". *Journal of dental research*. 2015;94(12):1628-37. doi: 10.1177/0022034515606045. PubMed PMID: 26377570.
47. Hajishengallis E, Parsaei Y, Klein MI, Koo H. Advances in the microbial etiology and pathogenesis of early childhood caries. *Molecular oral microbiology*. 2017;32(1):24-34. doi: 10.1111/omi.12152. PubMed PMID: 26714612; PubMed Central PMCID: PMC4929038.
48. Takahashi N, Saito K, Schachtele CF, Yamada T. Acid tolerance and acid-neutralizing activity of *Porphyromonas gingivalis*, *Prevotella intermedia* and *Fusobacterium nucleatum*. *Oral microbiology and immunology*. 1997;12(6):323-8. PubMed PMID: 9573805.
49. Hall MW, Singh N, Ng KF, Lam DK, Goldberg MB, Tenenbaum HC, et al. Interpersonal diversity and temporal dynamics of dental, tongue, and salivary microbiota in the healthy oral cavity. *NPJ biofilms and microbiomes*. 2017;3:2. Epub 2017/06/27. doi: 10.1038/s41522-016-0011-0. PubMed PMID: 28649403; PubMed Central PMCID: PMC5445578.
50. Costello EK, Lauber CL, Hamady M, Fierer N, Gordon JI, Knight R. Bacterial community variation in human body habitats across space and time. *Science*. 2009;326(5960):1694-7. Epub 2009/11/07. doi: 10.1126/science.1177486. PubMed PMID: 19892944; PubMed Central PMCID: PMC3602444.
51. Turnbaugh PJ, Gordon JI. The core gut microbiome, energy balance and obesity. *The Journal of physiology*. 2009;587(Pt 17):4153-8. Epub 2009/06/06. doi: 10.1113/jphysiol.2009.174136. PubMed PMID: 19491241; PubMed Central PMCID: PMC2754355.

52. Nasidze I, Li J, Quinque D, Tang K, Stoneking M. Global diversity in the human salivary microbiome. *Genome research*. 2009;19(4):636-43. Epub 2009/03/03. doi: 10.1101/gr.084616.108. PubMed PMID: 19251737; PubMed Central PMCID: PMC2665782.
53. Lazarevic V, Whiteson K, Hernandez D, Francois P, Schrenzel J. Study of inter- and intra-individual variations in the salivary microbiota. *BMC genomics*. 2010;11:523. Epub 2010/10/06. doi: 10.1186/1471-2164-11-523. PubMed PMID: 20920195; PubMed Central PMCID: PMC2997015.
54. Stahringer SS, Clemente JC, Corley RP, Hewitt J, Knights D, Walters WA, et al. Nurture trumps nature in a longitudinal survey of salivary bacterial communities in twins from early adolescence to early adulthood. *Genome research*. 2012;22(11):2146-52. Epub 2012/10/16. doi: 10.1101/gr.140608.112. PubMed PMID: 23064750; PubMed Central PMCID: PMC3483544.
55. Cameron SJ, Huws SA, Hegarty MJ, Smith DP, Mur LA. The human salivary microbiome exhibits temporal stability in bacterial diversity. *FEMS microbiology ecology*. 2015;91(9):fiv091. Epub 2015/07/25. doi: 10.1093/femsec/fiv091. PubMed PMID: 26207044.
56. Belstrom D, Holmstrup P, Bardow A, Kokaras A, Fiehn NE, Paster BJ. Temporal Stability of the Salivary Microbiota in Oral Health. *Plos One*. 2016;11(1):e0147472. Epub 2016/01/23. doi: 10.1371/journal.pone.0147472. PubMed PMID: 26799067; PubMed Central PMCID: PMC4723053.
57. Rasiah IA, Wong L, Anderson SA, Sissons CH. Variation in bacterial DGGE patterns from human saliva: over time, between individuals and in corresponding dental plaque microcosms. *Archives of oral biology*. 2005;50(9):779-87. Epub 2005/06/23. doi: 10.1016/j.archoralbio.2005.02.001. PubMed PMID: 15970209.

Chapter 7

THE SPATIAL DISTRIBUTION OF THE ORAL MICROBIOME
IN PAEDIATRIC SLEEP DISORDER BREATHERS

Abstract

Sleep disorder breathing (SDB) describes a spectrum of breathing disorders where there is the complete or partial blockage of the airways during sleep. If left untreated in children, it can lead to serious health issues. Recently it has been shown that the absolute microbial abundance dynamics of the paediatric SDB oral cavity significantly differs to healthy participants. However, taxonomic shifts are yet to be investigated. Here we report for the first time, using 16S ribosomal RNA gene sequencing, a significant difference in the bacterial community composition among microhabitats within the paediatric SDB oral cavity. However, unlike the healthy oral cavity, these bacterial communities remain constant during sleep. We also show that the paediatric SDB oral cavity is significantly different in bacterial community composition to the healthy oral cavity, specifically after sleep at the tip of the tongue where there is a shift from the anaerobic bacteria *Veillonella*, to the aerobic bacteria *Haemophilus* in SDB. This suggests that mouth breathing during sleep in SDB influences the oral microbial communities. Therefore, future studies should be conducted into the causal relations between the oral microbiome and SDB, and what impact these microbial shifts have of overall health and wellbeing.

Introduction

Sleep disorder breathing (SDB) affects approximately 10% of the paediatric population and describes a range of breathing disorders from snoring to obstructive sleep apnoea [1]. In children with SDB, the obstruction of the upper airways is usually due to hypertrophy of the tonsils and adenoids [2]. This results in the partial or complete blockage of air flow during sleep, leading to the disruption of the normal sleeping pattern [3]. Within the paediatric population, these disturbances to the normal sleeping pattern can lead to inattentiveness, fatigue, aggressiveness and hyperactivity [4, 5]. This can ultimately result in growth impairment, behavioural problems and neurocognitive and cardiovascular issues for the child [6, 7].

Currently, human microbial studies are focusing on characterising the shifts within the healthy microbiome, particularly at the spatial and temporal scales, to explain the progression of various disease states [8-14]. The oral cavity is one niche where this has been applied [8, 9]. Within the oral cavity are microhabitats that vary in surface structure [8, 9]. These microhabitats have been shown to harbour different microbial communities that vary taxonomically and numerically [8, 9, 15-17]. Previously, we have demonstrated that the microbial abundance dynamics within the paediatric SDB oral cavity significantly differ to the healthy paediatric oral cavity, particularly with the viral communities [18]. However, the taxonomic variations among microhabitats in the SDB oral cavity before and after sleep are still unknown.

Recently it has been shown that sleep fragmentation, a common symptom of obstructive sleep apnoea, perturbs the gut microbiota [19, 20]. As the oral cavity is the gateway to the digestive system, understanding what, if any, affect irregular breathing has on the microbiome of the upper respiratory tract could assist in interpreting or

tracking the progression of microbial shifts further down the digestive system. Here, we compared the bacterial taxonomic community composition of the paediatric oral cavity between healthy and SDB using 16S rRNA sequencing. We examined the microbial spatial distribution of the SDB oral cavity at 6 locations before and after sleep. Here we report on a significant difference in the microbial community structure of the oral cavity between healthy and SDB.

Materials and Methods

Ethics statement

This study was approved by the Human Research Ethics Committees of the Women's and Children's Hospital and the University of Adelaide, South Australia. The study has been conducted in accordance with the 1964 declaration of Helsinki and its later amendments. Written consent was provided by all parents and children written assent for their involvement in the study. A child's health and behaviour questionnaire was also completed by the parents prior to sample collection.

Sample collection

Oral swabs were collected from 12 participants undergoing a polysomnography sleep test at the Women's and Children's Hospital as part of a larger study investigating the effects of sleep disorder breathing on the development of children. Of the 12 participants, 6 were healthy controls (female = 2, male = 4) and 6 were participants that had been diagnosed with SDB (female = 2, male = 4). Healthy participants ages ranged from 7.75 to 16.58 years with an overall average of 10.40 ± 3.99 years. SDB ages ranged from 6.33 to 15.92 years with an overall average of

10.01 ± 1.49 years. BMI's for the healthy group range between 14.2 to 19.7 (average = 18.63 ± 3.92). SDB had BMI's from 12.83 to 26.6 (average = 19.07 ± 2.10).

Oral swab samples were collected by methods previously described [15, 16, 18]. Briefly, sterile individually packaged rayon swabs (Copan, Brescia, Italy; product code: 155C; length: 13.3 cm, diameter: 5 mm) were used to collect samples from the middle of the tip of the tongue, middle of the palate, middle of the back of the tongue, the gingival margin of the last proximal molar on the right lower jaw, the left temporomandibular joint and the occlusal site of the last two distal molars on the bottom jaw. These samples will be referred to as the tip of the tongue, palate, back of tongue, gingivae, temporomandibular joint and molars respectively for the duration of this manuscript. Swabs were collected by rotating the swab tip clockwise 6 times at the sample location. Swabs were collected from each sample location just before lights out between 8.30-9.00 pm and again the following morning at the same locations between 6.00-6.30 am. These samples will be referred to as before and after sleep respectively. In total there were 144 swab samples collected from the 12 participants. All oral swabs were collected by the same researcher using the methods described above. All swab samples were then frozen at -80°C in their polypropylene tubes until analysis.

Swab preparation

The oral swabs used in this study were part of another study investigating the absolute bacterial and Virus-like particle (VLP) abundances within the oral cavity of healthy and SDB using flow cytometry [16, 18]. In brief, swab tips were cut off into 1 ml of sterile (0.2 µm filtered and UV treated) TE buffer (10 mM Tris, 1 mM EDTA pH 7.4, sigma) and vortexed for 3 minutes to elute the bacteria and VLP from the swab

[16, 18]. The swab tip was then removed from the sample and a small volume of the buffer was collected for flow cytometric analysis [16, 18]. The remaining sample was snap frozen in liquid nitrogen and stored at -80°C ready for 16S analysis. During the preparation of the samples, negative control samples were prepared in the same manner using sterile rayon swabs (Copan, Brescia, Italy; product code: 155C; length: 13.3 cm, diameter: 5 mm).

Bacterial 16S PCR amplification

Eluted oral swab samples and negative control samples were thawed at room temperature and vortexed briefly to ensure uniform microbial distribution within the samples. Direct PCR [21] was performed on the samples using primers 341F and 806R (with Illumina overhang adaptors attached) that targeted the V4-V5 region of the 16S gene. KAPA Taq HiFi Hotstart polymerase (Kapa Biosystems, Boston, MA, USA) was used for the PCR amplification of the samples. A total reaction volume of 25 µl was used. Ten microliters of sample were used in each reaction. The PCR reaction was then performed as followed: initial denaturing step at 95°C for 3 minutes followed by 30 cycles of 95°C for 30 seconds, 55°C for 30 seconds and 72°C for 30 seconds. A final extension step of 72°C for 5 minutes was performed, followed by storage at 4°C. An agarose gel (2.5%) was run on the PCR products to ensure the successful amplification of oral samples and clear negative controls. DNA Sequences were generated using an Illumina Miseq run (Genomics Facility, Flinders Medical Centre, Adelaide Australia).

Bioinformatic analysis

Paired-End reAd mergeR (PEAR) v0.9.4 was used to successfully assemble and quality filter 7,660,611 reads at a Phred score of 30 [22]. As per previously

described methods [23], sequences were processed using Quantitative Insights Into Microbial Ecology (QIIME) v.1.8.0 [24] and UPARSE [25]. Briefly, sequences were quality filtered: to a minimum quality score of 30, to a minimum 200bp in length, no more than 6 ambiguous bases and no primer mismatches using QIIME. Sequences were dereplicated using VSEARCH [26] and singletons removed in USEARCH [27]. The removal of chimeras and the clustering into operational taxonomic units (OTUs) at 97% similarity was achieved using the *cluster_otus* command in USEARCH. Taxonomy was assigned using the Greengenes database (13_08) using UCLUST [27] in QIIME. To remove biases due to differing sequencing depths, sequences were rarefied to 4920.

Sequence analysis

The multivariate statistics program PRIMER (version 7, Primer-E, Plymouth) was used to calculate Bray-Curtis similarity matrices were calculated from square root transformed relative abundance data [28, 29]. Permutational Multivariate Analysis of Variance (PERMANOVA+, version 1.0.3) was used to determine differences in overall bacterial composition between locations, time, gender, participants and health status using 9999 unrestricted permutations of the raw data [29]. Patterns of bacterial community variation were analysed using the Analysis of Similarity (ANOSIM) to test the null hypothesis of no differences among *a priori* group using 9999 permutations [28]. To test for multivariate dispersions within a group, the distance-based test for homogeneity (PERMDISP) was performed using 9999 permutations [30]. A similarity percentage analysis (SIMPER) was used to determine the top genera of bacteria driving the dissimilarity between samples (90% cut off) when statistical significance was observed from the PERMANOVA and ANOSIM results ($p < 0.05$) [30]. The spread and separation of samples were then visualised using a metric Multidimensional

Scaling (MDS) plot [28]. Five hundred bootstraps were run to determine the average centroid and where 95% of the averages lied within the multivariate space.

Results

Overall sequence statistics

One hundred and twenty-two samples were successfully sequenced. After paired-end assembly, 7,660,611 reads were successfully joined. After 97% OTU clustering 5,577,556 sequences were clustered into 536 OTUs. Each sample contained an average of 44,980 ($\pm 31,384$ SD) sequences, with a minimum of 598 and a maximum of 253,489 sequences.

Oral microhabitats vary in bacterial composition in SDB

Overall, bacterial communities in the paediatric SDB oral cavity separated by microhabitat (ANOSIM $R = 0.23$, $p < 0.0001$; PERMANOVA pseudo- $F = 3.45$, $p < 0.0001$). Ten of the 15 microhabitat pairwise ANOSIM comparisons were significantly different (Table 1; $R \geq 0.13$, $p < 0.05$). The back of the tongue was the only microhabitat observed to be significantly different in bacterial composition to all other locations in the SDB oral cavity (Table 1; $p < 0.05$). The palate and tip of tongue were observed to be similar in bacterial composition (Table 1; $R = 0.11$, $p = 0.066$). However, both were significantly different to the back of tongue, gingivae and molars (Table 1; $p < 0.05$). In addition, the palate was also significantly different in bacterial composition compared to the temporomandibular joint (Table 1; $R = 0.23$, $p = 0.008$). There were no significant differences between bacterial communities at the gingivae, temporomandibular joint and molars (Table 1; $p > 0.05$).

Table 1. Pairwise ANOSIM comparisons between the microhabitats in the paediatric SDB oral cavity. A significant difference in the patterns of bacterial community composition between microhabitats is denoted by an asterisk (*). Average Bray-Curtis dissimilarity percentages were calculated using SIMPER analysis.

Pairwise tests	R statistic	P value	Average Bray-Curtis dissimilarity
Temporomandibular joint, Back of tongue	0.56	0.006*	42.85%
Temporomandibular joint, Gingivae	-0.045	0.67	-
Temporomandibular joint, Palate	0.23	0.008*	31.88%
Temporomandibular joint, Molars	0.019	0.31	-
Temporomandibular joint, Tip of tongue	0.11	0.089	-
Back of tongue, Gingivae	0.55	0.003*	46.41%
Back of tongue, Palate	0.65	0.005*	34.96%
Back of tongue, Molars	0.75	0.0005*	45.00%
Back of tongue, Tip of tongue	0.70	0.001*	41.15%
Gingivae, Palate	0.39	< 0.0001*	35.99%
Gingivae, Molars	0.055	0.17	-
Gingivae, Tip of tongue	0.24	0.006*	36.44%
Palate, Molars	0.18	0.013*	30.78%
Palate, Tip of tongue	0.11	0.066	-
Molars, Tip of tongue	0.13	0.045*	31.61%

Distance-based tests for homogeneity of multivariate dispersions among microhabitats revealed an overall even distribution of data points (PERMDISP $F = 4.81$, $p = 0.0042$). However, pairwise PERMDISP comparisons showed significant differences between the dispersal of data between the back of the tongue with the temporomandibular joint ($t = 3.59$, $p = 0.0026$), palate ($t = 2.80$, $p = 0.027$), molars ($t = 3.92$, $p = 0.0023$), gingivae ($t = 3.97$, $p = 0.0033$) and tip of tongue ($t = 2.49$, $p = 0.041$). A significant difference in the dispersal of data was also observed between the palate and the gingivae ($t = 3.07$, $p = 0.0059$). The range in Bray-Curtis distance-to-centroid measures for microhabitats using PERMDISP were between 11.71 ± 0.93 at the back of the tongue to 24.93 ± 2.03 at the gingivae. A metric MDS plot using the Bray-Curtis bootstrap averages showed an overlap in the data between the temporomandibular joint, molars and gingivae (Fig. 1). An overlap in the 95% bootstrap region was also observed between the tip of the tongue and the palate (Fig. 1). No microhabitats were observed to overlap with the back of the tongue (Fig. 1).

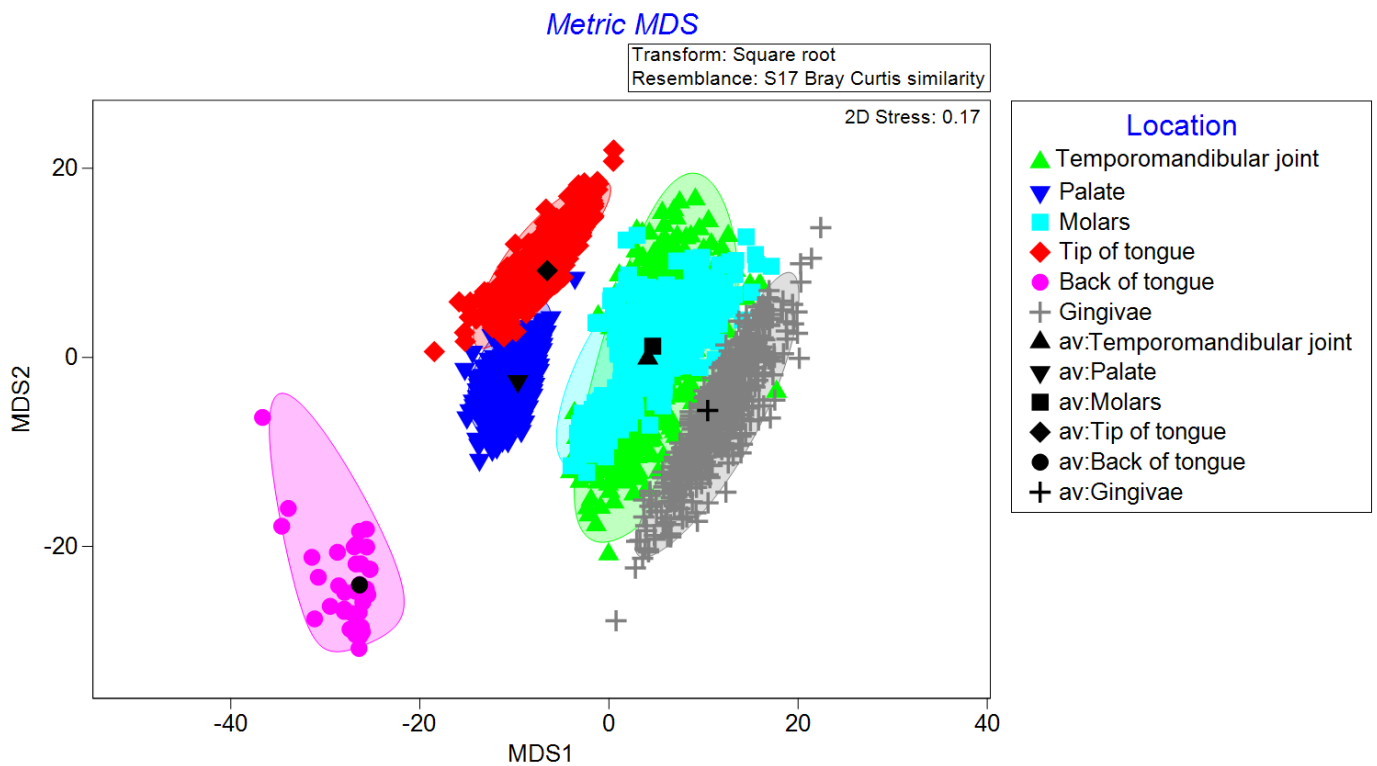


Figure 1. Metric Multidimensional Scaling (MDS) plot based on the Bray-Curtis dissimilarity for all samples at the temporomandibular joint (green triangle), palate (inverted dark blue triangles), molars (light blue squares), tip of tongue (red diamonds), back of tongue (pink circles) and gingivae (grey crosses) in the SDB paediatric oral cavity. Centroid values for each microhabitat are surrounded by a smooth bootstrap region where 95% of the 500 bootstrap averages lie.

SIMPER analysis on each oral microhabitat in SDB revealed average Bray-Curtis similarities of 66.75, 73.53, 69.23, 71.70, 80.48 and 63.28% for the temporomandibular joint, palate, molars, tip of tongue, back of tongue and gingivae respectively. *Streptococcus* was the most abundant genera at temporomandibular joint, palate, molars, tip of tongue and gingivae contributing to 22.62, 17.01, 21.08, 18.67 and 23.99% of the total within group similarity at each location respectively. At the back of the tongue, *Veillonella* was the top taxa among samples contributing to 18.12% of the within group similarity at this location. Pairwise SIMPER analysis revealed that the dissimilarity between the back of the tongue and the other microhabitats was driven by a higher relative abundance of *Veillonella* and a lower relative abundance of *Streptococcus*. This contributed to 17.31, 18.48, 19.30, 17.49 and 16.56% of the overall average dissimilarity between the back of the tongue and the temporomandibular joint, molars, palate, tip of tongue and gingivae respectively (Table 1; Fig. 2). In addition, the dissimilarity at temporomandibular joint, molars and gingivae were further driven by a higher relative abundance of *Prevotella* and *Actinomyces* at the back of the tongue contributing an additional 14.45, 12.99 and 14.66% to the overall dissimilarity at each location respectively (Fig. 2). At the tip of the tongue, the average dissimilarity with the molars and gingivae was driven by a higher relative abundance of *Rothia* and *Haemophilus* contributing to 13.19 and 14.75% of the overall dissimilarity respectively (Table 1; Fig. 2). *Neisseria* was also higher in relative abundance at the tip of the tongue and further contributed 5.84% to the dissimilarity at the gingivae (Fig. 2). Between the tip and back of tongue, 25.52% of the dissimilarity was driven by a higher relative abundance of *Rothia*, *Haemophilus* and *Neisseria* at the tip of the tongue and a higher relative abundance of *Prevotella* at the back of the tongue (Fig. 2).

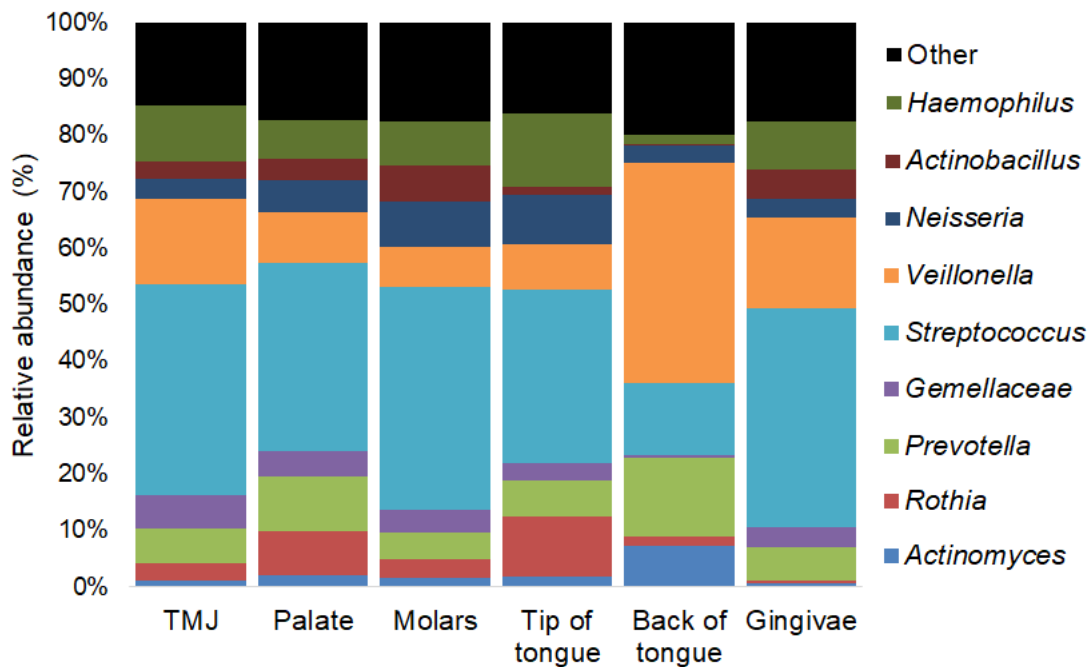


Figure 2. The top bacterial taxa driving the dissimilarity between microhabitats in the SDB oral cavity. Additional bacteria identified at each microhabitat that were not involved in driving the dissimilarity are grouped into Other. Bar graph is based on the average relative abundance of the bacteria at each microhabitat.

The temporomandibular joint was higher in relative abundance of *Haemophilus* and *Gemellaceae* compared to the back of the tongue and contributed to 10.25% of the average dissimilarity between microhabitats (Table 1; Fig. 2). The dissimilarity between the palate and the temporomandibular joint was driven by a higher relative abundance of *Rothia* and *Actinobacillus* at the palate and a higher relative abundance of *Veillonella* at the temporomandibular joint. Together, these taxa were responsible for 19.50% of the dissimilarity between the palate and temporomandibular joint (Table 1; Figure 2). *Rothia* was higher at the palate in comparison to the gingivae and drove 6.81% of the dissimilarity (Table 1; Fig. 2). *Actinobacillus* was higher in relative

abundance at the molars compared to the palate and the tip of the tongue and contributed to 7.04 and 6.86% of the dissimilarity between microhabitats respectively (Table 1; Fig. 2). At the gingivae, a higher relative abundance of *Veillonella* and *Actinobacillus* drove 12.43% of the dissimilarity with the palate (Table 1; Fig. 2).

Bacterial community composition among microhabitats when split by time

Pairwise ANOSIM comparisons between locations only before sleep revealed a significant difference in the relative abundance of bacterial communities at the back of the tongue compared with the temporomandibular joint ($R = 0.51$, $p = 0.024$), gingivae ($R = 0.61$, $p = 0.016$), palate ($R = 0.93$, $p = 0.005$), molars ($R = 0.88$, $p = 0.005$) and tip of the tongue ($R = 0.83$, $p = 0.008$). These differences were predominantly driven by a higher relative abundance of *Veillonella* and *Prevotella* at the back of the tongue (SIMPER). The higher relative abundance of these bacterial genera combined with the observed lower abundance of *Streptococcus* and *Haemophilus* at the back of the tongue drove 32.61, 28.93, 31.77, 32.82 and 32.90% of the Bray-Curtis dissimilarity between the temporomandibular joint (Avg Diss = 43.58), gingivae (Avg Diss = 46.00), palate (Avg Diss = 39.24), molars (Avg Diss = 48.15) and tip of tongue (Avg Diss = 43.58) respectively (SIMPER). Pairwise ANOSIM comparisons also revealed a significant difference in bacterial community composition between the palate and gingivae ($R = 0.33$, $p = 0.013$). The average dissimilarity between these two locations was 35.96 and was predominantly driven by higher relative abundances of *Rothia* and *Actinobacillus* at the palate and *Veillonella* at the gingivae (SIMPER). Combined, these differences contributed to 22.22% of the overall dissimilarity between these two locations (SIMPER). After sleep, the only significant differences observed were between the palate and the temporomandibular joint (ANOSIM $R = 0.36$, $p = 0.033$) and the palate and gingivae (ANOSIM $R = 0.45$, $p =$

0.004). SIMPER analysis revealed that a higher relative abundance of *Prevotella* at the palate was the top contributing taxa driving 11.70 and 10.85% of the 29.64 and 35.64 Bray-Curtis dissimilarity at the temporomandibular joint and gingivae respectively.

When grouped by time of sampling (i.e. before and after sleep), bacterial communities in the paediatric SDB oral cavity did not significantly shift in overall bacterial composition during sleep (ANOSIM $R = 0.033$, $p = 0.10$; PERMANOVA Pseudo-F = 1.75, $p = 0.10$). No significant difference was also observed between pairwise comparisons at each microhabitat before and after sleep (ANOSIM $p > 0.05$).

Bacterial communities differ in composition among participants and between genders in SDB

Bacterial community structure among participants was observed to be significantly different (ANOSIM $R = 0.52$, $p < 0.0001$; PERMANOVA Pseudo-F = 7.33, $p < 0.0001$). This was further supported through the visualisation of the MDS plots where all samples collected from a participant grouped together (Fig. 3). Participant 4 had the greatest spread of data with an average Bray-Curtis distance-to-centroid measure of 19.40 ± 2.61 and was observed to slightly overlap with participant 15 on the metric MDS plot of Bray-Curtis bootstrap averages (Fig. 3). However, there was no significant difference in the dispersal of participant 4's data with any other participant (PERMDISP $p > 0.05$). No other overlaps were observed between participants (Fig. 3). Samples collected from each participant had overall average Bray-Curtis similarities ranging between 71 and 76%. *Streptococcus* was the dominant

taxa identified within each participant and contributed to between 14% and 24% of the overall Bray-Curtis similarities (SIMPER).

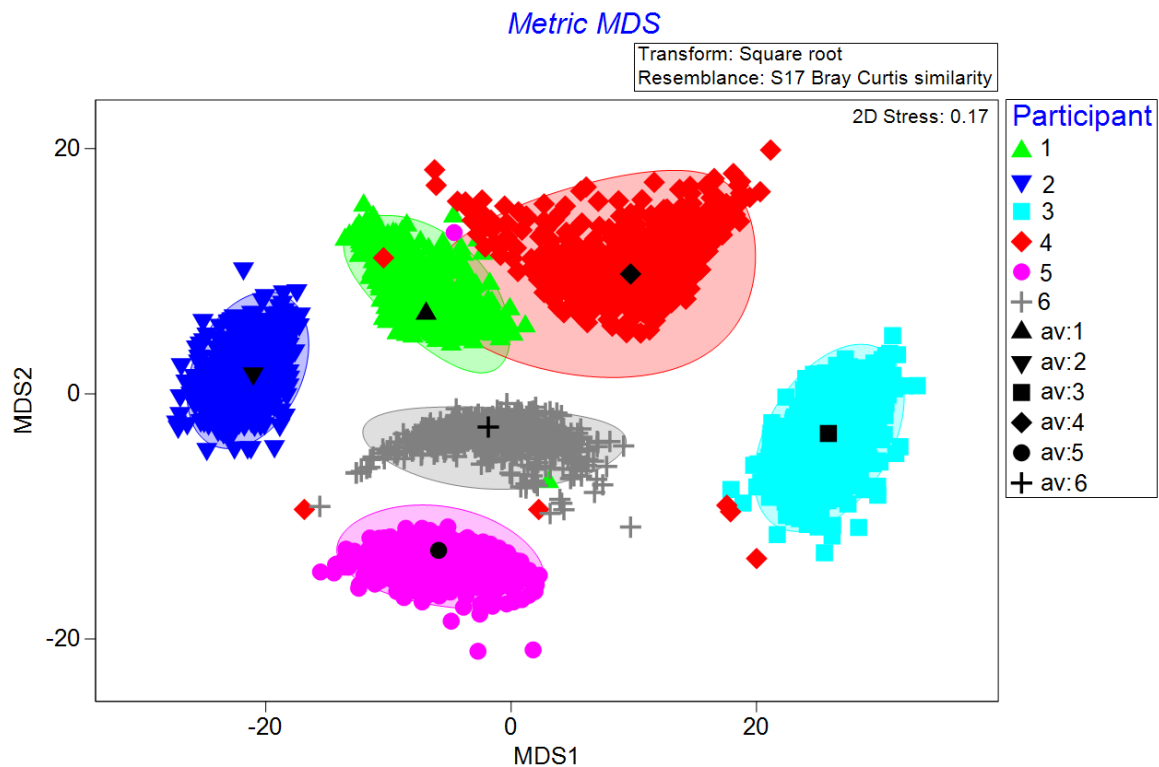


Figure 3. Metric Multidimensional Scaling (MDS) plot based on the Bray-Curtis dissimilarity of each SDB participant (n = 6). Centroid values for each participant are surrounded by a smooth bootstrap region where 95% of the 500 bootstrap averages lie.

Significant differences in the bacterial composition between genders was revealed within the SDB cohort (ANOSIM $R = 0.172$, $p = 0.002$; PERMANOVA Pseudo-F = 7.86, $p < 0.0001$). No overlap was observed between the spread of the 95% Bray-Curtis bootstrap regions between genders (Fig. 4). The multivariate dispersions between genders were heterogeneous (PERMDISP $F = 4.23$, $p = 0.059$) with males (23.26 ± 1.02) having a greater level of dispersion than females ($20.01 \pm$

1.04) as determined by the average Bray-Curtis distance-to-centroid measure. The significant difference in bacterial composition between genders was predominantly driven by a higher relative abundance of *Actinobacillus* and *Haemophilus* in males and a higher relative abundance of *Veillonella* in females (SIMPER). These three taxa were responsible for driving 20.14% of the overall Bray-Curtis dissimilarity of 35.10% between locations (SIMPER).

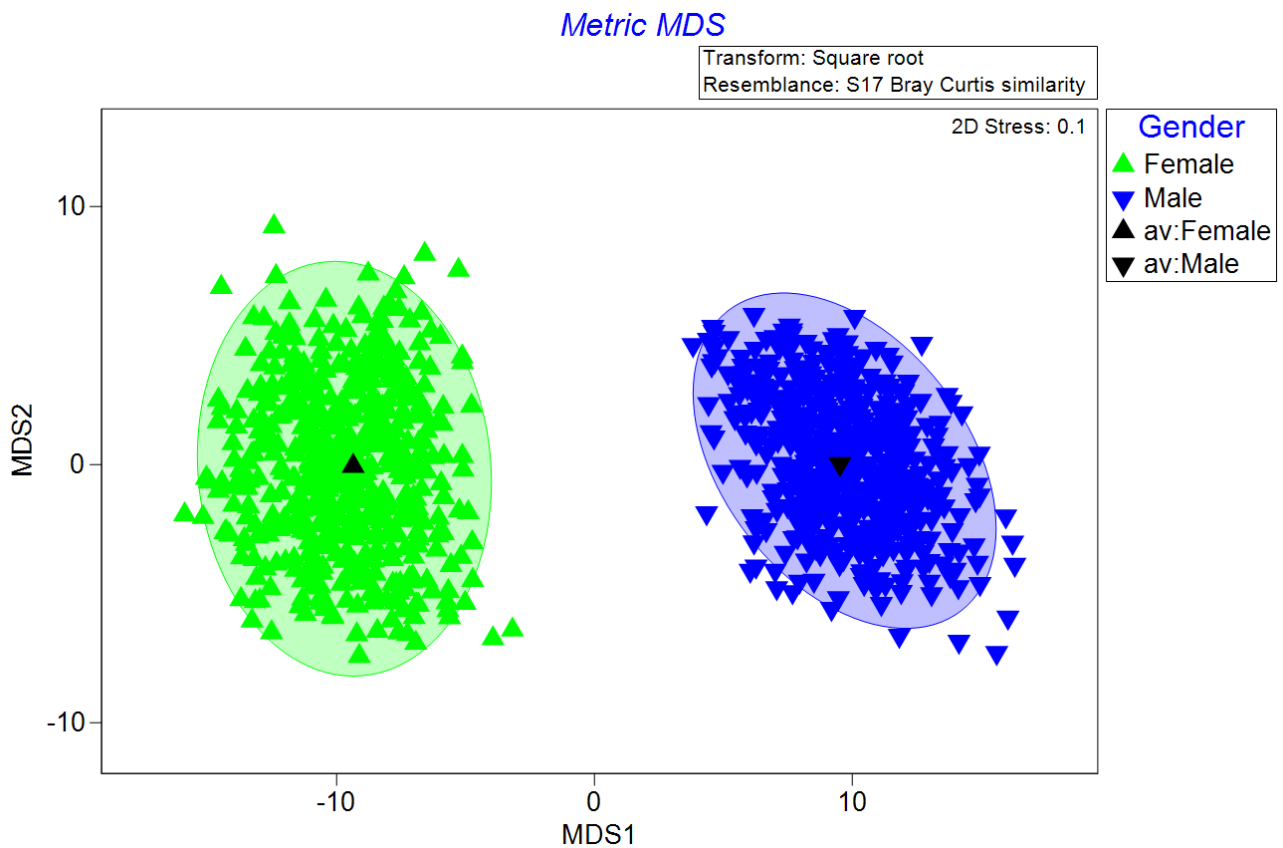


Figure 4. Metric Multidimensional Scaling (MDS) plot based on the Bray-Curtis dissimilarity for gender from the SDB cohort. Centroid values are for each gender are surrounded by a smooth bootstrap region where 95% of the 500 bootstrap averages lie.

Bacterial communities in paediatric SDB significantly differ to healthy participants

Comparisons between the overall bacterial communities in healthy and SDB participants revealed a significant shift between health states (ANOSIM $R = 0.075$, $p = 0.0002$; PERMANOVA Pseudo- $F = 3.80$, $p = 0.0023$). The metric MDS plot of Bray-Curtis bootstrap averages showed clear separation between healthy and SDB participants (Fig. 5). SDB had a slightly greater dispersal of data with an average Bray-Curtis distance-to-centroid measure of 23.57 ± 0.87 compared to 22.80 ± 0.66 for healthy participants (Fig. 5). However, the distribution of the multivariate data between

health states was not significant (PERMDISP $F = 0.51$, $p = 0.50$). An average similarity of 67.57% was reported for all healthy samples ($n = 65$) and 66.48% for all SDB samples ($n = 57$). *Streptococcus* was the top taxa contributing to 21.05 and 20.09% of the overall similarity within all healthy and SDB samples respectively. SIMPER comparison between healthy and SDB showed that there was a 33.94% average dissimilarity between health states and 6.67% of this was driven by a higher relative abundance of *Veillonella* in SDB (relative abundance: healthy = 10%; SDB = 13%). However, pairwise ANOSIM analysis based on health, microhabitat and time revealed only the tip of the tongue after sleep was the microhabitat where bacterial communities were reported to be significantly different between health states ($R = 0.28$, $p = 0.026$). Pairwise PERMDISP results revealed that the multivariate dispersal of data between these two locations was homogeneous ($t = 1.54$, $p = 0.25$). The average similarity for all tip of the tongue samples collected after sleep in healthy and SDB participants were 78.64 ($n = 6$) and 71.17 ($n = 5$) respectively. SIMPER comparisons revealed an average dissimilarity of 26.46 between these two sample groups. Of this dissimilarity, 14.42% was driven by a higher relative abundance of *Veillonella* (relative abundance: healthy = 16%; SDB = 10%) at the tip of the tongue in healthy participants and a higher relative abundance of *Haemophilus* at the tip of the tongue in SDB (relative abundance: healthy = 11%; SDB = 14%).

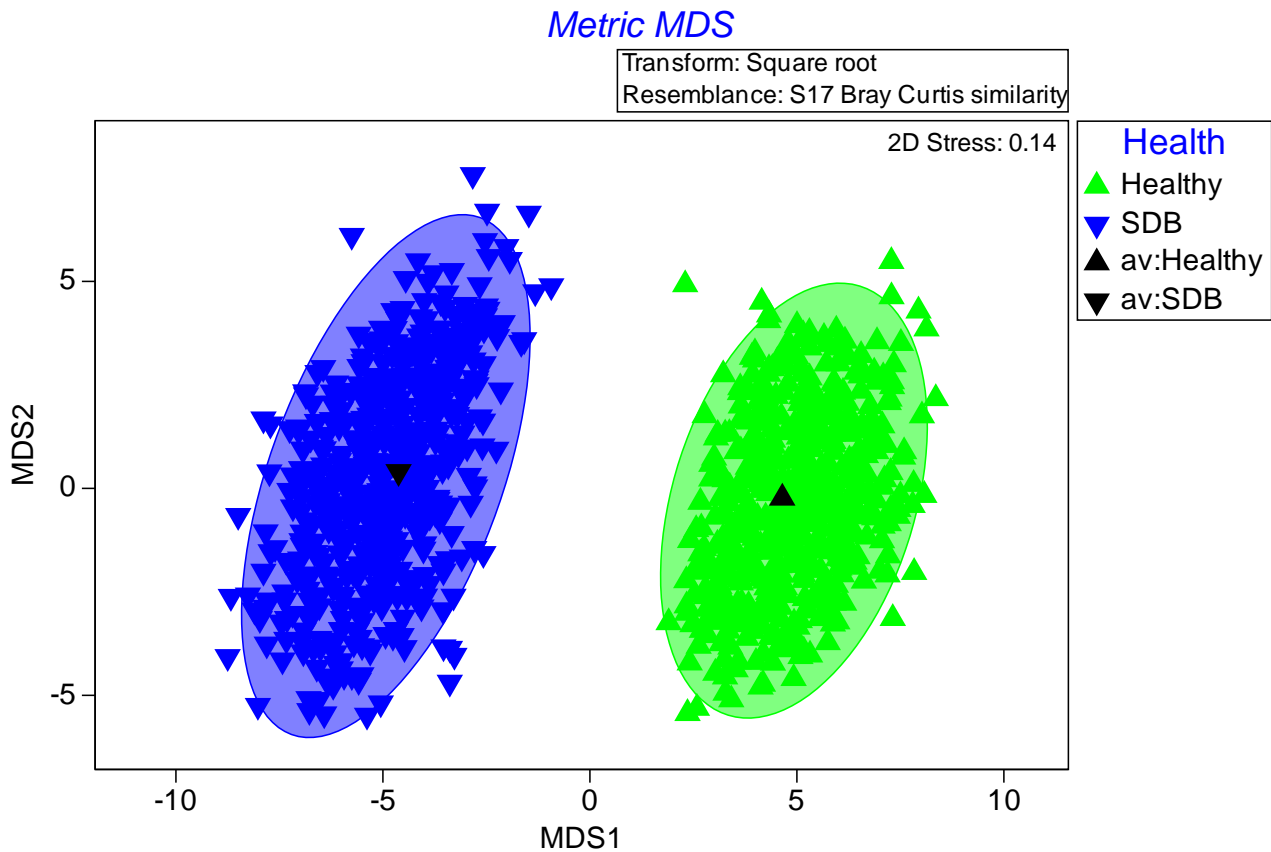


Figure 5. Metric Multidimensional Scaling (MDS) plot based on the Bray-Curtis dissimilarity between healthy (green triangles) and SDB (inverted dark blue triangles). Centroid values are for each health state are surrounded by a smooth bootstrap region where 95% of the 500 bootstrap averages lie.

Discussion

Here we present the first study to report on the microhabitat variation within the oral cavity of SDB. In addition, we report that these bacterial communities significantly differ to what is observed within the healthy paediatric oral cavity. This suggests that disruptions to the normal sleeping pattern of children may have an impact on the oral microbial communities present. Therefore, understanding what affect these shifts have on overall health and wellbeing may provide further insight into a potential link between the oral microbiome and SDB.

The microbial communities within the oral microhabitats of SDB are expected to be influenced by a number of factors including salivary flow, oral anatomy, oral hygiene, moisture levels, abrasion (i.e. from the tongue), surface structure, host immune response and oxygen, nutrient, temperature and pH gradients [8, 15, 31-39]. Here we show that like the healthy oral cavity [17], the overall bacterial community composition among microhabitats within the SDB oral cavity are different (Fig. 1; $p < 0.05$). Specifically, the back of the tongue compared with all other sampled microhabitats (Table 1; $p < 0.05$). A higher relative abundance of the anaerobic bacteria *Veillonella*, *Prevotella* and *Actinomyces* at this microhabitat were driving the dissimilarity among other sampled locations (Fig. 2). A similar trend was observed within the healthy oral cavity with *Prevotella* and *Veillonella* also the top taxa driving the dissimilarity between microhabitats [17]. The high relative abundance of these anaerobic bacteria is thought to be due to the papillae structures on the surface of the tongue [40]. Between these protrusions are anaerobic crevasses that trap nutrients and protect bacterial communities from salivary clearance [40]. However, as the tip of the tongue is the location in the oral cavity most exposed to the external environment,

and is directly exposure to the air we breathe, a higher relative abundance of aerobic bacteria is reported here compared to the back of the tongue (Fig. 2). This was also observed in the healthy oral cavity and was suggested to demonstrate a decreasing oxygen gradient from the tip to the back of the tongue [17].

Bacterial communities at palate in SDB were similar in composition to the tip of the tongue (Table 1; $p > 0.05$). As the surface of the tongue is in direct contact with the palate, it is understandable that these two locations share a similarity in bacterial communities. However, in healthy individuals the bacterial communities at the palate closely resemble the anaerobic ones found at the back of the tongue, rather than the aerobic ones at the tip [17]. We believe that this difference between health states is due to the common symptom of mouth breathing in SDB [4, 5, 41, 42]. However, due to the increased oxygen exposure to both surfaces, the palate is more likely to reflect and support the growth of the aerobic bacterial communities found at the tip of the tongue rather than the anaerobic bacterial communities at the back of the tongue.

In healthy individuals, the normal route of breathing at rest during the day and during sleep is through the nose [43, 44]. In the case of SDB, upper airway resistance, usually due to hypertrophy of the tonsils and adenoids, results in a shift to mouth breathing [41, 42]. We believe that this shift in the normal route of breathing is a major contributor to most of the bacterial dissimilarities observed between health states. For example, in healthy participants during sleep, overall bacterial communities in the oral cavity significantly shift towards a more anaerobic system, where the bacterial genera *Prevotella* and *Veillonella* increase in relative abundance [17]. Here we report that SDB oral bacterial communities do not significantly shift in composition during sleep ($p > 0.05$). Previously it has been reported that absolute bacterial concentrations in

the SDB oral cavity significantly increase by counts of up to 70 million [18]. Here, we show that these absolute abundance increases are not indicative of a significant shift in bacterial taxonomy ($p > 0.05$). One possible explanation for this bacterial continuity in SDB could lie in the microbial community's continuous exposure to oxygen due to mouth breathing during the day and at night. Therefore, there is no considerable shift in oxygen concentration within the oral cavity during the day compared to during sleep. However, further tests would be required to confirm this.

Microhabitat pairwise comparisons revealed a significant difference in the relative abundance of bacterial communities at the tip of the tongue after sleep between healthy and SDB. In healthy participants, the anaerobic genera of bacteria *Veillonella* were higher in relative abundance at the tip of the tongue after sleep [17]. Whereas, the aerobic bacteria *Haemophilus* was higher in relative abundance at the tip of the tongue after sleep in SDB. This could again reflect the high incidence of mouth breathing in SDB compared to healthy participants [4, 5, 41, 42]. These results could suggest that direct exposure to oxygen is a major contributing factor in shaping the paediatric oral bacterial communities. However, during sleep, oxygen concentrations in the oral cavity are not the only environmental factors to change. Studies have shown within the healthy oral cavity, temperature, pH and salivary flow rates also change [33, 35] influencing the oral microbial communities present [36, 45]. How these factors change within the SDB oral cavity are unknown. Therefore, further investigations into whether these environmental factors also change during sleep in SDB should be conducted to determine if they play a role in maintaining the bacterial continuity during sleep.

Sleep deprivation in healthy humans alters the gut microbiota [19]. This suggests that sleep disturbances influence the human microbiota. Here we show for the first time a significant difference in the oral bacterial communities between SDB and healthy individuals (Fig. 5). Overall, a higher relative abundance of *Veillonella* in the oral cavity of SDB was seen to be the top contributing taxa driving the dissimilarity between healthy individuals. This genus of bacteria is one of the top abundant 'core' taxa found within the healthy oral microbiome [46]. Within the healthy and SDB oral cavity, this genus of bacteria is commonly found at a higher abundance within the anaerobic microhabitats of the back of the tongue and subgingival plaque [17]. However, an increased relative abundance has been linked to dental caries and periodontal disease [47, 48]. Periodontal disease has also been linked to obstructive sleep apnoea [49] and to atherosclerosis [50], a cardiovascular disease that is also associated with obstructive sleep apnoea [51, 52]. However, further studies into why *Veillonella* is increased overall within the SDB oral cavity and its implications to overall health is required as it is beyond the scope of this study.

Here we show that even during disease, oral microhabitats within individuals display a level of interpersonal similarity (Fig. 3). This is not uncommon in human microbiome studies [17, 53-57] and is thought to reflect differences in environments, diets and immune responses among individuals [58-60]. This individuality supports the idea of personalised treatment options for oral related diseases. Differences between genders were also identified within the SDB cohort of this study with males seen to have a higher relative abundance of *Actinobacillus* and *Haemophilus* within their oral cavity. (Fig. 4). This dissimilarity was not observed within healthy paediatric oral studies [17]. As SDB has a higher prevalence and severity in males [1, 61], further

research into whether these bacterial differences reflect hormonal variances between genders [62], or an underlining microbial link to SDB should be investigated.

Limitations of this study include the small sample size of participants within the healthy (n = 6) and SDB (n = 6) groups. In addition, not all the sampled microhabitats from each participant successfully sequenced, particularly at the back of the tongue. As a result, the numbers of possible permutations run in the ANOSIM pairwise comparisons between the back of the tongue and the other microhabitats were much lower and did not meet the specified 9999 permutations. Significant differences in the distribution of the multivariate data between genders and the back of the tongue with the other microhabitats, as identified through PERMDISP, could mean that the significant differences observed reflected differences in the spread of the data rather than the bacterial communities. A repeat of this experiment with a larger sample size will give a higher confidence of significant differences among microhabitats.

Microbial communities in the healthy paediatric oral cavity display signs of a circadian rhythm where bacterial and viral communities shift during sleep [17]. Here we show that within the SDB oral cavity, this rhythm is disrupted, and bacterial communities remain constant during sleep. In addition, we report of a significant difference in the overall bacterial communities between the paediatric SDB and healthy oral cavities. Our results suggest that these shifts in bacterial communities maybe a result of mouth breathing during sleep in SDB. This suggests that bacterial communities in the paediatric oral cavity are predominantly shaped by the direct exposure to oxygen.

Acknowledgements

This study was supported by Flinders University, Adelaide University and grants from the Australian Research Council, Channel 7 Research Foundation and the Australian Office of Learning and Teaching.

References

1. Lumeng JC, Chervin RD. Epidemiology of pediatric obstructive sleep apnea. *Proceedings of the American Thoracic Society*. 2008;5(2):242-52. Epub 2008/02/06. doi: 10.1513/pats.200708-135MG. PubMed PMID: 18250218; PubMed Central PMCID: PMC2645255.
2. Marcus CL. Sleep-disordered breathing in children. *Am J Respir Crit Care Med*. 2001;164(1):16-30. doi: 10.1164/ajrccm.164.1.2008171. PubMed PMID: 11435234.
3. Loughlin GM, Brouillette RT, Brooke LJ, Carroll JL, Chipps BE, England SJ, et al. Standards and indications for cardiopulmonary sleep studies in children (vol 153, pg 866, 1995). *Am J Resp Crit Care*. 1996;153(6):U54-U. PubMed PMID: WOS:A1996UR22300046.
4. Chervin RD, Archbold KH, Dillon JE, Panahi P, Pituch KJ, Dahl RE, et al. Inattention, hyperactivity, and symptoms of sleep-disordered breathing. *Pediatrics*. 2002;109(3):449-56. Epub 2002/03/05. PubMed PMID: 11875140.
5. Sinha D, Guilleminault C. Sleep disordered breathing in children. *The Indian journal of medical research*. 2010;131:311-20. Epub 2010/03/24. PubMed PMID: 20308756.
6. Gozal D, O'Brien LM. Snoring and obstructive sleep apnoea in children: Why should we treat? *Paediatric Respiratory Reviews*. 2004;5, Supplement 1(0):S371-S6. doi: [http://dx.doi.org/10.1016/S1526-0542\(04\)90066-8](http://dx.doi.org/10.1016/S1526-0542(04)90066-8).

7. Yeshuroon-Koffler K, Shemer-Avni Y, Keren-Naus A, Goldbart AD. Detection of common respiratory viruses in tonsillar tissue of children with obstructive sleep apnea. *Pediatr Pulm.* 2014;n/a-n/a. doi: 10.1002/ppul.23005.
8. Aas JA, Paster BJ, Stokes LN, Olsen I, Dewhirst FE. Defining the normal bacterial flora of the oral cavity. *J Clin Microbiol.* 2005;43(11):5721-32. doi: 10.1128/JCM.43.11.5721-5732.2005. PubMed PMID: 16272510; PubMed Central PMCID: PMC1287824.
9. Xu X, He J, Xue J, Wang Y, Li K, Zhang K, et al. Oral cavity contains distinct niches with dynamic microbial communities. *Environmental Microbiology.* 2014;n/a-n/a. doi: 10.1111/1462-2920.12502.
10. Thaïss CA, Zeevi D, Levy M, Zilberman-Schapira G, Suez J, Tengeler AC, et al. Transkingdom control of microbiota diurnal oscillations promotes metabolic homeostasis. *Cell.* 2014;159(3):514-29. Epub 2014/11/25. doi: 10.1016/j.cell.2014.09.048. PubMed PMID: 25417104.
11. Lazarevic V, Whiteson K, Hernandez D, Francois P, Schrenzel J. Study of inter- and intra-individual variations in the salivary microbiota. *BMC genomics.* 2010;11:523. Epub 2010/10/06. doi: 10.1186/1471-2164-11-523. PubMed PMID: 20920195; PubMed Central PMCID: PMCPMC2997015.
12. Stahring SS, Clemente JC, Corley RP, Hewitt J, Knights D, Walters WA, et al. Nurture trumps nature in a longitudinal survey of salivary bacterial communities in twins from early adolescence to early adulthood. *Genome research.* 2012;22(11):2146-52. Epub 2012/10/16. doi: 10.1101/gr.140608.112. PubMed PMID: 23064750; PubMed Central PMCID: PMCPMC3483544.
13. Cameron SJ, Huws SA, Hegarty MJ, Smith DP, Mur LA. The human salivary microbiome exhibits temporal stability in bacterial diversity. *FEMS microbiology*

ecology. 2015;91(9):fiv091. Epub 2015/07/25. doi: 10.1093/femsec/fiv091. PubMed PMID: 26207044.

14. Belstrom D, Holmstrup P, Bardow A, Kokaras A, Fiehn NE, Paster BJ. Temporal Stability of the Salivary Microbiota in Oral Health. *Plos One*. 2016;11(1):e0147472. Epub 2016/01/23. doi: 10.1371/journal.pone.0147472. PubMed PMID: 26799067; PubMed Central PMCID: PMC4723053.

15. Carlson-Jones J, Kontos A, Paterson J, Smith R, Dann L, Speck P, et al. Flow Cytometric Enumeration of Bacterial and Virus-Like Particle Populations in the Human Oral Cavity Pre and Post Sleep. *J Sleep Res*. 2016;25:86-. PubMed PMID: WOS:000393032700215.

16. Carlson-Jones JA, Kontos A, Kennedy D, Martin J, McKerral J, Paterson JS, et al. The microbial abundance dynamics of the human oral cavity before and after sleep. *Plos One* (Submitted). 2018.

17. Carlson-Jones JA, Kontos A, Kennedy D, Martin J, McKerral J, Dann LM, et al. The spatial distribution of the bacterial communities within the healthy paediatric oral cavity before and after sleep. In Prep. 2018;Thesis chapter 6.

18. Carlson-Jones JA, Kontos A, Kennedy D, Martin J, McKerral J, Paterson JS, et al. The microbial abundance dynamics of the paediatric sleep disorder breather oral cavity before and after sleep. In Prep. 2018;Thesis chapter 5.

19. Benedict C, Vogel H, Jonas W, Woting A, Blaut M, Schurmann A, et al. Gut microbiota and glucometabolic alterations in response to recurrent partial sleep deprivation in normal-weight young individuals. *Mol Metab*. 2016;5(12):1175-86. Epub 2016/12/03. doi: 10.1016/j.molmet.2016.10.003. PubMed PMID: 27900260; PubMed Central PMCID: PMC5123208.

20. Poroyko VA, Carreras A, Khalyfa A, Khalyfa AA, Leone V, Peris E, et al. Chronic Sleep Disruption Alters Gut Microbiota, Induces Systemic and Adipose Tissue Inflammation and Insulin Resistance in Mice. *Scientific reports*. 2016;6:35405. Epub 2016/10/16. doi: 10.1038/srep35405. PubMed PMID: 27739530; PubMed Central PMCID: PMC5064361.
21. Dann LM, Smith RJ, Tobe SS, Paterson JS, Oliver RL, Mitchell JG. Microscale distributions of freshwater planktonic viruses and prokaryotes are patchy and taxonomically distinct. *Aquatic Microbial Ecology*. 2016;77(2):65-77.
22. Zhang J, Kobert K, Flouri T, Stamatakis A. PEAR: a fast and accurate Illumina Paired-End reAd mergeR. *Bioinformatics*. 2014;30(5):614-20. doi: 10.1093/bioinformatics/btt593. PubMed PMID: 24142950; PubMed Central PMCID: PMC3933873.
23. Pylro VS, Roesch LF, Morais DK, Clark IM, Hirsch PR, Totola MR. Data analysis for 16S microbial profiling from different benchtop sequencing platforms. *Journal of microbiological methods*. 2014;107:30-7. doi: 10.1016/j.mimet.2014.08.018. PubMed PMID: 25193439.
24. Kuczynski J, Stombaugh J, Walters WA, Gonzalez A, Caporaso JG, Knight R. Using QIIME to analyze 16S rRNA gene sequences from microbial communities. *Current protocols in bioinformatics*. 2011;Chapter 10:Unit 10 7. doi: 10.1002/0471250953.bi1007s36. PubMed PMID: 22161565; PubMed Central PMCID: PMC3249058.
25. Edgar RC. UPARSE: highly accurate OTU sequences from microbial amplicon reads. *Nature methods*. 2013;10(10):996-8. doi: 10.1038/nmeth.2604. PubMed PMID: 23955772.

26. Rognes T, Flouri T, Nichols B, Quince C, Mahe F. VSEARCH: a versatile open source tool for metagenomics. *PeerJ*. 2016;4:e2584. doi: 10.7717/peerj.2584. PubMed PMID: 27781170; PubMed Central PMCID: PMC5075697.
27. Edgar RC. Search and clustering orders of magnitude faster than BLAST. *Bioinformatics*. 2010;26(19):2460-1. doi: 10.1093/bioinformatics/btq461. PubMed PMID: 20709691.
28. Clarke K, Gorley, RN. PRIMER v7: User Manual/Tutorial. Plymouth: PRIMER-E; 2015.
29. Anderson M, Gorley R, Clarke K. PERMANOVA+ for PRIMER: Guide to Software and Statistical Methods. Plymouth UK: PRIMER-E; 2008.
30. Clarke KR. Non-parametric multivariate analyses of changes in community structure. *Austral ecology*. 1993;18(1):117-43.
31. Dewhirst FE, Chen T, Izard J, Paster BJ, Tanner AC, Yu WH, et al. The human oral microbiome. *Journal of bacteriology*. 2010;192(19):5002-17. doi: 10.1128/JB.00542-10. PubMed PMID: 20656903; PubMed Central PMCID: PMC2944498.
32. Human Microbiome Project C. Structure, function and diversity of the healthy human microbiome. *Nature*. 2012;486(7402):207-14. doi: 10.1038/nature11234. PubMed PMID: 22699609; PubMed Central PMCID: PMC3564958.
33. Xu X, He J, Xue J, Wang Y, Li K, Zhang K, et al. Oral cavity contains distinct niches with dynamic microbial communities. *Environ Microbiol*. 2015;17(3):699-710. Epub 2014/05/08. doi: 10.1111/1462-2920.12502. PubMed PMID: 24800728.
34. Simon-Soro A, Tomas I, Cabrera-Rubio R, Catalan MD, Nyvad B, Mira A. Microbial geography of the oral cavity. *Journal of dental research*. 2013;92(7):616-21. Epub 2013/05/16. doi: 10.1177/0022034513488119. PubMed PMID: 23674263.

35. Mager DL, Ximenez-Fyvie LA, Haffajee AD, Socransky SS. Distribution of selected bacterial species on intraoral surfaces. *J Clin Periodontol*. 2003;30(7):644-54. Epub 2003/07/02. PubMed PMID: 12834503.
36. Proctor DM, Fukuyama JA, Loomer PM, Armitage GC, Lee SA, Davis NM, et al. A spatial gradient of bacterial diversity in the human oral cavity shaped by salivary flow. *Nat Commun*. 2018;9(1):681. Epub 2018/02/16. doi: 10.1038/s41467-018-02900-1. PubMed PMID: 29445174; PubMed Central PMCID: PMC5813034.
37. Choi JE, Waddell JN, Lyons KM, Kieser JA. Intraoral pH and temperature during sleep with and without mouth breathing. *J Oral Rehabil*. 2016;43(5):356-63. Epub 2015/12/17. doi: 10.1111/joor.12372. PubMed PMID: 26666708.
38. Aframian DJ, Davidowitz T, Benoliel R. The distribution of oral mucosal pH values in healthy saliva secretors. *Oral diseases*. 2006;12(4):420-3. Epub 2006/06/24. doi: 10.1111/j.1601-0825.2005.01217.x. PubMed PMID: 16792729.
39. Dawes C. A mathematical model of salivary clearance of sugar from the oral cavity. *Caries research*. 1983;17(4):321-34. Epub 1983/01/01. doi: 10.1159/000260684. PubMed PMID: 6575870.
40. Allaker RP, Waite RD, Hickling J, North M, McNab R, Bosma MP, et al. Topographic distribution of bacteria associated with oral malodour on the tongue. *Archives of oral biology*. 2008;53 Suppl 1:S8-S12. doi: 10.1016/S0003-9969(08)70003-7. PubMed PMID: 18460402.
41. Bhattacharjee R, Kheirandish-Gozal L, Spruyt K, Mitchell RB, Promchiarak J, Simakajornboon N, et al. Adenotonsillectomy Outcomes in Treatment of Obstructive Sleep Apnea in Children A Multicenter Retrospective Study. *Am J Resp Crit Care*. 2010;182(5):676-83. doi: DOI 10.1164/rccm.200912-1930OC. PubMed PMID: WOS:000281492000013.

42. Fitzpatrick MF, McLean H, Urton AM, Tan A, O'Donnell D, Driver HS. Effect of nasal or oral breathing route on upper airway resistance during sleep. *Eur Respir J*. 2003;22(5):827-32. Epub 2003/11/19. PubMed PMID: 14621092.
43. Lumb AB. *Nunn's applied respiratory physiology eBook*: Elsevier Health Sciences; 2016.
44. Fitzpatrick MF, Driver HS, Chatha N, Voduc N, Girard AM. Partitioning of inhaled ventilation between the nasal and oral routes during sleep in normal subjects. *J Appl Physiol* (1985). 2003;94(3):883-90. Epub 2002/11/16. doi: 10.1152/jappphysiol.00658.2002. PubMed PMID: 12433860.
45. van 't Hof W, Veerman EC, Nieuw Amerongen AV, Ligtenberg AJ. Antimicrobial defense systems in saliva. *Monogr Oral Sci*. 2014;24:40-51. Epub 2014/05/28. doi: 10.1159/000358783. PubMed PMID: 24862593.
46. Zarco MF, Vess TJ, Ginsburg GS. The oral microbiome in health and disease and the potential impact on personalized dental medicine. *Oral diseases*. 2012;18(2):109-20. Epub 2011/09/10. doi: 10.1111/j.1601-0825.2011.01851.x. PubMed PMID: 21902769.
47. Peterson SN, Snesrud E, Liu J, Ong AC, Kilian M, Schork NJ, et al. The dental plaque microbiome in health and disease. *Plos One*. 2013;8(3):e58487. Epub 2013/03/23. doi: 10.1371/journal.pone.0058487. PubMed PMID: 23520516; PubMed Central PMCID: PMC3592792.
48. Takeshita T, Nakano Y, Kumagai T, Yasui M, Kamio N, Shibata Y, et al. The ecological proportion of indigenous bacterial populations in saliva is correlated with oral health status. *Isme J*. 2009;3(1):65-78. Epub 2008/10/03. doi: 10.1038/ismej.2008.91. PubMed PMID: 18830275.

49. Gunaratnam K, Taylor B, Curtis B, Cistulli P. Obstructive sleep apnoea and periodontitis: a novel association? *Sleep Breath*. 2009;13(3):233-9. Epub 2009/02/10. doi: 10.1007/s11325-008-0244-0. PubMed PMID: 19198909.
50. Lockhart PB, Bolger AF, Papapanou PN, Osinbowale O, Trevisan M, Levison ME, et al. Periodontal disease and atherosclerotic vascular disease: does the evidence support an independent association?: a scientific statement from the American Heart Association. *Circulation*. 2012;125(20):2520-44. Epub 2012/04/20. doi: 10.1161/CIR.0b013e31825719f3. PubMed PMID: 22514251.
51. Levy P, Pepin JL, Arnaud C, Baguet JP, Dematteis M, Mach F. Obstructive sleep apnea and atherosclerosis. *Prog Cardiovasc Dis*. 2009;51(5):400-10. Epub 2009/03/03. doi: 10.1016/j.pcad.2008.03.001. PubMed PMID: 19249446.
52. Lui MM, Sau-Man M. OSA and atherosclerosis. *J Thorac Dis*. 2012;4(2):164-72. Epub 2012/07/27. doi: 10.3978/j.issn.2072-1439.2012.01.06. PubMed PMID: 22833822; PubMed Central PMCID: PMC3378220.
53. Hall MW, Singh N, Ng KF, Lam DK, Goldberg MB, Tenenbaum HC, et al. Interpersonal diversity and temporal dynamics of dental, tongue, and salivary microbiota in the healthy oral cavity. *NPJ biofilms and microbiomes*. 2017;3:2. Epub 2017/06/27. doi: 10.1038/s41522-016-0011-0. PubMed PMID: 28649403; PubMed Central PMCID: PMC5445578.
54. Costello EK, Lauber CL, Hamady M, Fierer N, Gordon JI, Knight R. Bacterial community variation in human body habitats across space and time. *Science*. 2009;326(5960):1694-7. Epub 2009/11/07. doi: 10.1126/science.1177486. PubMed PMID: 19892944; PubMed Central PMCID: PMC3602444.
55. Turnbaugh PJ, Gordon JI. The core gut microbiome, energy balance and obesity. *The Journal of physiology*. 2009;587(Pt 17):4153-8. Epub 2009/06/06. doi:

10.1113/jphysiol.2009.174136. PubMed PMID: 19491241; PubMed Central PMCID: PMCPMC2754355.

56. Bik EM, Long CD, Armitage GC, Loomer P, Emerson J, Mongodin EF, et al. Bacterial diversity in the oral cavity of 10 healthy individuals. *Isme J.* 2010;4(8):962-74. Epub 2010/03/26. doi: 10.1038/ismej.2010.30. PubMed PMID: 20336157; PubMed Central PMCID: PMCPMC2941673.

57. Nasidze I, Li J, Quinque D, Tang K, Stoneking M. Global diversity in the human salivary microbiome. *Genome research.* 2009;19(4):636-43. Epub 2009/03/03. doi: 10.1101/gr.084616.108. PubMed PMID: 19251737; PubMed Central PMCID: PMCPMC2665782.

58. Adler CJ, Dobney K, Weyrich LS, Kaidonis J, Walker AW, Haak W, et al. Sequencing ancient calcified dental plaque shows changes in oral microbiota with dietary shifts of the Neolithic and Industrial revolutions. *Nat Genet.* 2013;45(4):450-5, 5e1. Epub 2013/02/19. doi: 10.1038/ng.2536. PubMed PMID: 23416520; PubMed Central PMCID: PMCPMC3996550.

59. Wu J, Peters BA, Dominianni C, Zhang Y, Pei Z, Yang L, et al. Cigarette smoking and the oral microbiome in a large study of American adults. *Isme J.* 2016;10(10):2435-46. Epub 2016/03/26. doi: 10.1038/ismej.2016.37. PubMed PMID: 27015003; PubMed Central PMCID: PMCPMC5030690.

60. Kilian M, Chapple IL, Hannig M, Marsh PD, Meuric V, Pedersen AM, et al. The oral microbiome - an update for oral healthcare professionals. *British dental journal.* 2016;221(10):657-66. Epub 2016/11/20. doi: 10.1038/sj.bdj.2016.865. PubMed PMID: 27857087.

61. Young T, Palta M, Dempsey J, Skatrud J, Weber S, Badr S. The Occurrence of Sleep-Disordered Breathing among Middle-Aged Adults. *New Engl J Med.*

1993;328(17):1230-5. doi: 10.1056/nejm199304293281704. PubMed PMID: 8464434.

62. Lin CM, Davidson TM, Ancoli-Israel S. Gender differences in obstructive sleep apnea and treatment implications. *Sleep medicine reviews*. 2008;12(6):481-96. Epub 2008/10/28. doi: 10.1016/j.smrv.2007.11.003. PubMed PMID: 18951050; PubMed Central PMCID: PMC2642982.

Chapter 8

GENERAL DISCUSSION

Thesis overview

An increasing number of studies are beginning to show that sleep disorder breathing (SDB) in mice and adults is linked to a shift in the gut microbiome [1-6]. As it is well accepted that the human microbiome is linked to maintaining and promoting health [7, 8], understanding what affects these microbial community shifts have on our overall health is rapidly gaining momentum. However, little research has been conducted looking at the oral microbiome in SDB, in particular at the paediatric age group. As the oral cavity is linked to the digestive and respiratory systems [9], it is important to investigate any microbial shifts at this location as it may have further implications down the digestive and respiratory tracts [10]. Most oral microbiome studies in health and disease have focused on adults [7, 11, 12]. As the human oral microbiome shifts with age [12, 13], it is important to establish a healthy baseline at the paediatric age group so appropriate comparisons can be performed. Therefore, this thesis aimed to understand the spatial distribution of the healthy paediatric oral microbiome, and to establish if these communities differ in paediatric SDB. To do this we first established that flow cytometry could be used on medical samples to enumerate bacterial and viral populations (chapter 2). Following this, investigations using flow cytometry and 16S ribosomal RNA analyses were conducted to determine the numeric (chapters 3 and 4) and taxonomic (chapter 6) distribution of the of the healthy paediatric oral cavity before and after sleep to ultimately understand if these microbial community dynamics differ in SDB (chapters 5 and 7). This final chapter will summarise and address the main findings from this thesis in regards to the overall objectives presented in the introduction.

Synthesis of research

Flow cytometric enumeration of bacteria and VLP in maxillary sinus flush samples

Chapter 2 investigated using flow cytometry as a method of enumerating bacterial and viral particles within the maxillary sinuses of chronic rhinosinusitis patients. Previously used in environmental studies to monitor microbial abundance dynamics [14-16], flow cytometry provides a rapid method for enumerating absolute bacterial and VLP abundances within a sample. However, this method of microbial enumeration is not commonly applied to medical samples. Here we present the first study to enumerate bacterial and viral populations within the maxillary sinuses of humans. Results from this chapter demonstrate that flow cytometry can successfully be applied to medical samples and hence can be used to assess microbial dynamics within other niches of the human body.

We also identified that in CRS patients, bacterial and VLP concentrations ranged between 10^4 to 10^8 bacterial ml^{-1} and 10^5 to 10^{10} VLP ml^{-1} . This shows that microbial abundances among patients with disease are not found at a similar level, implying that infection levels of bacteria and VLP are dependent on an individual. This highlights the potential for personalised treatment options when treating microbial related infections. One treatment method currently being investigated in this field is the use of phage therapy [17]. Knowledge that viruses are prominent within the sinuses of CRS patients may help in determining the appropriate dosage requirements for this treatment option [18]. Understanding the microbial abundances in the sinuses may also assist in interpreting the microbial dynamics within the oral cavity. Post-nasal drip down the back of the throat to the back of the tongue may also influence the

microbial abundance dynamics of the oral cavity as it could facilitate the transfer and inoculation of microbial communities from the sinuses to the oral cavity.

The healthy paediatric oral cavity is a numerically dynamic heterogeneous environment

Chapters 3 and 4 investigated the spatial distribution and dynamic of bacterial and viral populations in the healthy paediatric oral cavity. This was achieved through utilising the successful flow cytometric methods applied in chapter 2. Previously it has been shown that microhabitats in the oral cavity significantly different in taxonomic composition [7, 11, 12]. However, absolute abundance variation of bacteria and viruses among these microhabitats was unknown. Here we demonstrate for the first time that the oral bacterial and viral communities within microhabitats are numerally heterogeneous. This further supports and complements previous oral microbiome studies that suggest the oral microbiome be defined by its various microhabitats [7, 11, 12]. Bacterial abundances in the oral cavity ranged from $7.2 \pm 2.8 \times 10^5$ at the palate before sleep to $1.3 \pm 0.2 \times 10^8$ at the back of the tongue after sleep. Viruses ranged between $1.9 \pm 1.0 \times 10^6$ VLP at the palate before sleep to $9.2 \pm 5.0 \times 10^7$ VLP at the back of the tongue after sleep. However, viral abundances were observed to display homogeneity among microhabitats after sleep. This could be suggesting of a factor controlling viral dispersal during sleep.

This chapter also demonstrates that the oral cavity is a dynamic environment during sleep where bacteria and viruses significantly increase in abundance ($p < 0.05$). Bacteria were reported to increase by counts of 100 million and viruses by 70 million. As conditions in the oral environment change during sleep [19-22], this chapter suggests that these changes can have a large impact on the resulting microbial community abundance. As microbial communities also shift with age [12, 13], it was

important to establish a healthy paediatric 'baseline' of absolute bacterial and viral counts, so comparisons could be made with paediatric SDB in chapter 5.

Viral community abundances differ between healthy and SDB

In chapter 5, utilising the same techniques from chapters 2-4, we present the first study to enumerate microhabitat variation the bacterial and viral communities in the paediatric SDB oral cavity. Here we see that like the healthy paediatric oral cavity (chapters 3 and 4); the paediatric SDB oral cavity is also numerically heterogeneous in bacteria and viruses. Bacterial counts ranged between $9.55 \pm 3.88 \times 10^5$ at the palate before sleep to $8.94 \pm 1.49 \times 10^7$ at the back of the tongue after sleep. Viruses were reported to range between $1.38 \pm 0.64 \times 10^6$ at the palate before sleep to $7.72 \pm 3.13 \times 10^7$ at the gingivae after sleep. All microhabitat communities were also seen to be dynamic with significant increases in both bacteria and viruses during sleep. However, unlike healthy participants, SDB had more regions of heterogeneity in microbial communities, specifically in viruses after sleep. These differences may reflect variances in environmental conditions due to differences in sleeping patterns between healthy and SDB. These include but are not limited to snoring and mouth breathing [23-25].

Bacterial counts at the back of the tongue in SDB were significantly lower than healthy participants by a count of approximately 46 million after sleep. We suspect this is a result of increased friction at the back of the tongue in SDB due to snoring. This increased friction at the back of the tongue causes the dislodgment and shedding of mucosal fragments, ultimately resulting in the loss of the microbial communities residing there [12, 26, 27]. Therefore, microbial communities at this location in SDB are unable to develop to the same abundance as healthy participants. Viral

communities in SDB were also significantly different to counts in healthy participants. These differences could be a result of the differing environmental conditions between health states, or it could reflect a difference in the bacterial taxonomic structure.

Microbial communities shift anaerobically during sleep in healthy paediatric participants

Chapter 6 used 16S ribosomal RNA sequencing to investigate the taxonomic composition of the bacterial communities at the 6 oral microhabitats in healthy participants. Overall PERMANOVA and ANOSIM results on microhabitats indicated a significant difference in bacterial community structure (PERMANOVA $p < 0.05$, ANOSIM $p < 0.05$). This supports previous taxonomic studies on adult oral cavities [7, 11, 12]. However, pairwise ANOSIM comparisons revealed similarities among certain microhabitats (ANOSIM $p > 0.05$). The temporomandibular joint, gingivae and molars were similar in overall microbial composition (ANOSIM $p > 0.05$) and were higher in relative abundance of *Streptococcus* (SIMPER) than the palate, tip of tongue and back of tongue. The back of the tongue and the palate were also similar in microbial composition (ANOSIM $p > 0.05$) with a higher relative abundance of the anaerobic bacteria *Prevotella* and *Veillonella* driving the dissimilarity among microhabitats (SIMPER). We suspect that the direct contact between both locations facilitates the transfer of microbial communities resulting in the similarities observed. At the tip of the tongue the aerobic bacteria *Haemophilus* and *Rothia* were identified as the top genera driving the dissimilarity among all locations tested. This is suggestive of a decreasing oxygen gradient from the tip to the back of the tongue.

This chapter also reports for the first time a significant shift in oral bacterial communities during sleep within the healthy paediatric cohort (PERMANOVA $p < 0.05$,

ANOSIM $p < 0.05$). A higher relative abundance of the anaerobic bacteria *Veillonella* and *Prevotella* were observed to be the main genera driving the dissimilarity between time points. This suggests that the oral cavity shifts to a predominantly anaerobic system during sleep. This is likely a result of nasal breathing during the night [28] where air is not directly in contact with microhabitats in the oral cavity.

Bacterial communities in SDB significantly differ to healthy individuals

In chapter 7, 16S ribosomal RNA sequencing was also used to determine microhabitat variation within the SDB oral cavity before and after sleep. Here we show that like the healthy oral cavity (chapter 6), SDB oral microhabitats significantly differ in microbial community composition (PERMANOVA $p < 0.05$, ANOSIM $p < 0.05$). However, these oral bacterial communities do not significantly shift in composition during sleep ($p > 0.05$). This is thought to be a result of mouth breathing during the day and at night, a common symptom of SDB [29-32]. Therefore, oxygen concentrations in the oral cavity are not likely to change considerably during the day compared to at night, thus not resulting in a shift in oral microbial communities between time points. Therefore, the significant increase in absolute bacterial abundances in SDB during sleep (chapter 5) are not reflective of a significant difference in taxonomy.

Mouth breathing is also thought to be why there is a significant shift in bacterial communities between healthy and SDB oral bacterial communities (PERMANOVA $p < 0.05$, ANOSIM $p < 0.05$; Fig 1). Specifically, at the tip of the tongue after sleep where there is a shift from the anaerobic bacteria *Veillonella* in health participants to the aerobic bacteria *Haemophilus* in SDB (SIMPER). Unlike SDB, healthy participants breath through their nose during sleep [33, 34] creating an anaerobic environment in the oral cavity (chapter 6). However, the overall total relative abundance of *Veillonella*

in SDB was higher than healthy participants and was the main genera responsible for driving the dissimilarity between health states (SIMPER). This genus of bacteria is also found at a higher relative abundance in periodontal disease [35, 36], an oral disease which has been linked to obstructive sleep apnoea [37]. Determining that there is a significant shift in the oral bacterial communities between healthy and SDB means future studies can be conducted to ultimately understand why these shifts occur, what impact these shifts have on overall health and whether they are a cause or result of the sleep disorder.

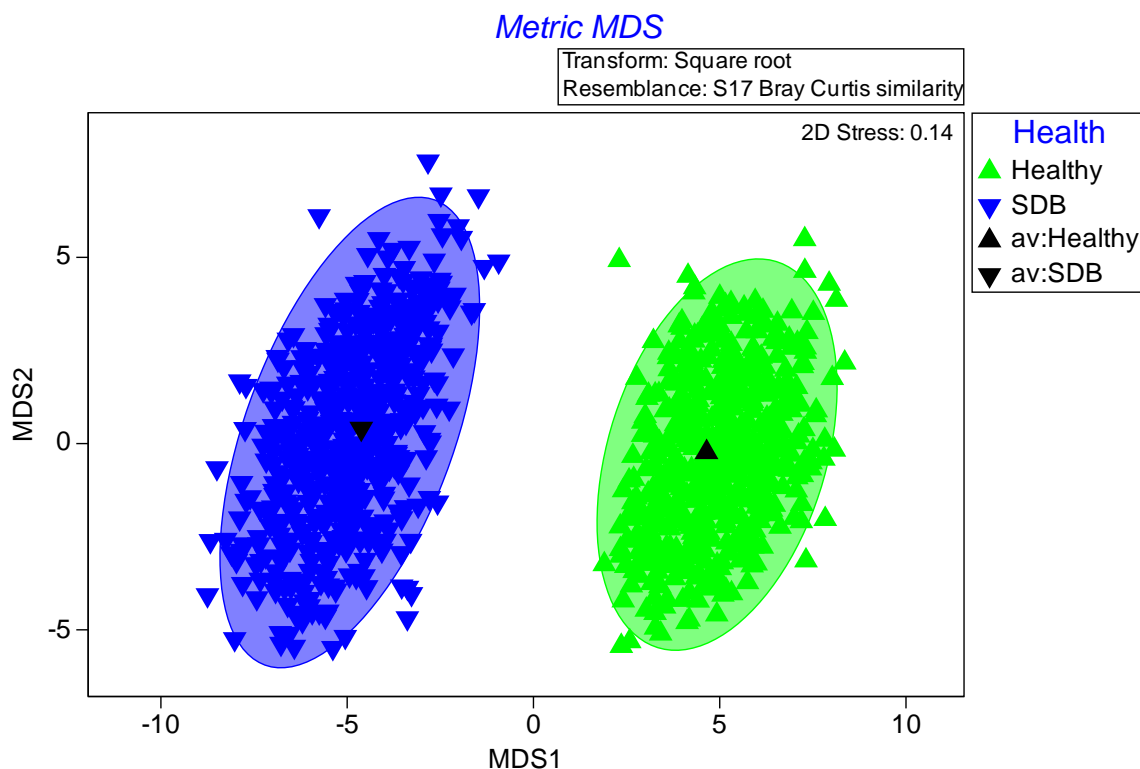


Figure 1. Metric Multidimensional Scaling (MDS) plot based on the Bray-Curtis dissimilarity between healthy (green triangles) and SDB (inverted dark blue triangles). Centroid values for each health state are surrounded by a smooth bootstrap region where 95% of the 500 bootstrap averages lie.

Significance

One of the main messages from this thesis is that flow cytometry can successfully be applied within the medical field to enumerate absolute microbial abundance dynamics from clinical samples using a DNA stain. We have established for the first time the absolute numerical range of bacterial and viral communities among microhabitats in the human oral cavity. In addition, we have also determined by how much these community dynamics change during sleep. As mentioned within chapters 2-5, flow cytometry has been used for decades to monitor microbial dynamics within environments such as marine and freshwater and ground water systems [14-16]. As the majority of bacteria isolated from the body is yet to be successfully cultured [11, 38-40], flow cytometry provides an inexpensive and rapid alternative to enumerate microbial communities without the biases culturing introduces [14, 41, 42].

As highlighted during the review process for chapter 4 (Appendix), investigations into the microbial dynamics of the oral cavity are relatively out dated. One study mentioned in the review process as a current method of measuring bacterial dynamics over time was a study published in 1989 that used photography to calculate plaque extension over time [43]. In brief, after plaque disclosure, tooth surfaces were photographed at 11 time points over a period of 96 hours to determine the rate of plaque growth. The bacterial dynamics at this location were determined based on the percentage of total plaque coverage on the surface of the teeth over the 96 hours. No absolute bacterial counts were performed in this study. Another study used fluorescent *in situ* hybridisation (FISH) using specific bacterial probes to count bacteria in plaque scrapings [44]. The specificity of the bacterial probes does not make it a good representation of the total bacterial community within this environment. To our

knowledge, there have been no studies investigating the viral abundance dynamics within the oral cavity. Therefore, there was a need for the development of a method that could be applied in the medical field to enumerate both bacterial and viral communities. Here we present in chapters 2- 5 of this thesis the first bacterial and viral abundance dynamics of the oral cavity using flow cytometry.

Previous studies on the salivary microbiome have shown that bacterial communities remain stable over time [45-49]. However, results in this thesis have demonstrated that this is not the case for microhabitats within the oral cavity. Significant count increase in bacterial and viral communities were observed over a 9-9½ hour period. Taxonomically, these microbial communities significantly shifted favouring anaerobic bacterial genera. Therefore, results from this thesis demonstrate the need for careful regulation of sample collection time when comparing oral related diseases to healthy controls.

Future directions

With the successful application of flow cytometry to in monitoring microbial dynamics in the sinuses and oral cavity (chapters 2-5), we propose that this technique be applied to other locations within the human body. Like the oral cavity, most other human microbiome studies focus on the taxonomic distribution and relative abundances of bacterial and viral communities within an environment [7, 50-52]. However; the absolute microbial dynamics of these environments are unknown. Flow cytometry could also be used to monitor temporal dynamics within the body, specifically in microbial related diseases or infections.

In some cases like chronic rhinosinusitis, specific bacterial species are thought to be involved in the pathogenesis of the disease [53, 54]. Therefore we propose that FISH in conjunction with flow cytometry [55-57] could be used to in microbial related diseases where there is a known pathogen of interest. This will enable the differentiation and enumeration of these specific bacterial species from the overall bacterial populations identified when using a general DNA stain like SYBR-Green. Knowledge of total bacterial communities in microbial related infections/diseases may assist in the future in determining appropriate dosages for antibiotics or even concentrations of bacteriophage in phage therapy.

Here we provide the first insight into the numeric and taxonomic differences between the microhabitats of the healthy and SDB paediatric oral cavity. Whether these differences are a cause or a result of SDB is beyond the scope of this thesis. However, the main finding of a significant difference in viral abundance and taxonomic communities between health states (chapters 5 and 7) warrants further investigations into what is causing these dissimilarities. Future metagenomics analysis into the genetic profiles of the oral bacterial and viral communities in SDB may provide a better insight into the metabolic functions of these microbial communities [10].

Conclusions

This thesis provides an overview of the bacterial and viral abundance dynamics within the paediatric oral cavity of healthy and SDB. Here we present, to the best of our knowledge, the first studies into the absolute microbial abundance dynamics of the healthy and SDB paediatric oral cavity during sleep. Results demonstrate that the oral cavity is a numerically heterogeneous environment where counts of bacterial and viruses can increase by 100 million. Absolute viral counts significantly differ between

health states suggesting the potential involvement or impact of SDB on viral communities within the oral cavity. Furthermore, a taxonomic and numeric shift in bacterial and viral communities during sleep show that time of sample collection is important when designing and collecting samples for oral microbiome studies. Further bacterial and viral metagenomics analyses will assist in determining what role SDB has on the distribution of microbial communities within the oral cavity, and what if any, impact these shifts have on overall health and wellbeing.

References

1. Benedict C, Vogel H, Jonas W, Woting A, Blaut M, Schurmann A, et al. Gut microbiota and glucometabolic alterations in response to recurrent partial sleep deprivation in normal-weight young individuals. *Molecular metabolism*. 2016;5(12):1175-86. doi: 10.1016/j.molmet.2016.10.003. PubMed PMID: 27900260; PubMed Central PMCID: PMC5123208.
2. Poroyko VA, Carreras A, Khalyfa A, Khalyfa AA, Leone V, Peris E, et al. Chronic Sleep Disruption Alters Gut Microbiota, Induces Systemic and Adipose Tissue Inflammation and Insulin Resistance in Mice. *Scientific reports*. 2016;6:35405. Epub 2016/10/16. doi: 10.1038/srep35405. PubMed PMID: 27739530; PubMed Central PMCID: PMCPMC5064361.
3. Moreno-Indias I, Torres M, Montserrat JM, Sanchez-Alcoholado L, Cardona F, Tinahones FJ, et al. Intermittent hypoxia alters gut microbiota diversity in a mouse model of sleep apnoea. *Eur Respir J*. 2015;45(4):1055-65. Epub 2014/12/30. doi: 10.1183/09031936.00184314. PubMed PMID: 25537565.
4. Durgan DJ, Ganesh BP, Cope JL, Ajami NJ, Phillips SC, Petrosino JF, et al. Role of the Gut Microbiome in Obstructive Sleep Apnea-Induced Hypertension.

- Hypertension. 2016;67(2):469-74. Epub 2015/12/30. doi: 10.1161/HYPERTENSIONAHA.115.06672. PubMed PMID: 26711739; PubMed Central PMCID: PMC4713369.
5. Santisteban MM, Qi Y, Zubcevic J, Kim S, Yang T, Shenoy V, et al. Hypertension-Linked Pathophysiological Alterations in the Gut. *Circ Res.* 2017;120(2):312-23. Epub 2016/11/02. doi: 10.1161/CIRCRESAHA.116.309006. PubMed PMID: 27799253; PubMed Central PMCID: PMC4713369.
 6. Li J, Zhao F, Wang Y, Chen J, Tao J, Tian G, et al. Gut microbiota dysbiosis contributes to the development of hypertension. *Microbiome.* 2017;5(1):14. Epub 2017/02/02. doi: 10.1186/s40168-016-0222-x. PubMed PMID: 28143587; PubMed Central PMCID: PMC4713369.
 7. Human Microbiome Project C. Structure, function and diversity of the healthy human microbiome. *Nature.* 2012;486(7402):207-14. Epub 2012/06/16. doi: 10.1038/nature11234. PubMed PMID: 22699609; PubMed Central PMCID: PMC3564958.
 8. Cho I, Blaser MJ. The human microbiome: at the interface of health and disease. *Nat Rev Genet.* 2012;13(4):260-70. Epub 2012/03/14. doi: 10.1038/nrg3182. PubMed PMID: 22411464; PubMed Central PMCID: PMC3418802.
 9. Proctor DM, Relman DA. The Landscape Ecology and Microbiota of the Human Nose, Mouth, and Throat. *Cell host & microbe.* 2017;21(4):421-32. doi: 10.1016/j.chom.2017.03.011. PubMed PMID: 28407480; PubMed Central PMCID: PMC5538306.
 10. Xu P, Gunsolley J. Application of metagenomics in understanding oral health and disease. *Virulence.* 2014;5(3):424-32. doi: 10.4161/viru.28532. PubMed PMID: 24642489; PubMed Central PMCID: PMC3979870.

11. Dewhirst FE, Chen T, Izard J, Paster BJ, Tanner AC, Yu WH, et al. The human oral microbiome. *Journal of bacteriology*. 2010;192(19):5002-17. doi: 10.1128/JB.00542-10. PubMed PMID: 20656903; PubMed Central PMCID: PMC2944498.
12. Xu X, He J, Xue J, Wang Y, Li K, Zhang K, et al. Oral cavity contains distinct niches with dynamic microbial communities. *Environmental Microbiology*. 2014:n/a-n/a. doi: 10.1111/1462-2920.12502.
13. Crielaard W, Zaura E, Schuller AA, Huse SM, Montijn RC, Keijser BJJ. Exploring the oral microbiota of children at various developmental stages of their dentition in the relation to their oral health. *Bmc Med Genomics*. 2011;4. doi: Artn 22 10.1186/1755-8794-4-22. PubMed PMID: WOS:000288378200001.
14. Marie D, Brussaard CPD, Thyraug R, Bratbak G, Vaulot D. Enumeration of marine viruses in culture and natural samples by flow cytometry. *Appl Environ Microbiol*. 1999;65(1):45-52. PubMed PMID: 9872758; PubMed Central PMCID: PMC90981.
15. Brussaard CP. Optimization of procedures for counting viruses by flow cytometry. *Appl Environ Microbiol*. 2004;70(3):1506-13. PubMed PMID: 15006772; PubMed Central PMCID: PMC368280.
16. Robertson BR, Button DK. Characterizing aquatic bacteria according to population, cell size, and apparent DNA content by flow cytometry. *Cytometry*. 1989;10(1):70-6. doi: 10.1002/cyto.990100112. PubMed PMID: 2465113.
17. Drilling A, Morales S, Jardeleza C, Vreugde S, Speck P, Wormald PJ. Bacteriophage reduces biofilm of *Staphylococcus aureus* ex vivo isolates from chronic rhinosinusitis patients. *American journal of rhinology & allergy*. 2014;28(1):3-11. doi: 10.2500/ajra.2014.28.4001. PubMed PMID: 24717868.

18. Payne RJ, Phil D, Jansen VA. Phage therapy: the peculiar kinetics of self-replicating pharmaceuticals. *Clin Pharmacol Ther.* 2000;68(3):225-30. Epub 2000/10/03. doi: S0009923600889559 [pii]
10.1067/mcp.2000.109520. PubMed PMID: 11014403.
19. Humphrey SP, Williamson RT. A review of saliva: normal composition, flow, and function. *The Journal of prosthetic dentistry.* 2001;85(2):162-9. doi: 10.1067/mpr.2001.113778. PubMed PMID: 11208206.
20. Schneyer LH, Pigman W, Hanahan L, Gilmore RW. Rate of flow of human parotid, sublingual, and submaxillary secretions during sleep. *Journal of dental research.* 1956;35(1):109-14. PubMed PMID: 13286394.
21. Simon-Soro A, Tomas I, Cabrera-Rubio R, Catalan MD, Nyvad B, Mira A. Microbial geography of the oral cavity. *Journal of dental research.* 2013;92(7):616-21. doi: 10.1177/0022034513488119. PubMed PMID: 23674263.
22. Choi JE, Waddell JN, Lyons KM, Kieser JA. Intraoral pH and temperature during sleep with and without mouth breathing. *J Oral Rehabil.* 2016;43(5):356-63. doi: 10.1111/joor.12372. PubMed PMID: WOS:000374339900005.
23. Izu SC, Itamoto CH, Pradella-Hallinan M, Pizarro GU, Tufik S, Pignatari S, et al. Obstructive sleep apnea syndrome (OSAS) in mouth breathing children. *Brazilian journal of otorhinolaryngology.* 2010;76(5):552-6. PubMed PMID: 20963335.
24. Oksenberg A, Fromm P, Melamed S. Dry mouth upon awakening in obstructive sleep apnea. *J Sleep Res.* 2006;15(3):317-20. doi: DOI 10.1111/j.1365-2869.2006.00527.x. PubMed PMID: WOS:000239691900010.
25. Liistro G, Stanescu DC, Veriter C, Rodenstein DO, Aubert-Tulkens G. Pattern of snoring in obstructive sleep apnea patients and in heavy snorers. *Sleep.* 1991;14(6):517-25. PubMed PMID: 1798885.

26. Li Y, Ku CY, Xu J, Saxena D, Caufield PW. Survey of oral microbial diversity using PCR-based denaturing gradient gel electrophoresis. *Journal of dental research*. 2005;84(6):559-64. PubMed PMID: 15914595.
27. Fabian TK, Fejerdy P, Csermely P. Salivary Genomics, Transcriptomics and Proteomics: The Emerging Concept of the Oral Ecosystem and their Use in the Early Diagnosis of Cancer and other Diseases. *Curr Genomics*. 2008;9(1):11-21. doi: 10.2174/138920208783884900. PubMed PMID: 19424479; PubMed Central PMCID: PMC2674305.
28. Pevernagie DA, De Meyer MM, Claeys S. Sleep, breathing and the nose. *Sleep medicine reviews*. 2005;9(6):437-51. Epub 2005/10/26. doi: 10.1016/j.smrv.2005.02.002. PubMed PMID: 16242364.
29. Chervin RD, Archbold KH, Dillon JE, Panahi P, Pituch KJ, Dahl RE, et al. Inattention, hyperactivity, and symptoms of sleep-disordered breathing. *Pediatrics*. 2002;109(3):449-56. Epub 2002/03/05. PubMed PMID: 11875140.
30. Sinha D, Guillemineault C. Sleep disordered breathing in children. *The Indian journal of medical research*. 2010;131:311-20. Epub 2010/03/24. PubMed PMID: 20308756.
31. Bhattacharjee R, Kheirandish-Gozal L, Spruyt K, Mitchell RB, Promchiarak J, Simakajornboon N, et al. Adenotonsillectomy Outcomes in Treatment of Obstructive Sleep Apnea in Children A Multicenter Retrospective Study. *Am J Resp Crit Care*. 2010;182(5):676-83. doi: DOI 10.1164/rccm.200912-1930OC. PubMed PMID: WOS:000281492000013.
32. Fitzpatrick MF, McLean H, Urton AM, Tan A, O'Donnell D, Driver HS. Effect of nasal or oral breathing route on upper airway resistance during sleep. *Eur Respir J*. 2003;22(5):827-32. Epub 2003/11/19. PubMed PMID: 14621092.

33. Lumb AB. Nunn's applied respiratory physiology eBook: Elsevier Health Sciences; 2016.
34. Fitzpatrick MF, Driver HS, Chatha N, Voduc N, Girard AM. Partitioning of inhaled ventilation between the nasal and oral routes during sleep in normal subjects. *J Appl Physiol* (1985). 2003;94(3):883-90. Epub 2002/11/16. doi: 10.1152/jappphysiol.00658.2002. PubMed PMID: 12433860.
35. Peterson SN, Snesrud E, Liu J, Ong AC, Kilian M, Schork NJ, et al. The dental plaque microbiome in health and disease. *Plos One*. 2013;8(3):e58487. Epub 2013/03/23. doi: 10.1371/journal.pone.0058487. PubMed PMID: 23520516; PubMed Central PMCID: PMC3592792.
36. Takeshita T, Nakano Y, Kumagai T, Yasui M, Kamio N, Shibata Y, et al. The ecological proportion of indigenous bacterial populations in saliva is correlated with oral health status. *Isme J*. 2009;3(1):65-78. Epub 2008/10/03. doi: 10.1038/ismej.2008.91. PubMed PMID: 18830275.
37. Gunaratnam K, Taylor B, Curtis B, Cistulli P. Obstructive sleep apnoea and periodontitis: a novel association? *Sleep Breath*. 2009;13(3):233-9. Epub 2009/02/10. doi: 10.1007/s11325-008-0244-0. PubMed PMID: 19198909.
38. Siqueira JF, Jr., Rocas IN. As-yet-uncultivated oral bacteria: breadth and association with oral and extra-oral diseases. *Journal of oral microbiology*. 2013;5. Epub 2013/05/30. doi: 10.3402/jom.v5i0.21077. PubMed PMID: 23717756; PubMed Central PMCID: PMC3664057.
39. Wade W, Thompson H, Rybalka A, Vartoukian S. Uncultured Members of the Oral Microbiome. *Journal of the California Dental Association*. 2016;44(7):447-56. Epub 2016/08/16. PubMed PMID: 27514156.

40. Eckburg PB, Bik EM, Bernstein CN, Purdom E, Dethlefsen L, Sargent M, et al. Diversity of the human intestinal microbial flora. *Science*. 2005;308(5728):1635-8. Epub 2005/04/16. doi: 10.1126/science.1110591. PubMed PMID: 15831718; PubMed Central PMCID: PMC1395357.
41. Lavergne C, Beaugeard L, Dupuy C, Courties C, Agogue H. An efficient and rapid method for the enumeration of heterotrophic prokaryotes in coastal sediments by flow cytometry. *Journal of microbiological methods*. 2014;105:31-8. Epub 2014/07/16. doi: 10.1016/j.mimet.2014.07.002. PubMed PMID: 25017902.
42. Brown MR, Hands CL, Coello-Garcia T, Sani BS, Ott AIG, Smith SJ, et al. A flow cytometry method for bacterial quantification and biomass estimates in activated sludge. *Journal of microbiological methods*. 2019;160:73-83. Epub 2019/03/31. doi: 10.1016/j.mimet.2019.03.022. PubMed PMID: 30926316.
43. Quirynen M, Steenberghe D. Is early plaque growth rate constant with time? *J Clin Periodontol*. 1989;16(5):278-83. doi: doi:10.1111/j.1600-051X.1989.tb01655.x.
44. Dige I, Schlafer S, Nyvad B. Difference in initial dental biofilm accumulation between night and day. *Acta Odontologica Scandinavica*. 2012;70(6):441-7. doi: 10.3109/00016357.2011.634833.
45. Lazarevic V, Whiteson K, Hernandez D, Francois P, Schrenzel J. Study of inter- and intra-individual variations in the salivary microbiota. *BMC genomics*. 2010;11:523. Epub 2010/10/06. doi: 10.1186/1471-2164-11-523. PubMed PMID: 20920195; PubMed Central PMCID: PMC2997015.
46. Stahringer SS, Clemente JC, Corley RP, Hewitt J, Knights D, Walters WA, et al. Nurture trumps nature in a longitudinal survey of salivary bacterial communities in twins from early adolescence to early adulthood. *Genome research*.

2012;22(11):2146-52. Epub 2012/10/16. doi: 10.1101/gr.140608.112. PubMed PMID: 23064750; PubMed Central PMCID: PMC3483544.

47. Cameron SJ, Huws SA, Hegarty MJ, Smith DP, Mur LA. The human salivary microbiome exhibits temporal stability in bacterial diversity. *FEMS microbiology ecology*. 2015;91(9):fiv091. Epub 2015/07/25. doi: 10.1093/femsec/fiv091. PubMed PMID: 26207044.

48. Belstrom D, Holmstrup P, Bardow A, Kokaras A, Fiehn NE, Paster BJ. Temporal Stability of the Salivary Microbiota in Oral Health. *Plos One*. 2016;11(1):e0147472. Epub 2016/01/23. doi: 10.1371/journal.pone.0147472. PubMed PMID: 26799067; PubMed Central PMCID: PMC4723053.

49. Rasiah IA, Wong L, Anderson SA, Sissons CH. Variation in bacterial DGGE patterns from human saliva: over time, between individuals and in corresponding dental plaque microcosms. *Archives of oral biology*. 2005;50(9):779-87. Epub 2005/06/23. doi: 10.1016/j.archoralbio.2005.02.001. PubMed PMID: 15970209.

50. Backhed F, Roswall J, Peng Y, Feng Q, Jia H, Kovatcheva-Datchary P, et al. Dynamics and Stabilization of the Human Gut Microbiome during the First Year of Life. *Cell host & microbe*. 2015;17(6):852. doi: 10.1016/j.chom.2015.05.012. PubMed PMID: 26308884.

51. Oh J, Byrd AL, Park M, Program NCS, Kong HH, Segre JA. Temporal Stability of the Human Skin Microbiome. *Cell*. 2016;165(4):854-66. doi: 10.1016/j.cell.2016.04.008. PubMed PMID: 27153496; PubMed Central PMCID: PMC4860256.

52. Wang Z, Bafadhel M, Haldar K, Spivak A, Mayhew D, Miller BE, et al. Lung microbiome dynamics in COPD exacerbations. *Eur Respir J*. 2016;47(4):1082-92. doi: 10.1183/13993003.01406-2015. PubMed PMID: 26917613.

53. Feazel LM, Robertson CE, Ramakrishnan VR, Frank DN. Microbiome complexity and *Staphylococcus aureus* in chronic rhinosinusitis. *The Laryngoscope*. 2012;122(2):467-72. doi: 10.1002/lary.22398. PubMed PMID: 22253013; PubMed Central PMCID: PMC3398802.
54. Boase S, Foreman A, Cleland E, Tan L, Melton-Kreft R, Pant H, et al. The microbiome of chronic rhinosinusitis: culture, molecular diagnostics and biofilm detection. *BMC infectious diseases*. 2013;13:210. doi: 10.1186/1471-2334-13-210. PubMed PMID: 23656607; PubMed Central PMCID: PMC3654890.
55. Biegala IC, Not F, Vaultot D, Simon N. Quantitative assessment of picoeukaryotes in the natural environment by using taxon-specific oligonucleotide probes in association with tyramide signal amplification-fluorescence in situ hybridization and flow cytometry. *Appl Environ Microbiol*. 2003;69(9):5519-29. PubMed PMID: 12957941; PubMed Central PMCID: PMC194996.
56. Lay C, Dore J, Rigottier-Gois L. Separation of bacteria of the *Clostridium leptum* subgroup from the human colonic microbiota by fluorescence-activated cell sorting or group-specific PCR using 16S rRNA gene oligonucleotides. *FEMS microbiology ecology*. 2007;60(3):513-20. doi: 10.1111/j.1574-6941.2007.00312.x. PubMed PMID: 17428302.
57. Czechowska K, Johnson DR, van der Meer JR. Use of flow cytometric methods for single-cell analysis in environmental microbiology. *Curr Opin Microbiol*. 2008;11(3):205-12. doi: <https://doi.org/10.1016/j.mib.2008.04.006>.

APPENDICES

The following publications and poster presentations have been produced from the chapters within this thesis.

Publications

Carlson-Jones JA, Paterson JS, Newton K, Smith RJ, Dann LM, Speck P, Mitchell JG, Wormald PJ. Enumerating Virus-Like Particles and Bacterial Populations in the Sinuses of Chronic Rhinosinusitis Patients Using Flow Cytometry. *Plos One*. 2016;11(5):e0155003. doi: 10.1371/journal.pone.0155003. PubMed PMID: 27171169; PubMed Central PMCID: PMC4865123

Carlson-Jones J, Kontos A, Paterson J, Smith R, Dann L, Speck P, Lushington K, Martin J, Kennedy D, Mitchell J. Flow Cytometric Enumeration of Bacterial and Virus-Like Particle Populations in the Human Oral Cavity Pre and Post Sleep. *J Sleep Res*. 2016;25:86-. PubMed PMID: WOS:000393032700215.

Poster presentations

Carlson-Jones J, Dann LM, Newton K, Paterson JS, Smith RJ, Speck P, Mitchell JG, Wormald PJ. Enumeration of virus-like particles in the sinus washes of chronic rhinosinusitis patients. Poster presented at: Australian Society for Microbiology, 2014 July 6-9, Melbourne, Australia

Carlson-Jones J, Dann LM, Newton K, Paterson JS, Smith RJ, Speck P, Mitchell JG, Wormald PJ. Enumeration of virus-like particles in the sinus washes of chronic rhinosinusitis patients. Poster presented at: 15th International Symposium on Microbial Ecology, 2014 August 24-29, Seoul, Korea.

Carlson-Jones, J, Kontos A, Paterson J, Smith R, Dann LM, Speck P, Lushington K, Martin J, Kennedy D, Mitchell J. Flow Cytometric Enumeration of Bacterial and Virus-Like Particle Populations in the Human Oral Cavity Pre and Post Sleep. Poster presented: 16th International Symposium on Microbial Ecology, 2016 August 21-25, Montréal, Canada.

Carlson-Jones, J, Kontos A, Paterson J, Smith R, Dann LM, Speck P, Lushington K, Martin J, Kennedy D, Mitchell J. Flow Cytometric Enumeration of Bacterial and Virus-Like Particle Populations in the Human Oral Cavity Pre and Post Sleep. Poster presented: Sleep Down Under, 2016 October 20-22, Adelaide, Australia.

RESEARCH ARTICLE

Enumerating Virus-Like Particles and Bacterial Populations in the Sinuses of Chronic Rhinosinusitis Patients Using Flow Cytometry

Jessica A. P. Carlson-Jones^{1*}, James S. Paterson¹, Kelly Newton¹, Renee J. Smith¹, Lisa M. Dann¹, Peter Speck¹, James G. Mitchell¹, Peter-John Wormald²

1 School of Biological Sciences, Flinders University, Adelaide, South Australia, Australia, **2** Department of Surgery-Otolaryngology Head & Neck Surgery, The University of Adelaide, South Australia, Australia

* jessica.carlsonjones@flinders.edu.au



 OPEN ACCESS

Citation: Carlson-Jones JAP, Paterson JS, Newton K, Smith RJ, Dann LM, Speck P, et al. (2016) Enumerating Virus-Like Particles and Bacterial Populations in the Sinuses of Chronic Rhinosinusitis Patients Using Flow Cytometry. PLoS ONE 11(5): e0155003. doi:10.1371/journal.pone.0155003

Editor: Jean-Luc EPH Darlix, Institut National de la Santé et de la Recherche Médicale, FRANCE

Received: October 29, 2015

Accepted: March 25, 2016

Published: May 12, 2016

Copyright: © 2016 Carlson-Jones et al. This is an open access article distributed under the terms of the [Creative Commons Attribution License](https://creativecommons.org/licenses/by/4.0/), which permits unrestricted use, distribution, and reproduction in any medium, provided the original author and source are credited.

Data Availability Statement: All relevant data are within the paper and Supporting Information files.

Funding: Consumables and general support was provided by Flinders University and grants to JGM by the Australian Research Council. The funders had no role in study design, data collection and analysis, decision to publish, or preparation of the manuscript.

Competing Interests: The authors have declared that no competing interests exist.

Abstract

There is increasing evidence to suggest that the sinus microbiome plays a role in the pathogenesis of chronic rhinosinusitis (CRS). However, the concentration of these microorganisms within the sinuses is still unknown. We show that flow cytometry can be used to enumerate bacteria and virus-like particles (VLPs) in sinus flush samples of CRS patients. This was achieved through trialling 5 sample preparation techniques for flow cytometry. We found high concentrations of bacteria and VLPs in these samples. Untreated samples produced the highest average bacterial and VLP counts with $3.3 \pm 0.74 \times 10^7$ bacteria ml^{-1} and $2.4 \pm 1.23 \times 10^9$ VLP ml^{-1} of sinus flush ($n = 9$). These counts were significantly higher than most of the treated samples ($p < 0.05$). Results showed 10^3 and 10^4 times inter-patient variation for bacteria and VLP concentrations. This wide variation suggests that diagnosis and treatment need to be personalised and that utilising flow cytometry is useful and efficient for this. This study is the first to enumerate bacterial and VLP populations in the maxillary sinus of CRS patients. The relevance of enumeration is that with increasing antimicrobial resistance, antibiotics are becoming less effective at treating bacterial infections of the sinuses, so alternative therapies are needed. Phage therapy has been proposed as one such alternative, but for dosing, the abundance of bacteria is required. Knowledge of whether phages are normally present in the sinuses will assist in gauging the safety of applying phage therapy to sinuses. Our finding, that large numbers of VLP are frequently present in sinuses, indicates that phage therapy may represent a minimally disruptive intervention towards the nasal microbiome. We propose that flow cytometry can be used as a tool to assess microbial biomass dynamics in sinuses and other anatomical locations where infection can cause disease.

Introduction

Chronic rhinosinusitis (CRS) is a common disease amongst the human population, and there is increasing evidence to show that microorganisms are involved in the inflammation of the sinus mucosal layer leading to exacerbation of the disease [1–3]. It is well established that the healthy sinus is not sterile, but is colonised by a diverse community of microorganisms [1, 2, 4, 5]. These microorganisms exist in the sinuses within exopolysaccharide biofilms, the presence of which leads to difficulties in treating the disease [6–12]. As antibiotics are a common treatment option for CRS patients, there is concern surrounding the growing antimicrobial resistance [13, 14]. Bacteria within these biofilms are able to secrete a polysaccharide matrix that acts as a protective barrier against host defences and antimicrobial agents [15]. This protective barrier makes it difficult when it comes to treating CRS with antibiotics. An alternative treatment is phage therapy which utilises specific bacteriophages (phage) that infect and kill pathogenic bacteria [16]. Trials of bacteriophage cocktails consisting of multiple types of phage, on sheep models of sinusitis have proven to be effective in eliminating *S. aureus* in biofilms and its free floating form [17]. Through the use of these phage cocktails, the development of phage resistant bacteria is reduced [18]. Knowledge of population abundance of bacteria and phage in the sinuses is important for the development of appropriate phage concentrations for use in this therapy [19].

Flow cytometry has been used as a method for enumerating heterotrophic bacteria and virus-like particles (VLPs) in environmental samples for decades [20–22]. This non-culture based technology is a quick, inexpensive way to rapidly enumerate a large number of cells and particles to provide data without the enrichment bias culturing introduces [20]. This technique yields highly reproducible counts and enumeration of VLPs at a concentration that would be too low for transmission electron microscopy (TEM) [20]. Here, we investigate methods to enumerate bacteria and VLPs within sinus flush fluid samples and present the first data, produced using flow cytometry, describing bacterial and VLP abundance within the maxillary sinuses of CRS patients. We, therefore, aim to measure the variation in abundance of bacteria and VLPs in the sinuses of CRS patients to determine if they are present at the same level among patients.

Materials and Methods

Ethics Statement

Maxillary sinus flush fluid samples were obtained from nine patients diagnosed with CRS in accordance to criteria defined by the Chronic Rhinosinusitis Task Force [23]. This study was approved by The Queen Elizabeth Hospital Human Research Ethics Committee, reference number: HREC/13/TQEHLMH/49. All nine patients involved in the study gave written consent prior to their sinus surgery. All sinus flush fluid samples were collected by the senior author (P.J.W) during the patient's endoscopic sinus surgery. Due to the highly invasive nature of the operating procedure, healthy controls were not ethically justifiable, nor are they relevant to the question of how much abundance variation is there among infected patients.

Sample collection. Immediately after opening the maxillary sinus, approximately 5 ml of sterile saline was used to flush the sinus and re-collected in sterile specimen containers. Volume of flush fluid collected ranged from approximately 2 to 4 ml. Once samples were collected, they were transported on ice ready for immediate fixation with glutaraldehyde (0.5% final concentration) on ice in the dark, then snap freezing in liquid nitrogen and storage at -80°C until analysis [21].

Sample Preparation

Five sample preparation techniques for flow cytometry were investigated. Fixed sinus flush fluid samples were thawed before each treatment was applied.

Sputasol. Sputasol was made using 0.02 μm filtered MilliQ water according to the manufacturer's instructions (Oxoid). Equal volumes of Sputasol and fixed sinus sample were mixed together then incubated at 37°C for 15 minutes.

Methanol. Methanol, 0.2 μm filtered, was added to fixed sinus samples to a final concentration of 20% [24]. Samples were incubated at 37°C for 15 minutes then sonicated for 30 seconds in a SoniClean™ sonicating bath (Model 160TD, 60 W, 50/60Hz).

Potassium citrate. Potassium citrate tribasic solution (1M, Sigma) was added to the fixed sample to a 1% final concentration [24]. The sample was then vortexed for 30 seconds [24].

Sodium pyrophosphate. Sodium pyrophosphate solution was added to 100 μl of fixed sample to a final concentration of 10 mM [24]. Samples were vortexed for 1 minute and incubated at room temperature for 15 minutes [24]. Samples were then sonicated for 30 seconds in a SoniClean™ sonicating bath (Model 160TD, 60 W, 50/60Hz).

Untreated. Fixed samples were diluted in 0.2 μm filtered TE buffer (10 mM Tris, 1 mM EDTA, pH 7.4) without pre-treatment [21].

Flow Cytometric Analysis

Bacterial and VLP populations present in sinus flush fluid were identified and enumerated using a BD ACCURI C6 flow cytometer (Becton Dickinson). Samples using each extraction technique were run in triplicate for each patient. Samples were diluted (1:100) in 0.2 μm filtered TE buffer, stained with the DNA-binding dye SYBR-I Green (1:20,000 final dilution; Molecular Probes) then incubated at 80°C in the dark for 10 minutes [21]. For each preparation method control samples were generated prior to each flow cytometry session. These samples were prepared in the same manner as patient samples in 0.9% sterile saline, the same concentration used to flush patient sinuses. These samples were used to eliminate background artefacts introduced during sample preparation.

Samples were analysed using an Accuri C6 flow cytometer (Accuri C6) and BD ACCURI CFlow software. All samples were run for 2 minutes at machine fluidics setting of fast, with the threshold set to FL-1 (green fluorescence). As a control, 1 μm diameter fluorescent beads (Molecular Probes) were used. Beads were added to each sample to a final concentration of 10^5 beads ml^{-1} [25]. The beads allow for flow cytometric parameters to be normalised according to bead fluorescence and concentration, and to give an indication of viral and bacterial cell size [25]. Phosphate-buffered saline (PBS) was used as sheath fluid for flow cytometry analysis. For each sample, green fluorescence, side angle light scatter and forward angle light scatter were recorded.

Data Analysis

Flow cytometry data was analysed using FlowJo software (Tree Star, Inc.). VLP and bacterial populations were categorised based on variations in side scatter, a representation of cell size, and SYBR Green fluorescence, an indication of nucleic acid content [20, 21, 26]. For some patients, only one bacterial population was observed, whereas others showed multiple. Therefore, one overall bacterial population was created to remain consistent across all patient samples.

Rank abundance plots were generated for bacterial and VLP concentrations using all method triplicates and their averages to distinguish between any patient groupings formed on

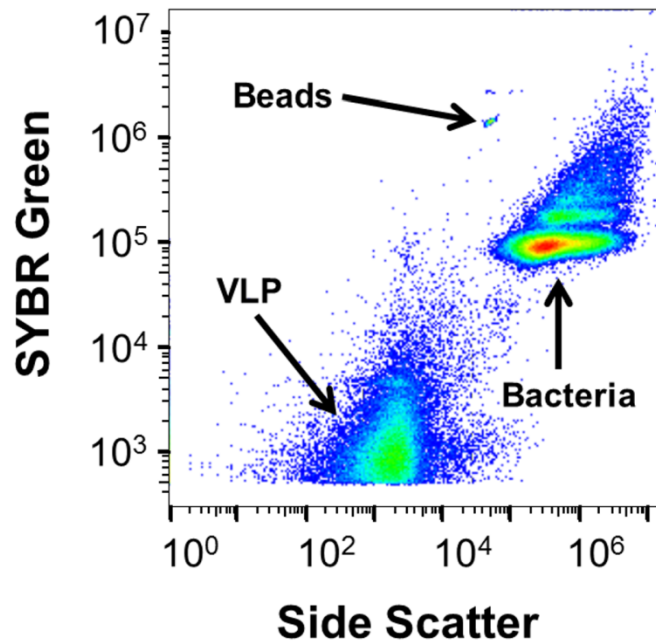


Fig 1. Bacterial and VLP identification using side-scatter and green fluorescence. Representative cytogram shows the VLP and bacterial populations in a patient's untreated sinus wash.

doi:10.1371/journal.pone.0155003.g001

abundance. Comparisons between bacterial and VLP abundances for each treatment method were made using the statistical analysis program SPSS version 22 (IBM Corp. Released 2013. IBM SPSS Statistics for Windows, Version 22.0. Armonk, NY: IBM Corp.) using the Wilcoxon signed-rank test. Statistical significance between treatments was considered when $p < 0.05$.

Results

Flow Cytometric Analysis

Cytograms showed discrete bacterial and VLP populations present within the sinus fluid of CRS patients (Fig 1). Some patients exhibited one distinct bacterial population, whereas others patients exhibited up to four (Fig 1). Variations in bacterial and VLP abundance were observed between patients regardless of the treatment method used on the samples. Mean bacterial and VLP abundances for each treatment method are shown in Table 1.

Table 1. Mean concentration of bacteria and VLP per ml of sinus flush fluid for each treatment method tested. Error represents standard error of the mean.

Treatment	Bacteria ml ⁻¹ (±SE)	VLP ml ⁻¹ (±SE)
Untreated	3.3 × 10 ⁷ (7.4 × 10 ⁶)	2.4 × 10 ⁹ (1.2 × 10 ⁹)
Sodium pyrophosphate	2.9 × 10 ⁷ (6.7 × 10 ⁶)	2.0 × 10 ⁹ (9.9 × 10 ⁸)
Sputasol	2.2 × 10 ⁷ (6.5 × 10 ⁶)	1.8 × 10 ⁹ (9.1 × 10 ⁸)
Methanol	2.0 × 10 ⁷ (4.3 × 10 ⁶)	2.2 × 10 ⁹ (9.9 × 10 ⁸)
Potassium citrate	1.9 × 10 ⁷ (4.6 × 10 ⁶)	2.2 × 10 ⁹ (1.1 × 10 ⁹)

doi:10.1371/journal.pone.0155003.t001

Bacterial Sample Preparation Method Optimisation

For patient samples, the mean bacterial abundance for untreated samples was the highest of all treatments, with $3.3 \pm 0.74 \times 10^7$ cells ml^{-1} ($n = 27$; [Table 1](#); [S1 Table](#)). The lowest mean abundance was for potassium citrate treated samples with $1.9 \pm 0.46 \times 10^7$ cells ml^{-1} ($n = 27$; [Table 1](#); [S1 Table](#)). In testing the differences between treatments, the untreated and sodium pyrophosphate samples yielded significantly higher bacterial abundance than potassium citrate ($p < 0.001$ and $p < 0.001$), methanol ($p = 0.002$ and $p < 0.001$) and Sputasol ($p = 0.003$ and $p < 0.001$). There was no significant difference in bacterial abundance between sodium pyrophosphate treated and untreated samples ($p = 0.39$).

VLP Sample Preparation Method Optimisation

VLP mean abundance for the untreated method was the highest for all patient samples with $2.4 \pm 1.2 \times 10^9$ cells ml^{-1} ($n = 27$; [Table 1](#); [S2 Table](#)). Sputasol treated patient samples yielded the lowest VLP abundances with $1.8 \pm 0.91 \times 10^9$ cells ml^{-1} ($n = 27$; [Table 1](#); [S2 Table](#)). Untreated samples yielded significantly higher VLP abundances than potassium citrate ($p = 0.031$), methanol ($p = 0.010$), and Sputasol ($p = 0.019$) treated samples. There was no significant difference between VLP abundance for untreated samples and sodium pyrophosphate treated samples ($p = 0.08$). Sodium pyrophosphate also did not yield significantly higher VLP abundances than potassium citrate ($p = 0.44$) and methanol ($p = 0.53$) treated samples. There was, however, a significant difference between VLP abundances for sodium pyrophosphate and Sputasol ($p = 0.008$).

Bacterial Rank Abundance

Rank abundance was used to identify possible groupings among the patient's bacterial abundance. Breaks in the plot suggest 3 groupings of patients with bacterial abundances classified as high, greater than 10^7 cells ml^{-1} , medium, between 10^5 to 10^6 cells ml^{-1} , and low, less than 10^5 cells ml^{-1} ([Fig 2](#)). The high bacterial group consisted of triplicates from 5 patients. The medium bacterial group contained triplicates from 3 patients and the low bacterial abundance group consisted of 1 patient. There was approximately one order of magnitude difference between each of the 3 groups ([Fig 2](#)). The overall average bacterial rank abundance using all treatment triplicates fit a logarithmic trend; however this was achieved by a series of step down power laws for each bacterial group ([Fig 3](#)).

VLP Rank Abundance

A rank abundance plot for VLP abundance was generated using the method triplicates of untreated, sodium pyrophosphate, potassium citrate, Sputasol and methanol samples ([Fig 4](#)). VLP abundances show an even distribution across 5 orders of magnitude. Three patients had values above 10^8 VLP ml^{-1} . These are classified as high VLP, with the proviso that they are separated from each other by an order of magnitude ([Fig 4](#)). Three patients make up the medium concentration group between 10^7 and 10^8 VLP ml^{-1} . However, in this group the loss of VLPs in the methanol and sodium pyrophosphate treatments makes the group appear fused with the lowest group. The lowest group was classified as concentrations below 10^7 VLP ml^{-1} . In this group the methanol treatment showed considerable loss of VLPs and in one patient a complete absence of VLPs ([Fig 4](#)). The overall average VLP rank abundance using all treatment triplicates fit a steep power law ([Fig 5](#)).

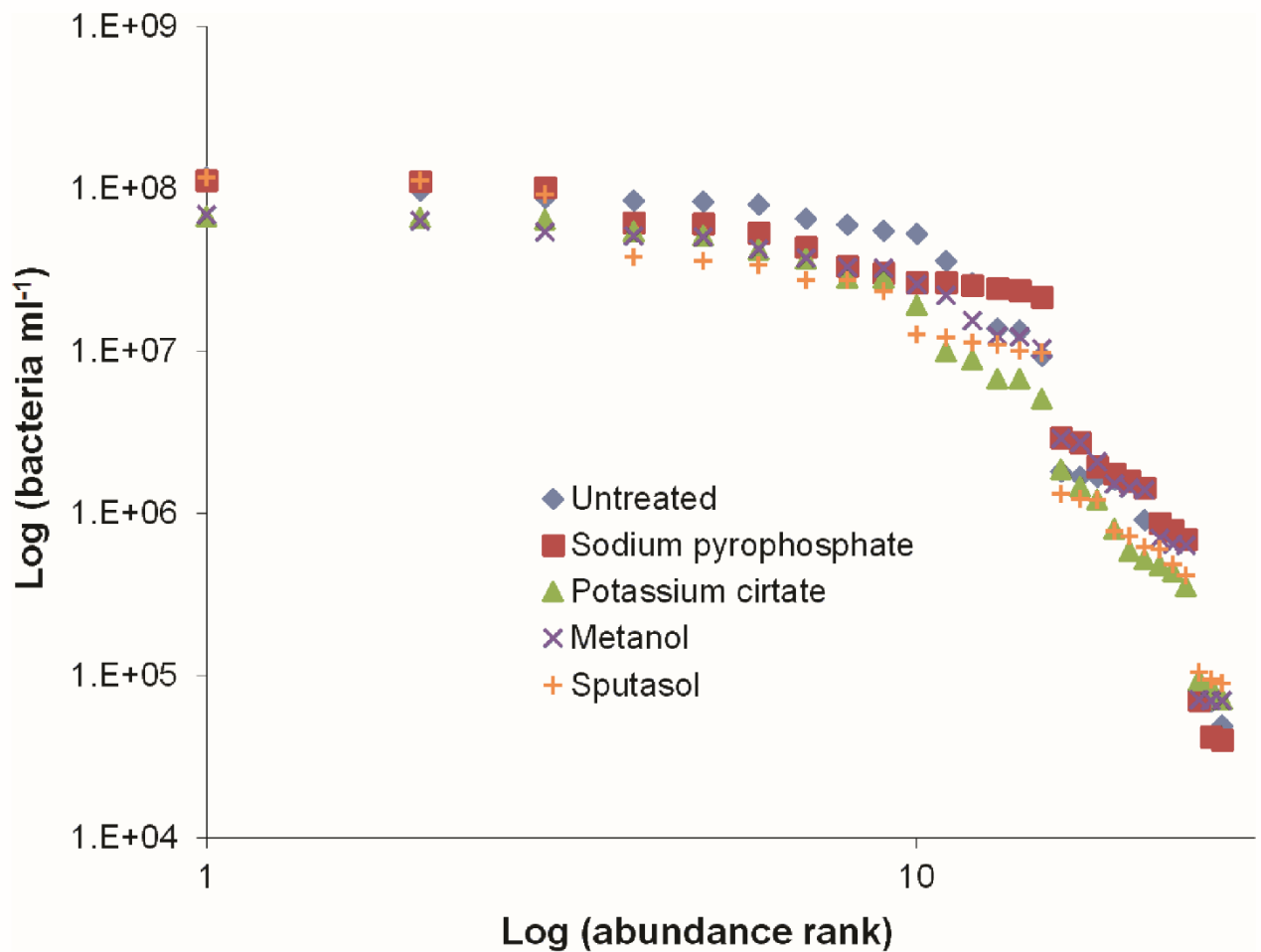


Fig 2. Rank abundance for each patient's bacterial abundance for each sample treatment method, with triplicates shown. Three clear groups of patients with high, medium and low bacterial abundances are apparent. Differences in treatments used on the samples can be seen not to influence steps of bacterial abundance for patients.

doi:10.1371/journal.pone.0155003.g002

Lack of Correlation with Patient Symptoms

Prior to sinus surgery, each patient completed a questionnaire regarding basic clinical information and provided a severity score from 0, being no problem, to 5, being a problem as bad as it can be, for CRS symptoms for the past two weeks. Based on the rank abundance plots (Figs 2 and 3), possible trends in the patient groups were investigated. There were no trends observed within the rank abundance patient groups for bacteria or VLPs.

Discussion

This is the first study to use flow cytometry to enumerate bacteria and VLPs within the maxillary sinus of CRS patients. We present a number of snapshot enumerations, using flow cytometry, of the microbial composition of sinuses of CRS patients. We tested a number of sample preparation techniques for bacterial and VLP enumeration that are used for environmental samples, in particular, techniques used for disruption of coral mucus, for microscopy [24, 27]. Our results showed that the sinus, at least in patients requiring sinus surgery, is an active microbiological environment. We speculate that most VLPs detected are likely to be bacteriophages

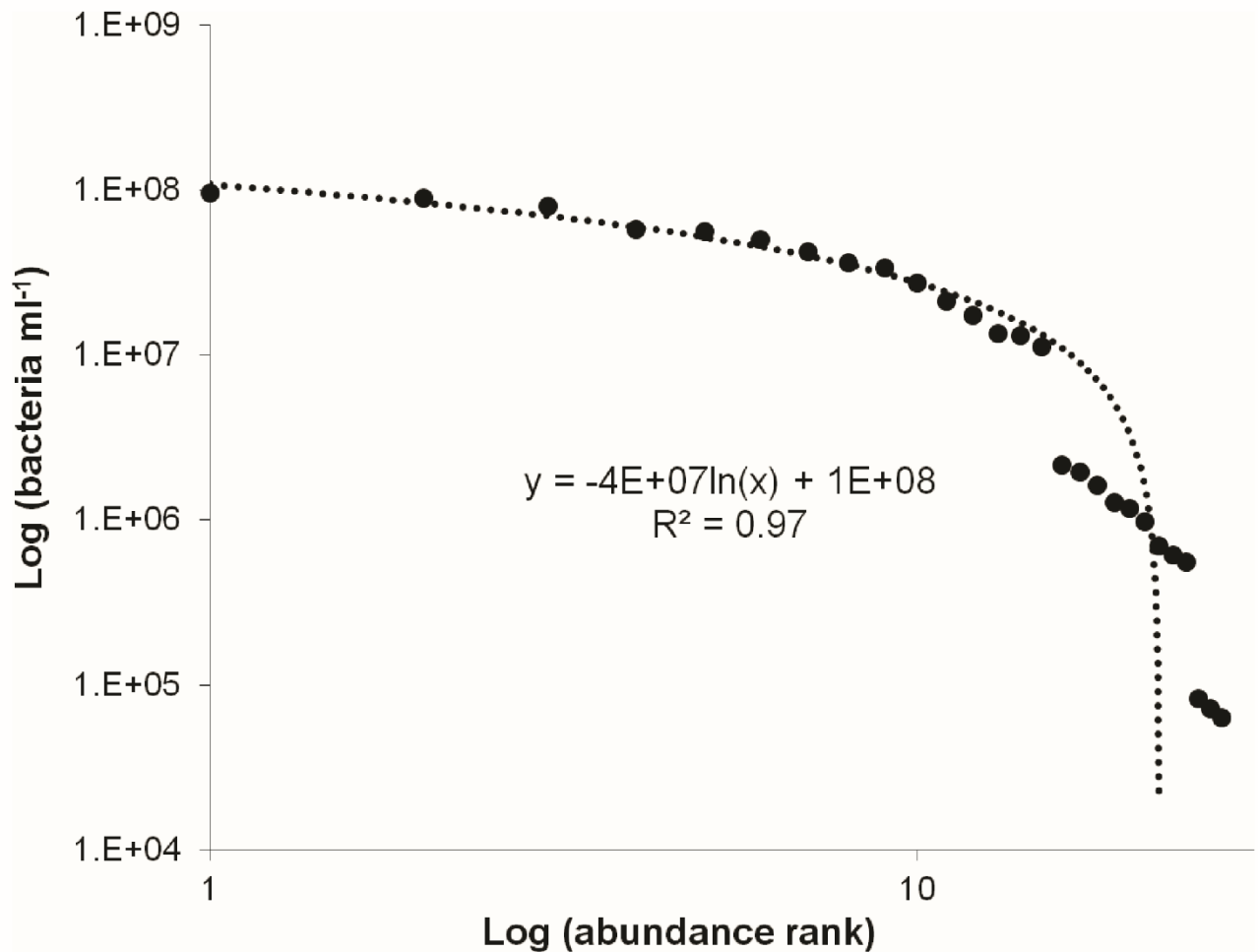


Fig 3. Average bacterial rank abundance using all treatment triplicates. Data points follow a logarithmic trend achieved by steps of power laws for each observed group. High medium and low bacterial concentration groups fit the power law equations $y = 2E+08x^{-0.84}$ ($R^2 = 0.84$), $y = 5E+10x^{-3.57}$ ($R^2 = 0.98$) and $y = 6E+09x^{-3.49}$ ($R^2 = 1$) respectively.

doi:10.1371/journal.pone.0155003.g003

as they are the most commonly found in association with their hosts, bacteria, which we find to be present in abundance in sinuses. The proposal that phages can be used to treat bacterial infections of the sinus [17] can now be viewed in the light of this data showing that phages appear to be present in sinuses in large numbers (Table 1).

Although the primary focus of this study was to enumerate the bacteria and VLPs in the sinus fluid, there was concern surrounding the presence of small fragments of mucus or biofilms within the samples prepared for flow cytometry. The mucus may have caused the bacteria and VLPs to clump together resulting in an overestimation on particle size, shape and DNA content. This is a similar concern in regards to analyzing bacteria and VLPs in coral mucus using microscopy [24, 27]. As bacterial and VLP flow cytometry on human samples is a new approach, various flow cytometry methods were investigated.

Common chemicals used in environmental sample preparation include potassium citrate, sodium pyrophosphate and methanol. Sodium pyrophosphate and potassium citrate are commonly used in environmental microbiology for desorbing viral particles from soil and marine sediment [28, 29]. Potassium citrate increases the electrostatic repulsion between viruses and

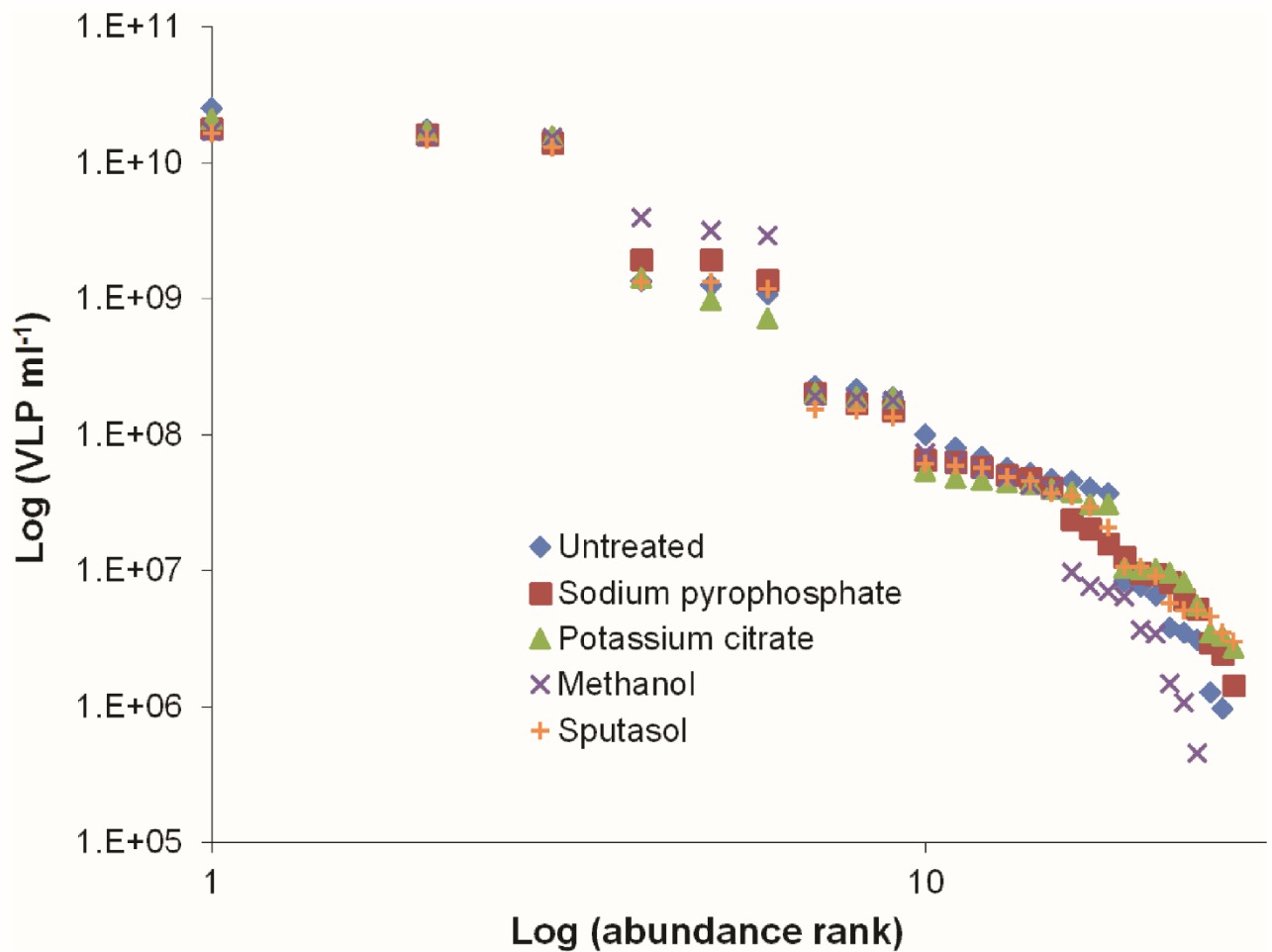


Fig 4. Rank abundance for each patient's VLP abundance for each sample preparation method, with triplicates shown. Highest abundances are rare while lower abundances are common. Differences in treatments used on the patient samples can be seen not to influence the high range of VLP origination levels.

doi:10.1371/journal.pone.0155003.g004

bacteria, and the mucus to which they are attached to by raising pH [24]. Sodium pyrophosphate weakens the hydrophilic links in mucus allowing for viruses and bacteria to be separated [30]. Dithiothreitol (DTT) has been used on sinus samples to improve the yield of fungal cultures and in studies involving quantification of inflammatory cells in nasal secretions [31–33]. Sputasol contains DTT and has been used to liquefy mucus in nasal lavage [34]. It does this by breaking disulfide bonds within mucin, causing liquefaction, releasing trapped viruses and bacteria [35, 36]. Methanol has the ability to break up exopolymeric substances in mucus which entrap bacteria and viruses [37].

Our results show that the untreated and sodium pyrophosphate treatment methods yielded significantly higher bacterial abundances than all other methods tested ($p < 0.05$). For VLP enumeration, no treatment (as in the untreated samples) was the optimal method. Although there was no significant difference between untreated and sodium pyrophosphate treated samples ($p < 0.05$), sodium pyrophosphate did not yield significantly higher VLP abundances than methanol and potassium citrate ($p < 0.05$). This result contrasts to previous microscopy studies which found potassium citrate better for viral enumeration in coral mucus [24]. Unlike

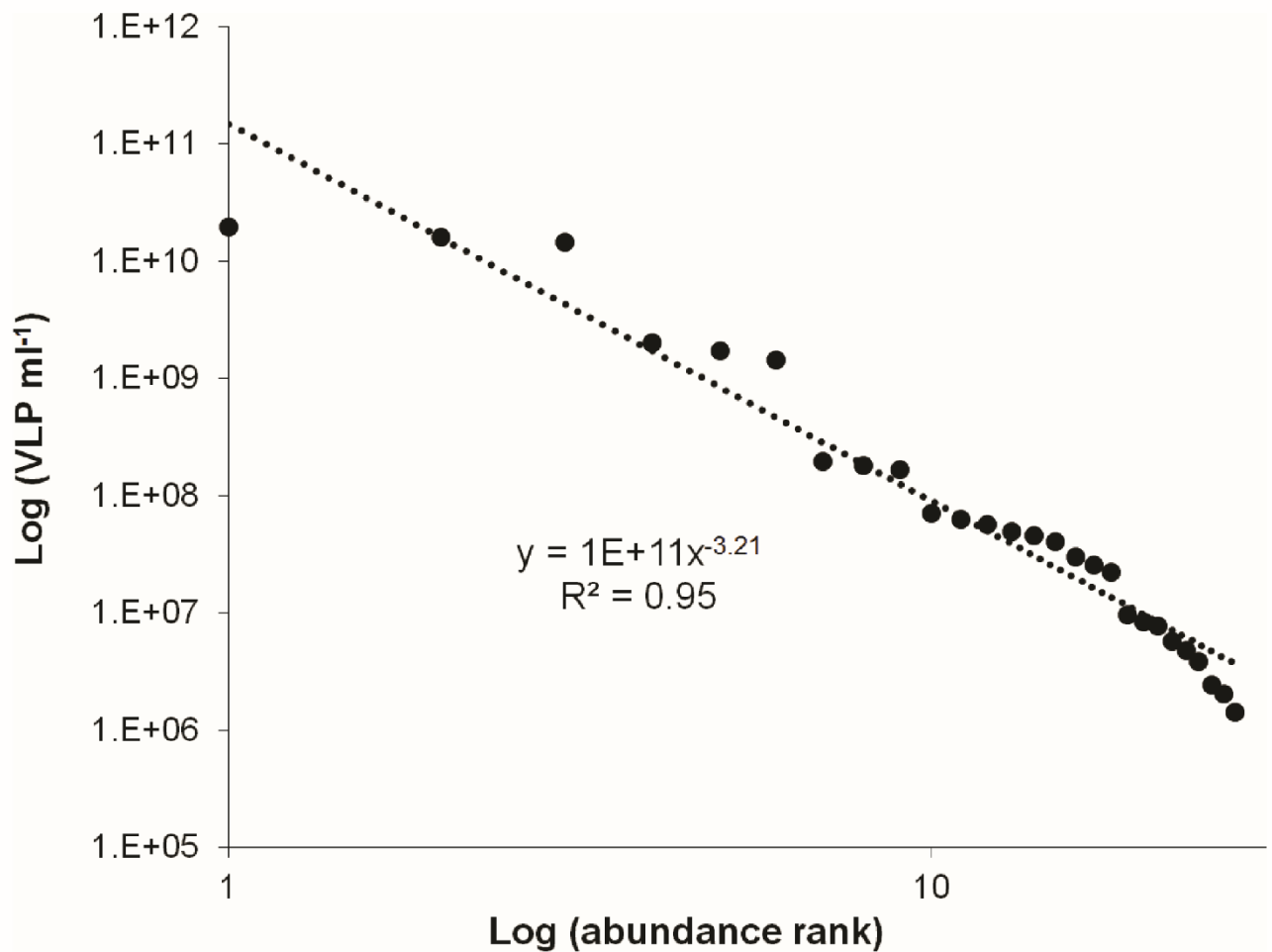


Fig 5. Average VLP rank abundance using all treatment triplicates. Data points follow a power law.

doi:10.1371/journal.pone.0155003.g005

sample preparation for coral mucus for microscopy, flow cytometry includes an incubation period after addition of SYBR Green. During this step viral capsids may partially and temporarily denature, facilitating a greater uptake of SYBR Green [20]. This may result in brighter VLP fluorescence resulting in higher counts for all samples. It is also possible that the extra processing steps involved with each treatment resulted in the loss of bacteria and VLPs. All samples were diluted for flow cytometry in TE buffer which contained 1 mM of EDTA. EDTA has been used to extract bacteria and viruses from photosynthetic microbial mats as it destroys cation links within exopolymeric substances, releasing bound bacteria and viruses [38]. It also permeabilises outer membranes, facilitating greater uptake of SYBR Green [39]. Additional treatment to each sample could have an adverse effect, causing damage to viral capsid proteins or to bacterial cell walls. Our data suggests that the least possible number of processing steps and addition of chemicals is the optimal method for analyzing sinus flush samples.

Previous studies have shown that the human sinus is colonized with an array of microbes [1, 2, 6–12, 40]. Flow cytometry enables categorization and enumeration of these microbes based on size and DNA content [21, 26]. Some patient's cytograms revealed numerous bacterial sub-populations (Fig 1). These populations displayed increased green fluorescence, an indication of DNA content, and size. These different sub-populations may be reflecting different

bacterial replication stages or are indicative of different bacterial species with different sized genomes. In the Sputasol treated patient samples, an unusual population was observed between the bacterial and VLP regions. This population appears to be an artifact of the Sputasol as it was also observed in the control samples (S1 Fig). Thus, there may be a component within Sputasol which autofluoresces or binds to SYBR Green.

Large variations were observed between patients bacterial and VLP concentrations, which is not uncommon with human microbial flora studies [41–45]. These findings suggest that the maxillary sinus is either extremely dynamic or highly individualised. These differences in the patient microbial concentrations could indicate the need for personalised dosages when treating CRS with antibiotics or with phage. The rank abundance plot for patient bacterial abundance revealed 3 groupings of high, medium and low abundance (Fig 2). As the treatments used on the samples were not seen to account for the differences in bacterial and VLP levels (Figs 2 and 4), an average of all treatment values was used to clearly demonstrate the obvious trends in bacterial concentration groups (Fig 3) and high episodic nature of the VLPs (Fig 5).

For the bacterial rank abundance, the three orders of magnitude range among the 9 patients may reflect temporal variation or that the bacterial abundances are defined by processes or a variable that was not measured. The skew of the distribution towards the lower concentrations in the VLP rank abundance is consistent with the highly episodic nature of viral infections, particularly in bacteriophage where large burst sizes can quickly reduce the concentrations of particular bacterial species, leaving high bacteriophage concentrations at least temporarily [46]. From this, one might posit that time series sampling would show an eventual decline in VLP concentration. While bacteriophage dynamics is one likely explanation for the observed distribution, at this point we cannot discount that some patients have chronically high VLP concentrations. To investigate this and its clinical significance would require flow cytometric and nucleic acid sequence analysis of time series samples from the identified patients. Due to the invasive nature of sampling used in this study, healthy controls and a time series using the same sampling method may not be a feasible option. Therefore there is the need to develop a proxy for an alternative less invasive sampling strategy, such as nasal swabbing. While this is beyond the scope of this paper, it is a potentially valuable future direction.

Knowledge of the abundance of microorganisms in CRS will further our understanding of the disease as the presence of certain bacterial species does not always imply infection. The aim of his research was to produce a snapshot enumeration of the sinus microbes of 9 patients known to suffer from CRS, and to determine if they had similar abundances of bacteria and VLPs. Within the group of 9 patients sampled, there was 3 orders of magnitude difference in abundance for bacterial populations and almost 4 orders of magnitude difference for VLPs. This suggests that not all CRS patients are infected at the same level of bacteria and VLPs. Knowledge of the differences in bacterial abundances may facilitate the development of personalised treatment options.

This work indicates the potential for future studies in other microbial disease related health conditions. We propose that flow cytometry has potential as a tool to monitor microbial dynamics in patients and in future may assist in determining appropriate dosages required when treating microbial related health conditions.

Supporting Information

S1 Fig. Representative cytogram showing the Sputasol artefact population observed between the VLP and bacterial populations.

(TIF)

S1 Table. Patients total bacterial abundances for each optimisation method. Replicates (Rep) for each method are shown.
(PDF)

S2 Table. Patients total VLP abundances for each optimisation method. Replicates (Rep) for each method are shown.
(PDF)

Acknowledgments

We would like to thank all the staff at the Flow Cytometry Unit in the Flinders Medical Centre for their technical support throughout the duration of this study. We would also like to extend our gratitude to the tissue registrars in Professor Wormald's research group for conducting the patient surveys and their assistance in sample collection.

Author Contributions

Conceived and designed the experiments: JAPCJ JSP KN RJS LMD PS JGM PJW. Performed the experiments: JAPCJ. Analyzed the data: JAPCJ JSP KN RJS LMD PS JGM. Contributed reagents/materials/analysis tools: JAPCJ JSP KN PJW. Wrote the paper: JAPCJ PS JGM PJW.

References

1. Feazel LM, Robertson CE, Ramakrishnan VR, Frank DN. Microbiome complexity and *Staphylococcus aureus* in chronic rhinosinusitis. *The Laryngoscope*. 2012; 122(2):467–72. doi: [10.1002/lary.22398](https://doi.org/10.1002/lary.22398) PMID: [22253013](https://pubmed.ncbi.nlm.nih.gov/22253013/); PubMed Central PMCID: PMC3398802.
2. Boase S, Foreman A, Cleland E, Tan L, Melton-Kreft R, Pant H, et al. The microbiome of chronic rhinosinusitis: culture, molecular diagnostics and biofilm detection. *BMC infectious diseases*. 2013; 13:210. doi: [10.1186/1471-2334-13-210](https://doi.org/10.1186/1471-2334-13-210) PMID: [23656607](https://pubmed.ncbi.nlm.nih.gov/23656607/); PubMed Central PMCID: PMC3654890.
3. Ooi EH, Wormald PJ, Tan LW. Innate immunity in the paranasal sinuses: a review of nasal host defenses. *American journal of rhinology*. 2008; 22(1):13–9. doi: [10.2500/ajr.2008.22.3127](https://doi.org/10.2500/ajr.2008.22.3127) PMID: [18284853](https://pubmed.ncbi.nlm.nih.gov/18284853/).
4. Jiang RS, Liang KL, Jang JW, Hsu CY. Bacteriology of endoscopically normal maxillary sinuses. *The Journal of laryngology and otology*. 1999; 113(9):825–8. PMID: [10664686](https://pubmed.ncbi.nlm.nih.gov/10664686/).
5. Wilson MT, Hamilos DL. The nasal and sinus microbiome in health and disease. *Current allergy and asthma reports*. 2014; 14(12):485. doi: [10.1007/s11882-014-0485-x](https://doi.org/10.1007/s11882-014-0485-x) PMID: [25342392](https://pubmed.ncbi.nlm.nih.gov/25342392/).
6. Cryer J, Schipor I, Perloff JR, Palmer JN. Evidence of bacterial biofilms in human chronic sinusitis. *ORL; journal for oto-rhino-laryngology and its related specialties*. 2004; 66(3):155–8. doi: [10.1159/000079994](https://doi.org/10.1159/000079994) PMID: [15316237](https://pubmed.ncbi.nlm.nih.gov/15316237/).
7. Ferguson BJ, Stolz DB. Demonstration of biofilm in human bacterial chronic rhinosinusitis. *American journal of rhinology*. 2005; 19(5):452–7. PMID: [16270598](https://pubmed.ncbi.nlm.nih.gov/16270598/).
8. Ramadan HH, Sanclement JA, Thomas JG. Chronic rhinosinusitis and biofilms. *Otolaryngology—head and neck surgery: official journal of American Academy of Otolaryngology-Head and Neck Surgery*. 2005; 132(3):414–7. doi: [10.1016/j.otohns.2004.11.011](https://doi.org/10.1016/j.otohns.2004.11.011) PMID: [15746854](https://pubmed.ncbi.nlm.nih.gov/15746854/).
9. Sanclement JA, Webster P, Thomas J, Ramadan HH. Bacterial biofilms in surgical specimens of patients with chronic rhinosinusitis. *The Laryngoscope*. 2005; 115(4):578–82. doi: [10.1097/01.mlg.0000161346.30752.18](https://doi.org/10.1097/01.mlg.0000161346.30752.18) PMID: [15805862](https://pubmed.ncbi.nlm.nih.gov/15805862/).
10. Sanderson AR, Leid JG, Hunsaker D. Bacterial biofilms on the sinus mucosa of human subjects with chronic rhinosinusitis. *The Laryngoscope*. 2006; 116(7):1121–6. doi: [10.1097/01.mlg.0000221954.05467.54](https://doi.org/10.1097/01.mlg.0000221954.05467.54) PMID: [16826045](https://pubmed.ncbi.nlm.nih.gov/16826045/).
11. Psaltis AJ, Ha KR, Beule AG, Tan LW, Wormald PJ. Confocal scanning laser microscopy evidence of biofilms in patients with chronic rhinosinusitis. *The Laryngoscope*. 2007; 117(7):1302–6. doi: [10.1097/MLG.0b013e31806009b0](https://doi.org/10.1097/MLG.0b013e31806009b0) PMID: [17603329](https://pubmed.ncbi.nlm.nih.gov/17603329/).
12. Foreman A, Psaltis AJ, Tan LW, Wormald PJ. Characterization of bacterial and fungal biofilms in chronic rhinosinusitis. *Am J Rhinol Allergy*. 2009; 23(6):556–61. doi: [10.2500/ajra.2009.23.3413](https://doi.org/10.2500/ajra.2009.23.3413) PMID: [19958600](https://pubmed.ncbi.nlm.nih.gov/19958600/).

13. Kingdom TT, Swain RE Jr. The microbiology and antimicrobial resistance patterns in chronic rhinosinusitis. *American journal of otolaryngology*. 2004; 25(5):323–8. PMID: [15334396](#).
14. Bhattacharyya N, Kepnes LJ. Assessment of trends in antimicrobial resistance in chronic rhinosinusitis. *Ann Oto Rhinol Laryn*. 2008; 117(6):448–52. WOS:000257026300008.
15. Flemming HC, Wingender J. The biofilm matrix. *Nature reviews Microbiology*. 2010; 8(9):623–33. doi: [10.1038/nrmicro2415](#) PMID: [20676145](#).
16. Abedon ST, Kuhl SJ, Blasdel BG, Kutter EM. Phage treatment of human infections. *Bacteriophage*. 2011; 1(2):66–85. Epub 2012/02/16. doi: [10.4161/bact.1.2.15845](#) 2159-7073-1-2-2 [pii]. PMID: [22334863](#); PubMed Central PMCID: PMC3278644.
17. Drilling A, Morales S, Jardeleza C, Vreugde S, Speck P, Wormald PJ. Bacteriophage reduces biofilm of *Staphylococcus aureus* ex vivo isolates from chronic rhinosinusitis patients. *American journal of rhinology & allergy*. 2014; 28(1):3–11. doi: [10.2500/ajra.2014.28.4001](#) PMID: [24717868](#).
18. Fu W, Forster T, Mayer O, Curtin JJ, Lehman SM, Donlan RM. Bacteriophage cocktail for the prevention of biofilm formation by *Pseudomonas aeruginosa* on catheters in an in vitro model system. *Antimicrob Agents Chemother*. 2010; 54(1):397–404. Epub 2009/10/14. doi: [10.1128/AAC.00669-09](#) AAC.00669-09 [pii]. PMID: [19822702](#); PubMed Central PMCID: PMC2798481.
19. Payne RJ, Phil D, Jansen VA. Phage therapy: the peculiar kinetics of self-replicating pharmaceuticals. *Clin Pharmacol Ther*. 2000; 68(3):225–30. Epub 2000/10/03. S0009923600889559 [pii] doi: [10.1067/mcp.2000.109520](#) PMID: [11014403](#).
20. Marie D, Brussaard CPD, Thyraug R, Bratbak G, Vault D. Enumeration of marine viruses in culture and natural samples by flow cytometry. *Appl Environ Microbiol*. 1999; 65(1):45–52. PMID: [9872758](#); PubMed Central PMCID: PMC90981.
21. Brussaard CP. Optimization of procedures for counting viruses by flow cytometry. *Appl Environ Microbiol*. 2004; 70(3):1506–13. PMID: [15006772](#); PubMed Central PMCID: PMC368280.
22. Robertson BR, Button DK. Characterizing aquatic bacteria according to population, cell size, and apparent DNA content by flow cytometry. *Cytometry*. 1989; 10(1):70–6. doi: [10.1002/cyto.990100112](#) PMID: [2465113](#).
23. Benninger MS, Ferguson BJ, Hadley JA, Hamilos DL, Jacobs M, Kennedy DW, et al. Adult chronic rhinosinusitis: definitions, diagnosis, epidemiology, and pathophysiology. *Otolaryngology—head and neck surgery: official journal of American Academy of Otolaryngology-Head and Neck Surgery*. 2003; 129(3 Suppl):S1–32. Epub 2003/09/06. S0194599803013974 [pii]. PMID: [12958561](#).
24. Leruste A, Bouvier T, Bettarel Y. Enumerating viruses in coral mucus. *Appl Environ Microbiol*. 2012; 78(17):6377–9. Epub 2012/06/26. doi: [10.1128/AEM.01141-12](#) AEM.01141-12 [pii]. PMID: [22729548](#); PubMed Central PMCID: PMC3416620.
25. Gasol JM, Del Giorgio PA. Using flow cytometry for counting natural planktonic bacteria and understanding the structure of planktonic bacterial communities. *Sci Mar*. 2000; 64(2):197–224. ISI:000088019800007.
26. Marie D, Partensky F, Jacquet S, Vault D. Enumeration and cell cycle analysis of natural populations of marine picoplankton by flow cytometry using the nucleic acid stain SYBR Green I. *Appl Environ Microb*. 1997; 63(1):186–93. WOS:A1997WA16800029.
27. Garren M, Azam F. New method for counting bacteria associated with coral mucus. *Appl Environ Microbiol*. 2010; 76(18):6128–33. doi: [10.1128/AEM.01100-10](#) PMID: [20656857](#); PubMed Central PMCID: PMC2937480.
28. Danovaro R, Dell'Anno A, Trucco A, Serresi M, Vanucci S. Determination of virus abundance in marine sediments. *Appl Environ Microbiol*. 2001; 67(3):1384–7. Epub 2001/03/07. doi: [10.1128/AEM.67.3.1384-1387.2001](#) PMID: [11229937](#); PubMed Central PMCID: PMC92740.
29. Williamson KE, Wommack KE, Radosevich M. Sampling natural viral communities from soil for culture-independent analyses. *Appl Environ Microbiol*. 2003; 69(11):6628–33. Epub 2003/11/07. PMID: [14602622](#); PubMed Central PMCID: PMC262263.
30. Danovaro R, Middelboe M. Separation of free virus particles from sediments in aquatic systems. *Manual of Aquatic Viral Ecology ASLO*. 2010:74–81.
31. Lee HS, Majima Y, Sakakura Y, Shinogi J, Kawaguchi S, Kim BW. Quantitative cytology of nasal secretions under various conditions. *The Laryngoscope*. 1993; 103(5):533–7. Epub 1993/05/01. doi: [10.1288/00005537-199305000-00010](#) PMID: [8483371](#).
32. Shinogi J, Majima Y, Takeuchi K, Harada T, Sakakura Y. Quantitative cytology of nasal secretions with perennial allergic rhinitis in children: comparison of noninfected and infected conditions. *The Laryngoscope*. 1998; 108(5):703–5. Epub 1998/05/20. doi: [10.1097/00005537-199805000-00014](#) PMID: [9591549](#).

33. Chisholm KM, Getsinger D, Vaughan W, Hwang PH, Banaei N. Pretreatment of sinus aspirates with dithiothreitol improves yield of fungal cultures in patients with chronic sinusitis. *International forum of allergy & rhinology*. 2013. Epub 2013/10/15. doi: [10.1002/alr.21230](https://doi.org/10.1002/alr.21230) PMID: [24124079](https://pubmed.ncbi.nlm.nih.gov/24124079/).
34. Hajioannou J, Maraki S, Vlachaki E, Panagiotaki I, Lagoudianakis G, Skoulakis C, et al. Mycology of the Nasal Cavity of Chronic Rhinosinusitis Patients with Nasal Polyps in the Island of Crete. *Research in Otolaryngology*. 2012; 1(2):6–10.
35. Cleland WW. Dithiothreitol, a New Protective Reagent for Sh Groups. *Biochemistry*. 1964; 3:480–2. Epub 1964/04/01. PMID: [14192894](https://pubmed.ncbi.nlm.nih.gov/14192894/).
36. Grebski E, Peterson C, Medici TC. Effect of physical and chemical methods of homogenization on inflammatory mediators in sputum of asthma patients. *Chest*. 2001; 119(5):1521–5. Epub 2001/05/12. PMID: [11348963](https://pubmed.ncbi.nlm.nih.gov/11348963/).
37. Lunau M, Lemke A, Walther K, Martens-Habbena W, Simon M. An improved method for counting bacteria from sediments and turbid environments by epifluorescence microscopy. *Environ Microbiol*. 2005; 7(7):961–8. Epub 2005/06/11. EMI767 [pii] doi: [10.1111/j.1462-2920.2005.00767.x](https://doi.org/10.1111/j.1462-2920.2005.00767.x) PMID: [15946292](https://pubmed.ncbi.nlm.nih.gov/15946292/).
38. Carreira C, Staal M, Middelboe M, Brussaard CP. Counting viruses and bacteria in photosynthetic microbial mats. *Appl Environ Microbiol*. 2015; 81(6):2149–55. doi: [10.1128/AEM.02863-14](https://doi.org/10.1128/AEM.02863-14) PMID: [25595761](https://pubmed.ncbi.nlm.nih.gov/25595761/); PubMed Central PMCID: [PMC4345377](https://pubmed.ncbi.nlm.nih.gov/PMC4345377/).
39. Vaara M. Agents That Increase the Permeability of the Outer-Membrane. *Microbiol Rev*. 1992; 56(3):395–411. WOS:A1992JN45300002. PMID: [1406489](https://pubmed.ncbi.nlm.nih.gov/1406489/)
40. Human Microbiome Project C. Structure, function and diversity of the healthy human microbiome. *Nature*. 2012; 486(7402):207–14. doi: [10.1038/nature11234](https://doi.org/10.1038/nature11234) PMID: [22699609](https://pubmed.ncbi.nlm.nih.gov/22699609/); PubMed Central PMCID: [PMC3564958](https://pubmed.ncbi.nlm.nih.gov/PMC3564958/).
41. Costello EK, Lauber CL, Hamady M, Fierer N, Gordon JI, Knight R. Bacterial community variation in human body habitats across space and time. *Science*. 2009; 326(5960):1694–7. doi: [10.1126/science.1177486](https://doi.org/10.1126/science.1177486) PMID: [19892944](https://pubmed.ncbi.nlm.nih.gov/19892944/); PubMed Central PMCID: [PMC3602444](https://pubmed.ncbi.nlm.nih.gov/PMC3602444/).
42. Turnbaugh PJ, Hamady M, Yatsunencko T, Cantarel BL, Duncan A, Ley RE, et al. A core gut microbiome in obese and lean twins. *Nature*. 2009; 457(7228):480–4. doi: [10.1038/nature07540](https://doi.org/10.1038/nature07540) PMID: [19043404](https://pubmed.ncbi.nlm.nih.gov/19043404/); PubMed Central PMCID: [PMC2677729](https://pubmed.ncbi.nlm.nih.gov/PMC2677729/).
43. Biswas K, Hoggard M, Jain R, Taylor MW, Douglas RG. The nasal microbiota in health and disease: variation within and between subjects. *Front Microbiol*. 2015; 9:134. doi: [10.3389/fmicb.2015.00134](https://doi.org/10.3389/fmicb.2015.00134) PMID: [25784909](https://pubmed.ncbi.nlm.nih.gov/25784909/); PubMed Central PMCID: [PMC4345913](https://pubmed.ncbi.nlm.nih.gov/PMC4345913/).
44. Nasidze I, Li J, Quinque D, Tang K, Stoneking M. Global diversity in the human salivary microbiome. *Genome research*. 2009; 19(4):636–43. doi: [10.1101/gr.084616.108](https://doi.org/10.1101/gr.084616.108) PMID: [19251737](https://pubmed.ncbi.nlm.nih.gov/19251737/); PubMed Central PMCID: [PMC2665782](https://pubmed.ncbi.nlm.nih.gov/PMC2665782/).
45. Grice EA, Kong HH, Conlan S, Deming CB, Davis J, Young AC, et al. Topographical and temporal diversity of the human skin microbiome. *Science*. 2009; 324(5931):1190–2. doi: [10.1126/science.1171700](https://doi.org/10.1126/science.1171700) PMID: [19478181](https://pubmed.ncbi.nlm.nih.gov/19478181/); PubMed Central PMCID: [PMC2805064](https://pubmed.ncbi.nlm.nih.gov/PMC2805064/).
46. Mitchell JG, Seuront L. Towards a seascape topology II: Zipf analysis of one-dimensional patterns. *J Marine Syst*. 2008; 69(3–4):328–38. doi: [10.1016/j.jmarsys.2006.03.026](https://doi.org/10.1016/j.jmarsys.2006.03.026) WOS:000252044800015.

Flow cytometric enumeration of bacterial and virus-like particle populations in the human oral cavity pre and post sleep

Jessica Carlson-Jones¹, Anna Kontos², James S Paterson¹, Renee J Smith¹, Lisa M Dann¹, Peter Speck¹, James Martin³, Declan Kennedy³, James G Mitchell¹
¹Flinders University, Australia, ²The University of Adelaide, Australia, ³Department of Respiratory and Sleep Medicine, Australia

Introduction¹⁻¹⁰

- Various microhabitats within the oral cavity
 - Tongue, palate, teeth, gingiva
- Different oral surfaces = different microbial communities
- Changes in oral environment over time
 - Oxygen levels, pH, dryness, nutrients (food)
- Flow cytometry as a tool for enumeration
 - Rapid enumeration of cells
 - Allows for counts of virus-like particles (VLPs) at low concentrations
 - Reduces enrichment biases

Objectives

To examine the spatial distribution of bacteria and VLPs within the healthy paediatric oral cavity

To determine changes in bacterial and VLP concentrations in the oral cavity after sleep

Methodology⁷⁻¹⁰

Sample collection:

- Oral swabs collected at Women's and Children's Hospital, Adelaide
 - Roof of mouth
 - Back of throat
 - Back of tongue
 - Tip of tongue
 - Top of molars
 - Gingiva
- Swabs taken before and after sleep

Enumeration:

- FACSCanto II flow cytometer

Results

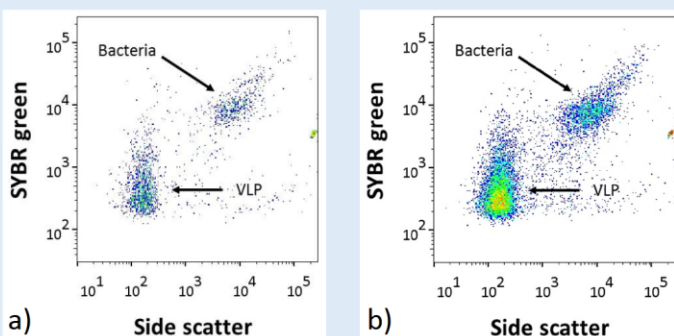


Figure 1: Cytograms from swab samples taken at the back of the throat a) before and b) after sleep from one healthy volunteer. An increase in both bacteria and VLP abundance can be seen after sleep.

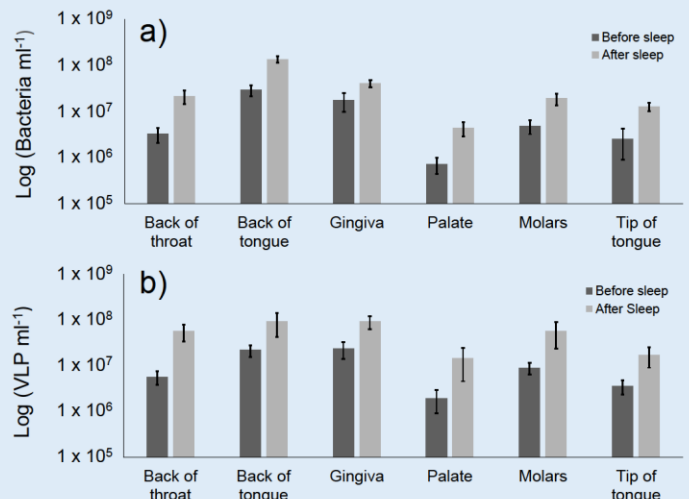


Figure 2: Average abundances of a) bacteria ml^{-1} and b) VLP ml^{-1} at various locations within the oral cavity. Error bars represent the standard error of the mean.

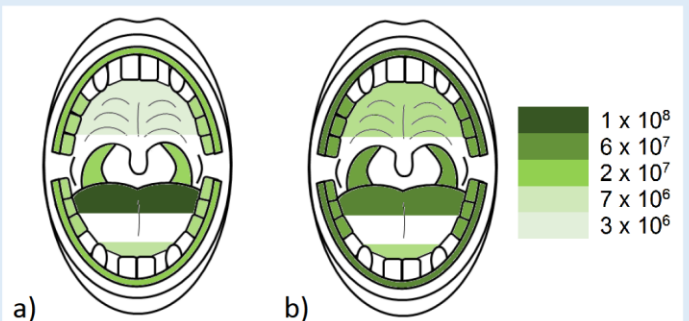


Figure 3: Heat maps showing the average increase in a) bacteria ml^{-1} and b) VLP ml^{-1} after sleep at sampled locations.

- Significant increase in both bacteria and VLP for all locations after sleep ($p < 0.05$)

Conclusions

Flow cytometry can be used as a tool to enumerate bacteria and VLPs from oral swab samples

The back of the tongue and gingiva have the highest abundances of bacteria and VLPs

The palate and tip of tongue have the lowest abundances of bacteria and VLPs

There is an average increase in the abundance of bacteria and VLP by 1000% during sleep

Bacterial abundances in the oral cavity can increase by a count of up to 100 million during sleep

References

- Dewhirst et al. (2010) Journal of bacteriology. 192(19):5002-17
- Human Microbiome Project (2012) Nature. 486(7402):207-14.
- Xu et al. (2014) Environmental Microbiology. n/a-n/a.
- Aas et al. (2005) J Clin Microbiol. 43(11):5721-32.
- Humphrey et al. (2001) The Journal of prosthetic dentistry. 85(2):162-9.
- Schneyer et al. (1956) Journal of dental research. 35(1):109-14.
- Marie D et al. (1999) Appl Environ Microbiol. 65(1):45-52.
- Bruissard et al. (2004) Applied and environmental microbiology. 70(3):1506-13.
- Robertson et al. (1989) Cytometry. 10(1):70-6.
- Carlson-Jones et al. (2016) PloS one. 11(5):e0155003

Email: jessica.carlsonjones@flinders.edu.au

Ethics: REC24953/16(HREC/12WCHN/52;SSA/12WCH/53)



Enumeration of virus-like particles in the sinus washes of chronic rhinosinusitis patients

Jessica Carlson-Jones¹, Lisa M Dann¹, Kelly Newton¹, James Paterson¹, Renee Smith¹, Peter Speck¹, James G Mitchell¹ and Peter-John Wormald²
¹School of Biological Sciences, Flinders University, GPO Box 2100, Adelaide SA 5001 ²Otolaryngology Head & Neck Surgery, Adelaide University, Adelaide, SA, Australia

Introduction

- Chronic rhinosinusitis (CRS)
 - Inflammation of paranasal sinuses for more than 12 weeks¹
 - Affects 12.5% of US population¹
 - \$2.4 billion healthcare expenditure annually²
- Bacterial infections thought to have a role in CRS³
 - Staphylococcus aureus*
- Not much known on viral populations in the sinuses
- Current CRS treatments have limitations⁴⁻⁵
 - Antibiotics: Bacterial resistance
 - Steroids: Health concerns from prolonged use
 - Surgery: Invasive
- Potential for phage therapy
 - Utilises specific bacteriophage that target, infect and kill pathogenic bacteria⁶
 - Success of the therapy may depend on the knowledge of abundance levels of bacterial and viral populations in CRS patients⁷
- Flow cytometry
 - Used in environmental studies to enumerate bacterial and viral populations⁸⁻⁹
 - Never used in CRS studies to enumerate bacterial and viral populations
- Presence of mucus in sinus washout samples may cause bacteria and viruses to clump together
 - Trial different methods to desorb bacteria and viruses from mucus¹⁰

Objective

Determine the presence and abundance of virus-like particles (VLP) in the maxillary sinus of patients with CRS.

Methodology

Experimental^{1, 8-12}

Patient selection:

- Full ethics approval (HERC/13/TQEHLMH/49)
- Consented patients underwent endoscopic sinus surgery for CRS (n = 9) (PJW)
- Patients gave written consent prior to surgery

Sample collection:

- Maxillary sinus flushed with sterile saline
- Sample fixed in 25% glutaraldehyde
- Snap frozen in liquid nitrogen

Sample treatment to desorb viruses and bacteria from mucus.

- 1% potassium citrate
- Methanol
- Sodium pyrophosphate
- Sputasol
- Untreated

Data analysis⁸⁻¹¹

Flow Cytometry

- BD Accuri™ C6 flow cytometer

FlowJo analysis software (© Tree Star)

- Viral and bacterial population definition
- Enumeration

Data processing¹³⁻¹⁴

PRIMER 6

- CLUSTER analysis
 - Euclidean distance – bacteria
 - Bray Curtis – VLP
- CAP analysis
- SIMPER analysis

Results

Virus-like particles present

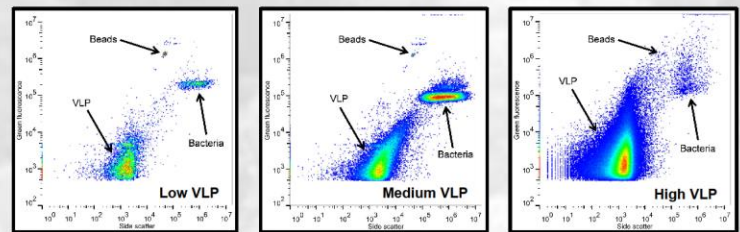


Figure 1: Cytograms from three patients using the untreated method showing low, medium and high VLP levels.

VLP range

$2.3 \times 10^6 \pm 7.3 \times 10^5$ → $2.0 \times 10^{10} \pm 5.2 \times 10^9$ VLP/ml

Bacterial range

$4.3 \times 10^4 \pm 6.6 \times 10^3$ → $1.0 \times 10^6 \pm 5.4 \times 10^6$ bacteria/ml

- No method significantly better for VLP enumeration (DNS)
- Untreated samples had significantly higher bacterial counts (DNS)

Findings

VLP are present in the maxillary sinus of CRS patients.

The sample treatment methods used did not affect VLP abundances.

The untreated method was most effective for bacterial enumeration.

This is the first study to enumerate VLP and bacterial populations in the maxillary sinus of CRS patients using flow cytometry.

References

- Benninger et al. (2003) *Otolaryngol Head Neck Surg.* 129:12
- Abreu et al. (2012) *Sci Transl Med.* 4: 151ra124
- Boase et al. (2013) *BMC Infect Dis.* 13: 210
- Hsu et al. (1998) *Am J Rhinol.* 12:243-8.
- Wood & Douglas (2010) *Postgrad Med J.* 86: 359-64
- Abedon et al. (2011) *Bacteriophage.* 1:66-85
- Payen et al. (2000) *Clin Pharmacol Ther.* 68: 225-30
- Marie et al. (1999) *Appl Environ Microbiol.* 65: 45-52
- Brussaard (2004) *Appl Environ Microbiol.* 70: 1506-13
- Gasol & Del Giorgio (2000) *Scientia Marina.* 64: 197-224
- Marie et al. (1997) *Appl Environ Microbiol.* 63: 186-93
- Leruste et al. (2012) *Appl Environ Microbiol.* 78: 6377-9
- Clarke & Gorley (2006) *Primer v6: User Manual/Tutorial.* PRIMER-E
- Clarke (1993) *Australian Journal of Ecology.* 18: 117-143

Background: Ramadan et al. (2005) *Otolaryngol Head Neck Surg.* 132: 414-7
(Standard preparation scanning microscopy micrograph of a CRS patient's mucosa)

Email: carl0092@flinders.edu.au

Response to reviewers (chapter 4)

The response to reviewers has been removed due to confidentiality.